

NASA CONTRACTOR REPORT 166587



An Experimental Evaluation of Advanced Rotorcraft Airfoils in the NASA Ames Eleven-Foot Transonic Wind Tunnel

Robert J. Flemming

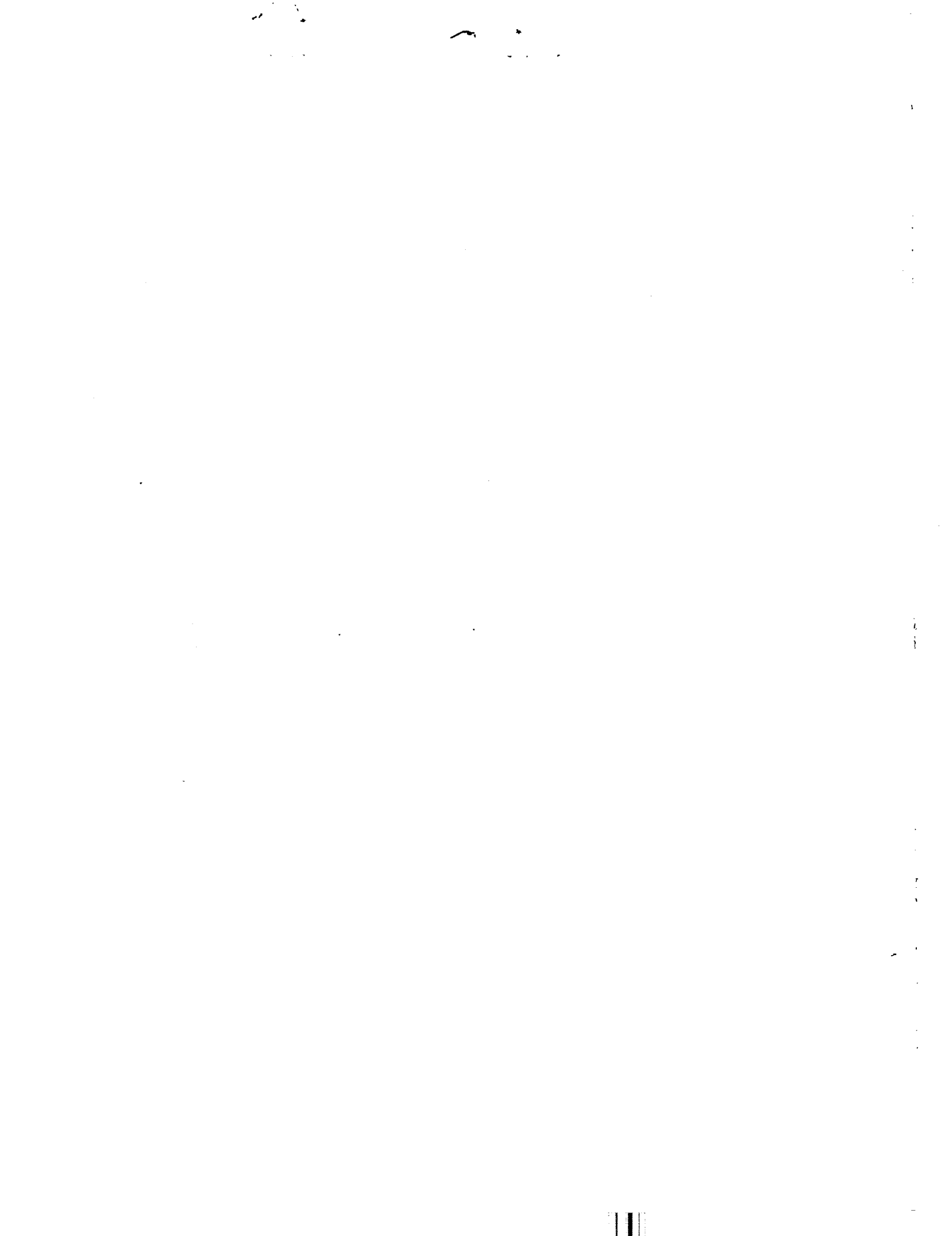
(NASA-CF-166587) AN EXPERIMENTAL EVALUATION OF ADVANCED ROTORCRAFT AIRFOILS IN THE NASA AMES ELEVEN-FOOT TRANSONIC WIND TUNNEL Contractor Report, Mar. 1982 - Apr. 1983 (Sikorsky Aircraft) 162 p Avail: NTIS HC

M88-11640

Unclas 0108482 G3/C2

CONTRACT MOA 14800-039
September 1984





NASA CONTRACTOR REPORT 166587

**An Experimental Evaluation of Advanced Rotorcraft Airfoils in
The NASA Ames Eleven-Foot Wind Tunnel**

Robert J. Flemming
United Technologies
Sikorsky Aircraft

Prepared for
Ames Research Center
under Contract MOA 14800-039



National Aeronautics and
Space Administration

Ames Research Center
Moffett Field, California 94035



FOREWORD

The test and data comparisons contained in this report are the result of a cooperative rotorcraft airfoil program between the Sikorsky Aircraft Division of United Technologies Corporation and the Ames Research Center of the National Aeronautics and Space Administration. While the tested airfoils are the product of Sikorsky design efforts, the test data and theoretical comparisons are published herein to advance the state of rotorcraft airfoil performance prediction. Several comparisons are contained in this report, but the reader is invited to use the data to provide additional insight into the areas where the available theoretical methods give valid results and where further theory development is required.

Many people provided the technical support to conduct this program. The principal personnel include:

Raymond Hicks	NASA Ames	Project Coordination
LeRoy Guist	NASA Ames	Test Engineer
Donald Jepson	Sikorsky Aircraft	Model Design
Anthony Saccullo	Sikorsky Aircraft	Test Engineer
David Lednicer	Sikorsky Aircraft	Aerodynamicist

PRECEDING PAGE BLANK NOT FILMED

TABLE OF CONTENTS

	<u>Page</u>
Foreword	iii
List of Tables	v
List of Figures	vi
Summary	1
Introduction	2
Symbols	3
Test Facility	4
Models	4
Instrumentation	5
Test Procedure	6
Data Reduction Methods	6
Test Results	8
Theory Correlation	10
Conclusions	12
Appendix A - Tabulated Test Data	126
References	152

LIST OF TABLES

		<u>Page</u>
I	Airfoil Model Geometric Characteristics	13
II	Coordinates for the SC1095 and SC1094 R8 Airfoils	14
III	Model Configuration Summary	15
IV	Run Log	16
V	Estimated Data Accuracy	26

LIST OF FIGURES

	<u>Page</u>
1. TSA installed in the Ames Eleven-Foot Transonic Wind Tunnel	27
2. TSA schematic	28
3. Airfoil section profiles	29
4. Airfoil metric sections	29
5. Test Reynolds numbers	30
6. Metric section calibration fixture	31
7. Representative manometer board wake rake profiles	31
8. Data repeatability - SC1095 airfoil, Mach number = 0.40	32
a. Lift coefficient versus angle of attack	
b. Drag coefficient versus lift coefficient	
c. Pitching moment coefficient versus lift coefficient	
9. Balance measurement correlation with pressure measurements	35
a. Lift	
b. Drag	
c. Pitching moment	
10. Drag for a drag coefficient of 0.008	38
11. Aerodynamic characteristics of the SC1095 airfoil	39
a. Lift coefficient versus angle of attack	
b. Drag coefficient versus lift coefficient	
c. Pitching moment coefficient versus lift coefficient	
12. Aerodynamic characteristics of the SSC-A09 airfoil	42
a. Lift coefficient versus angle of attack	
b. Drag coefficient versus lift coefficient	
c. Pitching moment coefficient versus lift coefficient	
13. Aerodynamic characteristics of the SSC-A07 airfoil	45
a. Lift coefficient versus angle of attack	
b. Drag coefficient versus lift coefficient	
c. Pitching moment coefficient versus lift coefficient	

LIST OF FIGURES (Cont'd)

	<u>Page</u>
14. Aerodynamic characteristics of the SSC-B08 airfoil	48
a. Lift coefficient versus angle of attack	
b. Drag coefficient versus lift coefficient	
c. Pitching moment coefficient versus lift coefficient	
15. Aerodynamic characteristics of the SC1094 R8 airfoil	51
a. Lift coefficient versus angle of attack	
b. Drag coefficient versus lift coefficient	
c. Pitching moment coefficient versus lift coefficient	
16. Aerodynamic characteristics at a Mach number of 0.30	54
a. Lift coefficient versus angle of attack	
b. Drag coefficient versus lift coefficient	
c. Pitching moment coefficient versus lift coefficient	
17. Aerodynamic characteristics at a Mach number of 0.40	57
a. Lift coefficient versus angle of attack	
b. Drag coefficient versus lift coefficient	
c. Pitching moment coefficient versus lift coefficient	
18. Aerodynamic characteristics at a Mach number of 0.50	60
a. Lift coefficient versus angle of attack	
b. Drag coefficient versus lift coefficient	
c. Pitching moment coefficient versus lift coefficient	
19. Aerodynamic characteristics at a Mach number of 0.60	63
a. Lift coefficient versus angle of attack	
b. Drag coefficient versus lift coefficient	
c. Pitching moment coefficient versus lift coefficient	
20. Aerodynamic characteristics at a Mach number of 0.70	66
a. Lift coefficient versus angle of attack	
b. Drag coefficient versus lift coefficient	
c. Pitching moment coefficient versus lift coefficient	
21. Aerodynamic characteristics at a Mach number of 0.80	69
a. Lift coefficient versus angle of attack	
b. Drag coefficient versus lift coefficient	
c. Pitching moment coefficient versus lift coefficient	

LIST OF FIGURES (Cont'd)

	<u>Page</u>
22. Aerodynamic characteristics at a Mach number of 0.85	72
a. Lift coefficient versus angle of attack	
b. Drag coefficient versus lift coefficient	
c. Pitching moment coefficient versus lift coefficient	
23. Variation in maximum lift coefficient versus Mach number	75
24. Variation in drag coefficient at zero lift versus Mach number	76
25. Maximum L/D versus Mach number	77
26. Lift curve slope correlation	78
27. Pressure coefficient distribution for the SC1095 airfoil	79
a. M = 0.40	
b. M = 0.60	
c. M = 0.80	
28. Pressure coefficient distribution for the SSC-A09 airfoil	82
a. M = 0.40	
b. M = 0.60	
c. M = 0.80	
29. Pressure coefficient distribution for the SSC-A07 airfoil	85
a. M = 0.40	
b. M = 0.60	
c. M = 0.80	
30. Pressure coefficient distribution for the SSC-B08 airfoil	88
a. M = 0.40	
b. M = 0.60	
c. M = 0.80	
31. Pressure coefficient distribution for the SC1094 R8 airfoil	91
a. M = 0.40	
b. M = 0.60	
c. M = 0.80	

LIST OF FIGURES (Cont'd)

	<u>Page</u>
32. Pressure coefficient distribution for low lift at high Mach numbers	94
a. M = .825	
b. M = .85	
c. M = .88	
d. M = .90	
e. M = .98	
f. M = 1.07	
33. Pressure coefficient correlation, M = 0.30, C ₁ = 0	100
a. SC1095	
b. SSC-A09	
c. SSC-A07	
d. SSC-B08	
e. SC1094 R8	
34. Pressure coefficient correlation, M = 0.30, C ₁ = 1.2	105
a. SC1095	
b. SSC-A09	
c. SSC-A07	
d. SSC-B08	
e. SC1094 R8	
f. SC1094 R8, C ₁ = 1.5	
35. Pressure coefficient correlation, M = 0.4, C ₁ = .7	111
a. SC1095	
b. SSC-A09	
c. SSC-A07	
d. SSC-B08	
e. SC1094 R8	
36. Pressure coefficient correlation, M = 0.6, C ₁ = .4	116
a. SC1095	
b. SSC-A09	
c. SSC-A07	
d. SSC-B08	
e. SC1094 R8	
37. Pressure coefficient correlation, M = 0.825, C ₁ = 0	121
a. SC1095	
b. SSC-A09	
c. SSC-A07	
d. SSC-B08	
e. SC1094 R8	



An Experimental Evaluation of Advanced Rotorcraft
Airfoils in the NASA Ames Eleven-Foot
Transonic Wind Tunnel

R. J. Flemming
Sikorsky Aircraft

SUMMARY

Five full scale rotorcraft airfoils were tested in March and April 1982 in the NASA Ames Eleven-Foot Transonic Wind Tunnel for full scale Reynolds numbers at Mach numbers from 0.3 to 1.07. The models, which spanned the tunnel from floor to ceiling, included two modern baseline airfoils, the SC1095 and SC1094 R8, which have been previously tested in other facilities. Three advanced transonic airfoils, designated the SSC-A09, SSC-A07, and SSC-B08, were tested to confirm predicted performance and provide confirmation of advanced airfoil design methods. This test has shown that the eleven-foot tunnel is suited to two-dimensional airfoil testing.

The maximum lift coefficients at a Mach number of 0.3 for the SC1095 and SC1094 R8 were 1.37 and 1.72, respectively, about 9% above prior test values. The transonic airfoils had maximum lift coefficients of 1.40, 1.22, and 1.15 for the SSC-A09, -B08 and -A07, respectively. Drag divergence Mach numbers at zero lift for these airfoils were .808, .780, .833, .848 and .860. Prior to stall and drag divergence the pitching moments were generally between 0.010 and -0.015. SC1095 and SC1094 R8 lift curve slopes were 8 to 17% below that of the solid-wall United Technologies Research Center tunnel, used to test the baseline airfoils in 1975.

The airfoil analysis codes agreed well with this data, with the Grumman GRUMFOIL code giving the best overall performance correlation. The NYU Transonic Airfoil code predicted airfoil pressures and drag divergence well, but errs in the calculation of pitching moment. The Texas A&M TRANDES/TRANSEP codes show good correlation over the full range of test conditions. The AMI CLMAX code predicts the relative maximum lift coefficient of the thicker airfoils well, but fails to predict the maximum lift coefficient of the SSC-A07. The maximum lift coefficients measured in the test exceed the CLMAX code prediction and available test data from the United Technologies tunnel by about 10%.

INTRODUCTION

Rotor systems must be improved to satisfy mission requirements which demand advancements in efficiency for higher cruise speeds and lower fuel consumption and for reductions in acoustic levels. Advances in methodology have provided more rigorous means to design improved airfoils, but these codes have not had a good correlation base for rotorcraft airfoils - airfoils that have compromises between high lift at low velocities and low drag at transonic velocities, all while maintaining low pitching moments.

Sikorsky Aircraft initiated a project in 1979 to replace the SC1095 airfoil family with a family of airfoils that maintain its maximum lift capability and pitching moment levels while increasing drag divergence Mach number by .03 or more. This airfoil family was designated the SSC-AXX family. An additional design incorporated a different design philosophy to provide a pitching moment near zero. This airfoil family was designated the SSC-BXX family. The design study used many airfoil codes, including TRANDES, NYU Transonic code (program H), AMI's CLMAX code, FLO 6, and GRUMFOIL (MCMJ-9) (refs. 1-5). While these codes correlate well with modern airfoils such as the SC1095, additional data was required to validate the new transonic airfoil designs and the theories that were used to design them. A cooperative two-dimensional test program between NASA's Ames Research Center and Sikorsky Aircraft was initiated in 1980 to satisfy these validation requirements. This report describes the test procedure, data analysis methods, processed data, and code correlation for this test program, conducted in the Ames Eleven-Foot Transonic Wind Tunnel.

SYMBOLS

A	Axial Force, kg (lb)
c	Airfoil Chord, m (ft)
C_A	Axial Force Coefficient, A/Sq
C_d	Drag Coefficient, D/Sq
C_l	Lift Coefficient, L/Sq
C_m	Pitching moment coefficient reference to quarter chord, PM/Scq
C_N	Normal Force Coefficient, N/Sq
C_p	Surface Pressure Coefficient, $\frac{P_1 - P_\infty}{q_\infty}$
D	Drag, newtons (lb)
h	Tunnel height, m (ft)
L	Lift, newtons (lb)
M	Mach number
M_{DD}	Mach number for drag divergence, $dC_d/dM = 0.1$
N	Normal Force, newtons (lb)
P	Pressure, newtons/m ² (psf)
PM	Pitching Moment, newton-m (ft-lb)
q	Dynamic pressure, $\frac{1}{2}\rho V^2$, newtons/m ² (psf)
R_N	Reynolds Number
S	Metric Section Area, m ² (ft ²)
t	Airfoil Thickness, cm (in)
V	Velocity, mps (fps)
α	Angle of Attack, deg
ρ	Air density, newtons/m ³ , (slugs/ft ³)

Subscripts

BAL	Balance
l	Local
max	Maximum
P	Pressure
W	Wake
∞	Free Stream

TEST FACILITY

The Eleven-Foot Transonic Wind Tunnel at NASA Ames is part of the Unitary Plan Wind Tunnel complex. It is a closed return, variable density tunnel with airflow produced by a three-stage axial-flow compressor. The tunnel can be operated at Mach numbers from 0.4 to 1.4 at stagnation pressures from 0.5 to 2.25 atmospheres and at lower Mach numbers at pressures above 1.4 atmospheres. For the advanced rotorcraft airfoil test the maximum Mach number was 1.07 and the stagnation pressure was held at 1.0 and 1.4 atmospheres. Stagnation temperature averaged 294°K (530°R).

The four walls of the test section are slotted with a normal porosity of 6.1%. To provide smooth flow near the ends of the airfoil model the slots adjacent to the model were taped, reducing porosity to 4.7%.

MODELS

The Sikorsky Tunnel Spanning Apparatus (TSA) was installed in the eleven-foot tunnel in a vertical orientation (see fig. 1). Dimensional data for the TSA is provided in figure 2. The base of the TSA's stainless steel spar was adapted to the tunnel yaw table and a turntable was fabricated to support the upper end of the spar. The turntables were controlled by one primary input with trim adjustments made with the upper turntable controller. Seven fiberglass-graphite airfoil panel segments for each airfoil model were attached to the spar. Surface pressures were measured using 24 upper surface and 11 lower surface .107 cm (.042 inch) orifices located 15.24 cm (6 inches) above the model centerline. The center 20.32 cm (8 inches) of the model contains a six-component Task balance and a single-component rear load cell. The metric section is sealed to the non-metric panels with .024 cm (.010 in) thick elastomeric material. Two struts with triangular cross-sections provided part-span support. The test of Reference 6 showed that the struts do not affect airfoil performance.

Five airfoil profiles (fig. 3) were fabricated for this test, including the SC1095 and SC1094 R8 for which test data in other facilities was already available. The chords of these two models are about 41 cm (16 inches). The three advanced airfoil models fabricated for this test have chords of 43.9 to 54.2 cm (17.3 to 21.3 inches). The chord increase was required to accommodate the spar for these airfoils, which are thinner than the SC1095. The airfoil metric sections are shown in figure 4. Tests near atmospheric pressure provide full scale data for aircraft in the size range of the Sikorsky S-76 and UH-60A, Bell UH-1H, and Hughes AH-64A.

While the tunnel can be operated over a wide range of stagnation pressures, data were acquired at pressures of 76 cm (30 inches) and 107 cm (42 inches) of mercury. The latter pressure was required at $M = 0.3$ because of minimum motor RPM constraints. The SSC-A09 airfoil was operated at Mach numbers up to .84 at both pressures to define Reynolds number trends. The test Reynolds numbers are summarized in figure 5.

Table I shows the basic geometric properties of the airfoil models. The coordinates for the SC1095 and SC1094 R8 airfoil sections are given on the first page of Table II. The coordinates for the SSC-A09 and SSC-A07 sections for which a patent is pending and the SSC-B08 section are included on the second page of Table II. The airfoil section profiles (fig. 3) were produced from aluminum molds using fiberglass with stiffening provided by graphite strips. This fabrication process generally produced airfoils to a tolerance within .03 cm (.012 inches). The panel segments of the SSC-A09 airfoil were reworked prior to Run 196 to reduce bolt head loads. This resulted in larger tolerance errors. Comparison of data taken prior to the modification with that after the modification indicates that the data of Runs 196-221 has a reduction in C_{lmax} of 0.11, an increase in drag of 0.0014 and an increase in pitching moment of .001. This is discussed further later in this report (see page 8). Surface finish was smooth, comparable to production blade finishes. Boundary layer transition devices were not used because full scale Reynolds numbers were used during testing.

At the end of the test, several out-of-contour modifications were made to the SSC-A09 airfoil using tape and wax. The description of these changes is given in the Test Results section of this report.

INSTRUMENTATION

The airfoil section forces and moments were derived from the balance readings and by pressure integrations. The center 20.3 cm (8 inches) of the TSA span is mounted to a 2.54 cm (one-inch) diameter six component Task balance and a single component load cell (see fig. 2). Calibration of this system was made with elastomeric seals in place, using special calibration fixtures (fig.6). The balance system was check loaded for each configuration during the test.

Pressures from the model orifices and the sting-mounted wake rake were measured by an automatic scanning system with precision transducers. Half of the wake rake tubes were teed to a mercury manometer board to aid in visualization and rake placement (fig. 7).

Model incidence was measured with potentiometers on both the lower and upper turntables. The TSA spar and struts were strain gauged to permit monitoring of the component loads. All parameters were displayed on digital voltmeters to permit continuous monitoring of the data. Data were recorded on the tunnel data system and transmitted to the Ames computer for on-line data reduction and stored for final post-test processing. Final data tapes were transmitted to Sikorsky Aircraft for preparation of final data listings and to facilitate the plotting of data.

TEST PROCEDURE

The test was conducted according to a test plan which prescribed angle of attack variation from -5 degrees through stall for Mach numbers between 0.3 and 1.07, except when limited by strut compression loads. Drag divergence Mach number was defined by a Mach number sweep at zero lift. The wake rake was generally covered at Mach numbers of 0.9 and above to prevent vibratory damage to the rake tubes. Ultra-violet oil flow photographs were taken for selected conditions.

Each data point was approached from a lower angle of attack with 30 seconds allowed for the tunnel and manometer board to stabilize prior to data acquisition. Data repeatability with angle of attack set in both the increasing and decreasing directions was evaluated during the initial test runs. Repeatability is excellent and there are no signs of hysteresis in any parameter (fig. 8). Test repeatability was checked during each run by repeating the Mach number of 0.4 case at angles of attack of 0 and 6 degrees.

The configurations tested are summarized in Table III. Run conditions are presented in Table IV.

DATA REDUCTION METHODS

The equations used to transform raw test data to aerodynamic coefficient follow accepted procedures. A description of the equations used in the data reduction process are given below to assist the reader in understanding the derivations of the coefficients.

The aerodynamic parameters contained in this report are corrected for the effect of the tunnel walls and spar torsion. The magnitude of the wall corrections that must be applied to the data are small. Since airfoil thickness ratios are 9.5% or less and height to chord ratios greater than 6, the wall

correction factors increase the free stream Mach number by 1%, the lift and drag coefficients decrease by 1½%, with small changes to pitching moment and angle of attack. The relationships used are given in Reference 7. An additional correction is made to the angle of attack to account for the change in angle at the metric section due to torsional moments. This correction increases the magnitude of the angle of attack about 2%. The lift curve slope in a slotted tunnel is less than that of a solid wall tunnel by 8 to 17%. The angles in this report are not corrected for the slot effect, but corrections are presented in the Test Results section of this report.

The coefficients of lift and drag are presented in the wind axis system. The wake rake drag is measured in the wind axis system, but the balance chord force and balance and surface pressure normal forces must be transformed as follows:

$$C_{L_P} = C_{N_P}(\cos \alpha + \tan \alpha \sin \alpha) - C_{D_W} \tan \alpha$$

$$C_{L_{BAL}} = C_{N_{BAL}} \cos \alpha - C_{A_{BAL}} \sin \alpha$$

$$C_{D_{BAL}} = C_{N_{BAL}} \sin \alpha + C_{A_{BAL}} \cos \alpha$$

The pitching moments for all of the airfoils, except the SC1094 R8, are referenced to the quarter chord. The SC1094 R8 pitching moment is referenced to the quarter chord of the SC1095. The quarter chord moment for the SC1094 R8 is

$$C_M = C_M - .0025 C_L - .015 C_D$$

Use of this transformation increases the nose down moment at high lift conditions by .005.

The wake rake data were analyzed following the procedures of Reference 8. Corrections for wall interference and the velocity gradient across the probes were applied.

TEST RESULTS

The airfoil surface pressure data, internal balance data, and wake rake pressure data were used to produce coefficients of lift, drag and quarter chord pitching moment, presented in tabular form in Appendix A. At low tunnel speeds the coefficients based on pressure data are inherently more accurate. Model flexibility results in errors in the transfer of loads to the balance, especially in the axial direction. As the tunnel speed is increased, and loads increase the agreement between pressure and balance measurements improve. At high Mach numbers the balance provides more accurate results, since the balance is not affected by force and moment pressure integration uncertainties due to rotational flow and shock position location between pressure ports. A comparison of force and moment coefficients derived from pressure and balance measurements is shown in Figure 9. The lift coefficient agreement is very good, even for cases with shock waves and for post-stall conditions (see fig. 9a). The estimated data accuracy for these measurements is given in Table V.

The wake rake provided much better drag coefficient repeatability than the balance measurements. The drag uncertainty for the balance was about 1.5 kilograms due to the flexibility in bond joints between the composite model skins and the balance clamps. (Future metric sections will be machined from solid metal to avoid this flexibility.) This 1.5 kilogram uncertainty exceeds the nominal minimum drag coefficient for Mach numbers below 0.64 (see fig. 10). Figure 9b shows the data scatter that exists in balance drag measurements. While points showing good agreement exist within the overall data scatter, balance drag values for points where the measured wake rake drag is less than 1.5 kilograms are generally not presented in Appendix A. The agreement between balance and pressure-derived pitching moment coefficients are good, improving with increasing Mach number. The plotted data presented in figures 11 through 25 are based on pressure measurements.

Figure 11 shows the force and moment coefficient data for the SC1095 airfoil for a range of Mach numbers. The maximum lift coefficient for the SC1095 at low Mach numbers as measured in the Ames 11-foot wind tunnels exceeds the maximum lift coefficient measured with the TSA in the UTRC 8-foot wind tunnel by 10%. Measured drag coefficients agree well. Force and moment coefficient data for the SSC-A09, SSC-A07, SSC-B08, and SC1094 R8 airfoils are presented in figures 12 through 15.

The SSC-A09 airfoil attachment points had to be reworked to reduce bolt head stresses. This resulted in a slight upward rotation of the leading edge piece and a corresponding dis-

continuity between the leading edge and trailing edge parts of the model for Runs 196 to 285. Post test evaluation of the data showed that this tolerance error caused a degradation in airfoil performance. The drag coefficient increased by 0.0014 and the pitching moment increased by 0.001. The maximum lift coefficient at a Mach number of 0.3 was lower by 0.11 after the rework and the point of zero lift occurs at a 0.3 degree higher angle of attack. Of this block of data only Run 196 is used in the graphical presentations in this report. This run is shown in figure 12 and exhibits a premature reduction in lift coefficient at angles of attack about 13 degrees. The dashed line in figure 12a shows the minimum performance expected for the airfoil at a Mach number of 0.4.

Figures 16 through 22 show the effect of airfoil configuration at constant Mach numbers. Figure 16a shows the low Mach number high lift characteristics of each airfoil. The high lift benefits of the leading edge camber of the SC1094 R8 are evident in this figure. The three transonic airfoils performed satisfactorily at this condition. The SSC-A09 airfoil exceeded the SC1095 airfoil maximum lift coefficient by 2%, and each transonic airfoil tested showed "gentler" stall characteristics. Low lift, low Mach number drag levels ranged from .0067 to .0088. The transonic airfoils had lower drag levels than the baseline airfoils.

The transonic airfoils produced significant performance improvements at higher Mach numbers. The maximum lift of the SSC-A09 exceeded that of the other airfoils tested at Mach numbers between 0.50 and 0.74. Above a Mach number of 0.74 the SSC-A07 had superior maximum lift capability (see fig. 23). Figure 24 shows the zero lift drag for the tested airfoils. The type of leading edge camber used for the SC1094 R8 results in an early drag rise and a drag divergence Mach number that is significantly lower than the other airfoils. The transonic airfoils maintain low drag characteristics to Mach numbers above 0.833. The drag divergence Mach number occurs at lower drag levels for the improved airfoils, providing more drag reduction than indicated by changes in drag divergence Mach number. The lift-drag ratios for the airfoils designed using modern design methods are superior to earlier rotorcraft airfoils. The airfoils in the SSC-AXX family have better maximum L/D values than the other tested airfoils (fig. 25).

Slotted wind tunnels give lower lift curve slopes than given in solid wall tunnels or by theory (see ref. 9). Figure 26 compares, for the SC1095 and SC1094 R8 airfoils, the lift curve slope derived from theory and the Ames and UTRC tunnels. The differences between tunnels ranges from 8% at low Mach numbers to 17% at high Mach numbers.

A limited number of runs at higher Reynolds numbers were made during the latter part of the test. These runs, which were at a Reynolds number 40% above the baseline, showed little change in maximum lift, a very small increase in drag coefficient (+.0008), and a small increase in pitching moment (+.004).

Five types of out-of-contour bumps and protruberances were added to the SSC-A09 airfoil at the end of the test and run over limited angle of attack and Mach number ranges. Each configuration showed a degradation in maximum lift coefficient and an increase in drag coefficient. Pitching moment coefficient changes were generally within ± 0.005 of the baseline value.

The first change (Configuration 6) was a simulated out-of-contour de-icing boot or abrasion strip. A soft duct tape was applied to the leading edge of the airfoil back to an x/c of 10% for both the upper and lower surfaces. The tape thickness was 0.35% of chord and ended in a step discontinuity. This resulted in a 15% reduction in maximum lift and an 80% increase in drag. This configuration was modified by adding a fairing behind the tape (Configuration 7). The fairings reduced the penalties for configuration 6 by 50%. The effect of miniature pressure transducers mounted on the blade surface was investigated (Configuration 8). Three rows of fifteen units, each having a diameter of 0.40 cm and a height of 0.08 cm with a simulated base and wiring, were placed on the model on the pressure orifice line, on the centerline of the metric section and 15 cm below the metric section centerline. The simulated transducers reduced the maximum lift by 4% and increased the drag by 18%.

Configurations 9 and 10 were smooth surface bumps. The first had a height of 0.3% of chord centered at the 50% chord station on the upper surface. The chordwise extent was 29%. This bump caused a 2% reduction in maximum lift and a 15% increase in drag. Adding a second bump at 10% chord (Configuration 10) with a height of 0.2% of chord and a chordwise extent of 14% resulted in a further loss in maximum lift of 1% and a further drag increase of 7%.

THEORY CORRELATION

Surface pressure data for the tested airfoils are presented in figures 27-32. These data have been used to compare several analysis methods (figs. 33-37). Figure 33 presents the surface pressure correlation for the five tested airfoils at low lifts and low Mach numbers. The computer codes produced similar results, and match the test data well. Pressure differences near the trailing edge are evident from these plots. Figure 34

shows similar data for high lift, low Mach number conditions. The data selected do not show separated flows on the upper surface as predicted by the AMI CLMAX code (ref. 3), although the angle of attack prediction for the input lift coefficient is good (prior to making lift curve slope corrections). The CLMAX code failed to converge at high angles of attack for the 7% thick airfoil. The Squire-Young drag coefficient ($C_{D_{S-Y}}$) in CLMAX tended to be optimistic. Additional CLMAX cases were run to evaluate the predicted maximum lift capability for each tested model. This code underpredicted the maximum lift coefficient measured in the Ames tunnel by about 10%. (It should be noted that the maximum lift from the Ames 11-foot wind tunnel exceeded that of the UTRC tunnel by 10%.) At a constant lift coefficient the pressures predicted by the NYU transonic (Korn, Garabedian, Bauer) code (ref. 2) are very good, although this code was not formulated for high lift, separated flow conditions and cannot show the same pressure distribution given by the CLMAX code. The TRANSEP code (ref. 1) predicted the pressure distributions well, showing the same or smaller separated zones at the trailing edge than the CLMAX code. The angle of attack correlation would improve if the slotted wall lift curve slope correction was applied to the data.

The surface pressures predicted by the NYU, TRANDES (see ref. 1) and MCMJ-9 GRUMFOIL code (see ref. 5) correlate very well for the moderate Mach number, moderate lift condition of figure 35. GRUMFOIL provides a better prediction of pitching moment. Similar correlation exists for the higher Mach number, moderate lift conditions of figure 36. Figure 37 shows the test data - theory comparison for a low lift, high Mach number condition. The shock position and the pitching moment for the SC1095 airfoil (fig. 37a) is predicted by GRUMFOIL, but GRUMFOIL shows the shock at a more rearward position for the SC1094 R8 airfoil. The three codes agree with the test data reasonably well for the transonic airfoils. GRUMFOIL exhibited much better pitching moment correlation than the other codes evaluated. The NYU, TRANDES and GRUMFOIL predicted the drag divergence Mach number within ± 0.015 . TRANDES tended to underpredict the drag divergence Mach number while the other two programs matched or slightly exceeded the drag divergence Mach number based on test data. The theoretical calculations for the SC1094 R8 airfoil had the largest deviations from the test data. The predicted drag levels for the cases of figures 35-37 were very good.

CONCLUSIONS

The test confirmed that the NASA Ames Research Center Eleven-Foot Transonic Wind Tunnel is well suited to airfoil testing. This test provided data for several airfoil designs including the SSC-AXX and SSC-BXX airfoil families, showing capability greater than that of the baseline SC1095 airfoil in the areas of maximum lift, maximum L/D and drag divergence Mach number.

Several modern airfoil theories were compared with the test data. The AMI CLMAX program had good angle of attack-lift correlation for low Mach number, high lift conditions but underpredicted drag. The Texas A&M TRANSEP program showed good surface pressure correlation, but the cases run failed to give reasonable drag levels. The TRANDES and NYU Transonic codes showed good drag, lift, and surface pressure correlation at low and moderate lifts but failed to predict airfoil pitching moment. GRUMFOIL gives good surface pressure, lift, drag and pitching moment correlation for these conditions.

TABLE I. AIRFOIL CHARACTERISTICS

Configuration Airfoil Designation Airfoil Type	1 SC1095 Modern	2, 6-10* SSC-A09 Advanced	3 SSC-A07 Advanced	4 SSC-B08 Advanced	5 SC1094 R8 Modern High Lift
Thickness Ratio, t/c	.095	.090	.070	.080	.094
Chord, inches	16.070	17.290	21.350	19.685	16.230
feet	1.3392	1.4408	1.7792	1.6404	1.3525
meters	.4082	.4392	.5423	.5000	.4122
x/c For Maximum Thickness	.27	.38	.38	.38	.27
x/c For Maximum Camber	.27	.17	.17	.34	.20
Model Aspect Ratio	8.21	7.63	6.18	6.71	8.13
Tunnel Height/Chord	8.21	7.63	6.18	6.71	8.13
Distance From Trailing Edge To Wake Rake, Chords	2.06	1.86	1.36	1.54	2.03
C_{Lmax} @ $M = 0.3$	1.37	1.40	1.15	1.22	1.71
C_{Lmax} @ $M = 0.4$	1.24	1.24	1.01	1.03	1.34
M_{DD} @ $C_L = 0$.808	.833	.850	.865	.78
<p>* Configuration 2 is clean SSC-A09 airfoil. Configurations 6-10 incorporate modifications to simulate deicing boots or abrasion strips (6 with step aft edge, 7 with faired aft edge), miniature pressure transducers (8), and contour bumps (9 and 10).</p>					

TABLE II. COORDINATES FOR THE SC1095 AND SC1094 R8 AIRFOILS

$\frac{X}{C}$	<u>SC1095</u>		<u>SC1094 R8</u>	
	$\frac{Y(C)}{u}$	$\frac{Y(C)}{l}$	$\frac{Y(C)}{u}$	$\frac{Y(C)}{l}$
0	0	0	-.01729	-.01729
.0008	.00389	-.00317	-.1172	-.0225
.004	.00898	-.00744	-.00333	-.0277
.01	.0155	-.0155	.0057	-.0318
.02	.0233	-.0185	.0158	-.0344
.04	.0334	-.0259	.0291	-.0369
.06	.0395	-.0303	.0367	-.0380
.08	.0438	-.0329	.0416	-.0386
.10	.0470	-.0346	.0452	-.0389
.125	.0497	-.0362	.0483	-.0390
.15	.0517	-.0375	.0506	-.0390
.20	.0546	-.0390	.0537	-.0390
.25	.0555	-.0394	.0549	-.0390
.30	.0554	-.0393	.0548	-.0389
.35	.0545	-.0387	.0541	-.0384
.40	.0529	-.0376	.0527	-.0374
.45	.0511	-.0362	.0508	-.0360
.50	.0485	-.0345	.0484	-.0343
.55	.0457	-.0324	.0455	-.0323
.60	.0421	-.0299	.0420	-.0298
.70	.0337	-.0239	.0337	-.0238
.80	.0236	-.0166	.0236	-.0165
.90	.0124	-.0087	.0123	-.0086
.95	.0064	-.0044	.0064	-.0044
1.00	.0017	-.0017	.0017	-.0017

TABLE II (concluded)
 COORDINATES FOR THE SSC-A09, SSC-A07
 AND SSC-B08 AIRFOILS

X/C	SSC-A09 (Patent Pending)		SSC-A07 (Patent Pending)		SSC-B08	
	Y/C) _u	Y/C) _l	Y/C) _u	Y/C) _l	Y/C) _u	Y/C) _l
0		0	0	0	0	0
.0008	.0039	-.0029	.0031	-.0022	.0031	-.0030
.0045	.0099	-.0064	.0077	-.0050	.0080	-.0076
.01	.0149	-.0089	.0116	-.0070	.0130	-.0104
.02	.0215	-.0117	.0167	-.0091	.0189	-.0133
.04	.0304	-.0157	.0237	-.0122	.0268	-.0168
.06	.0369	-.0186	.0287	-.0145	.0325	-.0191
.08	.0416	-.0209	.0323	-.0163	.0367	-.0207
.10	.0449	-.0228	.0349	-.0178	.0397	-.0220
.125	.0478	-.0249	.0372	-.0193	.0424	-.0233
.15	.0499	-.0266	.0388	-.0207	.0445	-.0244
.20	.0528	-.0295	.0410	-.0229	.0474	-.0260
.25	.0544	-.0317	.0423	-.0246	.0493	-.0273
.30	.0553	-.0332	.0430	-.0258	.0504	-.0282
.35	.0556	-.0342	.0432	-.0266	.0509	-.0289
.40	.0553	-.0346	.0430	-.0269	.0507	-.0293
.45	.0544	-.0344	.0423	-.0268	.0499	-.0294
.50	.0528	-.0336	.0410	-.0261	.0484	-.0292
.55	.0505	-.0320	.0393	-.0249	.0462	-.0287
.60	.0475	-.0298	.0369	-.0232	.0432	-.0280
.70	.0389	-.0238	.0303	-.1085	.0352	-.0253
.80	.0261	-.0159	.0203	-.0124	.0248	-.0207
.90	.0113	-.0074	.0088	-.0058	.0127	-.0128
.95	.0044	-.0030	.0034	-.0023	.0059	-.0069
.97	.0030	-.0023	.0023	-.0018	.0039	-.0049
.98	.0022	-.0016	.0017	-.0009	.0033	-.0037
.99	.0021	-.0009	.0016	-.0007	.0030	-.0022
1.00	.0024	-.0008	.0019	-.0006	.0029	-.0004



TABLE III. MODEL CONFIGURATION SUMMARY

Advanced Rotorcraft Airfoil Test
 NASA Ames 11-Foot Transonic Wind Tunnel

<u>Config</u>	<u>Identifier</u>	<u>Run Number</u>
1	SC1095 Airfoil	1 - 58
2	SSC-A09 Airfoil	59-83, 191-221
3	SSC-A07 Airfoil	84 - 115
4	SSC-B08 Airfoil	116 - 147
5	SC1094 R8 Airfoil	148 - 190
6	SSC-A09 Airfoil With Unfaired De-icing Boot	222 - 235
7	SSC-A09 Airfoil With Faired De-icing Boot	236 - 256
8	SSC-A09 Airfoil With Simulated Pressure Transducer	257 - 268
9	SSC-A09 Airfoil With Upper Surface Bump at X/C = 50%	269 - 284
10	SSC-A09 Airfoil With Upper Surface Bumps at X/C = 10% and 50%	285 - 286

TABLE IV. RUN LOG

Run No.	Total Pressure PT (in Hg)	Nominal Mach No.	Angle of Attack Range (deg)	Remarks
SC1095 Airfoil Installed, Configuration 1				
1	-	0	0	Data System Checks
2	→	→	→	Balance Trial Loading
3	→	→	→	Balance Trial Loading
4	→	→	→	Data System Checks
5	→	→	→	Balance Trial Loading
6	→	→	→	No Data
7	→	→	→	Balance Trial Loading
8	→	→	→	Balance Normal Force Check Loading
9	→	→	→	Balance Pitching Moment Check Loading
10	→	→	→	Balance Axial Force Check Loading
11	→	→	→	Balance Chord Force Check Loading
12	30	.5, .8	0	Shake Down Run
13	35	0	0	Scanivalve Check
14	30.0	.4	-5 to 20	Hysteresis and Repeatability Check Runs
15	→	→	20 to -5	
16	→	→	20 to -5	
17	→	→	0	
18	35	0	0 to 16	Scanivalve Check
19	42	.3	0 to 16	
20	42	.3	13	
21	30	.4	0, 6	
22	30	.5	-5 to 18	
23	30	.5	-0.6	
24	30	.6	-5 to 16	
25	30	.7	-5 to 2	
26	35	0	0	Run Terminated - Seals Split
27	30	.4	0	Scanivalve Check
28	30	.7	-5 to 11	Repeat of Run 25
29	35	0	0	Scanivalve Check
30	30	.8	-3 to 8	

TABLE IV. RUN LOG (Continued)

<u>Run No.</u>	<u>PT(in Hg)</u>	<u>Mach No.</u>	<u>Angle of Attack Range (deg)</u>	<u>Remarks</u>
31	30	.8	-1, 0	
32	30	.4	0, 6	
33	30	.6	0 to 11	Repeat of Run 24
34	30	.7	-6	
35	30	.75	-6	
36	30	.775	-6	
37	30	.80	-6	
38	30	.82	-6	
39	30	.4	-0.8, 0, 6	Includes Bilinear Scanivalve Check
40	30	.4	0, 6	
41	30	.7	-.6	
42	↓	.75	↓	
43	↓	.775	↓	
44	↓	.80	↓	
45	↓	.82	↓	
46	↓	.84	↓	
47	35	0	-0.6, -0.4	Scanivalve Check
48	30	.4	0, 6	
49	30	.9	-2 to 0	Shutdown to Check Seals. Two Screws broken Scanivalve Check
50	35	0	0	
51	30	.4	.0, 6	
52	30	.9	-1 to 5	
53	--	--	--	Continuation of Run 49 No Data
54	35	0	0	Scanivalve Check
55	30	.4	0, 6	
56	30	.98	-2 to 0	
57	30	1.07	-1 to 0	
58	--	0	0	N3 Check Load
SSC-A09 Airfoil Installed, Configuration 2				
59	35	0	0	
60	30	.4	0, 6	Scanivalve Check
61	42	.3	0 to 15	

TABLE IV. RUN LOG (Continued)

Run No.	PT (in Hg)	Mach No.	Angle of Attack Range (deg)	Remarks
62	35	0	0	Scanivalve Check
63	30	.5	-5 to 18	
64	↓	.4	0, 6	
65		.6	-4 to 13	
66	35	0	0	Scanivalve Check
67	30	.4	0, 6	
68	↓	.6	0, 11 to 16	Continuation of Run 65
69		.7	-3 to 11	
70		.8	-3 to 8	
71		.82	-0.7	
72		.84	-1.3 to -0.7	
73		.86	-1.3	
74		.88	-1.3	
75		.7	-1.3	
76		.75	-1.3	
77		.775	-1.3 to -0.8	
78		.8	-0.8	
79		.82	-0.8	
80		.84	-1.3	
81	35	0	0	Scanivalve Check
82	30	.75 to .90	-0.8 to 0	
83	30	.90	0	
SSC-A07 Airfoil Installed, Configuration 3				
84	35	0	0	Scanivalve Check
85	30	.4	-5, 0	
86	35	0	0	Scanivalve Check
87	30	.4	-5 to 14	
88	42	.3	0 to 14	
89	30	0	0	Static Data System Check
90	30	.4	0, 6, 12	Wake Rake Survey, Oil Flow
91	30	.5	-5 to 12	
92	35	0	0	Scanivalve Check
93	30	.6	-3 to 16	

TABLE IV. RUN LOG (Continued)

Run No.	PT(in Hg)	Mach No.	Angle of Attack Range (deg)	Remarks		
94	30	.7	-3 to 10	Scanivalve Check		
95	↓ 35	.4	0,6			
96	30	0	0			
97	↓ 30	.8	-2 to 6			
98	↓	.4	0,6			
99	↓	.7	0.1			
100	↓	.75	0.1, 0.2			
101	↓	.775	0.2 to 0.5			
102	↓	.8	0.4			
103	↓	.83	0.4			
104	↓	.85	-0.2 to 2.6			
105	↓	.87	0.6			
106	↓	.89	0.6			
107	35	0	0			
108	30	.4	0, 6			
109	↓	.9	-2 to 4			
110	↓	.98	-1 to 2			
111	↓	1.07	-1 to 2			
112	↓	0	0			
113	↓	↓	↓			
114	↓	↓	↓			
115	↓	↓	↓			
SSC-B08	Airfoil Installed, Configuration 4			Scanivalve Check		
116	↓	0	0			
117	↓	↓	↓			
118	↓	↓	↓			
119	↓	↓	↓			
120	↓	↓	↓			
121	↓	↓	↓			
122	30	.4	0,6			
123	↓	.4	-5 to 18			
124	↓	.5	-5 to 18			
125	35	0	0			
					End Zero Balance Normal Force Check Loading Balance Pitching Moment Check Loading Balance Chord Force Check Loading	
						No Data No Data Balance Normal Force Check Loading Balance Chord Force Check Loading Balance Pitching Moment Check Loading Repeat of 121 Includes Scanivalve Check at Pt = 35

TABLE IV. RUN LOG (Continued)

Run No.	PT (in Hg)	Mach No.	Angle of Attack Range (deg)	Remarks
126	42	.3	0 to 15	Scanivalve Check
127	35	0	0	
128	30	.4	0, 6, 12	Includes Repeat Points
129	↓	.6	-5 to 16	
130	↓	.7	-2 to 9	
131	↓	0	0	End Zero
132	35	0	0	Scanivalve Check
133	30	.8	-1.5 to 8	Oil Flow
134	↓	.7	1 to 0	
135	↓	.75	0	
136	↓	.775	0	
137	↓	.8	0	
138	↓	.82	0	
139	↓	.84	-0.4, 0.2	
140	↓	.86	-0.4, 0	
141	↓	.88	-0.5, 0	
142	↓	.4	0 to 13	
143	35	0	0	Scanivalve Check
144	30	.9	-2 to 4	
145	↓	.98	-1.3 to 2	
146	↓	1.07	-1.3 to 1	
147	↓	.4	0, 6, 12	
SC1094 R8 Airfoil Installed Configuration 5				
148	35	0	0	Scanivalve Check
149	30	.4	-0.2, -0.1, 6	Oil Flow
150	↓	.4	-5 to 18	
151	↓	.5	-5 to 18	
152	35	0	0	Scanivalve Check
153	42	.3	-5 to 18	
154	35	0	0	Scanivalve Check
155	30	.4	12 to 15	Repeat of Run 150, Oil Flow

TABLE IV. RUN LOG (Continued)

<u>Run No.</u>	<u>PT(in Hg)</u>	<u>Mach No.</u>	<u>Angle of Attack Range (deg)</u>	<u>Remarks</u>
156	30	.6	-5 to 10	Scanivalve Check
157	35	0	0	
158	30	.8	-0.3	Scanivalve Check
159	↓	.84	-0.3, 0.5	
160	↓	.4	0,6	
161	↓	.6	-5 to 16	
162	35	0	0	Scanivalve Check
163	30	.4	0,6	
164	↓	.7	-5.5 to 11	Scanivalve Check
165	↓	.8	-2 to 8	
166	↓	.85	0 to 5	
167	35	0	0	
168	42	.3	0 to 18	Scanivalve Check
169	30	0	0	
170	42	.4	0 to 20	End/Start Zeros
171	42	.35	0 to 20	
172	42	.4	0 to 20	Scanivalve Check
173	30	.6	1.6, 3.6	
174	↓	.65	1.3, 3.3	Scanivalve Check
175	↓	.7	-1 to 3	
176	↓	.725	-1 to 3	Scanivalve Check
177	↓	.75	-1 to 3	
178	↓	.775	-1 to 3	Scanivalve Check
179	↓	.8	-1 to 3	
180	↓	.82	-1 to 3.5	Scanivalve Check
181	↓	.84	-0.3, 2.2	
182	↓	.86	0.2, 2.5	Scanivalve Check
183	↓	.4	0, 6	
184	-	0	0	Balance Normal Force Check Loadings
185	↓	↓	↓	Balance Chord Force Check Loading
186	↓	↓	↓	Balance Normal Force Check Loading
187	↓	↓	↓	Balance Normal Force Check Loading
188	↓	↓	↓	Balance Pitching Moment Check Loading

TABLE IV. RUN LOG (Continued)

Run No.	PT (in Hg)	Mach No.	Angle of Attack Range (deg)	Remarks
189		0	0	
190		0	0	
191	30	0	0	Balance Chord Force Check Loading
192	30	0	0	Bilinear Scanivalve Check
193	30	0	0	Balance Normal Force Check Loading
194	35	0	0	Balance Chord Force Check Loading
195	30	0	0	Balance Pitching Moment Check Loading
196	35	0	0	Scanivalve Check
197	30	0	0	Wake Rake Survey
198	30	0	0	Repeat of Run 196
199	42	0	0	Repeat of Run 61
200	42	0	0	Scanivalve Check
201	35	0	0	
202	30	0	0	
203	42	0	0	
204	42	0	0	
205	35	0	0	
206	30	0	0	
207	42	0	0	
208	42	0	0	
209	30	0	0	
210	30	0	0	
211	30	0	0	
212	30	0	0	
213	30	0	0	
214	30	0	0	
215	42	0	0	
216	42	0	0	
217	42	0	0	
218	42	0	0	
219	42	0	0	

TABLE IV. RUN LOG (Continued)

Run No.	PT (in Hg)	Mach No.	Angle of Attack Range (deg)	Remarks
220	42	.84	1.4	
221	30	0	0	End Zero
SSC-A09 Airfoil Unfaired De-Icing Boot, Configuration 6				
222	30	.4	-2.3 to 17	
223	30	.6	-2.4 to 16	
224	30	.8	-2 to 8	
225	35	0	0	Scanivalve Check
226	42	.3	-2 to 17	
227	30	.4	0,6	
228		.75	0	
229		.775	0	
230		.8	0	
231		.82	0	
232		.84	0, -0.5	
233		.86	-0.5	
234		.88	-0.5	
235		0	0	End Zero
SSC-A09 Airfoil With Faired De-Icing Boot, Configuration 7				
236	30	.4	-2 to 15	
237	30	.4	0,6	
238	35	0	0	
239	30	.4	0	
240	30	.6	-2 to 16	
241	30	.8	0.1	
242	30	.75	0	
243		.775	-0.4	
244		.8	-0.3	
245		.81	-0.4	
246		.84	0	No Data
247		.86	-0.4	
248		.88	-0.4	
249		0	0	End Zero

TABLE IV. RUN LOG (Continued)

Run No.	PT (in Hg)	Mach No.	Angle of Attack Range (deg)	Remarks
250	42	.3	0	
251	35	0	0	Includes Scanivalve Check,
252	42	.3	-2 to 18	Aborted, bad α output
253	30	.4	0,6	Scanivalve Check
254	30	.8	0	
255	30	.84	0	
256	-	0	0	End Zero, Scanivalve Check
SSC-A09 Airfoil With Simulated Pressure Transducers, Configuration 8				
257	30	.4	-2 to 6	
258	↓	.4	-1 to 16	
259	↓	.6	-2 to 16	
260	↓	.8	-2 to 8	
261	42	.3	-2 to 16	
262	30	.75	0	
263	↓	.775	0	
264	↓	.8	0	
265	↓	.82	0	
266	↓	.84	0	
267	↓	.87	0	
268	↓	.88	0	
SSC-A09 Airfoil With Contour With Upper Surface Contour Bump at X/C = 50%, Configuration 9				
269	35	0	0	
270	30	.4	-1 to 16	
271	↓	.6	-1 to 12	
272	↓	.8	-2 to 7	
273	↓	.6	-2 to 16	
274	↓	0	0	End Zero
275	↓	.75	0,0.4	
276	↓	.775	0.4	
277	↓	.8	0.4	
278	↓	.82	0.4	
279	↓	.84	0.4	

TABLE IV. RUN LOG (Continued)

<u>Run No.</u>	<u>PT(in Hg)</u>	<u>Mach No.</u>	<u>Angle of Attack Range (deg)</u>	<u>Remarks</u>
280	30	.86	0.4	
281	↓	.88	0.4	
282		.4	0,6	
283	42	.3	-2 to 16	
284	30	0	0	End Zero
SCC-A09	Airfoil With Upper Surface Contour Bumps at X/C = 10% and 50%, Configuration 10			
285	30	.4	-0 to 18	
286	-	0	0	End Zero, End of Test

TABLE V. ESTIMATED DATA ACCURACY

(Based on 1σ Deviations)

	Balance Data		Pressure Data	
	Coefficient Values		Coefficient Values	
	M = 0.4	M = 0.6	M = 0.4	M = 0.6
Lift	± 1.9 kg	± 0.022	± 1.0 kg	± 0.012
Drag	± 1.5 kg	± 0.0170	± 0.07 kg	± 0.0008
Pitching Moment	± 3.1 n-m	± 0.009	± 1.4 n-m	± 0.004
Surface Pressure Coefficients	--	± 0.01	--	± 0.01
Angle of Attack	± 0.1 deg	--	± 0.1 deg	--

* Not including errors caused by non-axial wake disturbances.

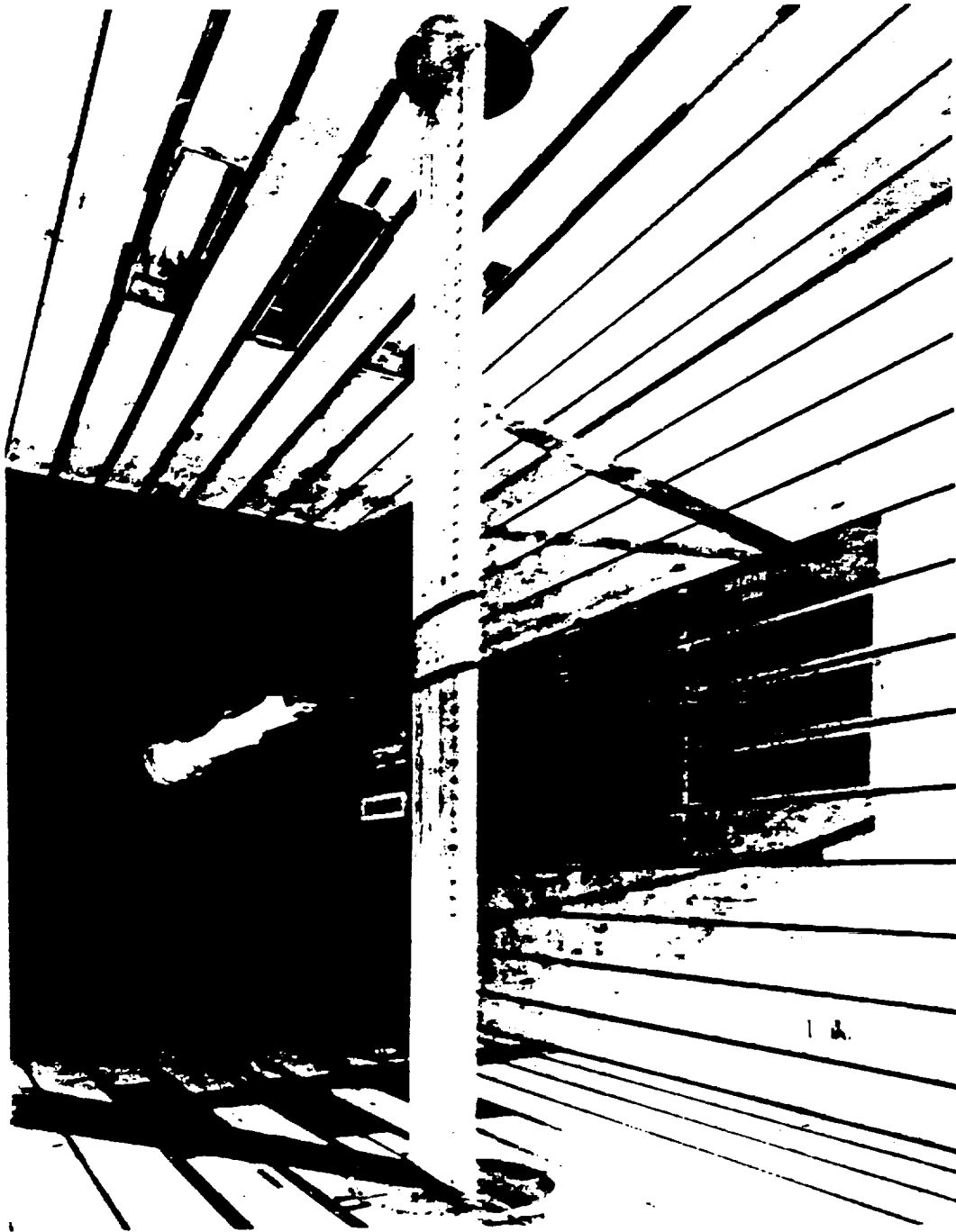


Figure 1. TSA installed in the Ames Eleven-Foot Transonic Wind Tunnel.

ORIGINAL PAGE IS
OF POOR QUALITY

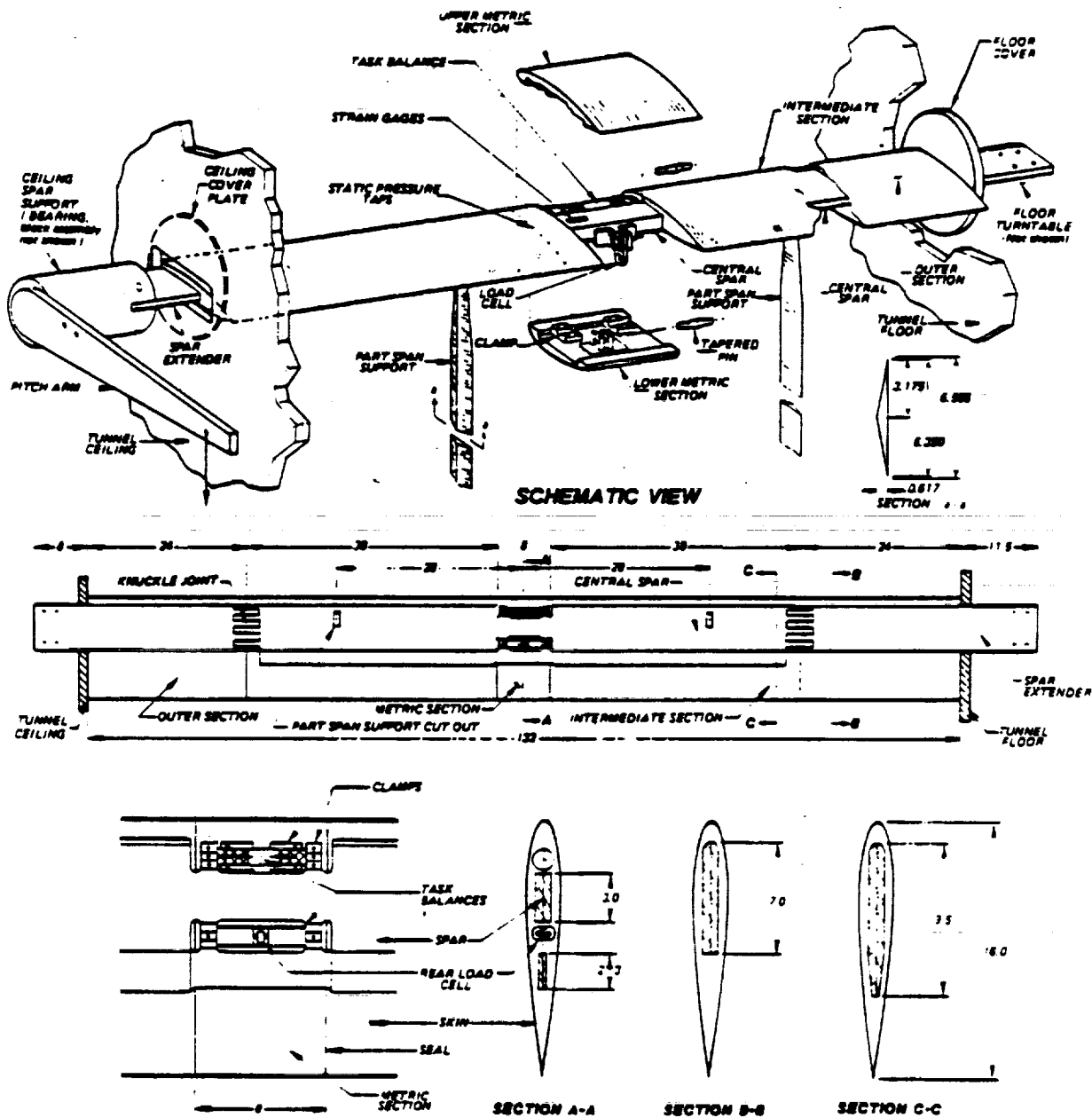


Figure 2. TSA schematic.

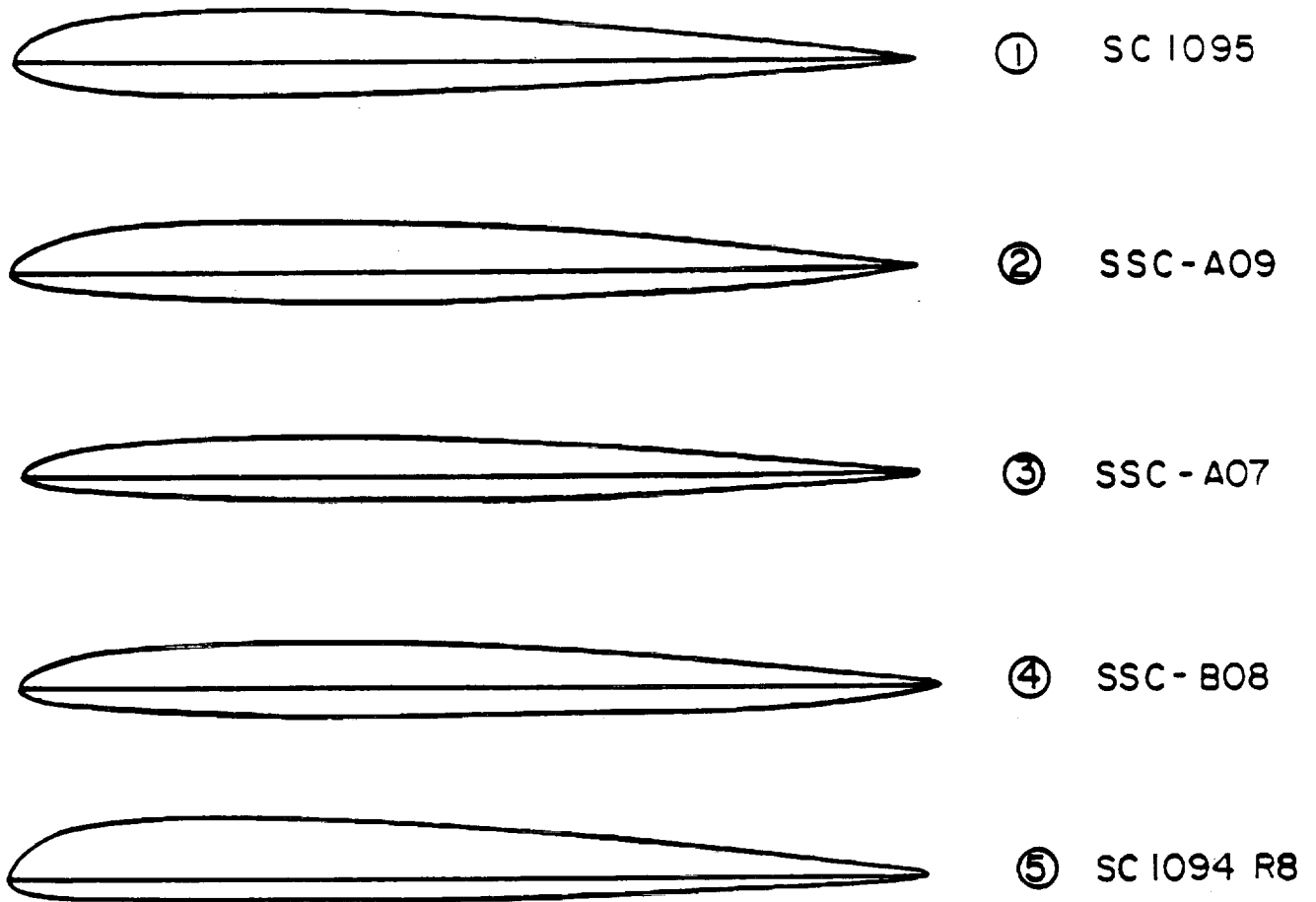


Figure 3. Airfoil section profiles.

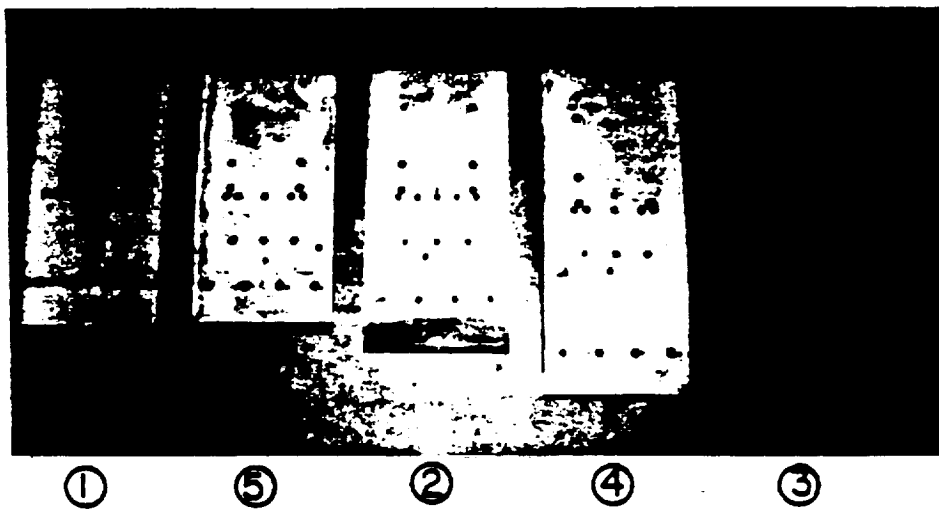


Figure 4. Airfoil metric sections.

M	RN/FT	
	$P_T = 30 \text{ PSF (1.0 ATM)}$	$P_T = 42 \text{ PSF (1.4 ATM)}$
.3	-	2.91
.4	2.07	3.73
.5	3.24	4.47
.6	3.66	5.00
.7	4.00	5.52
.8	4.22	5.80
.9	4.48	-
.98	4.51	-
1.07	4.44	-

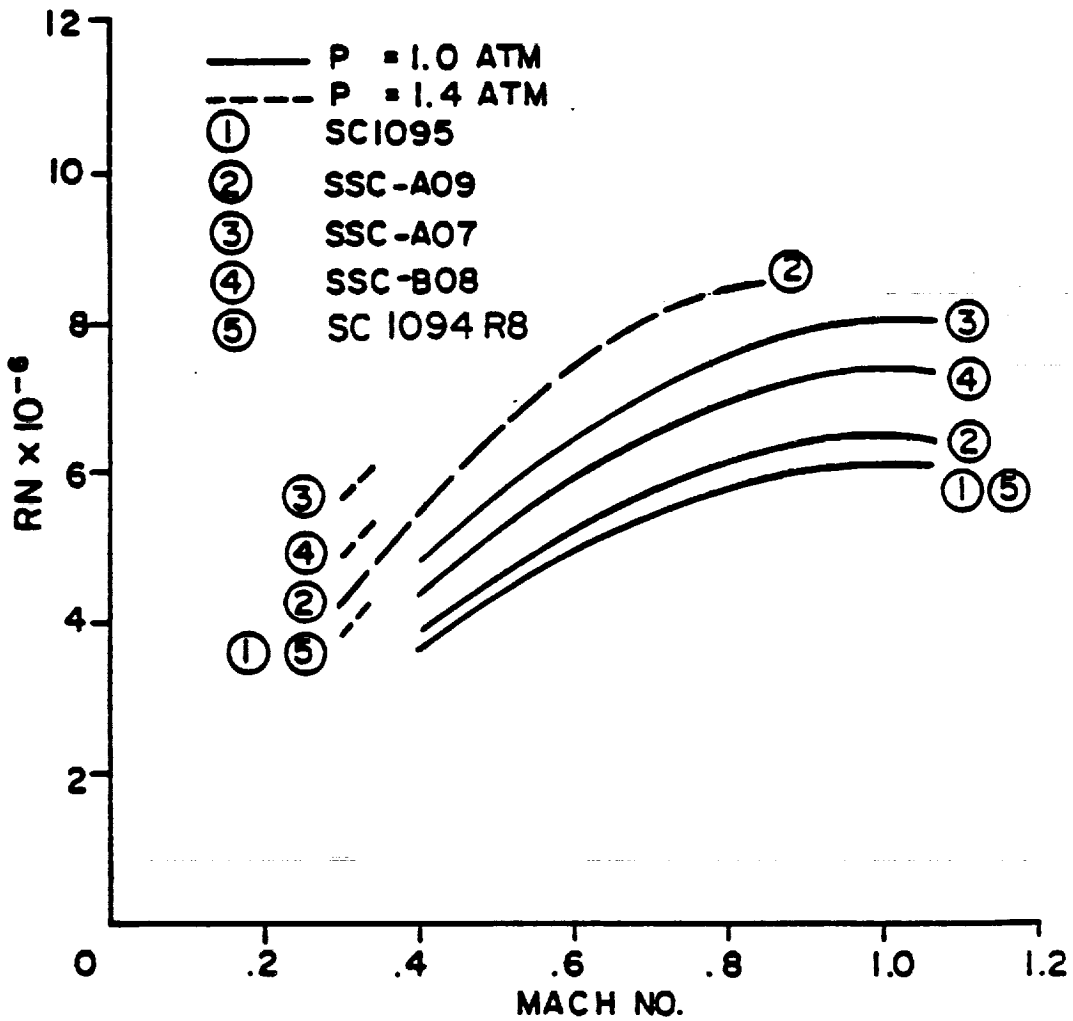


Figure 5. Test Reynolds numbers.

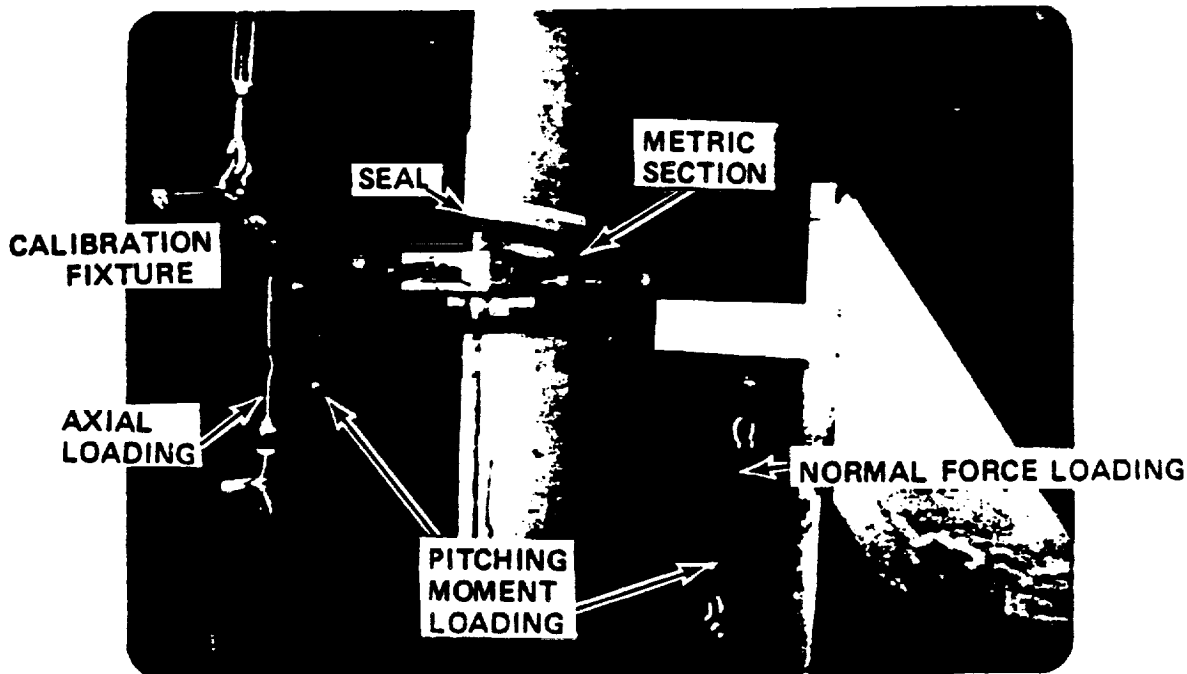


Figure 6. Metric section calibration fixture.

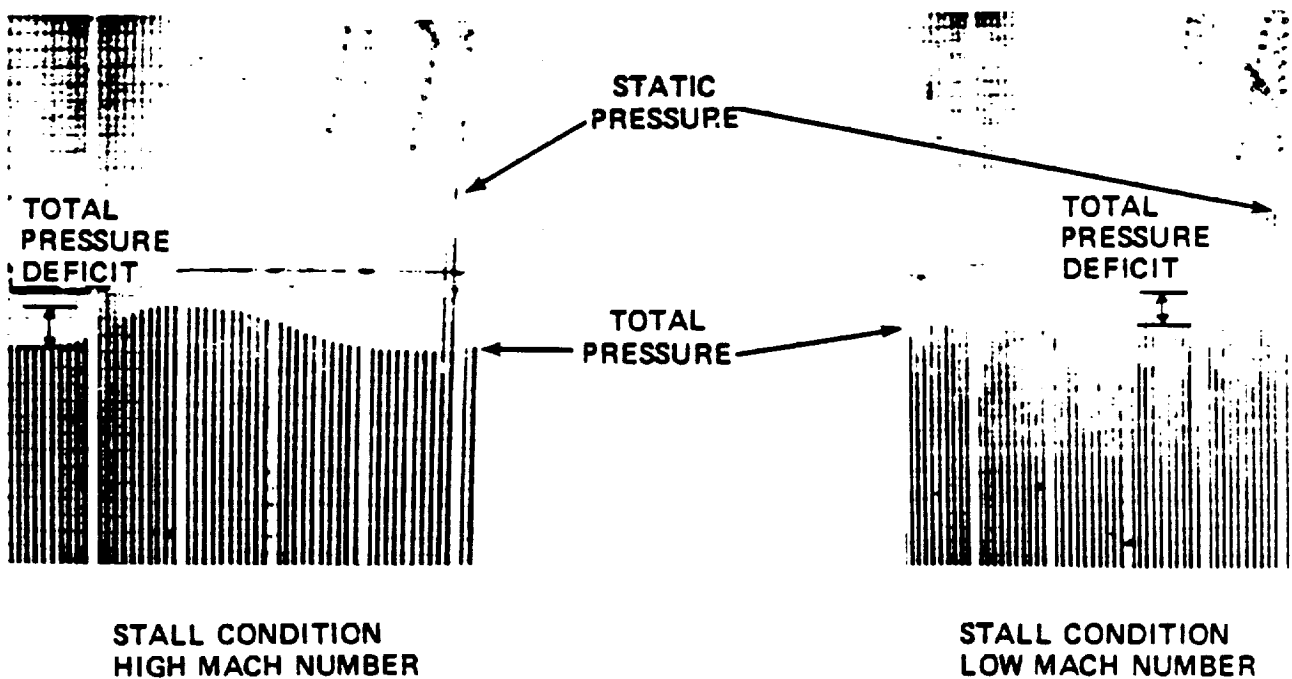
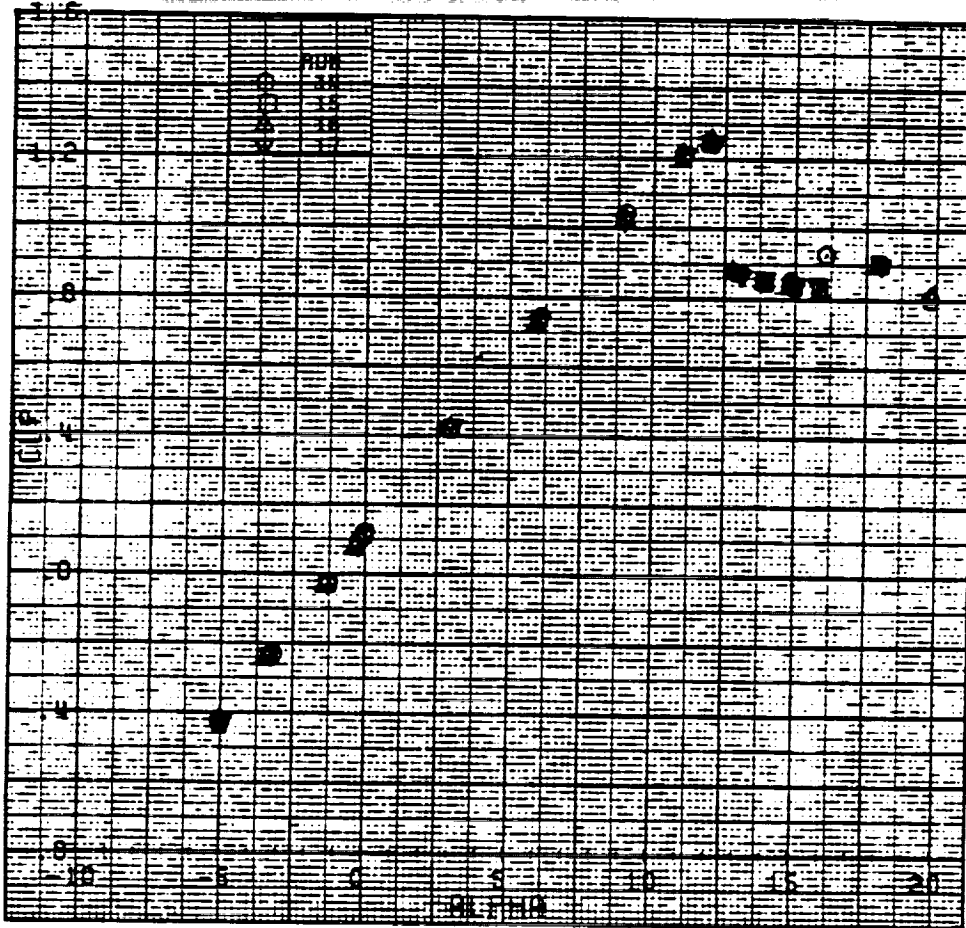
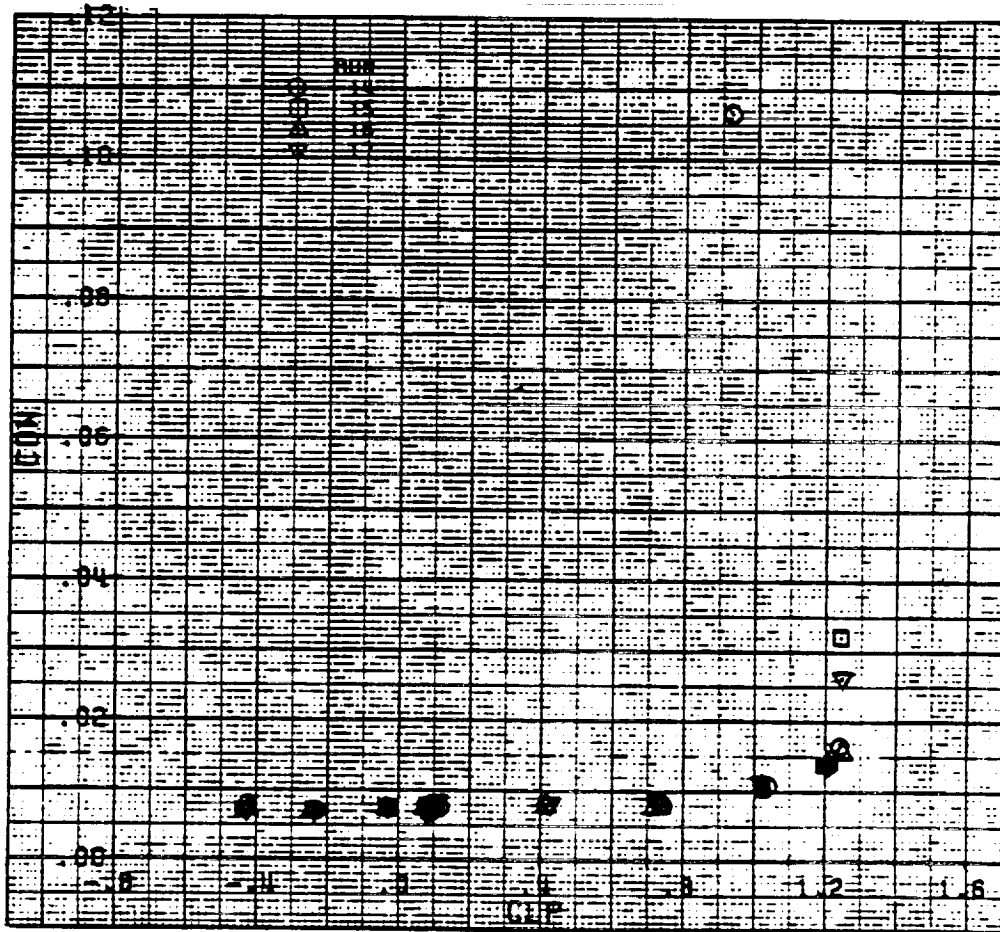


Figure 7. Representative manometer board wake rake profiles.

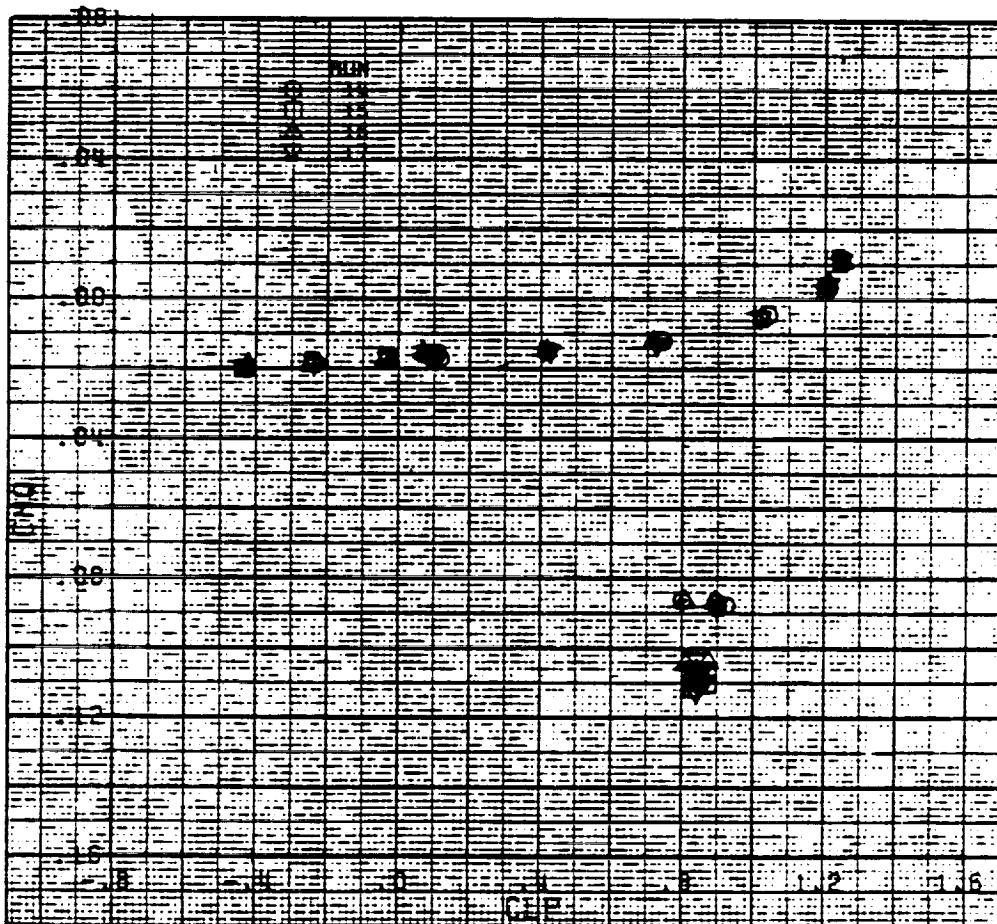


(a) Lift coefficient versus angle of attack
 Figure 8.-Data repeatability - SC1095 airfoil,
 Mach number = 0.40.



(b) Drag coefficient versus lift coefficient

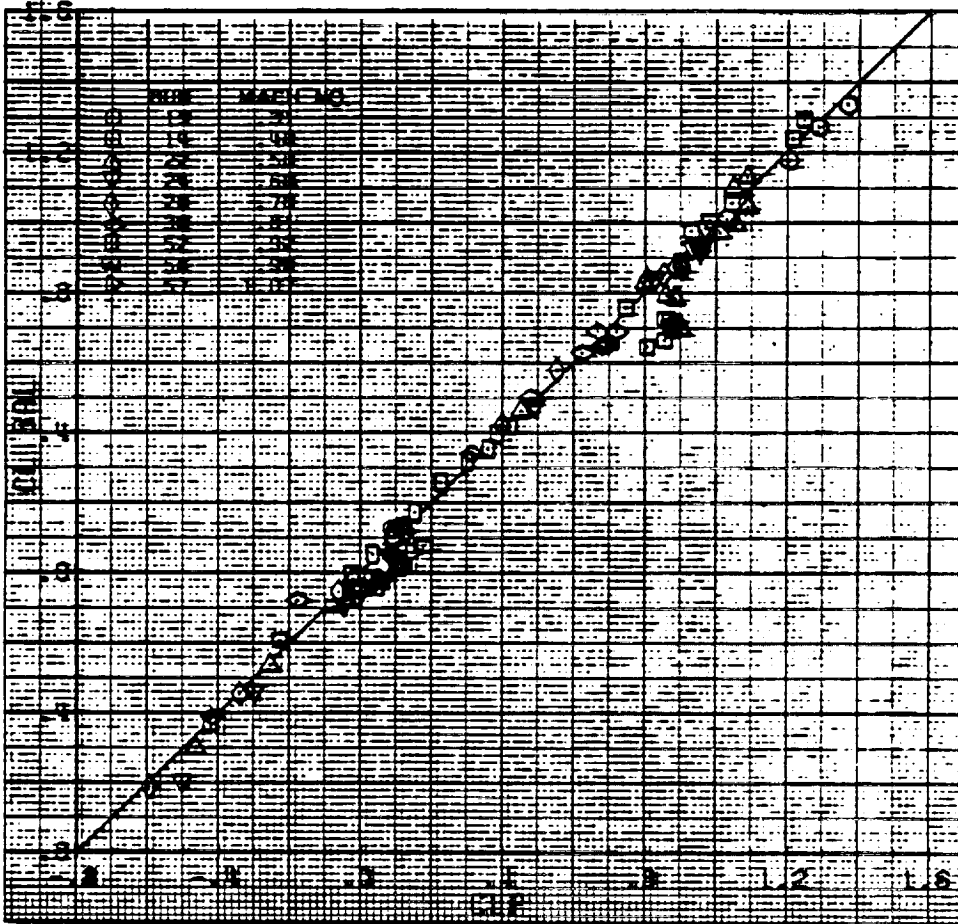
Figure 8.-Continued.



(c) Pitching Moment coefficient versus lift coefficient

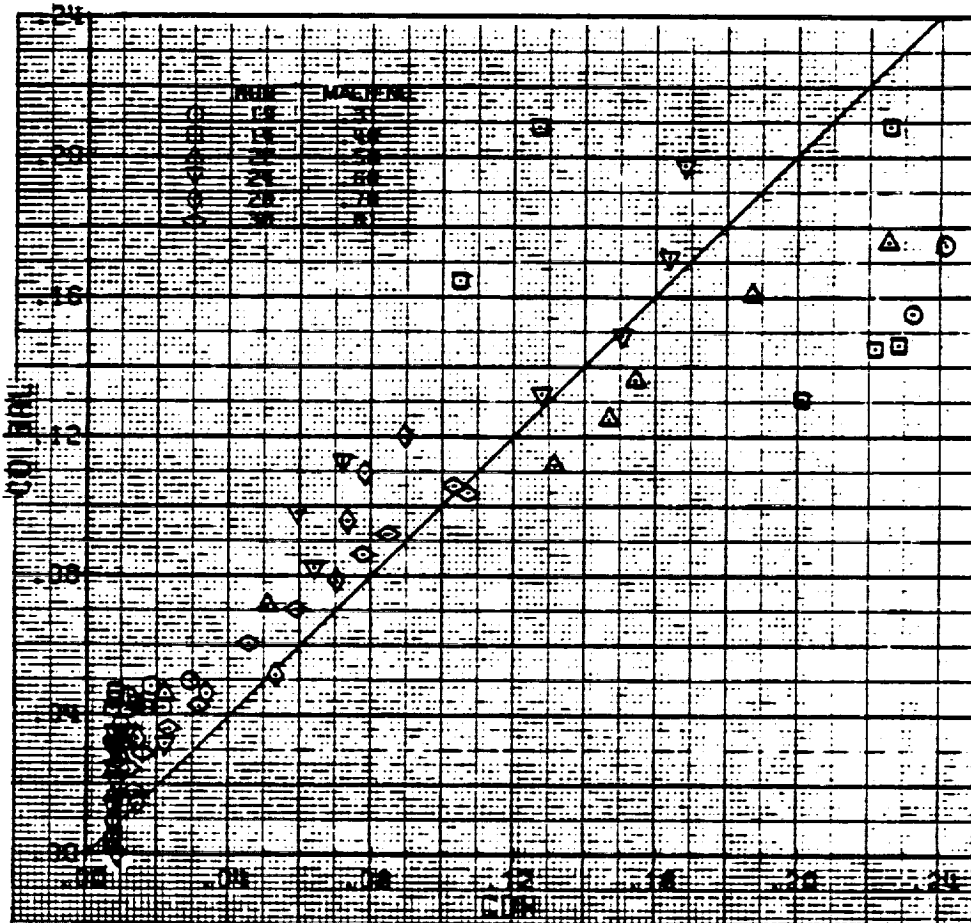
Figure 8.-Concluded.

ORIGINAL PAGE IS
OF POOR QUALITY



(a) Lift

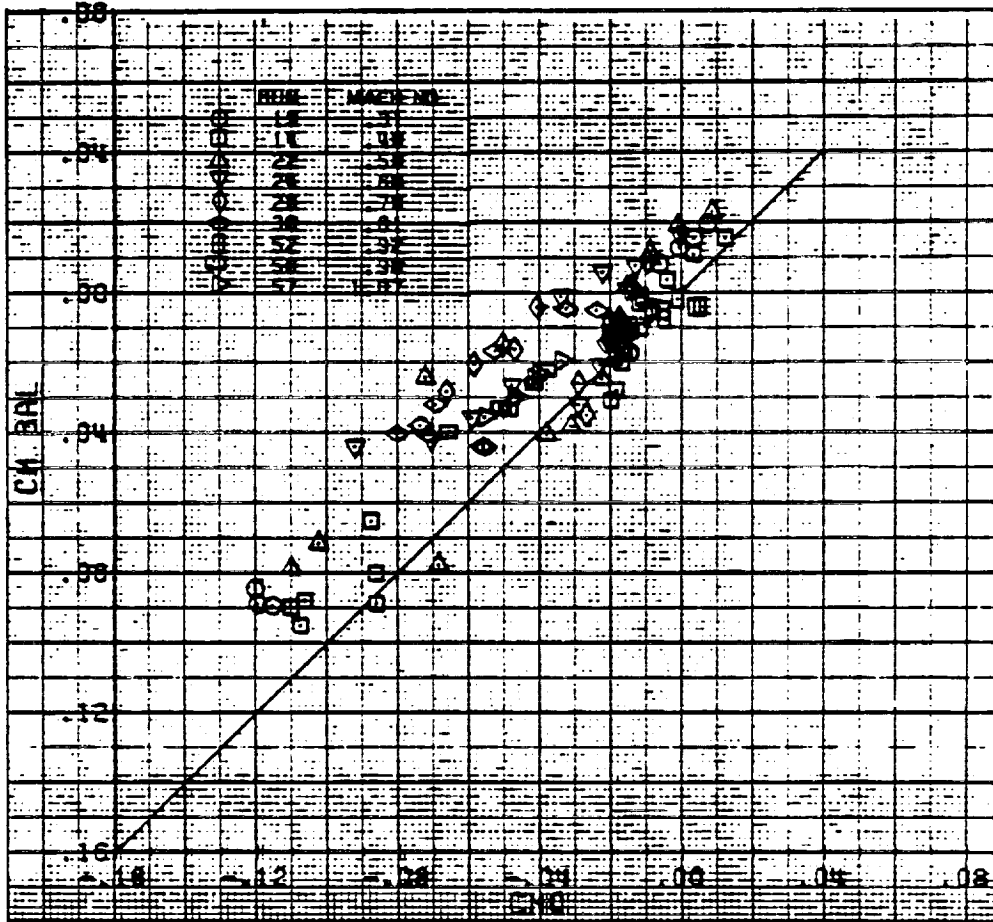
Figure 9.- Balance measurement correlation with pressure measurements.



(b) Drag

Figure 9.-Continued.

ORIGINAL PAGE IS
OF POOR QUALITY



(c) Pitching moment

Figure 9.-Concluded.

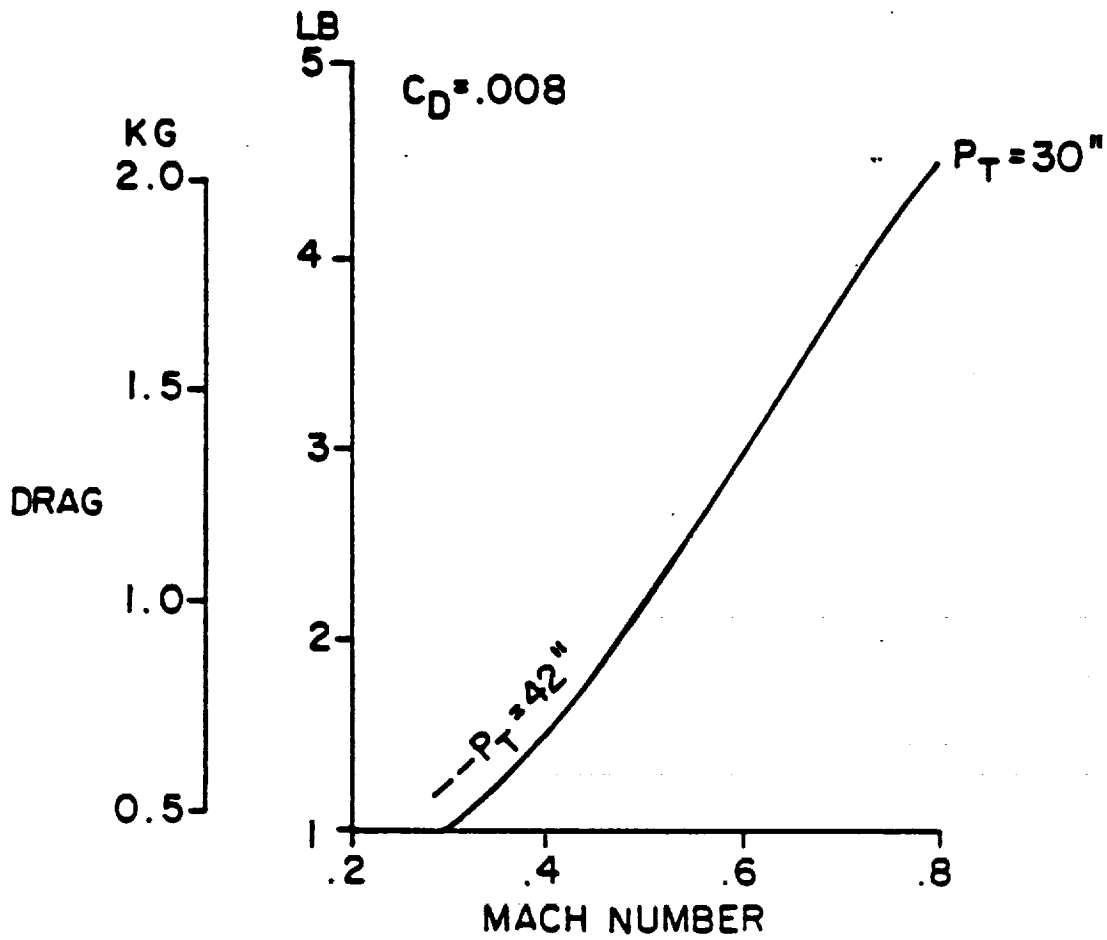
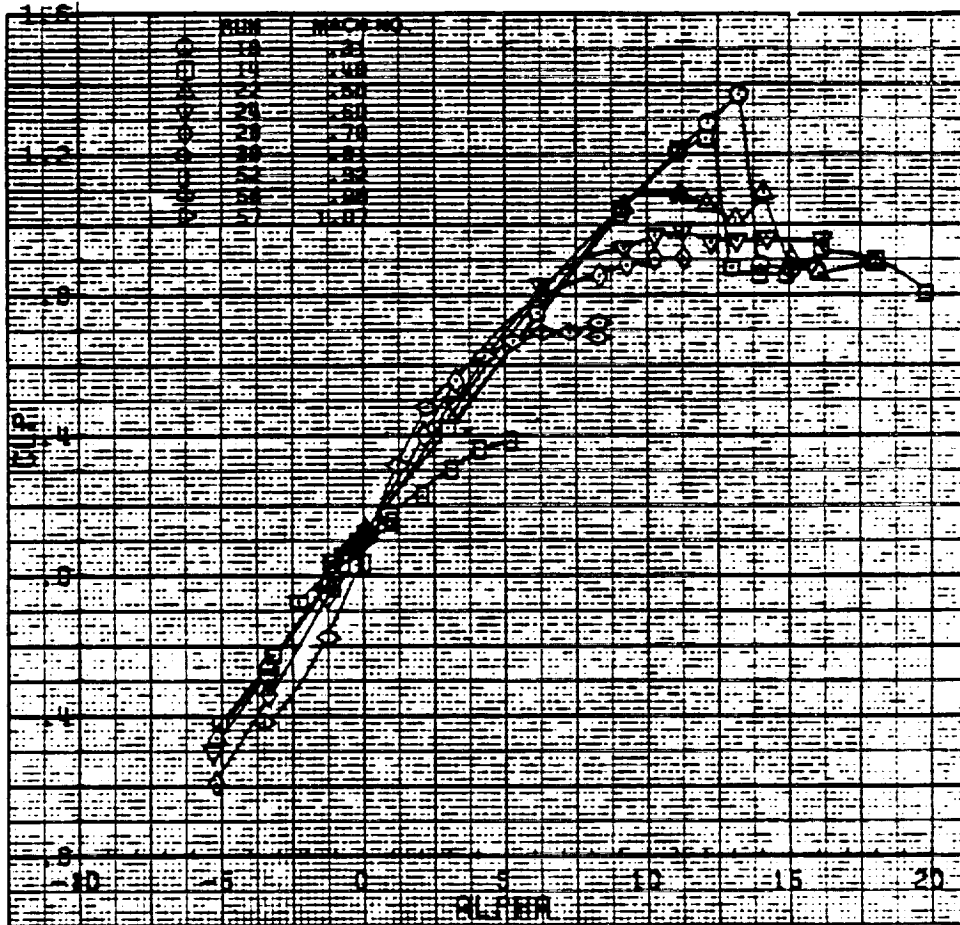
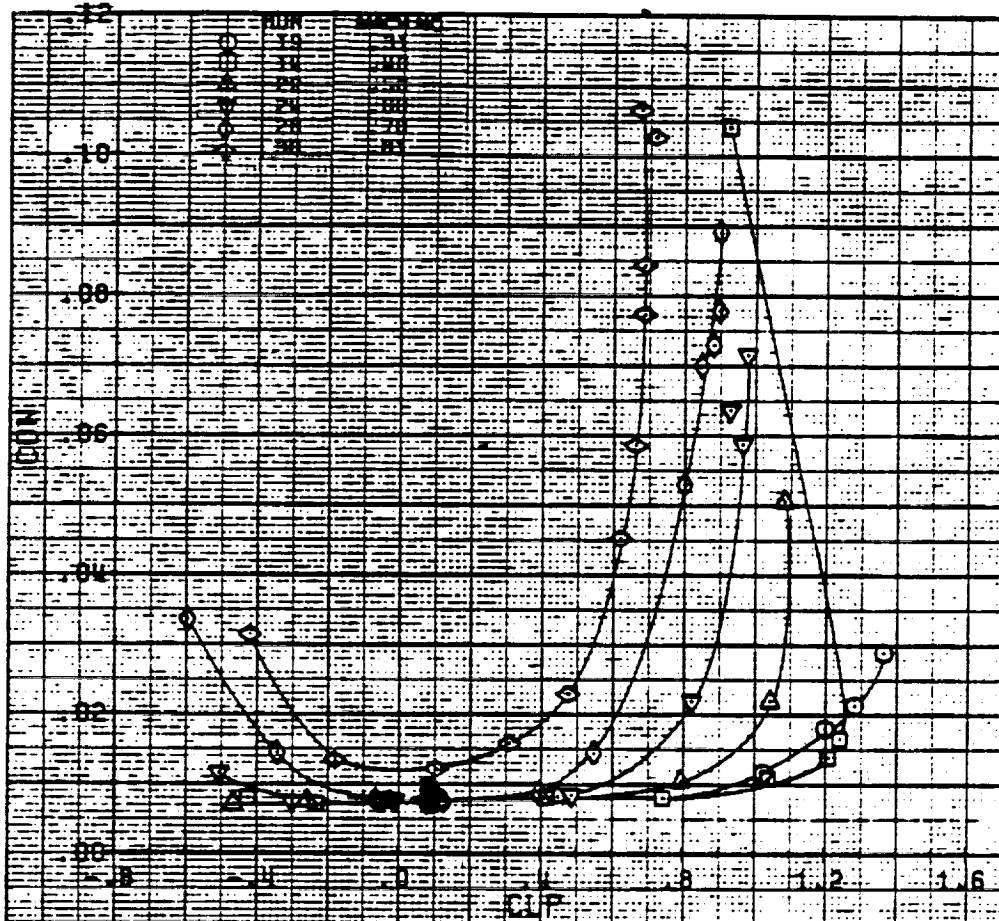


Figure 10. Drag for a drag coefficient of 0.008.



(a) Lift coefficient versus angle of attack

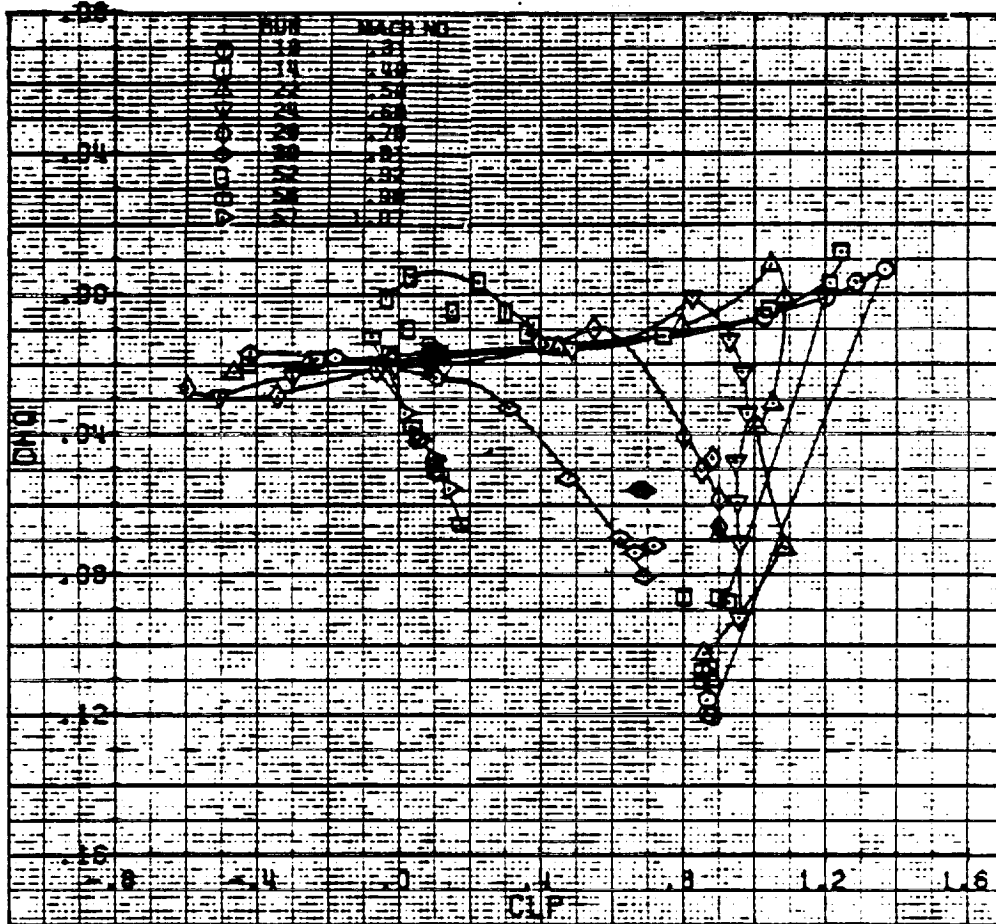
Figure 11.- Aerodynamic characteristics of the SC1095 airfoil.



(b) Drag coefficient versus lift coefficient

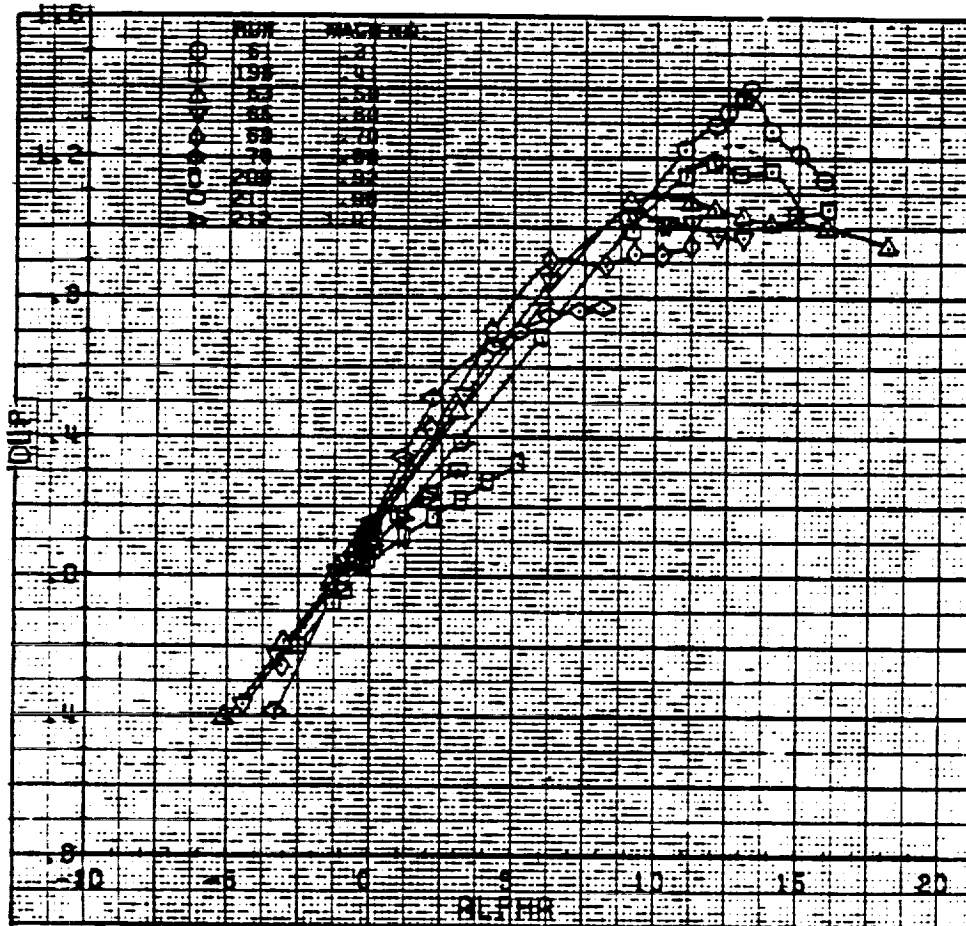
Figure 11.-Continued.

ORIGINAL PAGE IS
OF POOR QUALITY



(c) Pitching moment coefficient versus lift coefficient

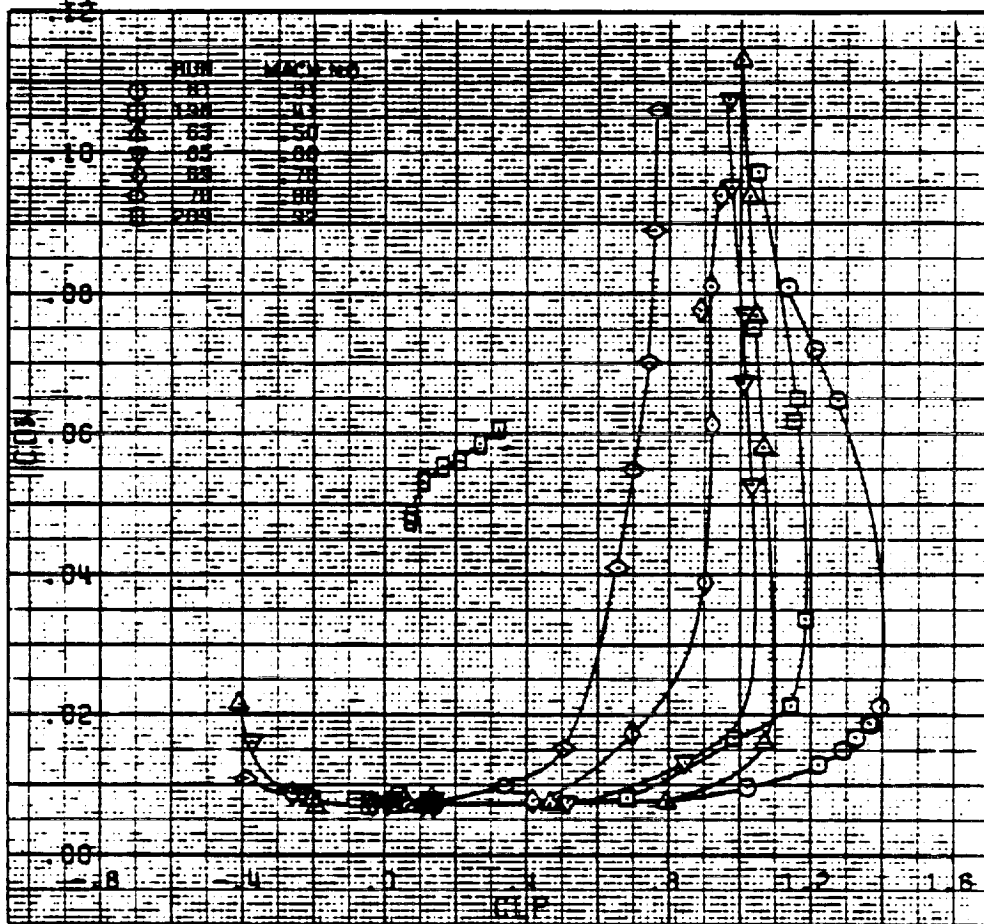
Figure 11.-Concluded.



(a) Lift coefficient versus angle of attack

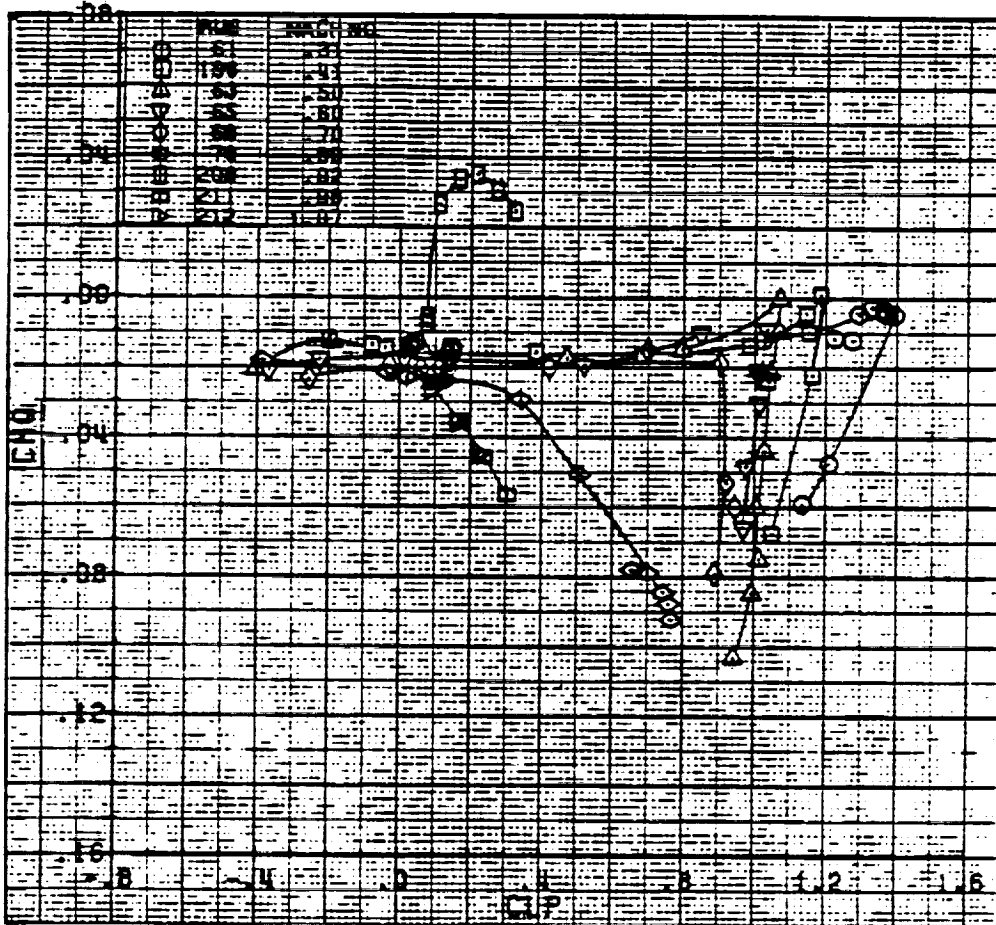
Figure 12.- Aerodynamic characteristics of the SSC-A09 airfoil.

ORIGINAL PAGE IS
OF POOR QUALITY



(b) Drag coefficient versus lift coefficient

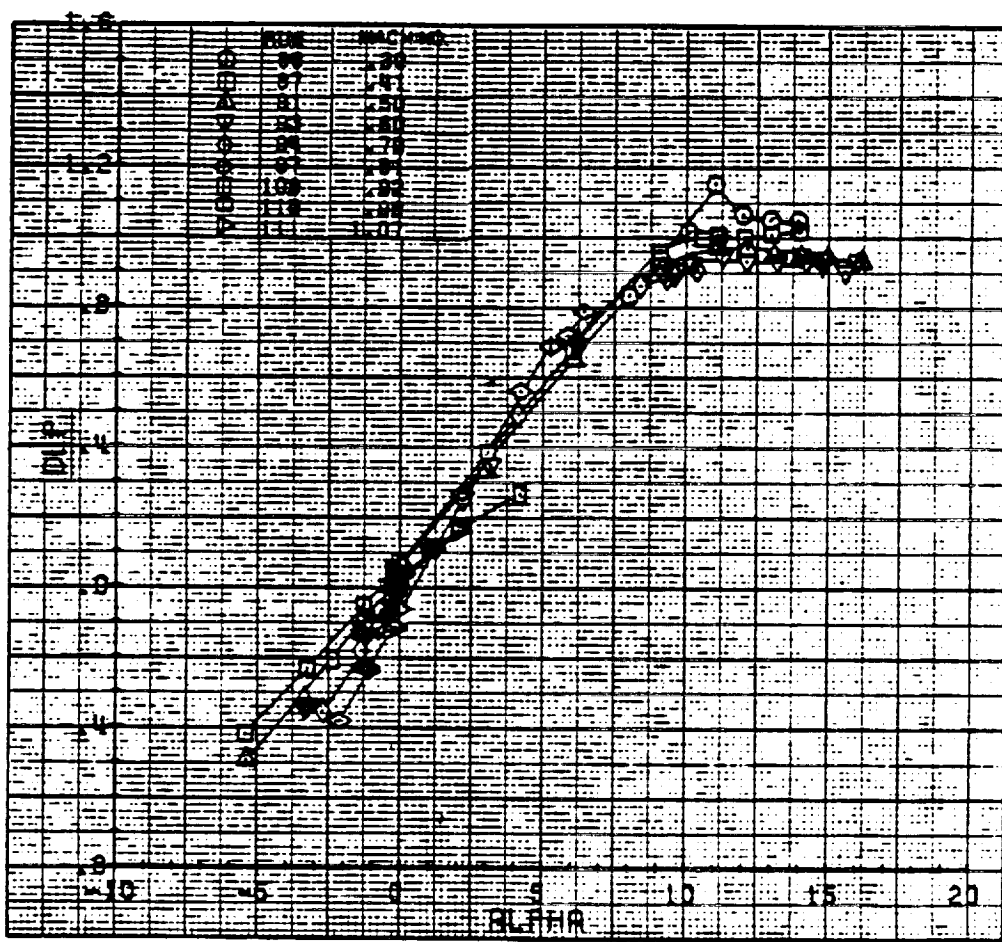
Figure 12.-Continued.



(c) Pitching moment coefficient versus lift coefficient

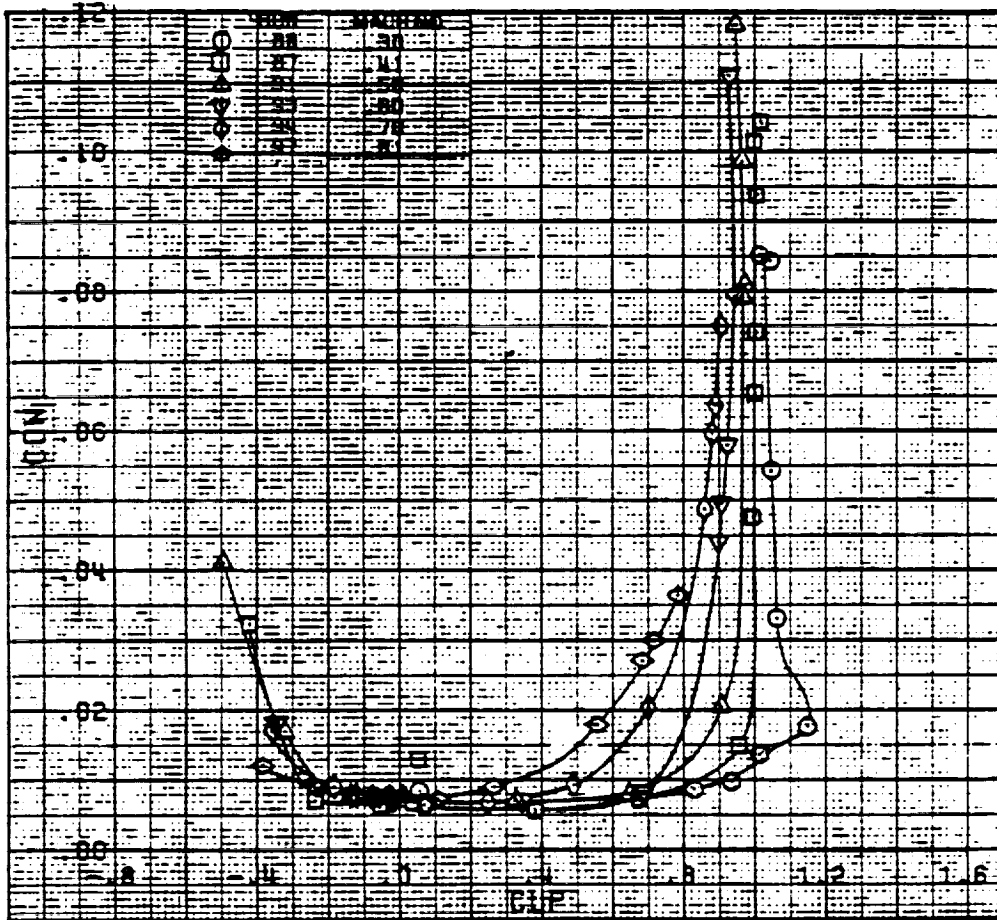
Figure 12.-Concluded.

ORIGINAL PAGE IS
 OF POOR QUALITY



(a) Lift coefficient versus angle of attack

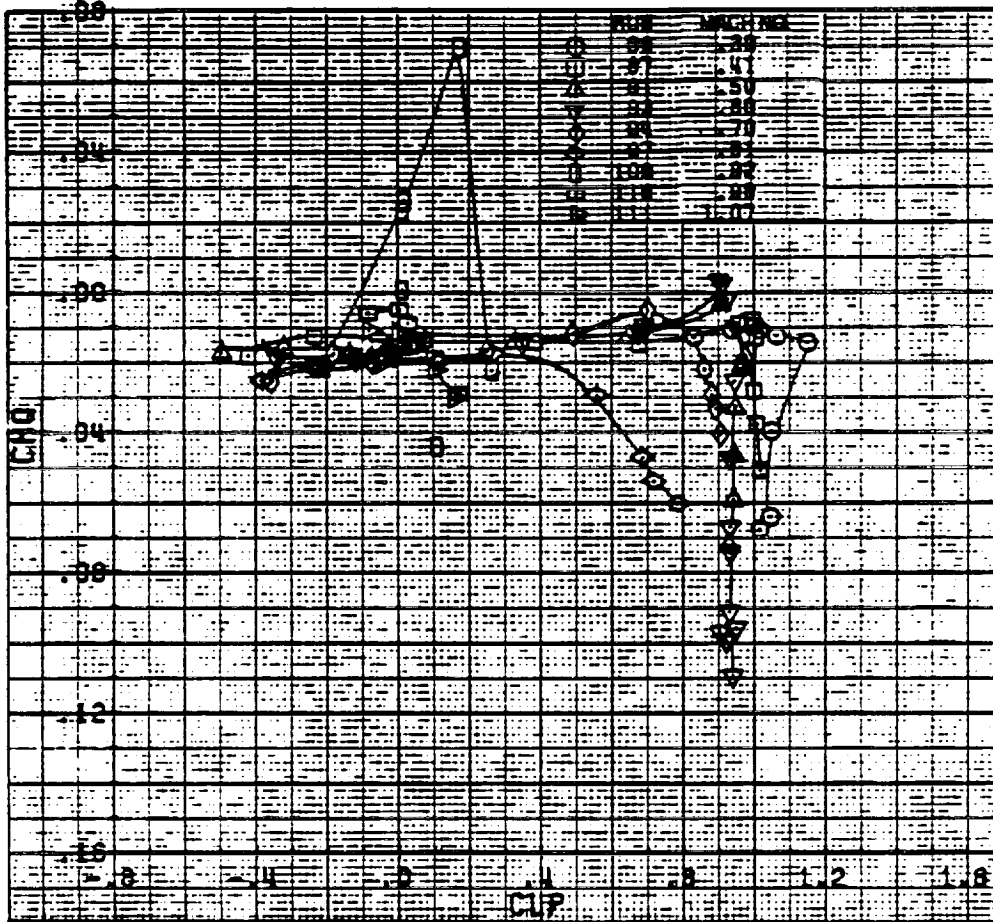
Figure 13. - Aerodynamic characteristics of the SSC-A07 airfoil.



(b) Drag coefficient versus lift coefficient

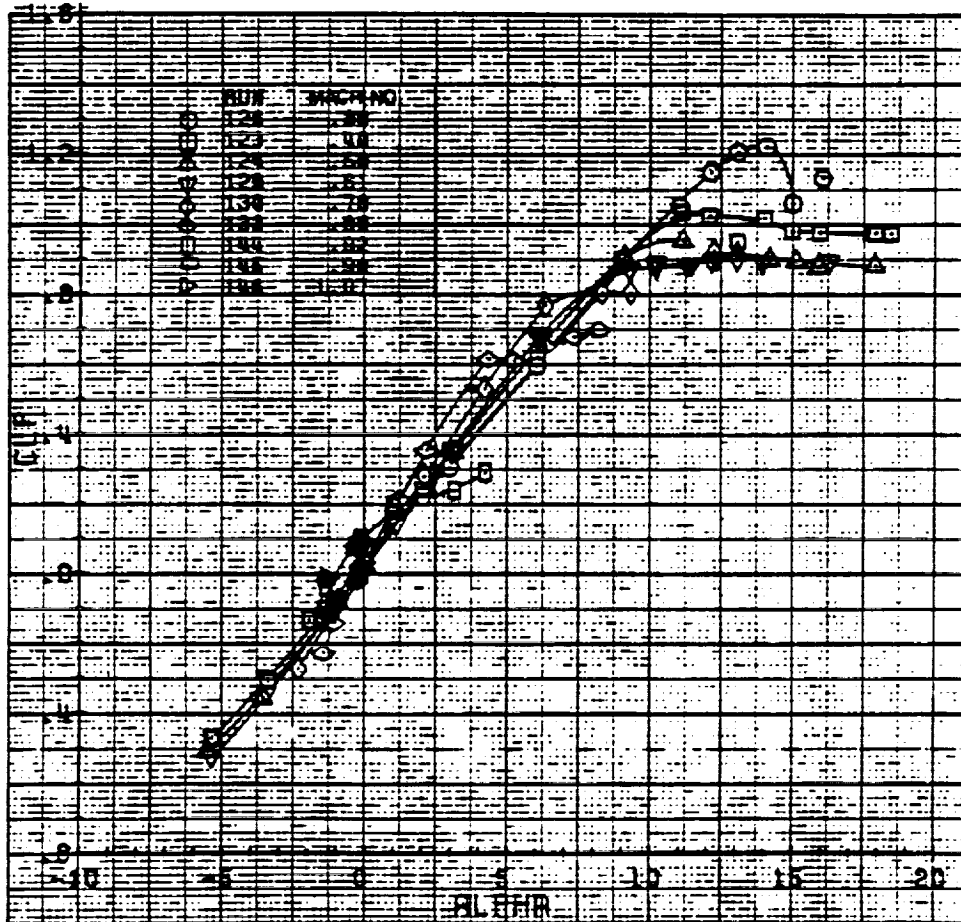
Figure 13.-Continued.

ORIGINAL PAGE IS
 OF POOR QUALITY.



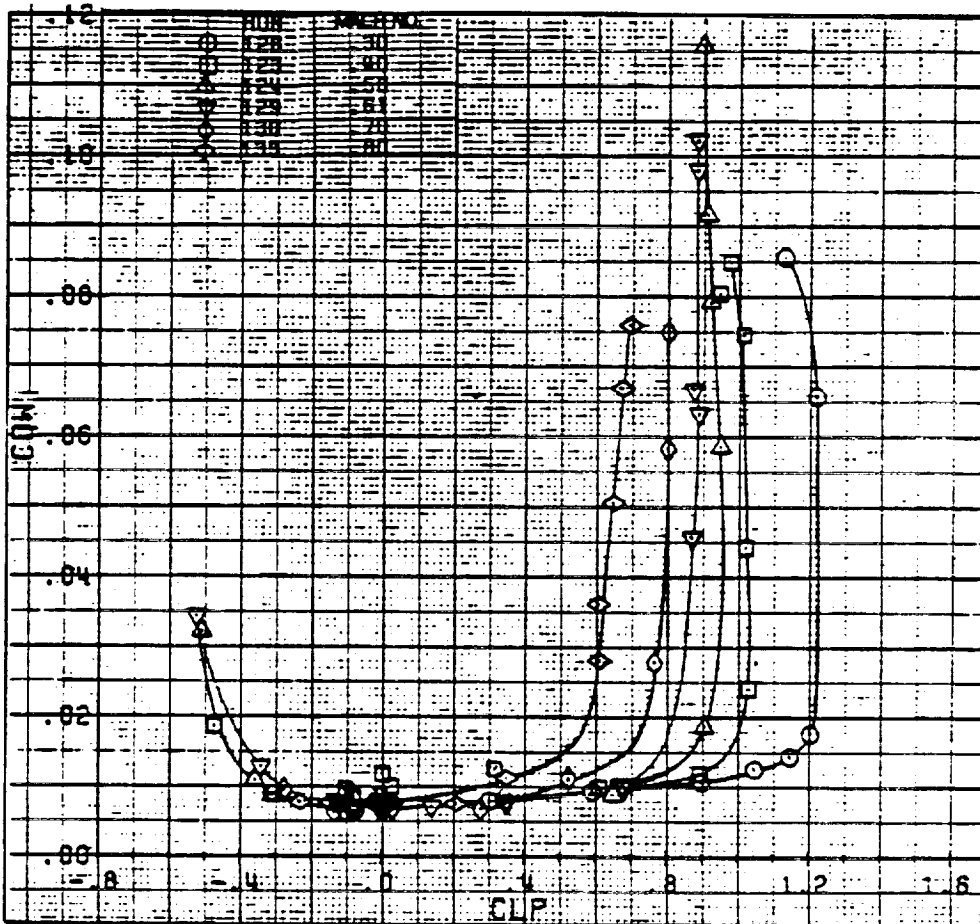
(c) Pitching moment coefficient versus lift coefficient

Figure 13.-Concluded.



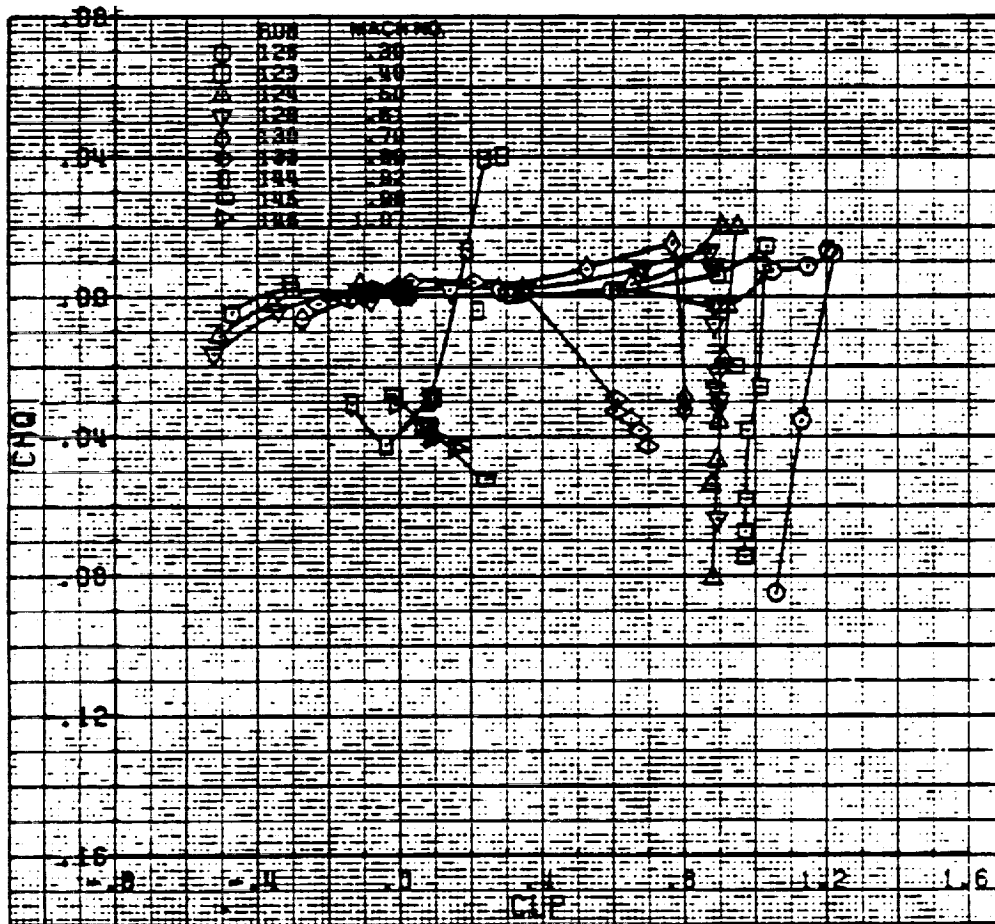
(a) Lift coefficient versus angle of attack

Figure 14.- Aerodynamic characteristics of the SSC-B08 airfoil.



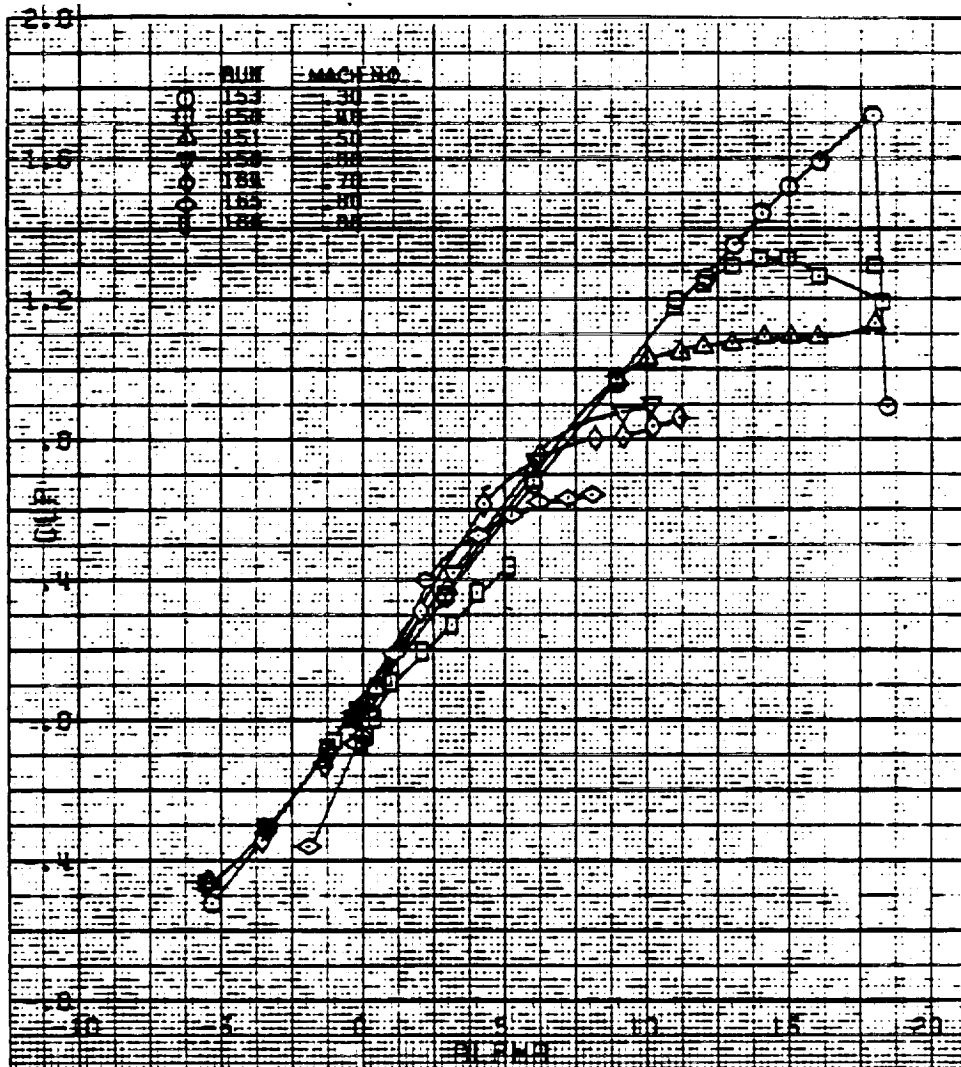
(b) Drag coefficient versus lift coefficient

Figure 14.-Continued.



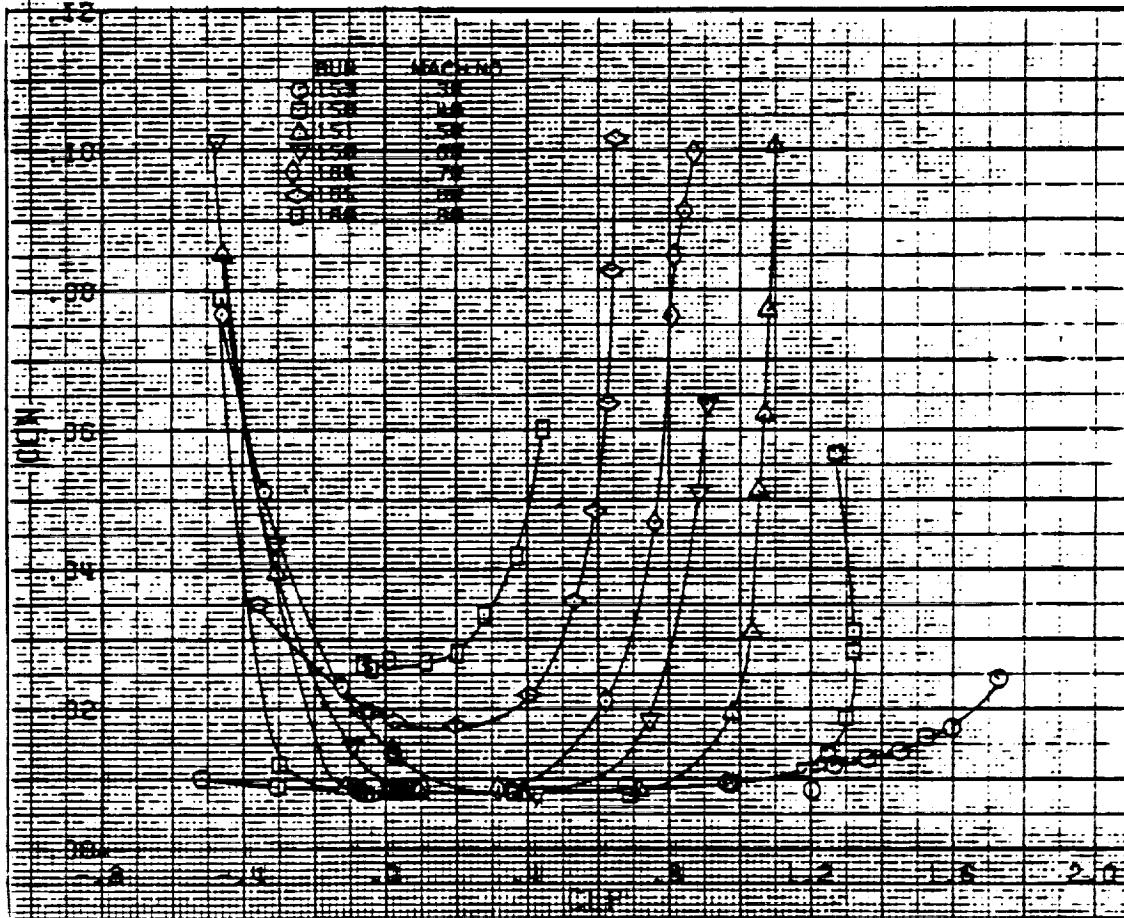
(c) Pitching moment coefficient versus lift coefficient

Figure 14.-Concluded.



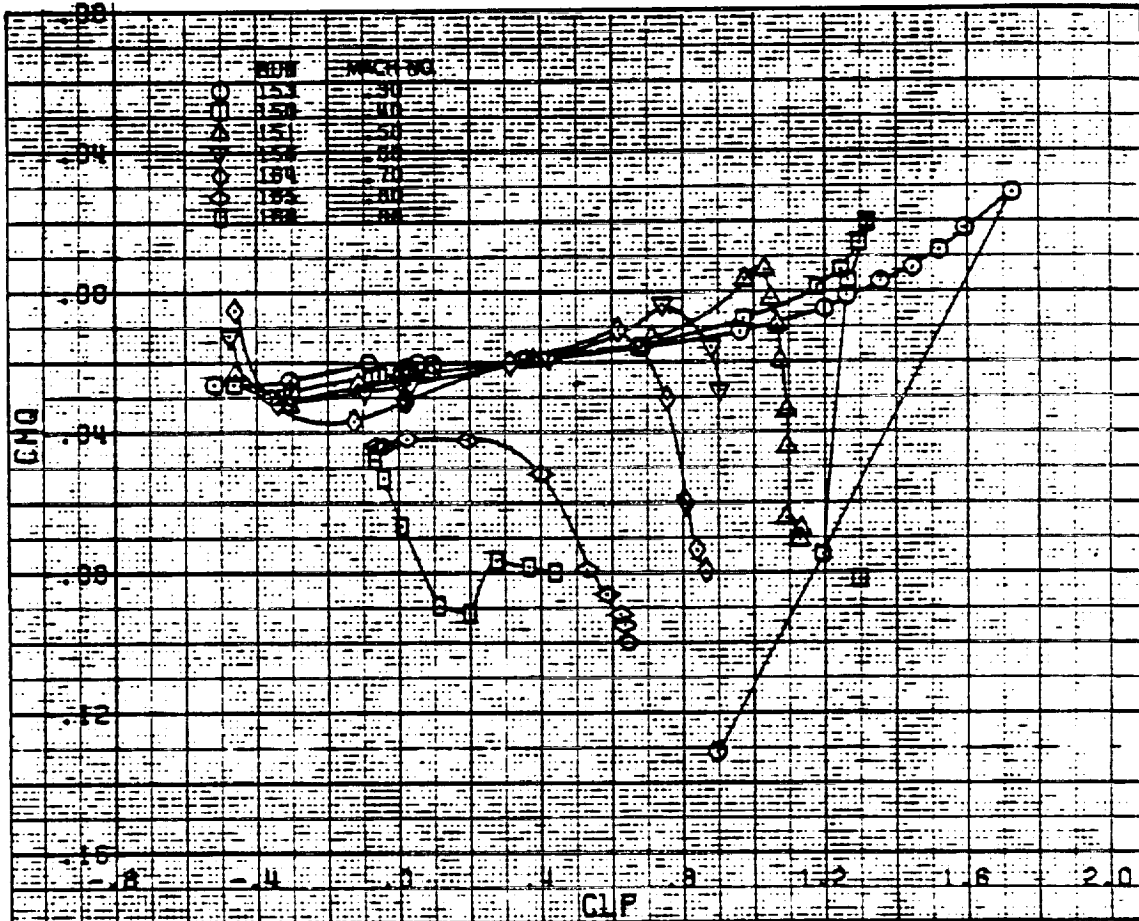
(a) Lift coefficient versus angle of attack

Figure 15. - Aerodynamic characteristics of the SC1094 R8 airfoil.



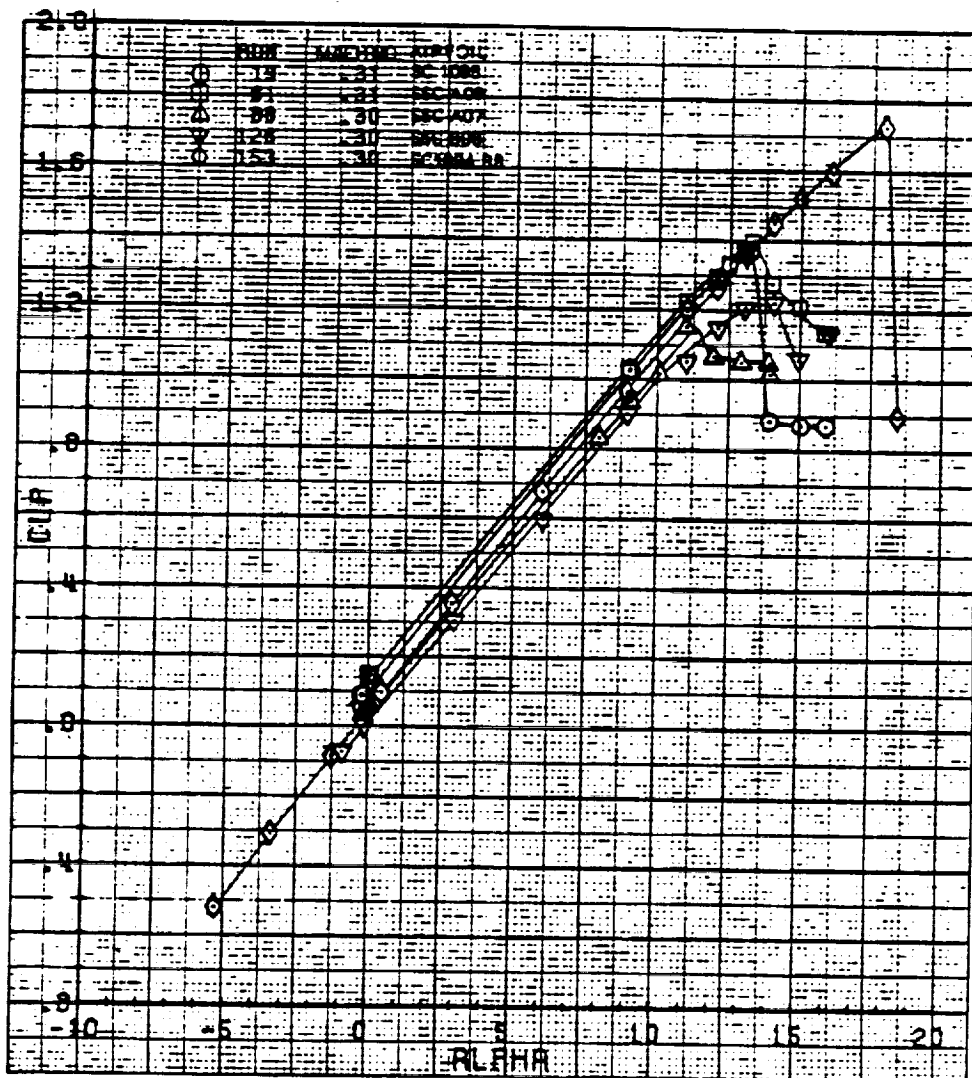
(b) Drag coefficient versus lift coefficient

Figure 15-Continued.



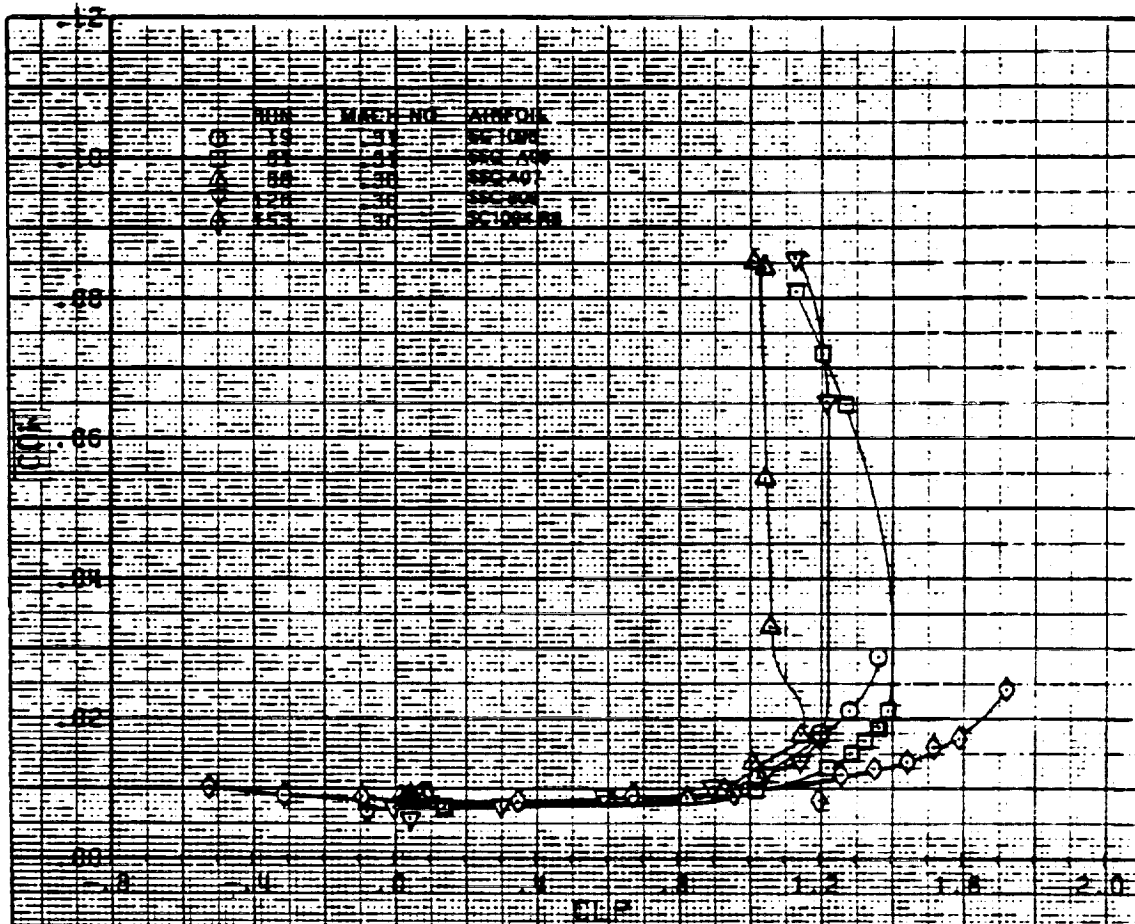
(c) Pitching moment coefficient versus lift coefficient

Figure 15.-Concluded.



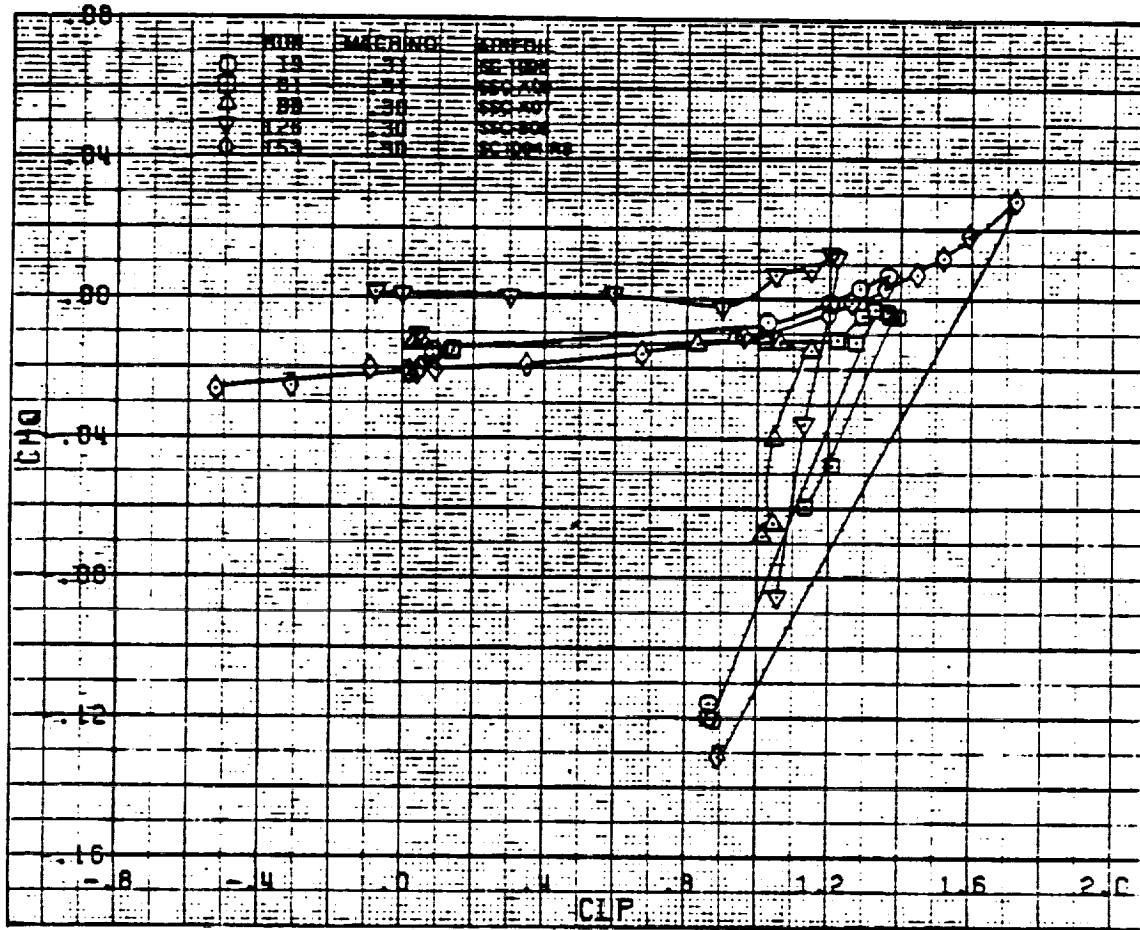
(a) Lift coefficient versus angle of attack

Figure 16.- Aerodynamic characteristics at a Mach number of 0.30.



(b) Drag coefficient versus lift coefficient

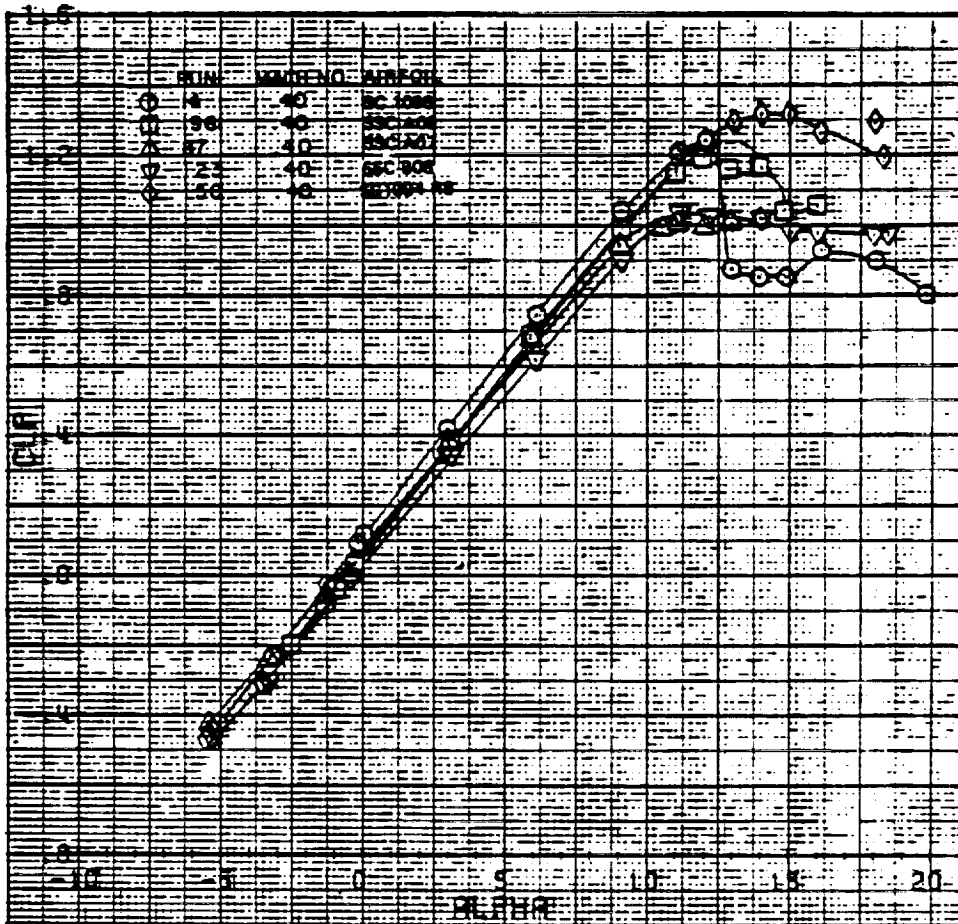
Figure 16.-Continued.



(c) Pitching moment coefficient versus lift coefficient

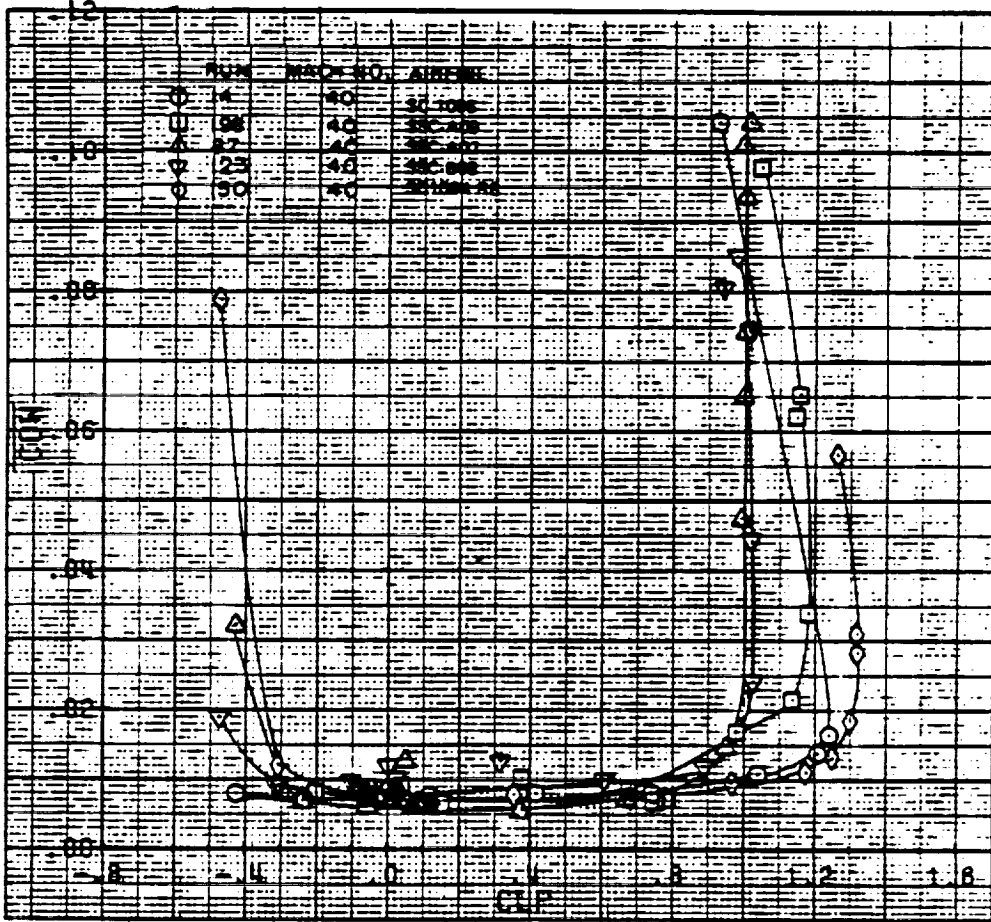
Figure 16.-Concluded.

TERMINAL PAGE IS
OF POOR QUALITY



(a) Lift coefficient versus angle of attack

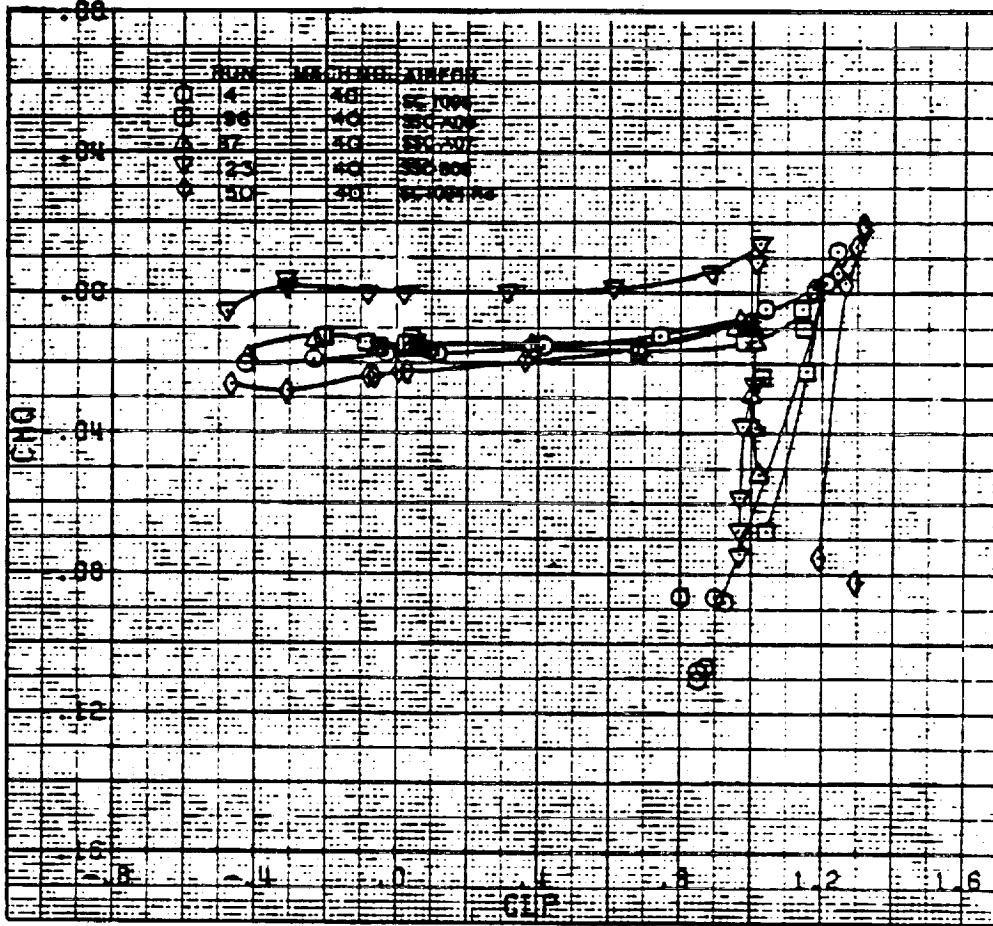
Figure 17.- Aerodynamic characteristics at a Mach number of 0.40.



(b) Drag coefficient versus lift coefficient

Figure 17.-Continued.

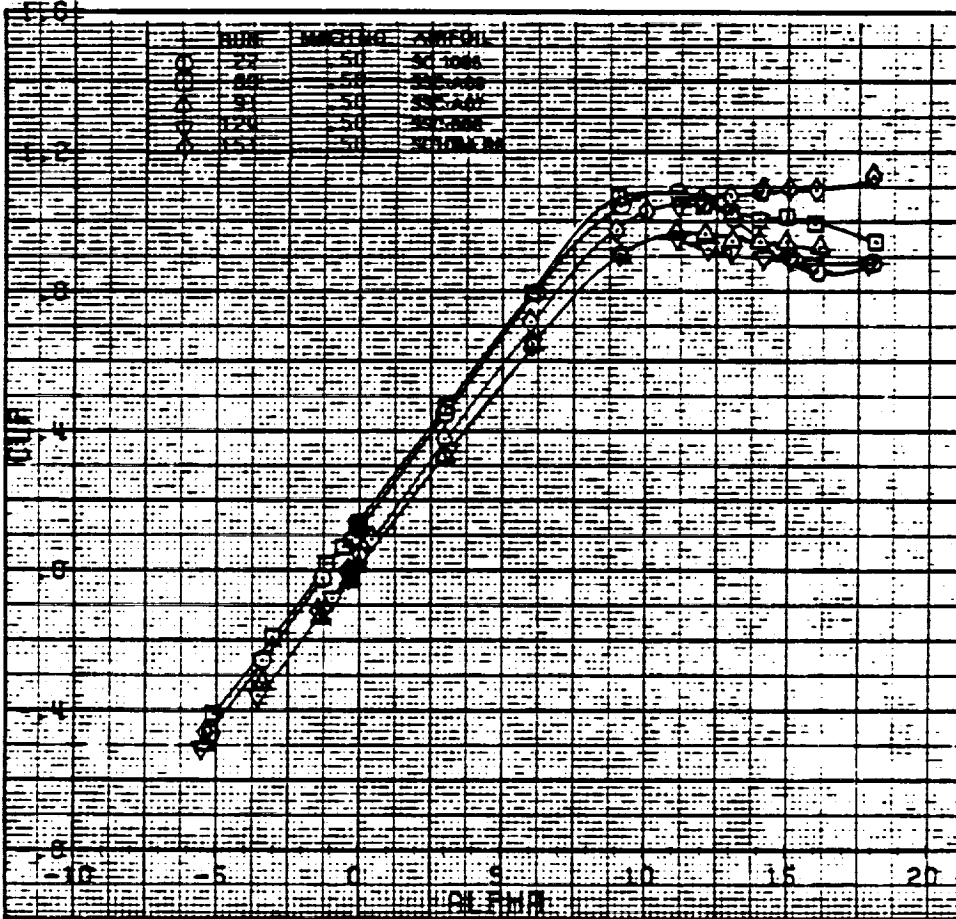
ORIGINAL PAGE IS
OF POOR QUALITY



(c) Pitching moment coefficient versus lift coefficient

Figure 17.-Concluded.

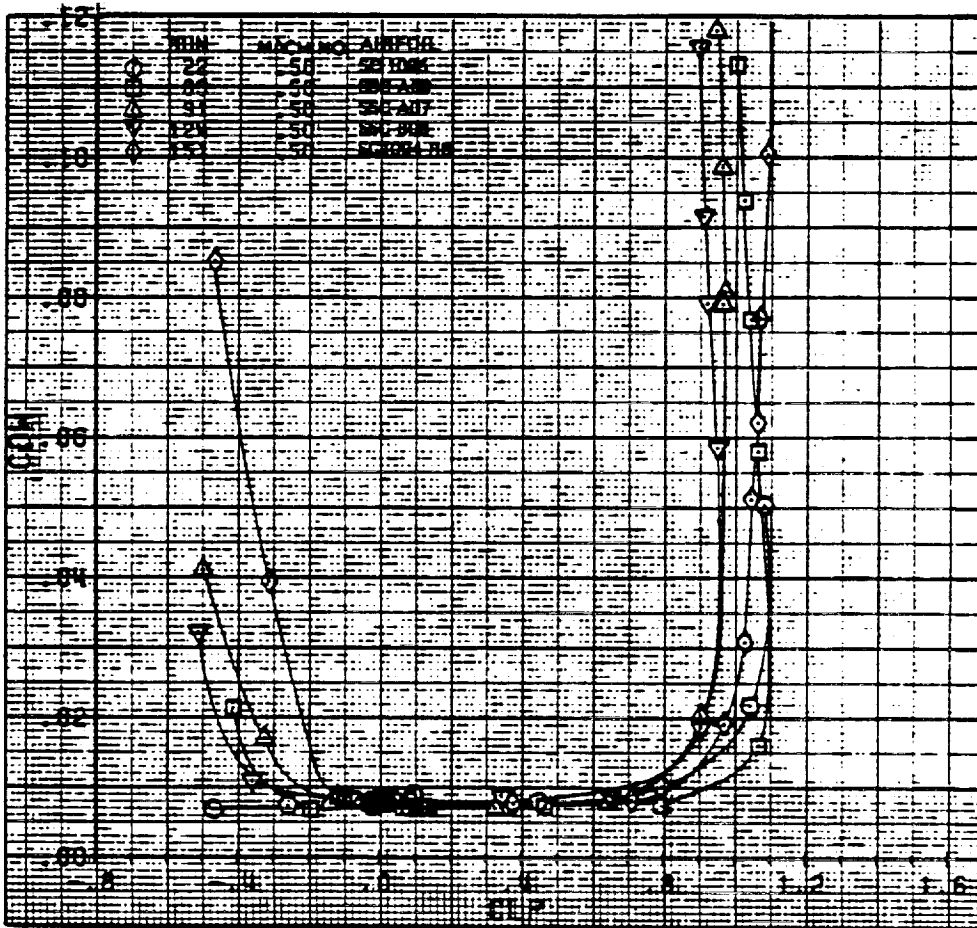
ORIGINAL PAGE IS
 OF POOR QUALITY



(a) Lift coefficient versus angle of attack

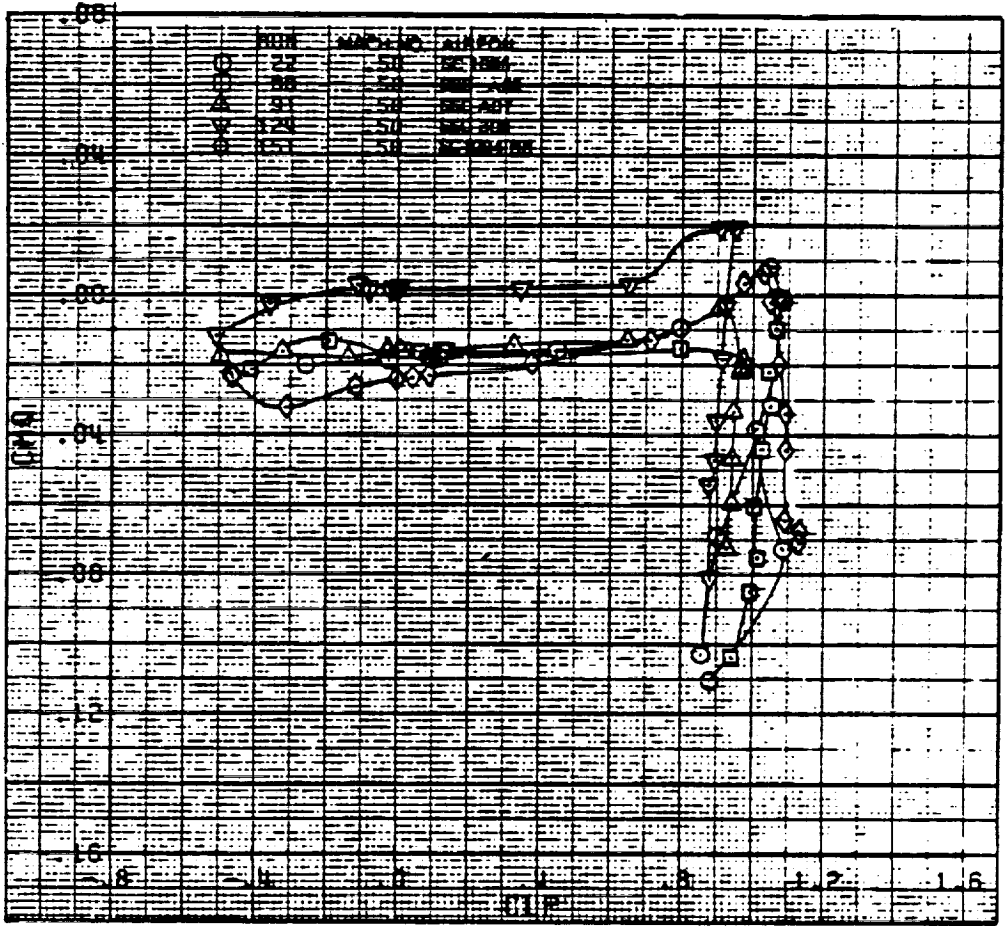
Figure 18.— Aerodynamic characteristics at a Mach number of 0.50.

ORIGINAL PAGE IS
OF POOR QUALITY



(b) Drag coefficient versus lift coefficient

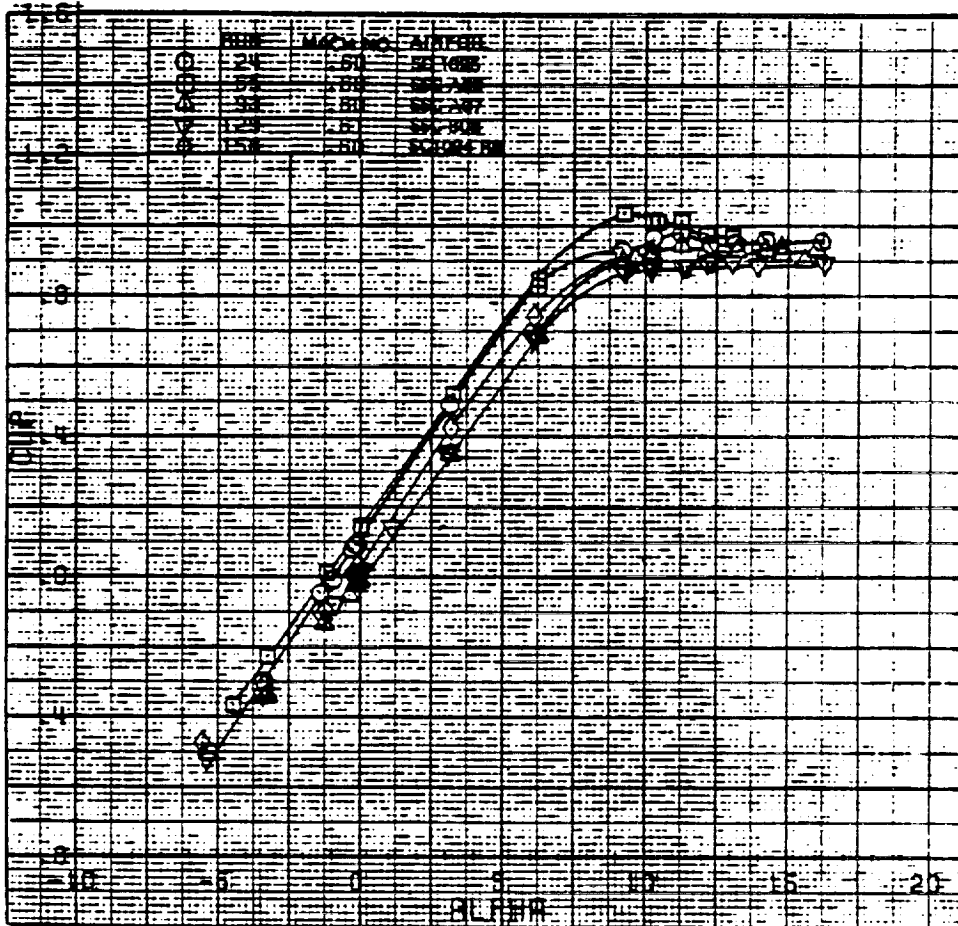
Figure 18.-Continued.



(c) Pitching moment coefficient versus lift coefficient

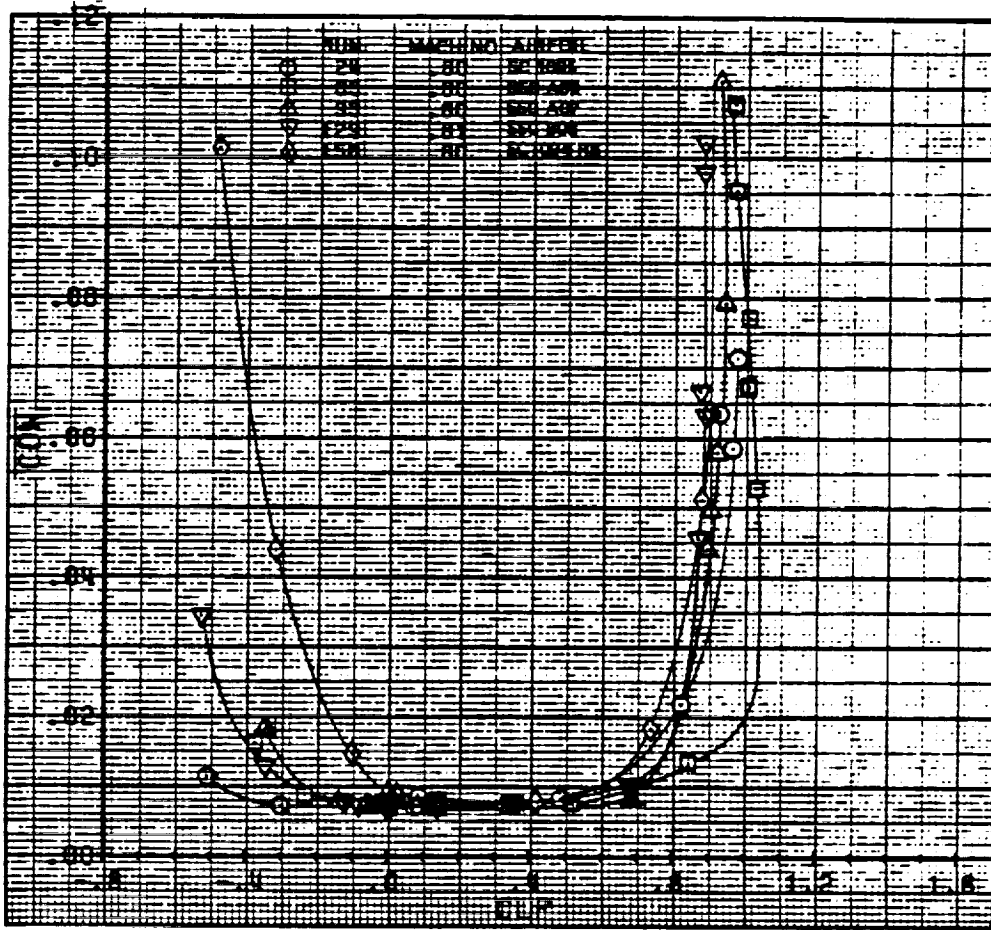
Figure 18.—Concluded.

ORIGINAL PAGE IS
OF POOR QUALITY



(a) Lift coefficient versus angle of attack

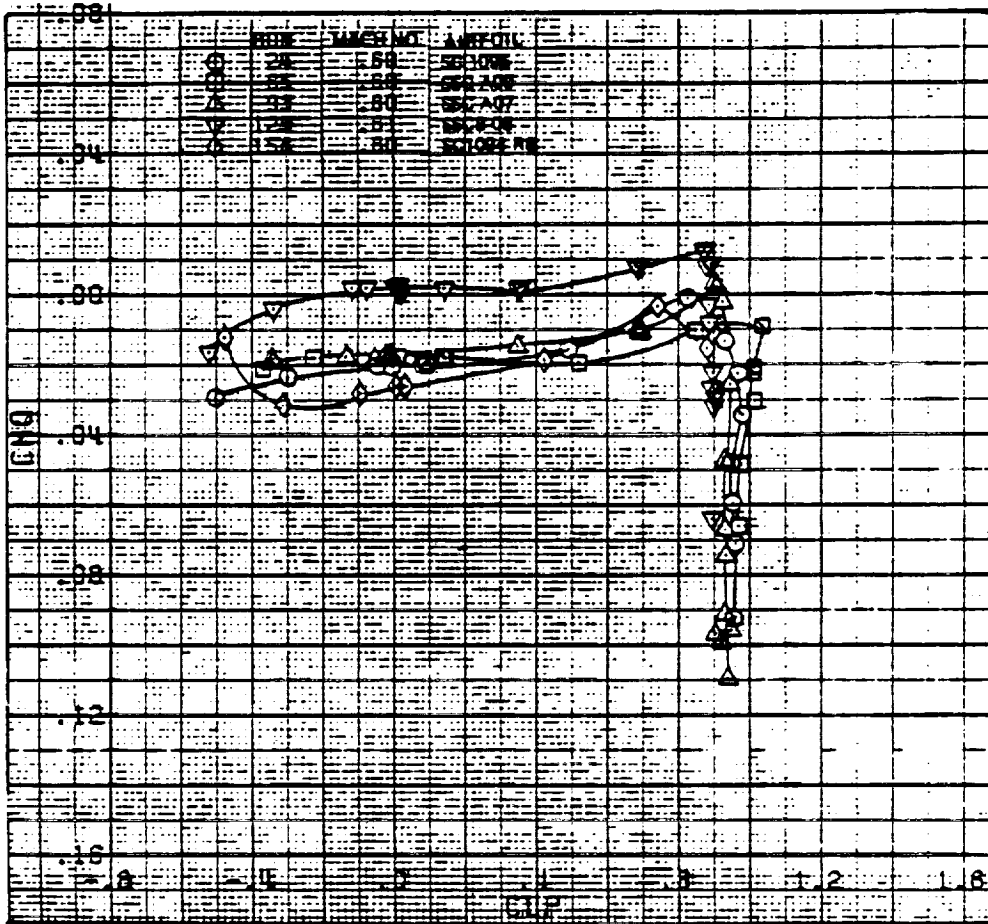
Figure 19.— Aerodynamic characteristics at a Mach number of 0.60.



(b) Drag coefficient versus lift coefficient

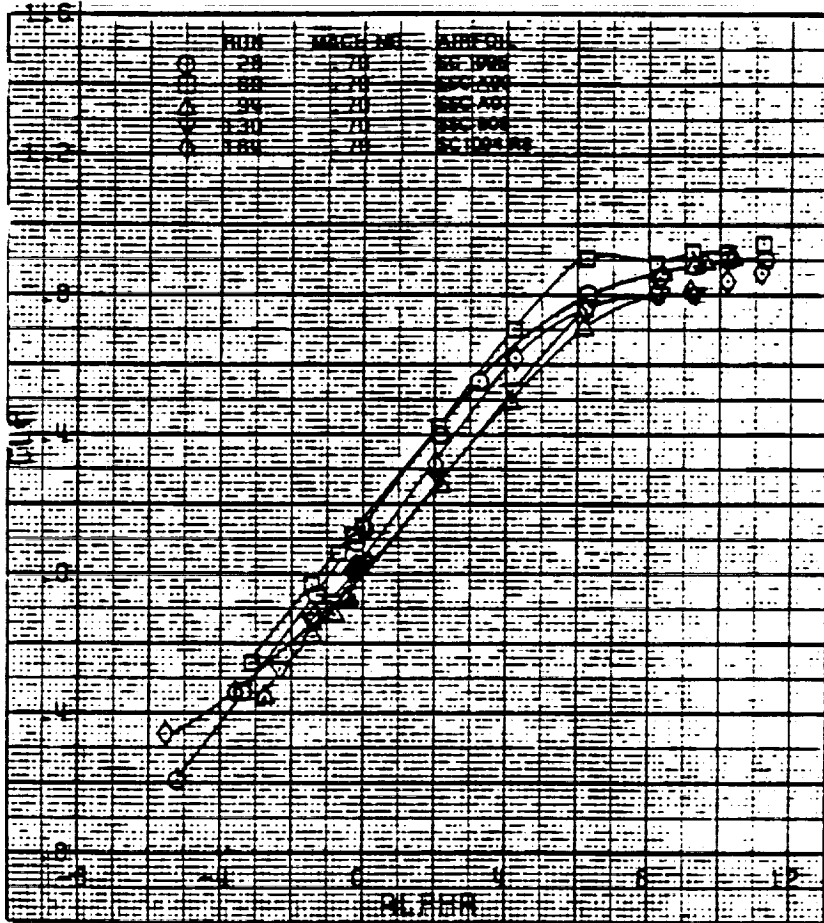
Figure 19.-Continued.

ORIGINAL PAGE IS
OF POOR QUALITY



(c) Pitching moment coefficient versus lift coefficient.

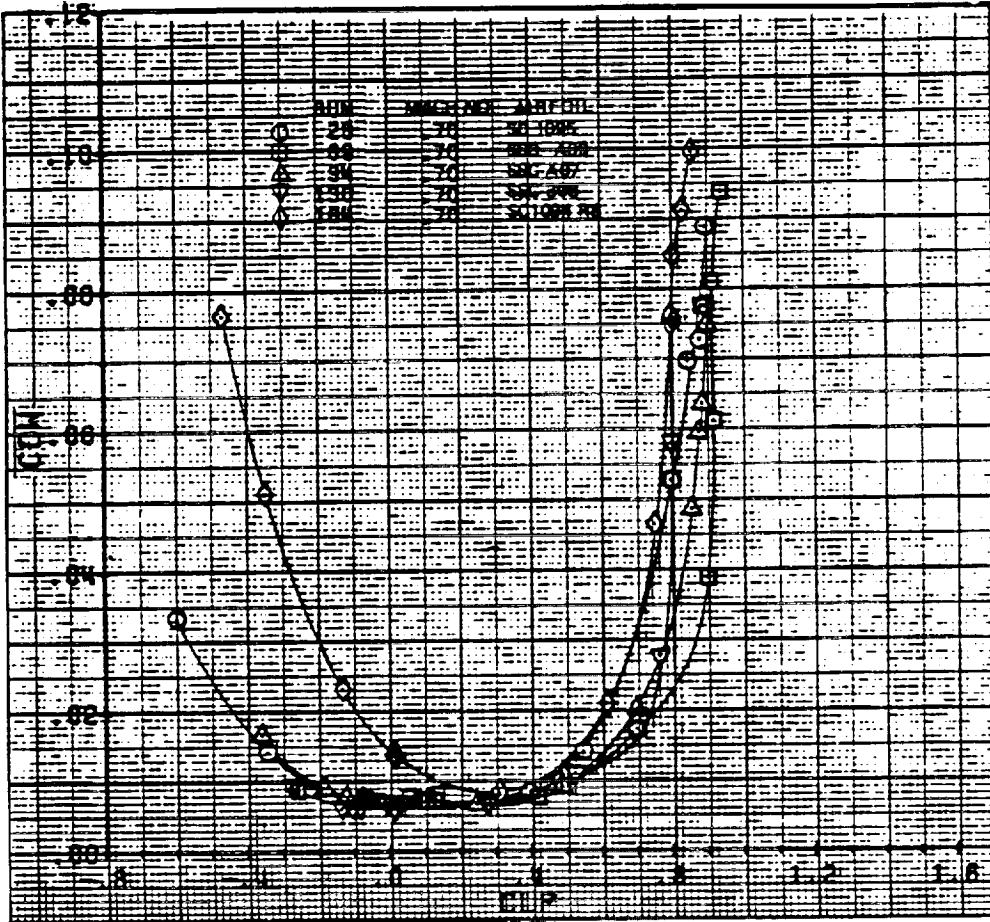
Figure 19.-Concluded.



(a) Lift coefficient versus angle of attack

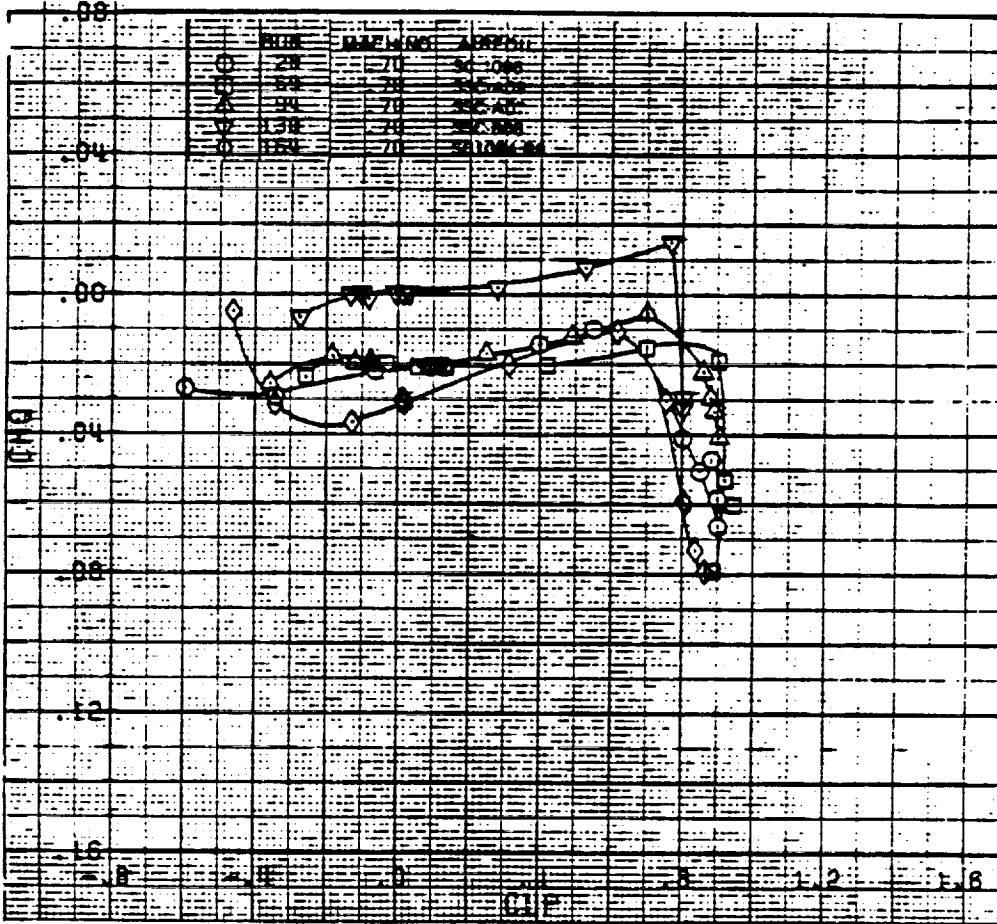
Figure 20.—Aerodynamic characteristics at a Mach number of 0.70.

ORIGINAL RATE IS
OF POOR QUALITY



(b) Drag coefficient versus lift coefficient

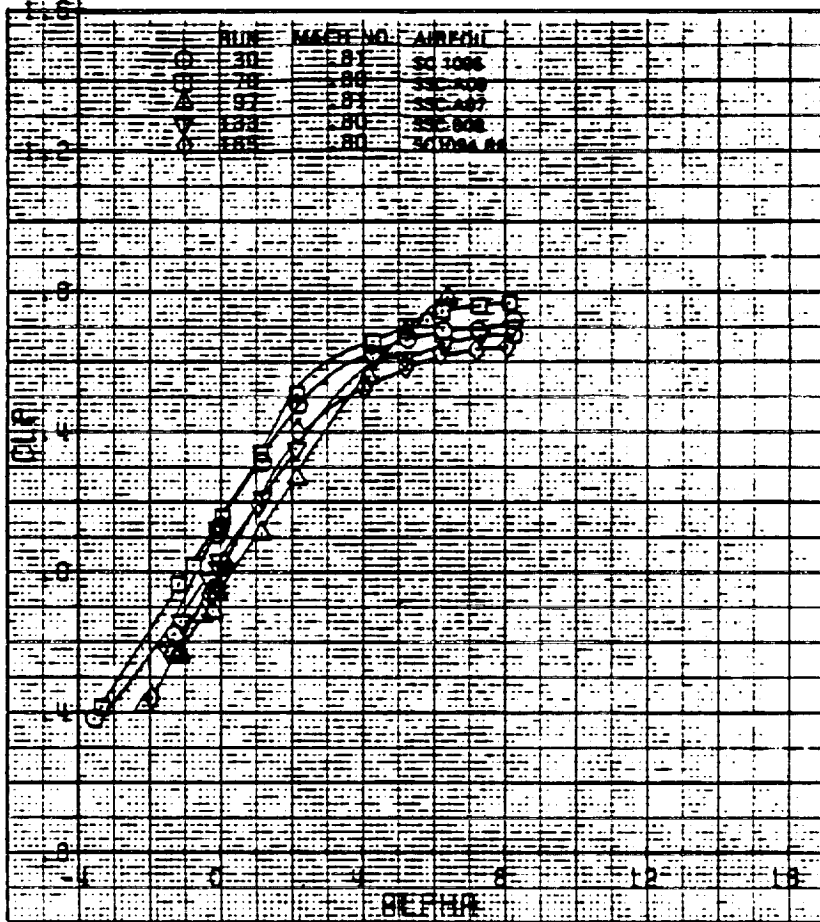
Figure 20.-Continued.



(c) Pitching moment coefficient versus lift coefficient

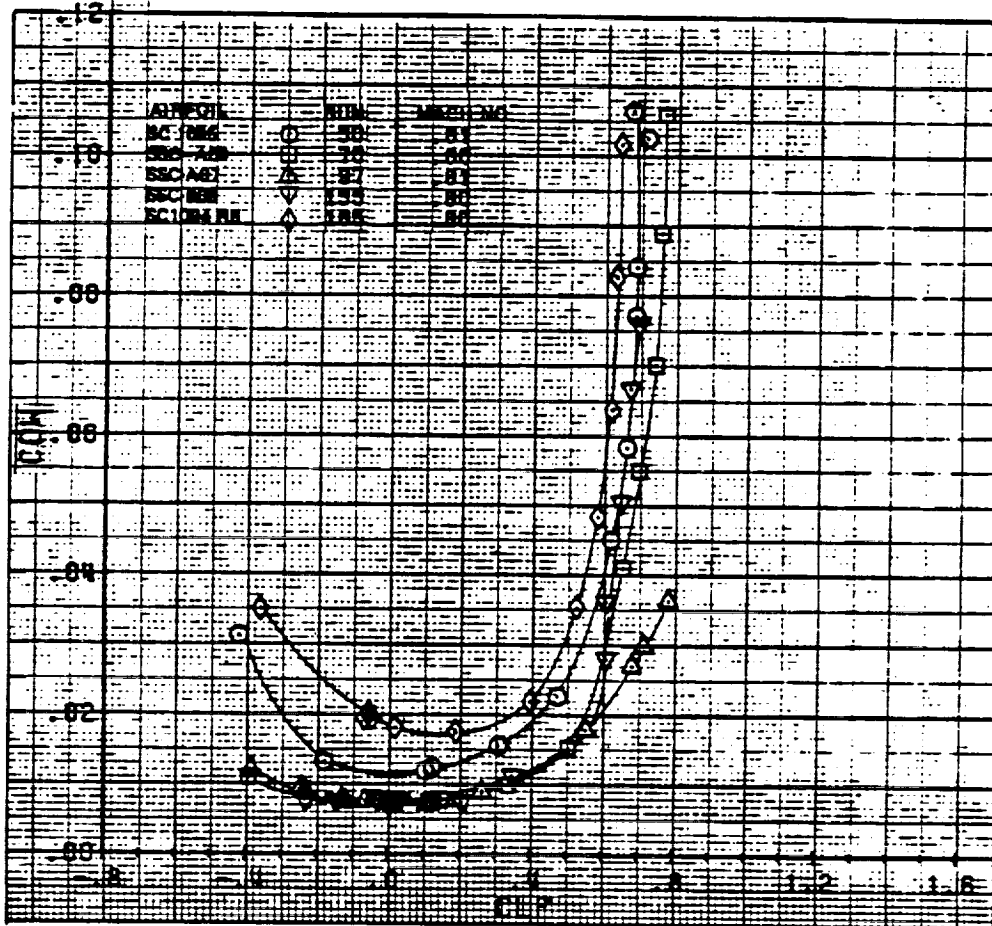
Figure 20.-Concluded.

ORIGINAL PAGE IS
 OF POOR QUALITY



(a) Lift coefficient versus angle of attack

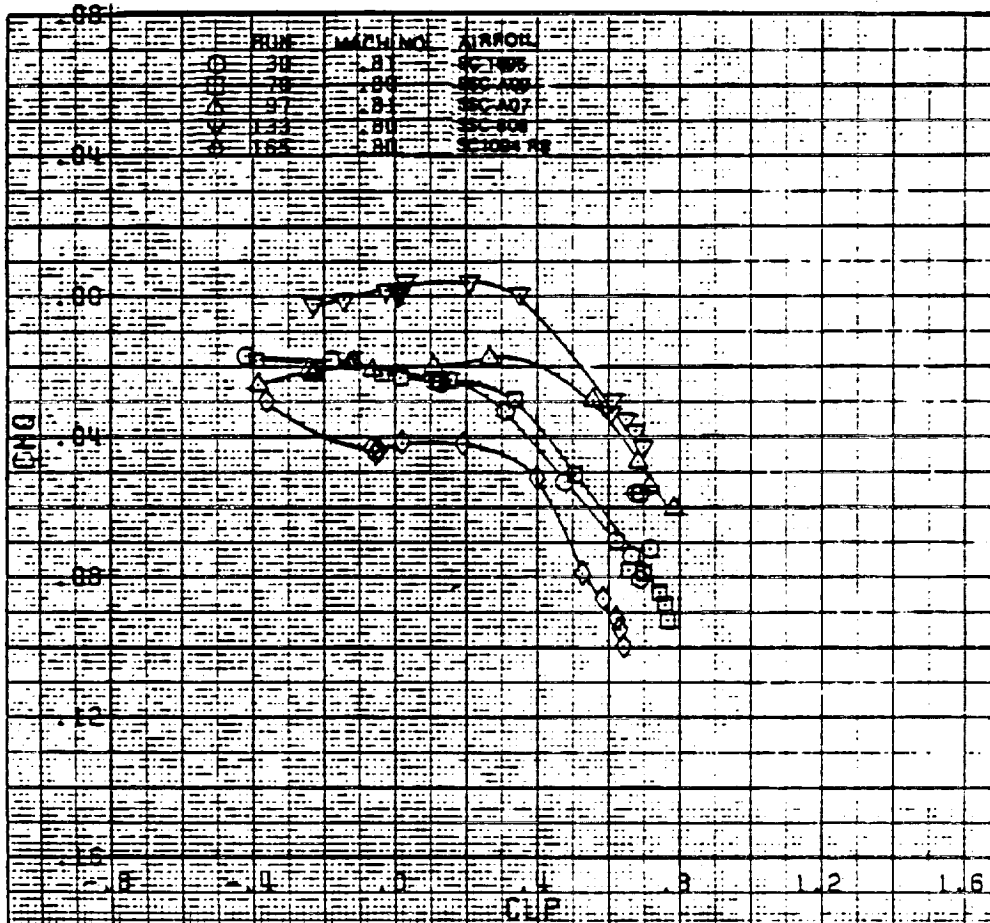
Figure 21.—Aerodynamic characteristics at a Mach number of 0.20.



(b) Drag coefficient versus lift coefficient

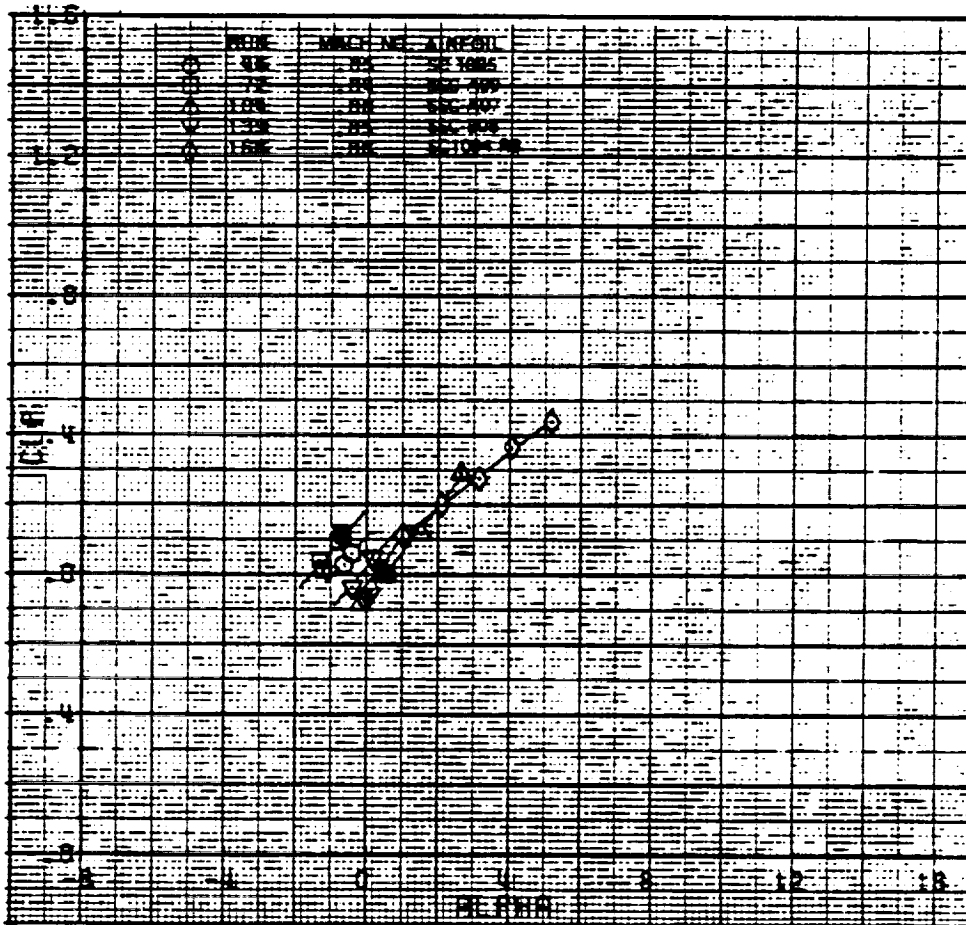
Figure 21.-Continued.

ORIGINAL PAGE IS
OF POOR QUALITY



(c) . Pitching moment coefficient versus lift coefficient

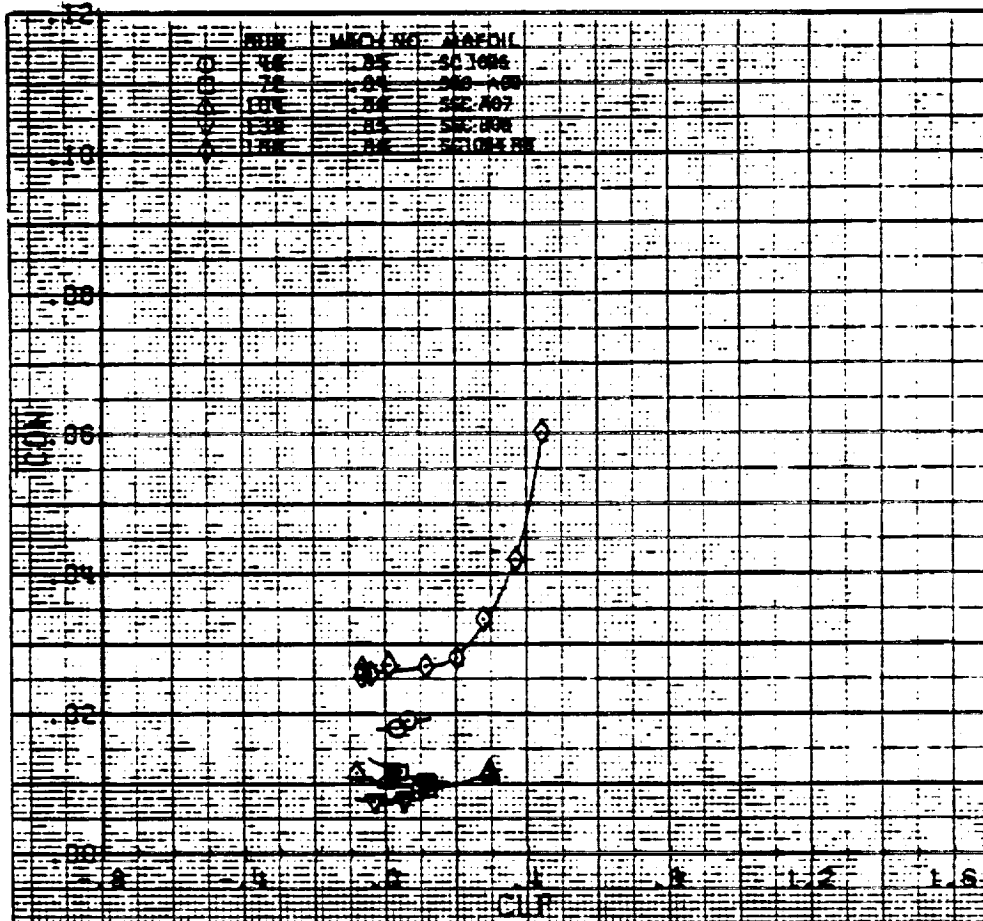
Figure 21.-Concluded.



(a) Lift coefficient versus angle of attack

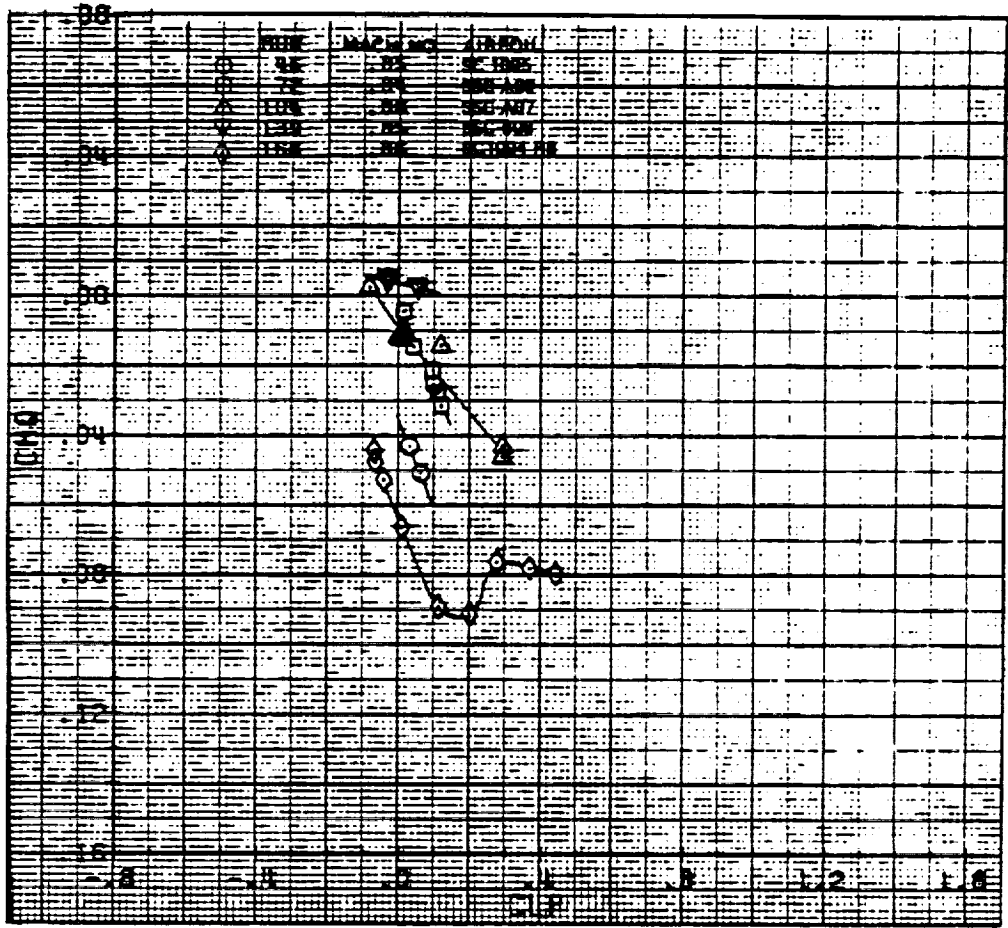
Figure 22.—Aerodynamic characteristics at a Mach number of 0.85.

ORIGINAL PAGE IS
OF POOR QUALITY.



(b) Drag coefficient versus lift coefficient

Figure 22.-Continued.



(c) Pitching moment coefficient versus lift coefficient

Figure 22.-Concluded.

ORIGINAL PAGE IS
OF POOR QUALITY

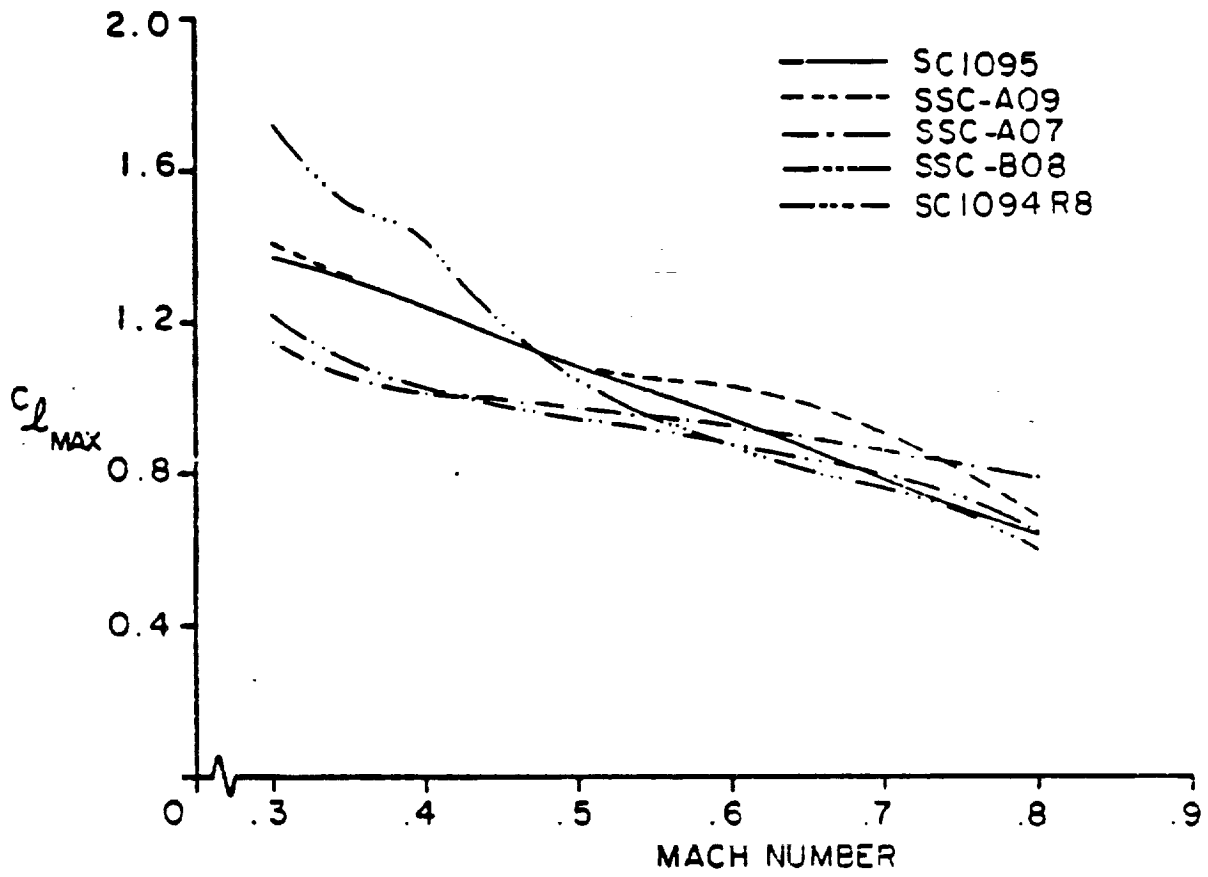


Figure 23.— Variation in maximum lift coefficient versus Mach number.

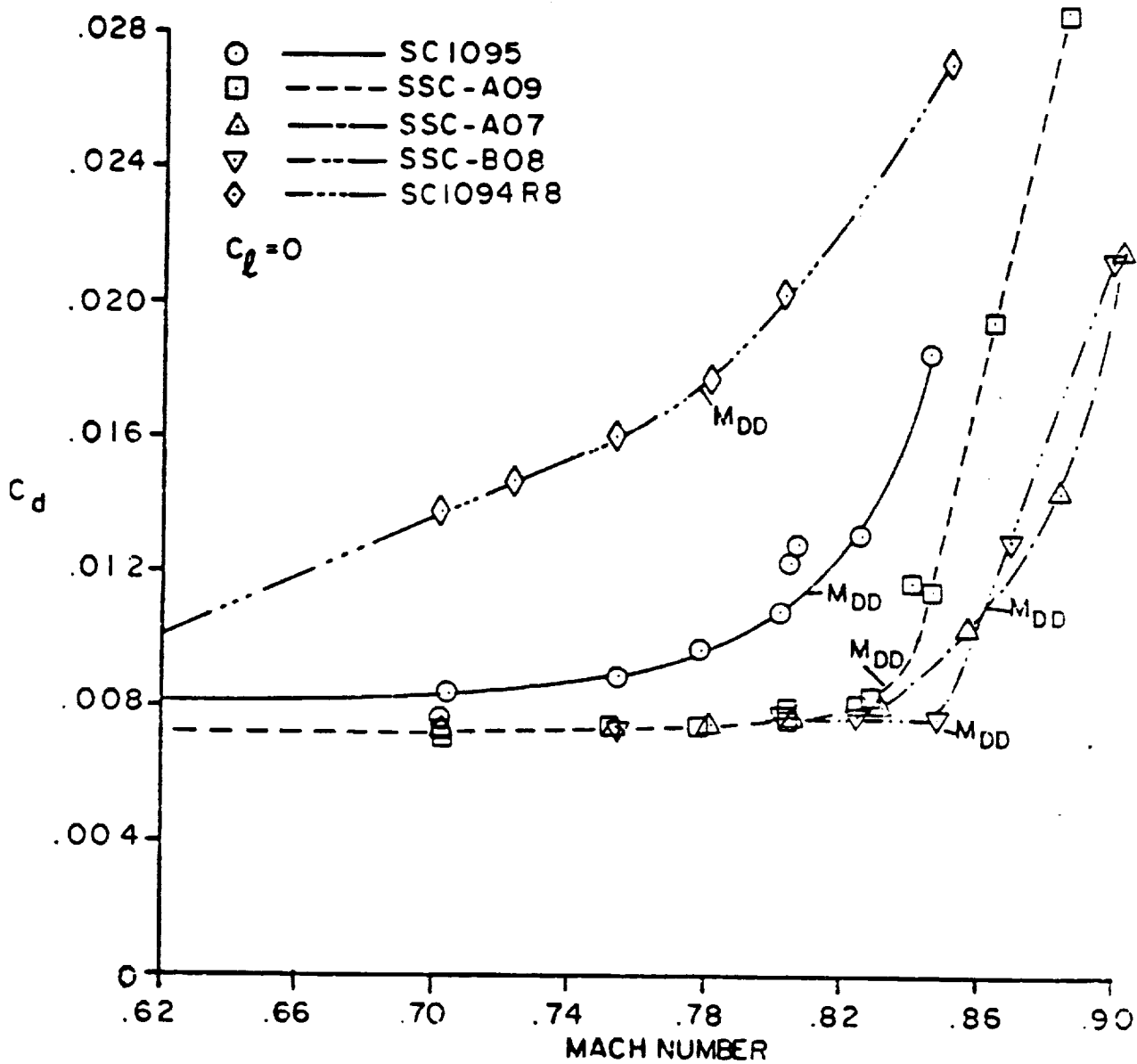


Figure 24.— Variation in drag coefficient at zero lift versus Mach number.

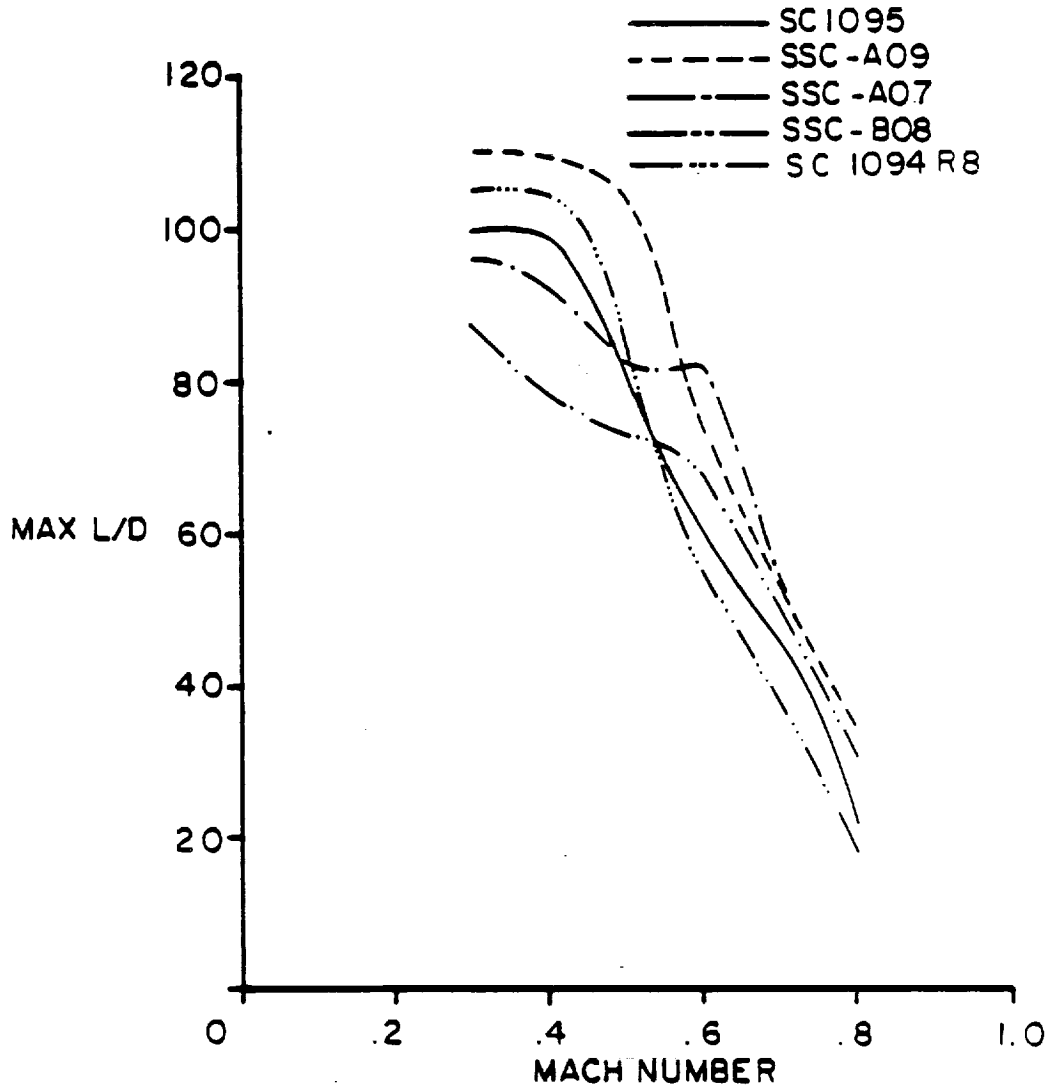


Figure 25.— Maximum L/D versus Mach number.

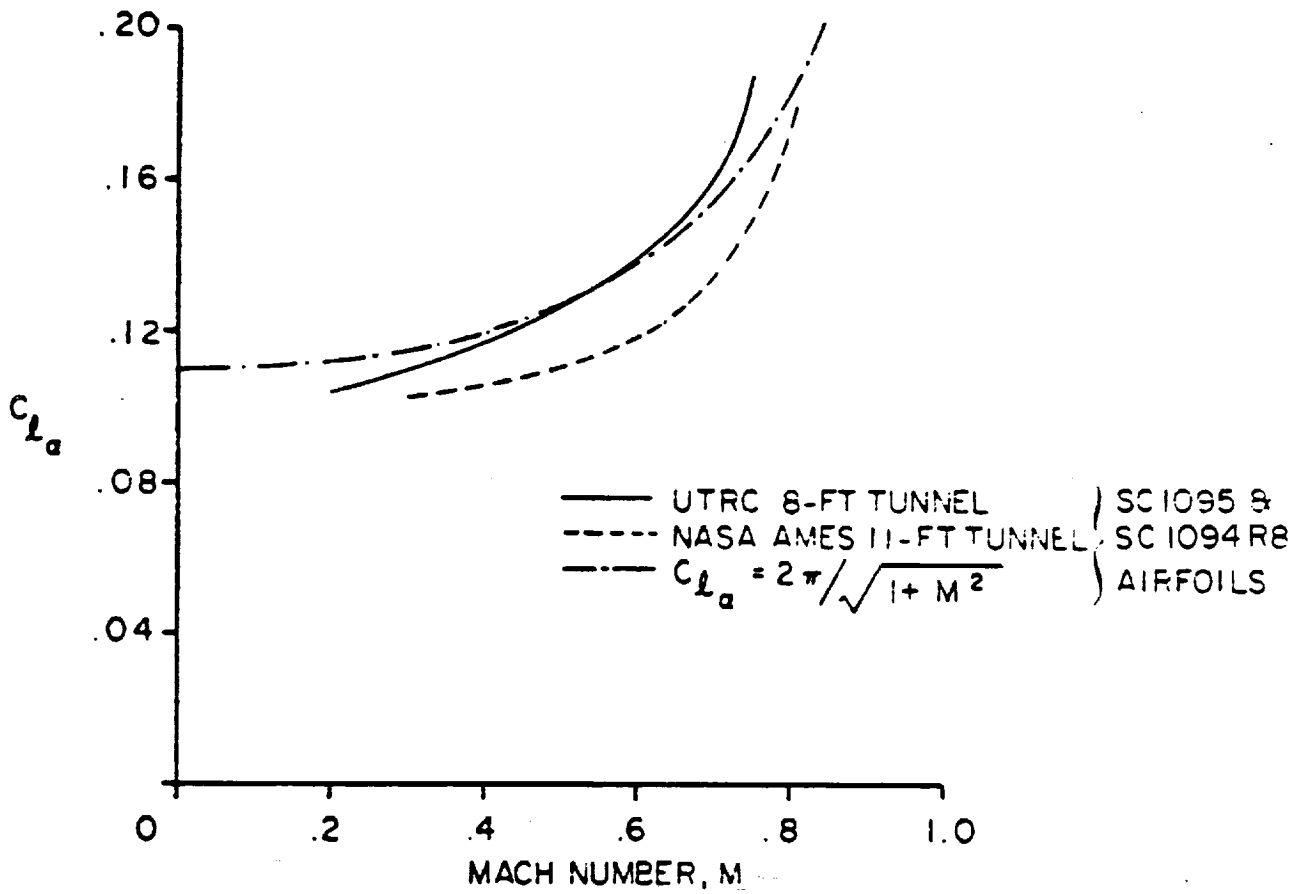
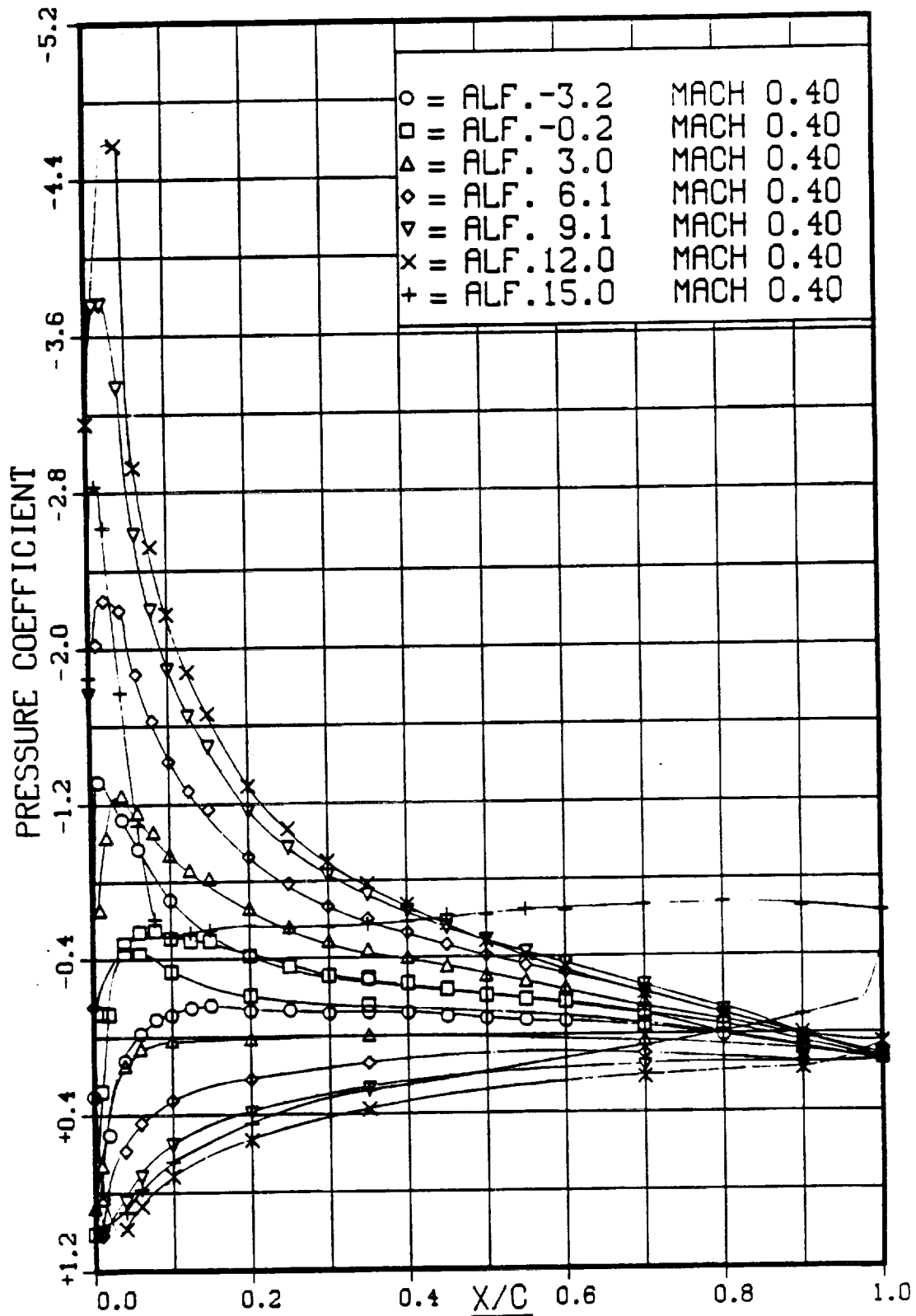
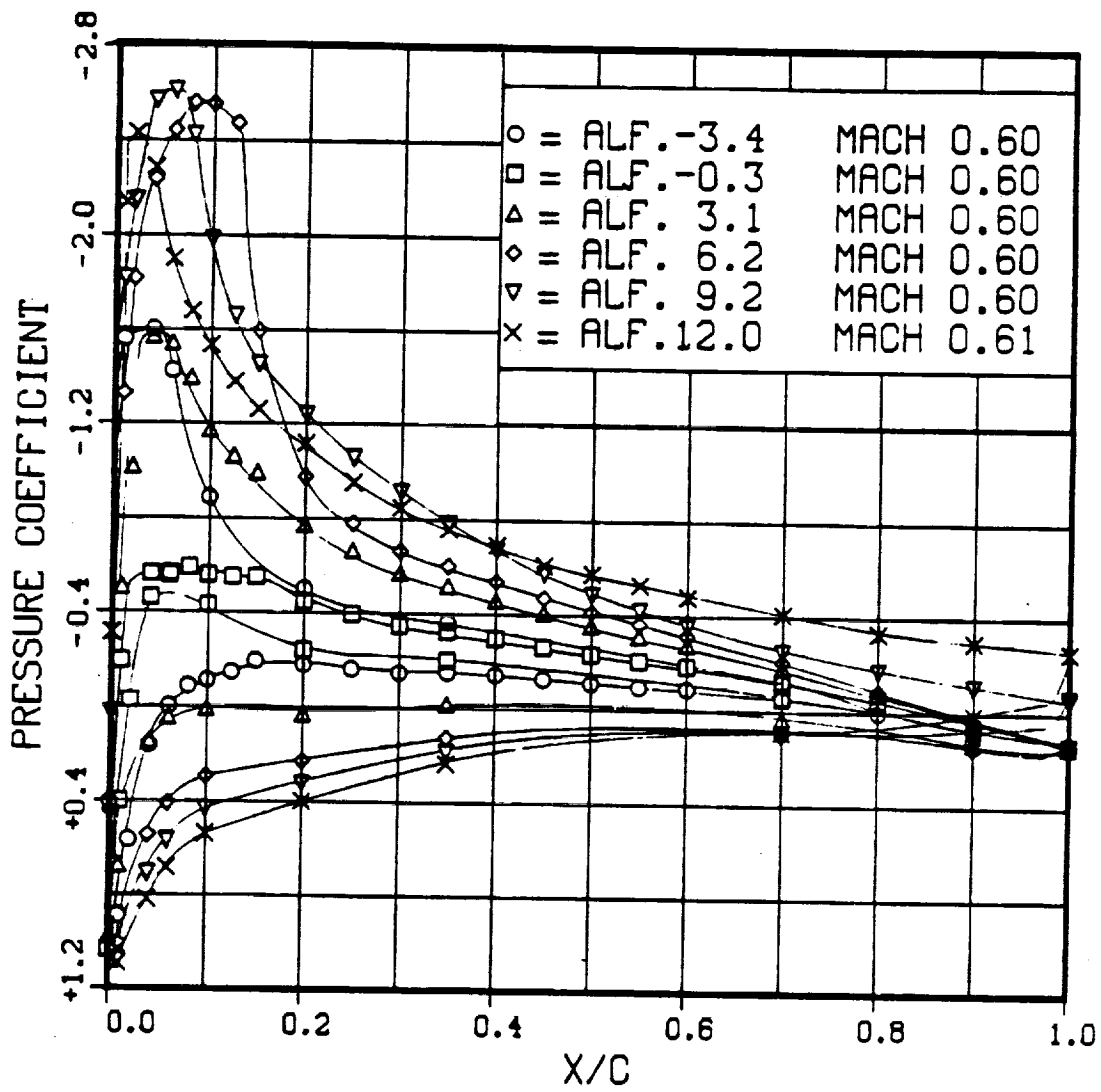


Figure 26.— Lift curve slope correlation.



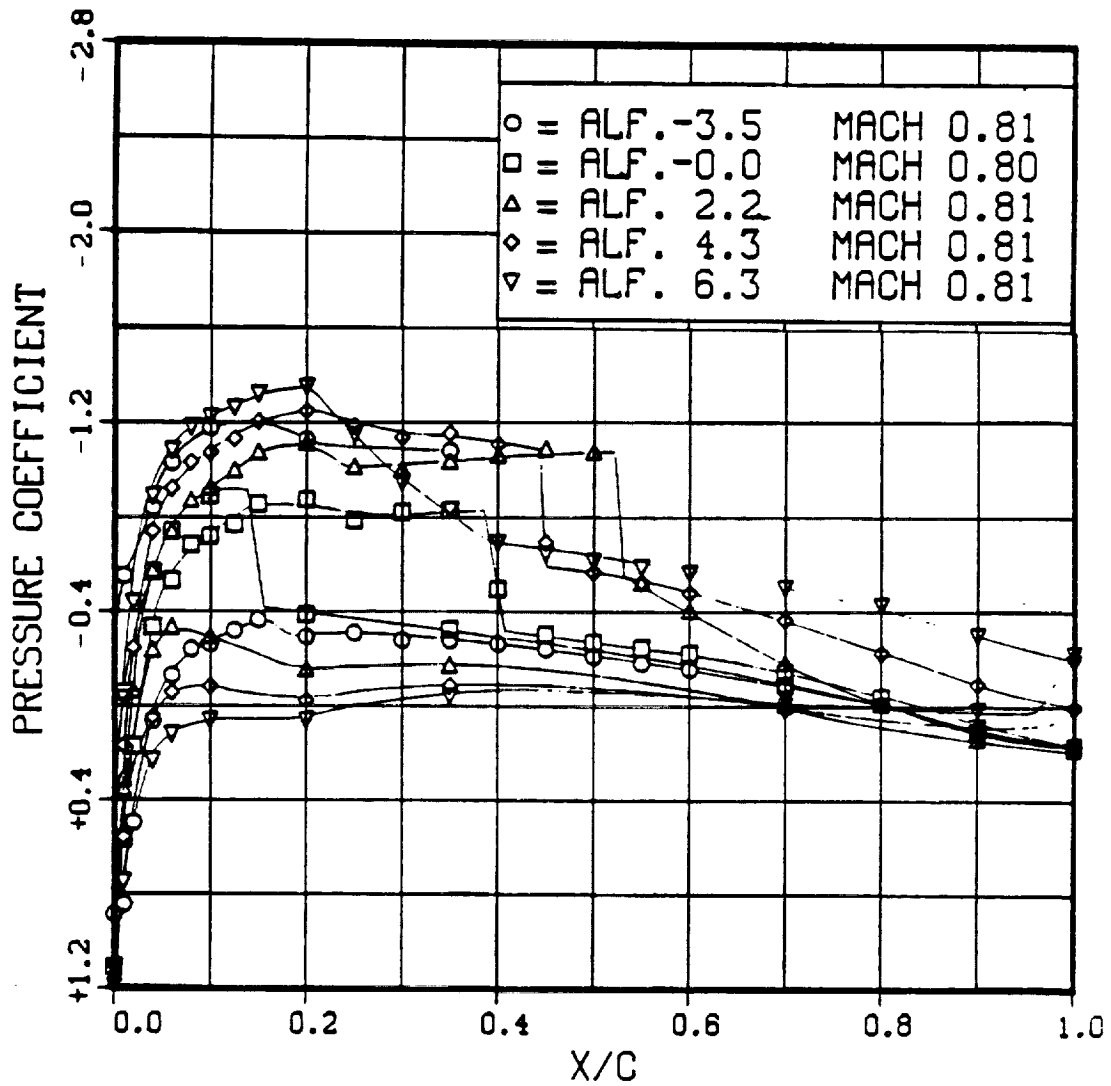
(a) M = 0.40

Figure 27.—Pressure coefficient distribution for the SC1095 airfoil.



(b) $M = 0.60$

Figure 27.-Continued.



(c) M = 0.80

Figure 27.-Concluded.

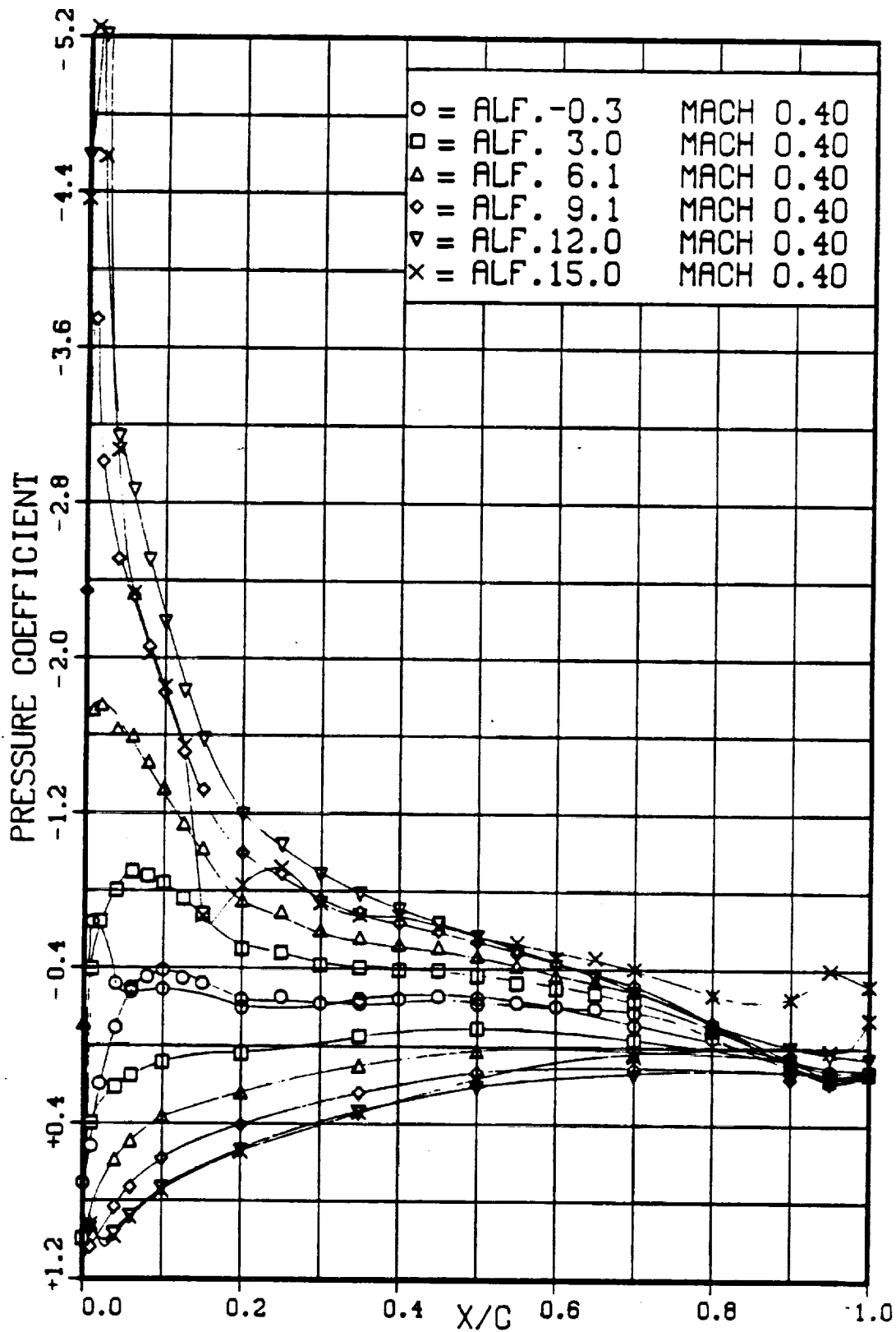
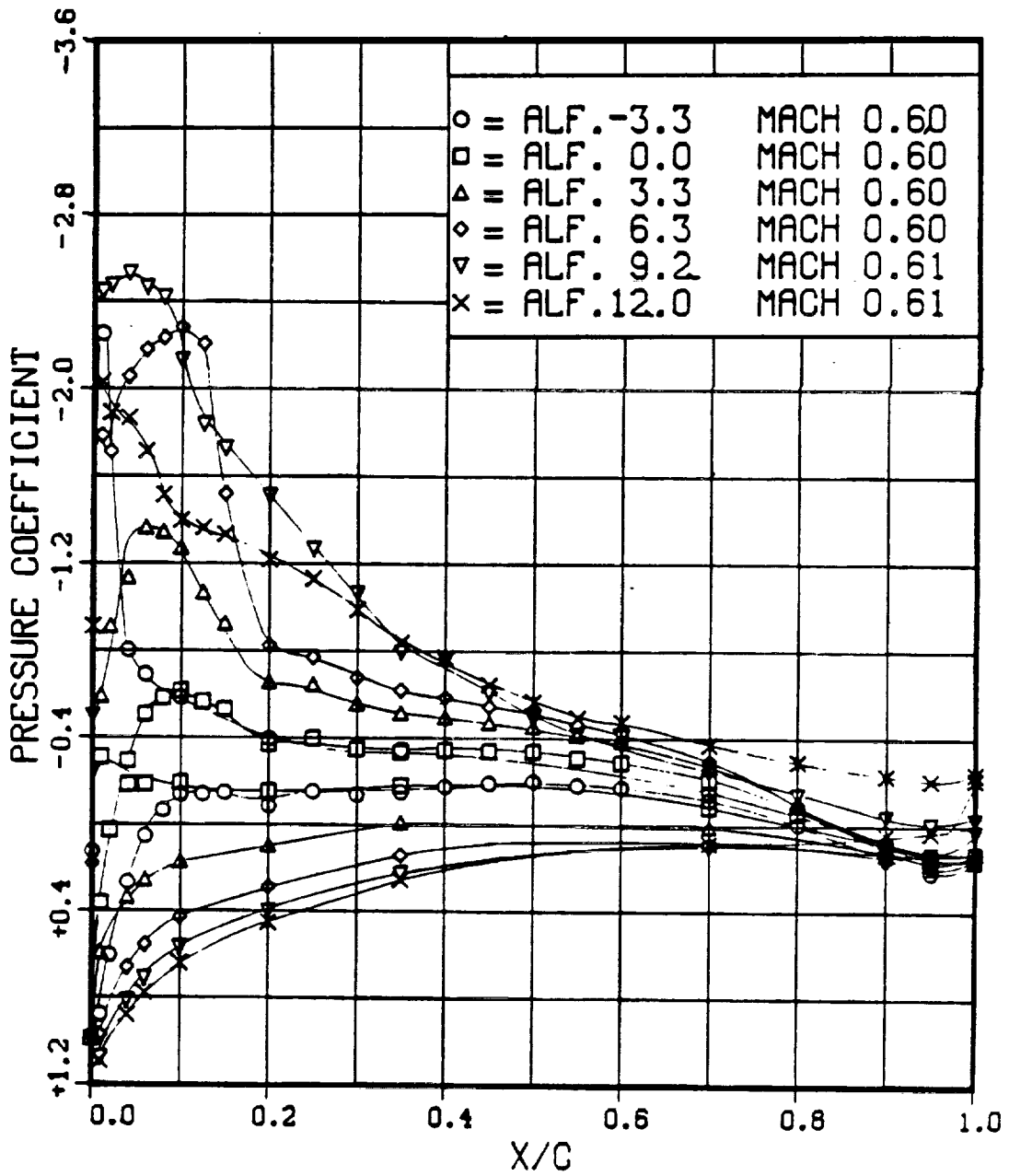
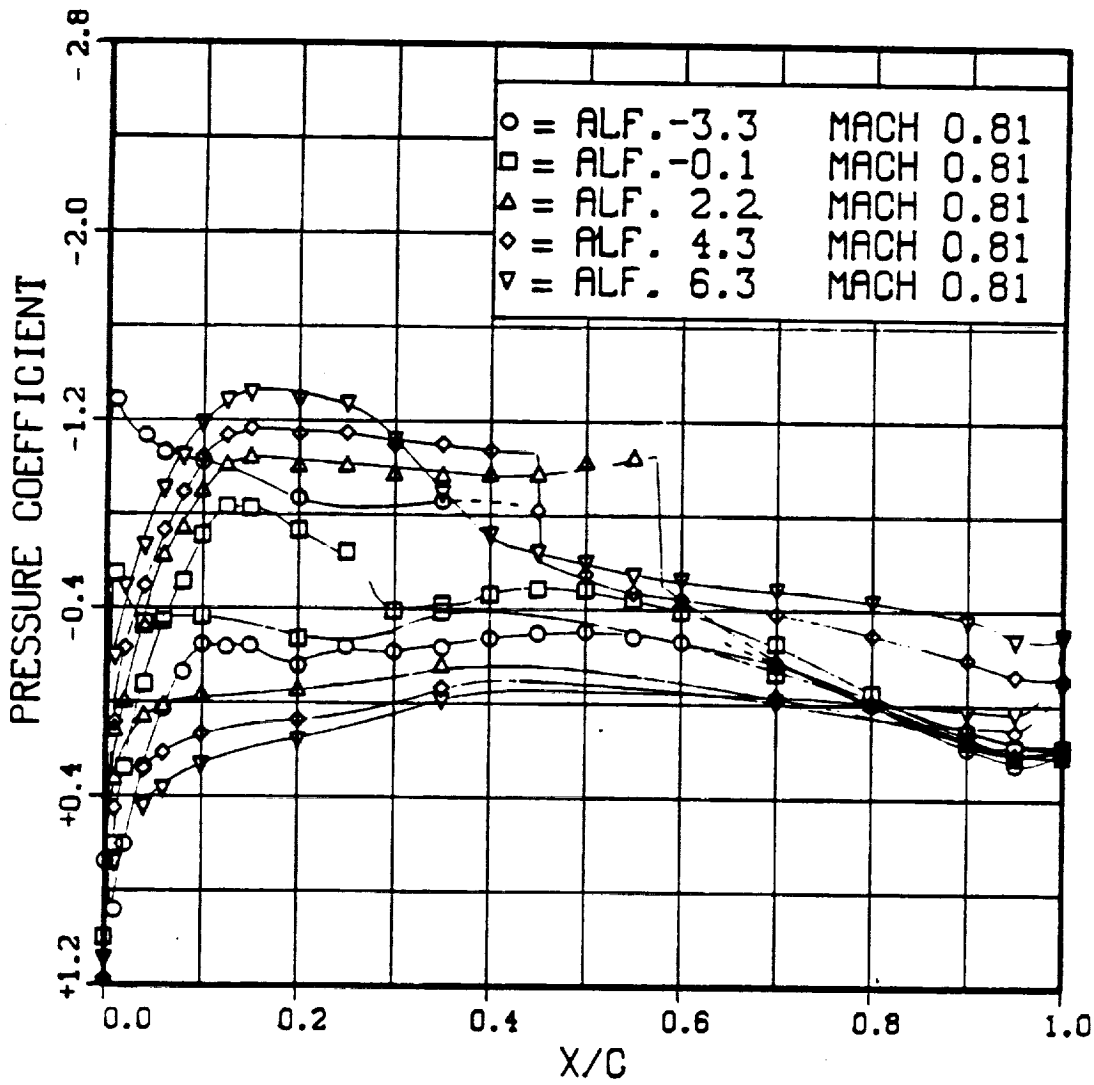


Figure 28.-Pressure coefficient distribution for the SSC-A09 airfoil.



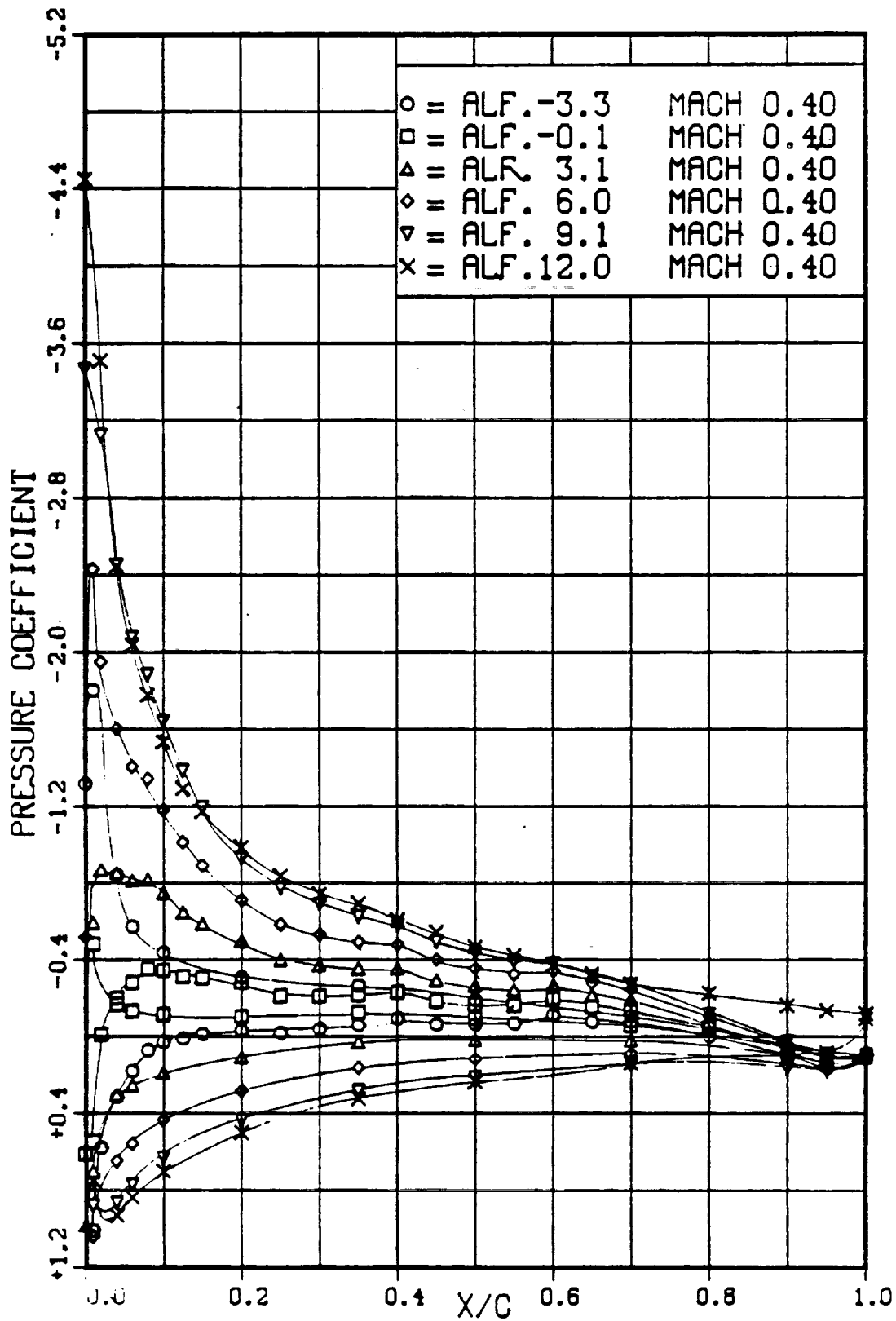
(b) $M = 0.60$

Figure 28.-Continued.



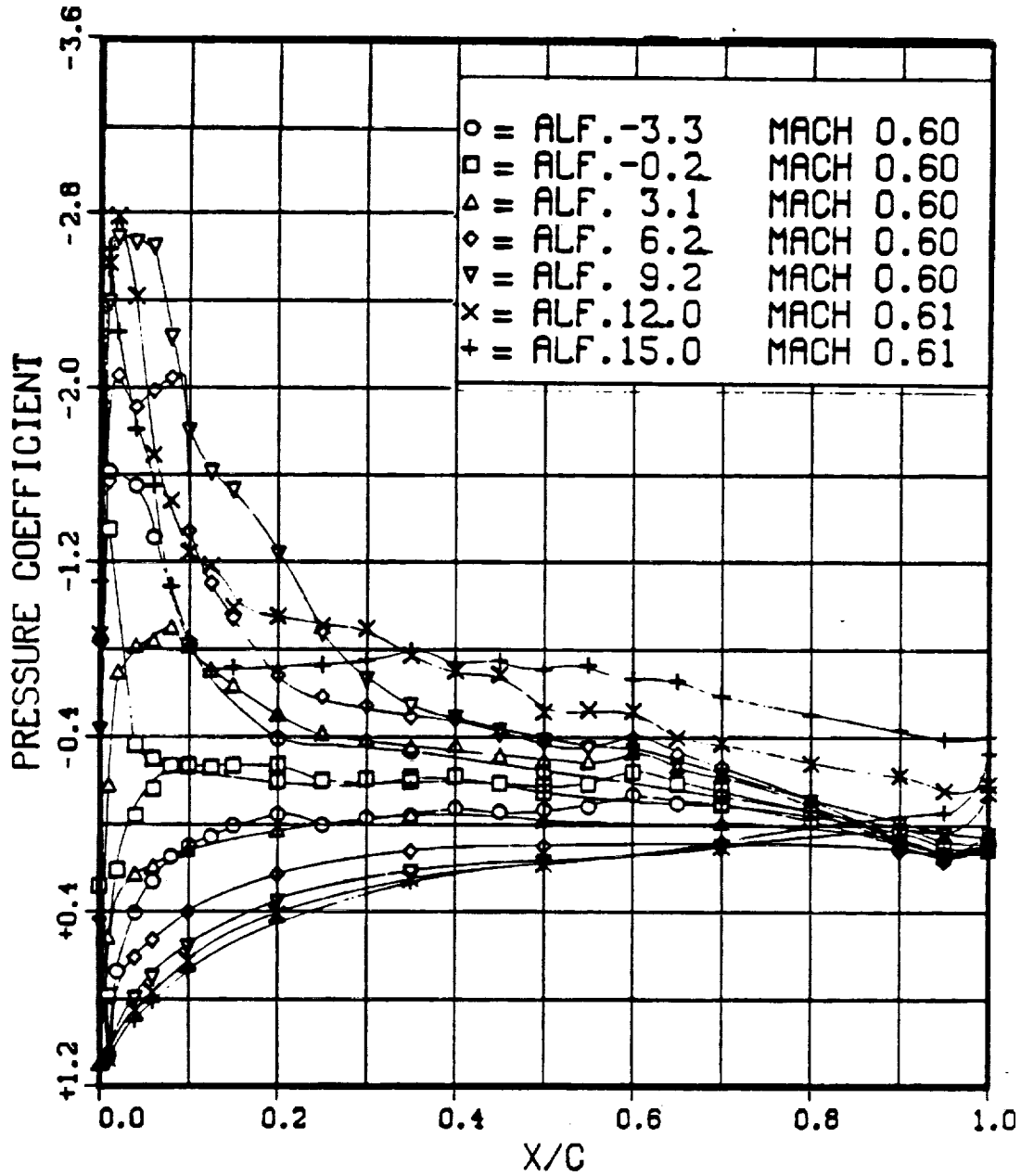
(c) M = 0.80

Figure 28.-Concluded.



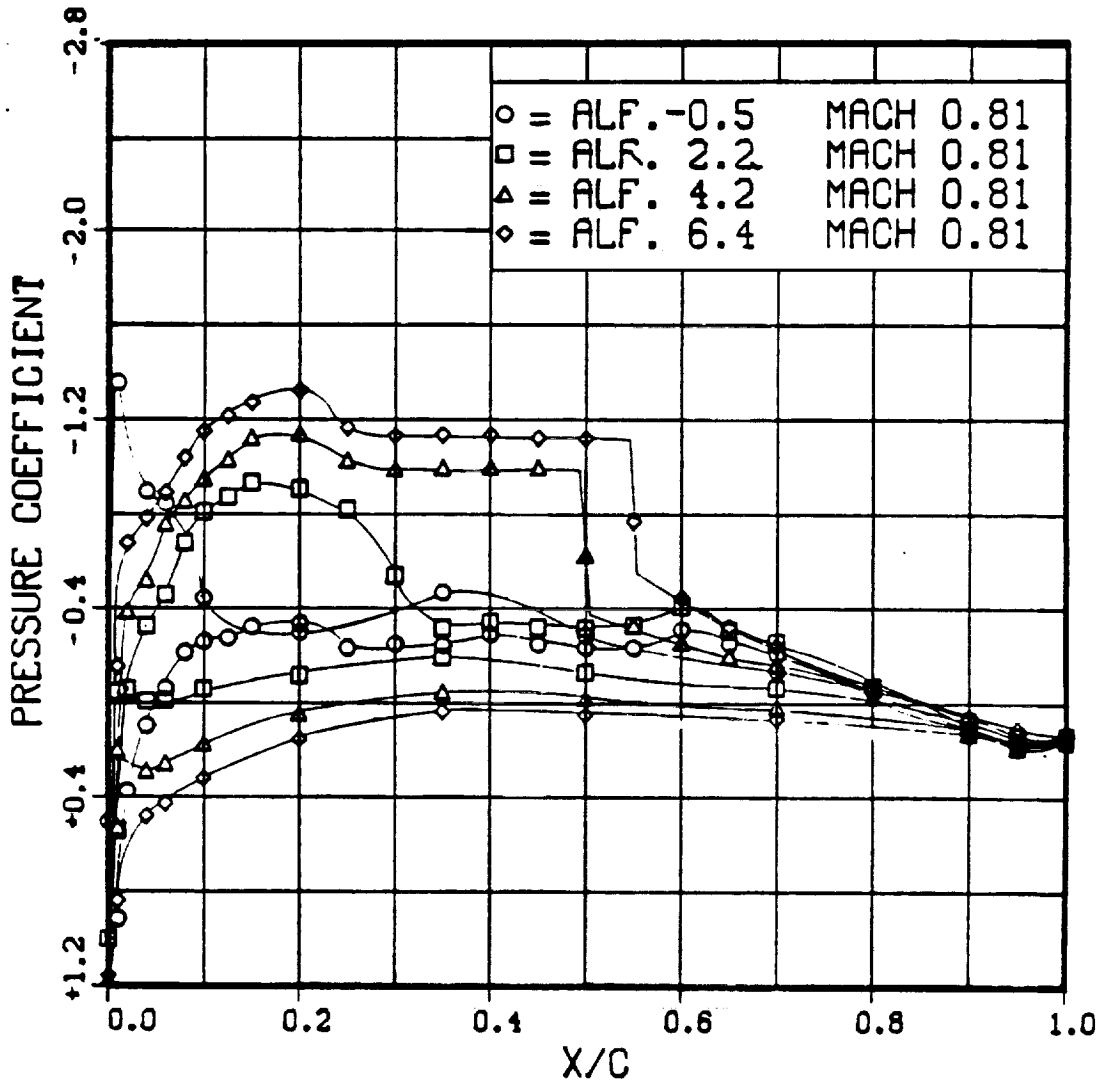
(a) $M = 0.40$

Figure 29.--Pressure coefficient distribution for the SSC-A07 airfoil.



(b) M = 0.60

Figure 29.-Continued.



(c) M = 0.80

Figure 29.-Concluded.

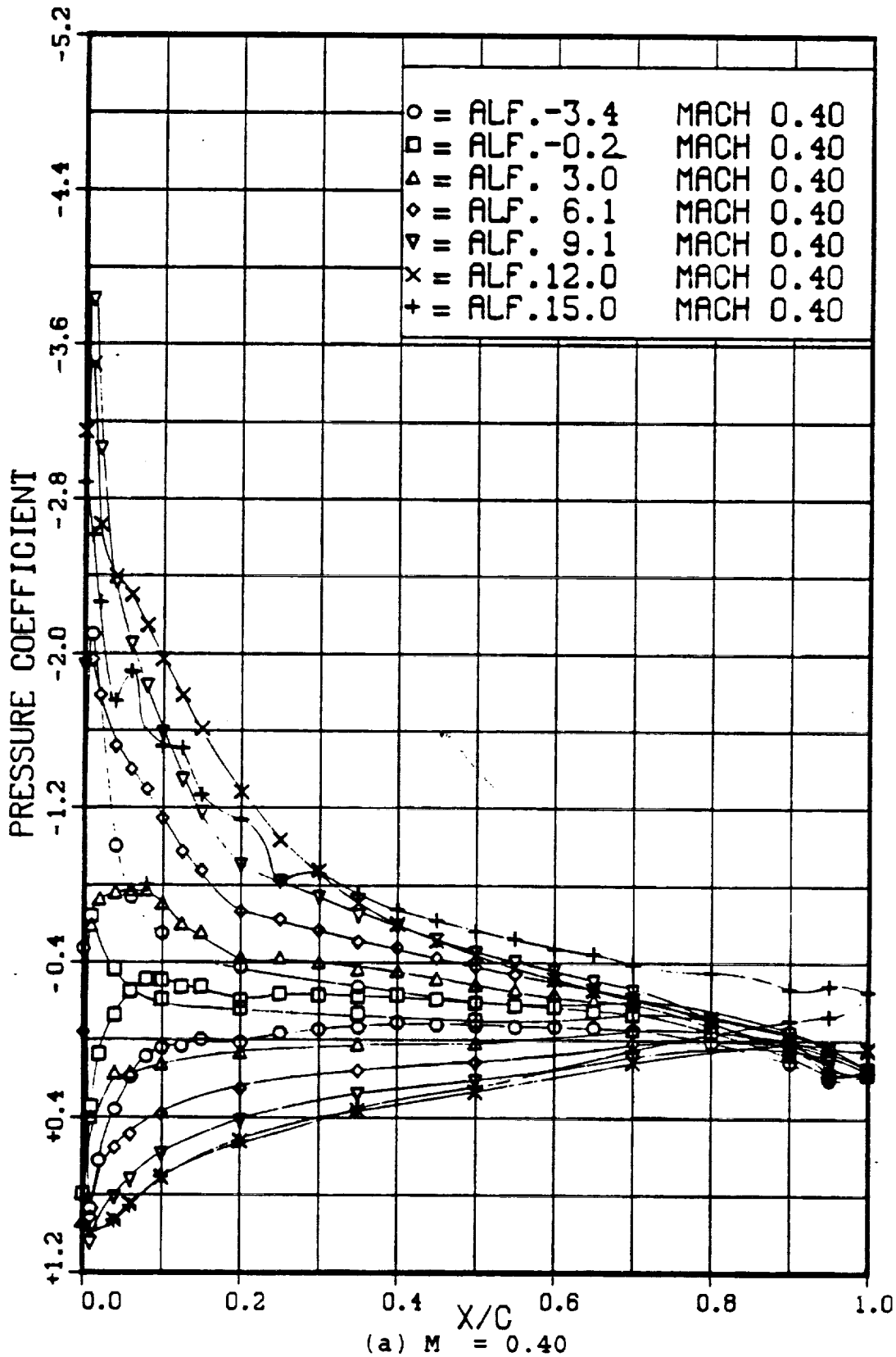
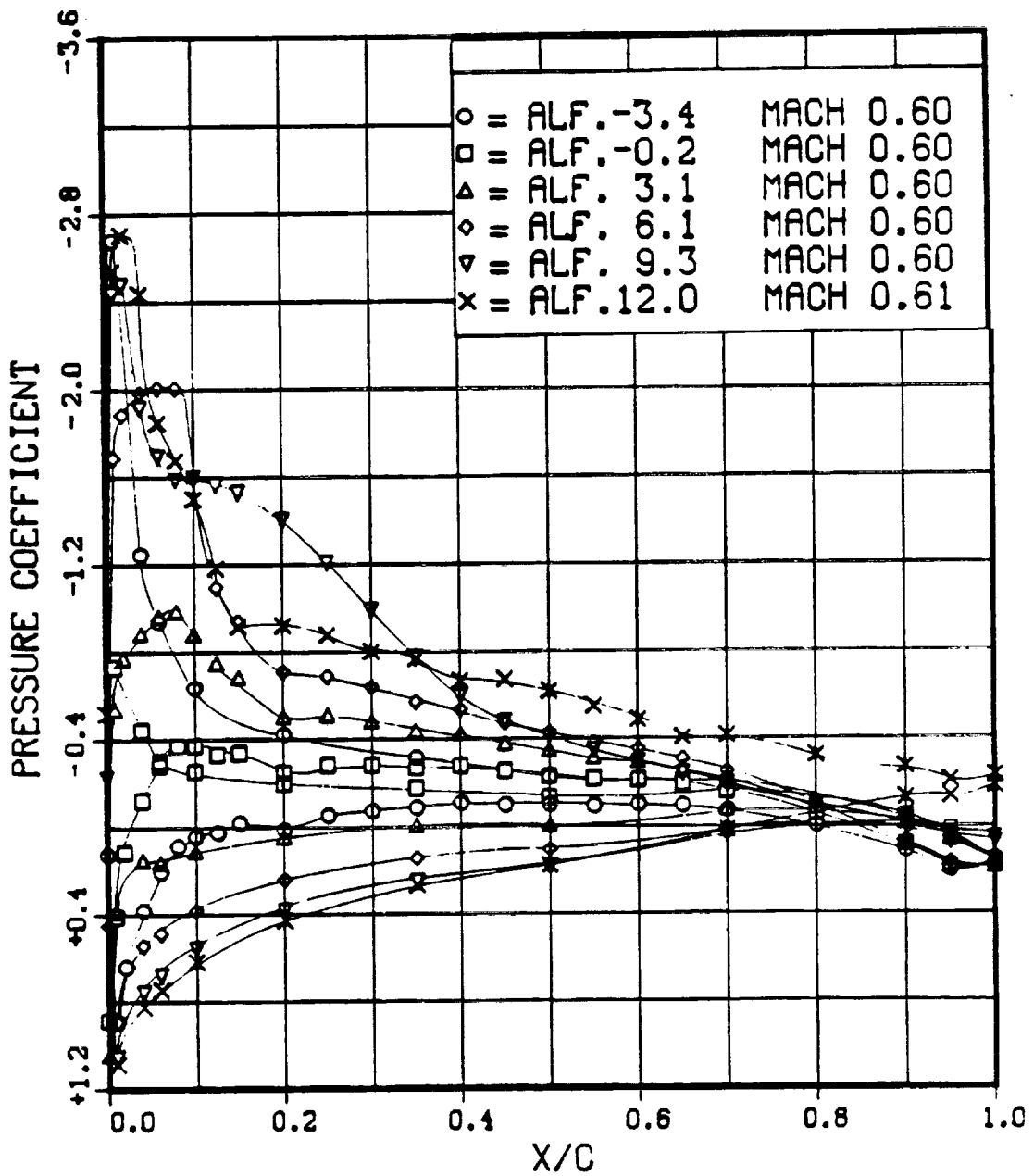


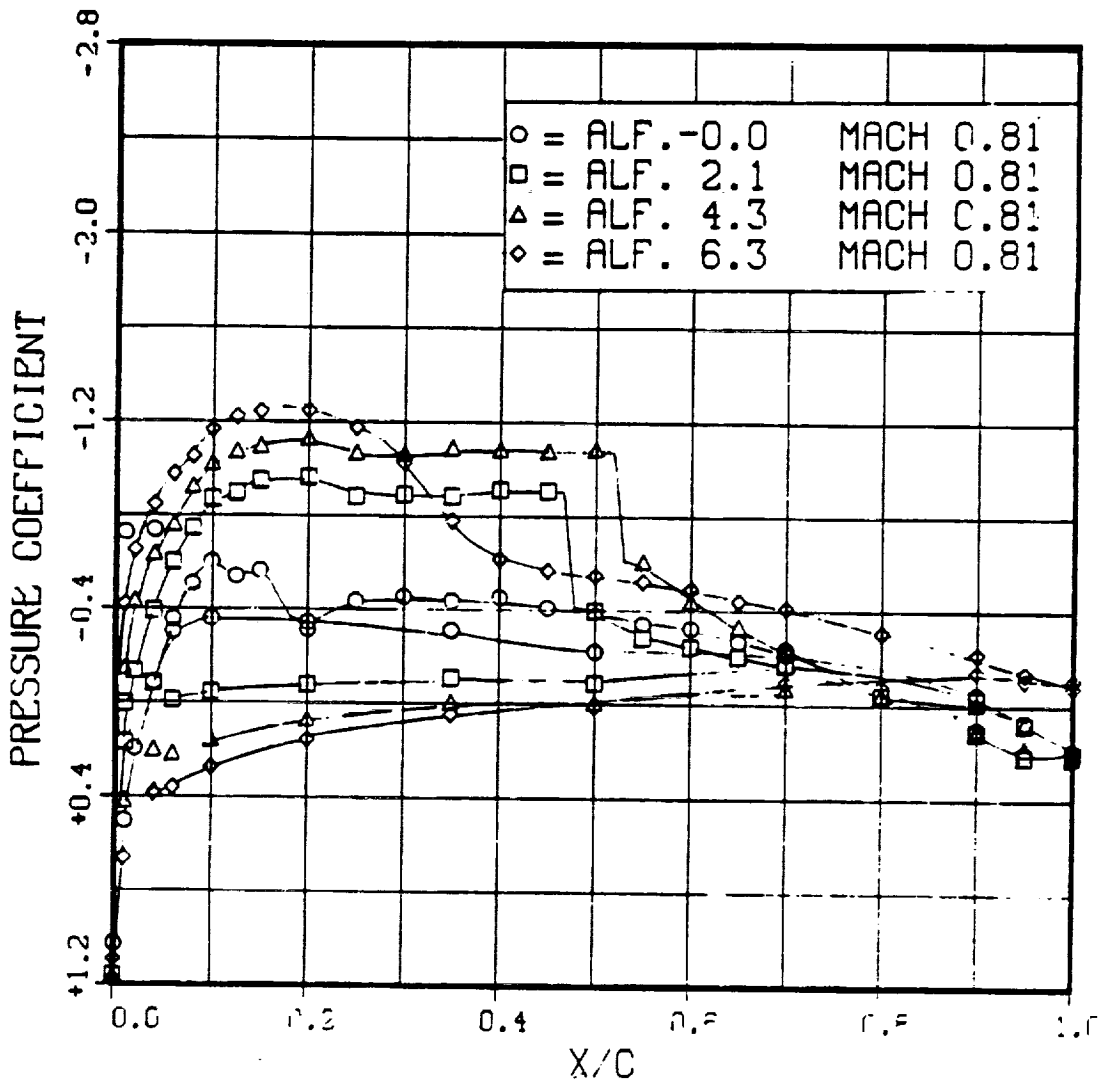
Figure 30.-Pressure coefficient distribution for the SSC-B08 airfoil.

0.2



(b) M = 0.60

Figure 30.-Continued.



(c) M = 0.80

Figure 30. Concluded

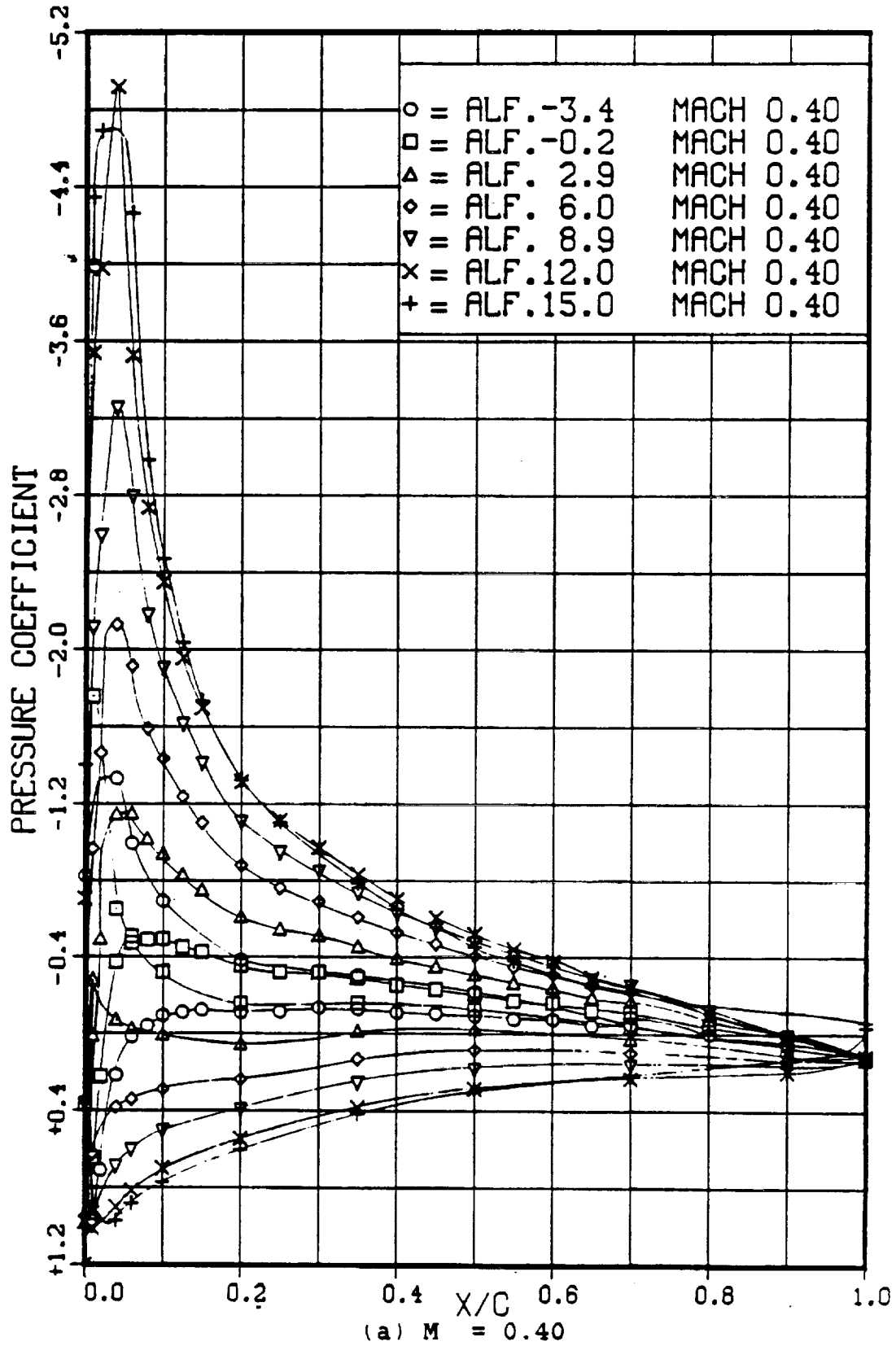
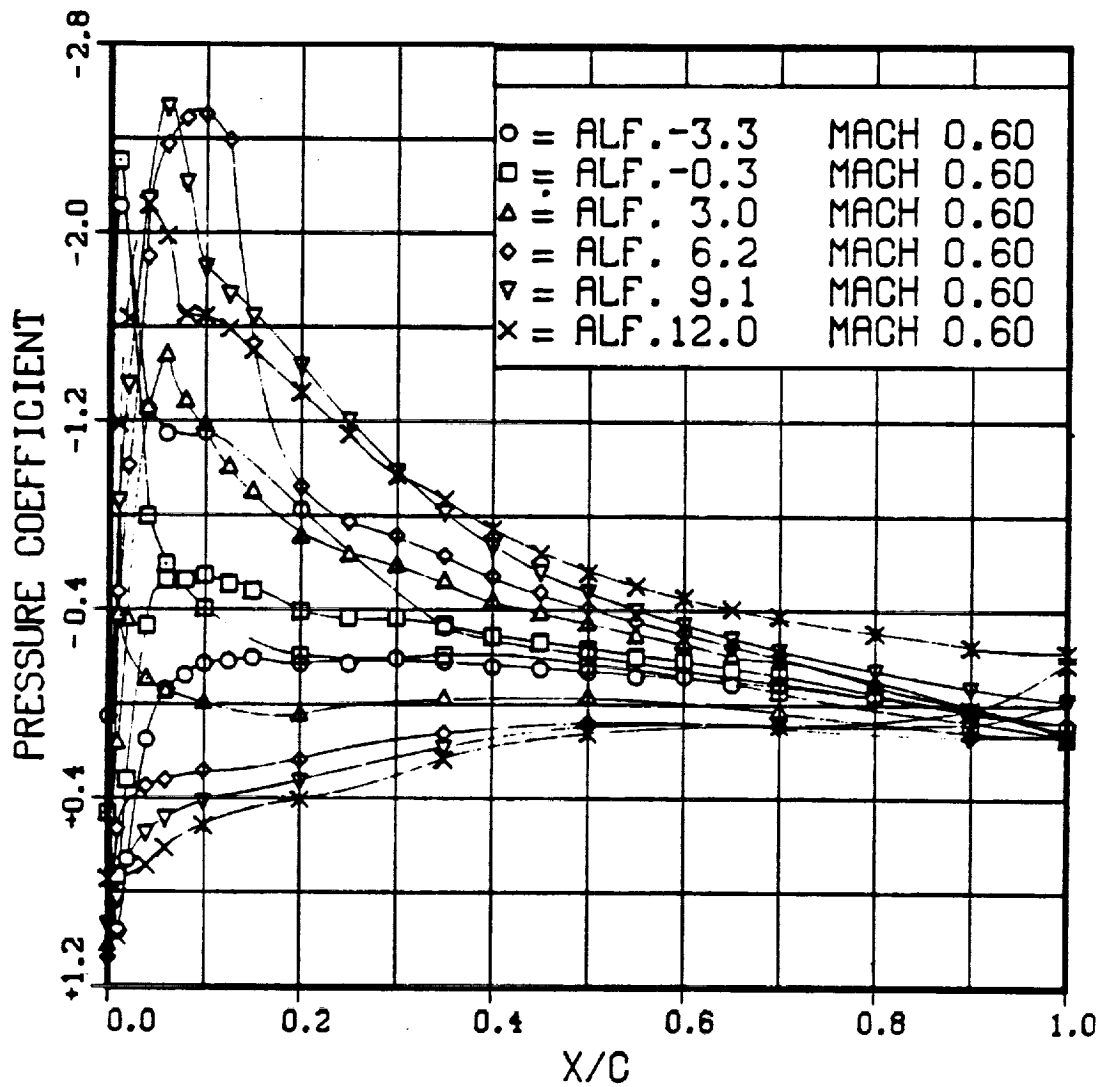
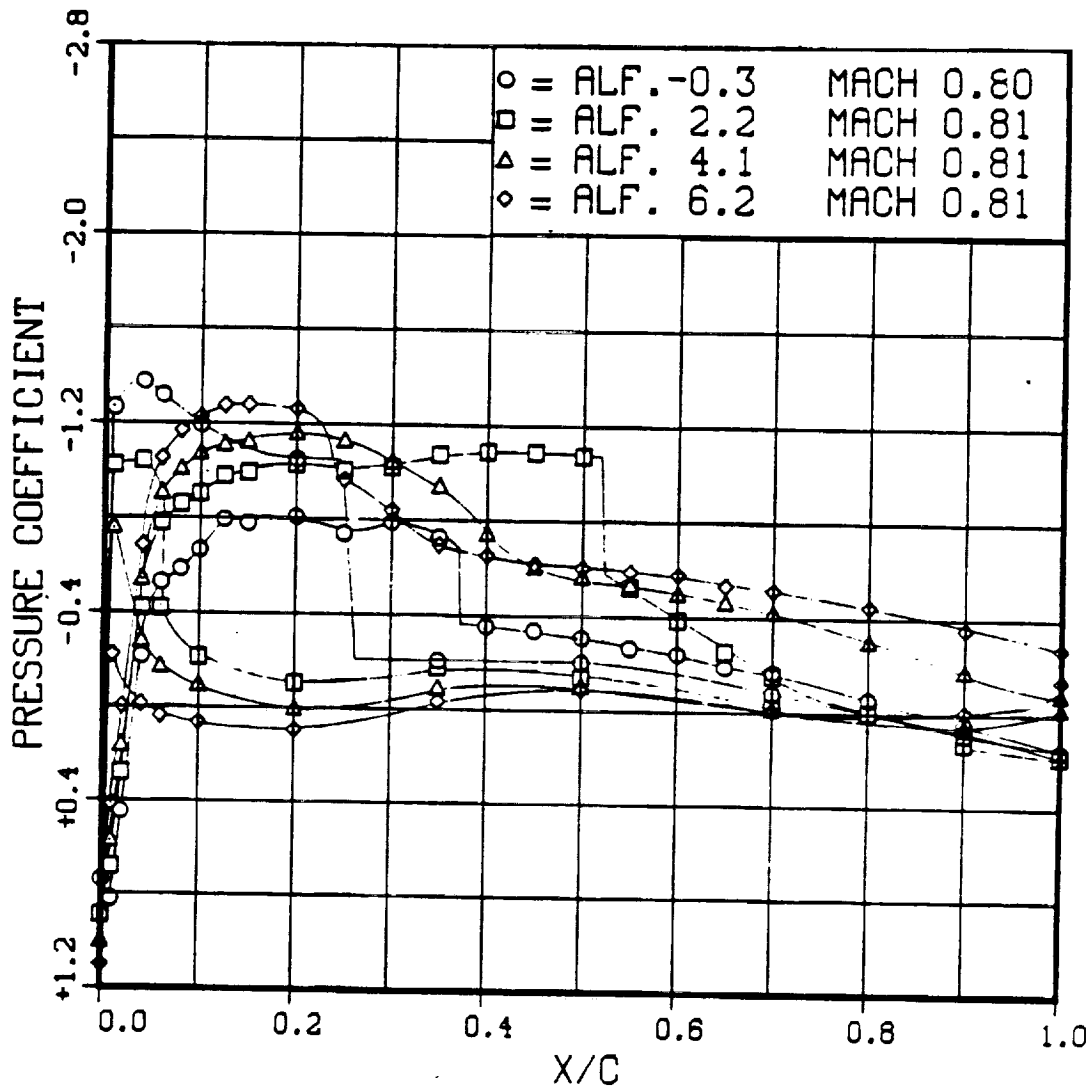


Figure 31.-Pressure coefficient distribution for the SC1094 R8 airfoil



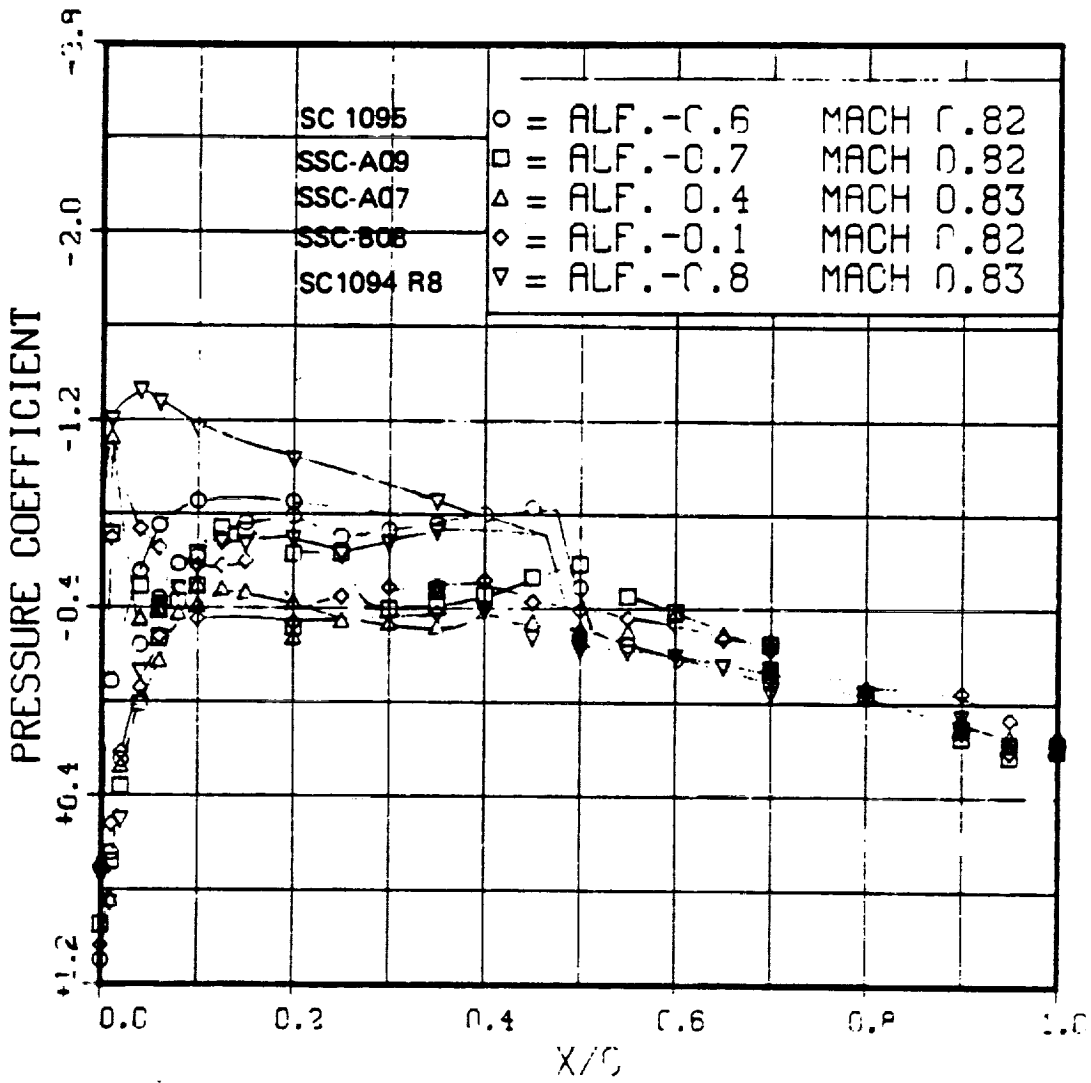
(b) M = 0.60

Figure 31.-Continued.



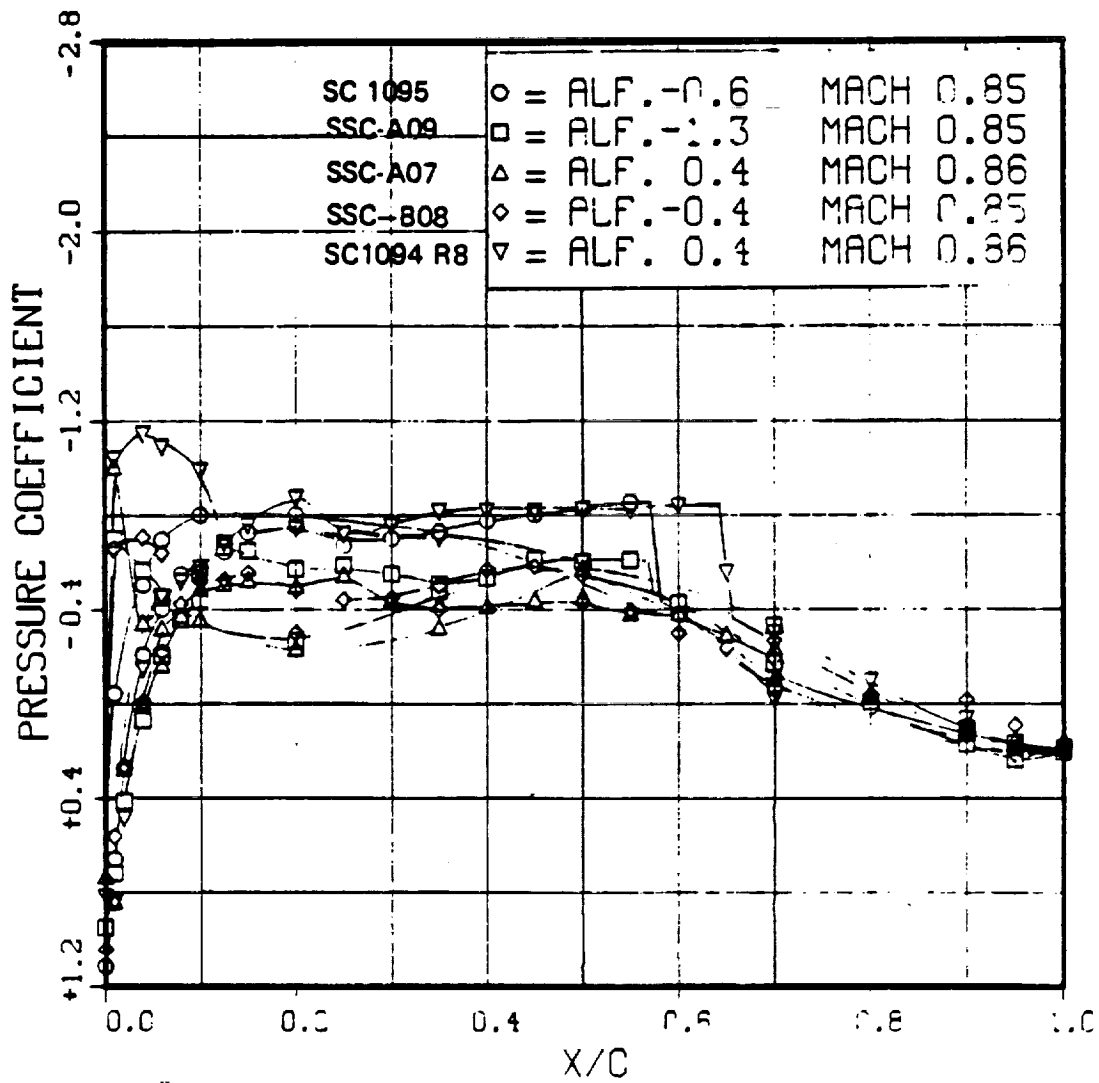
(c) M = 0.80

Figure 31.-Concluded.



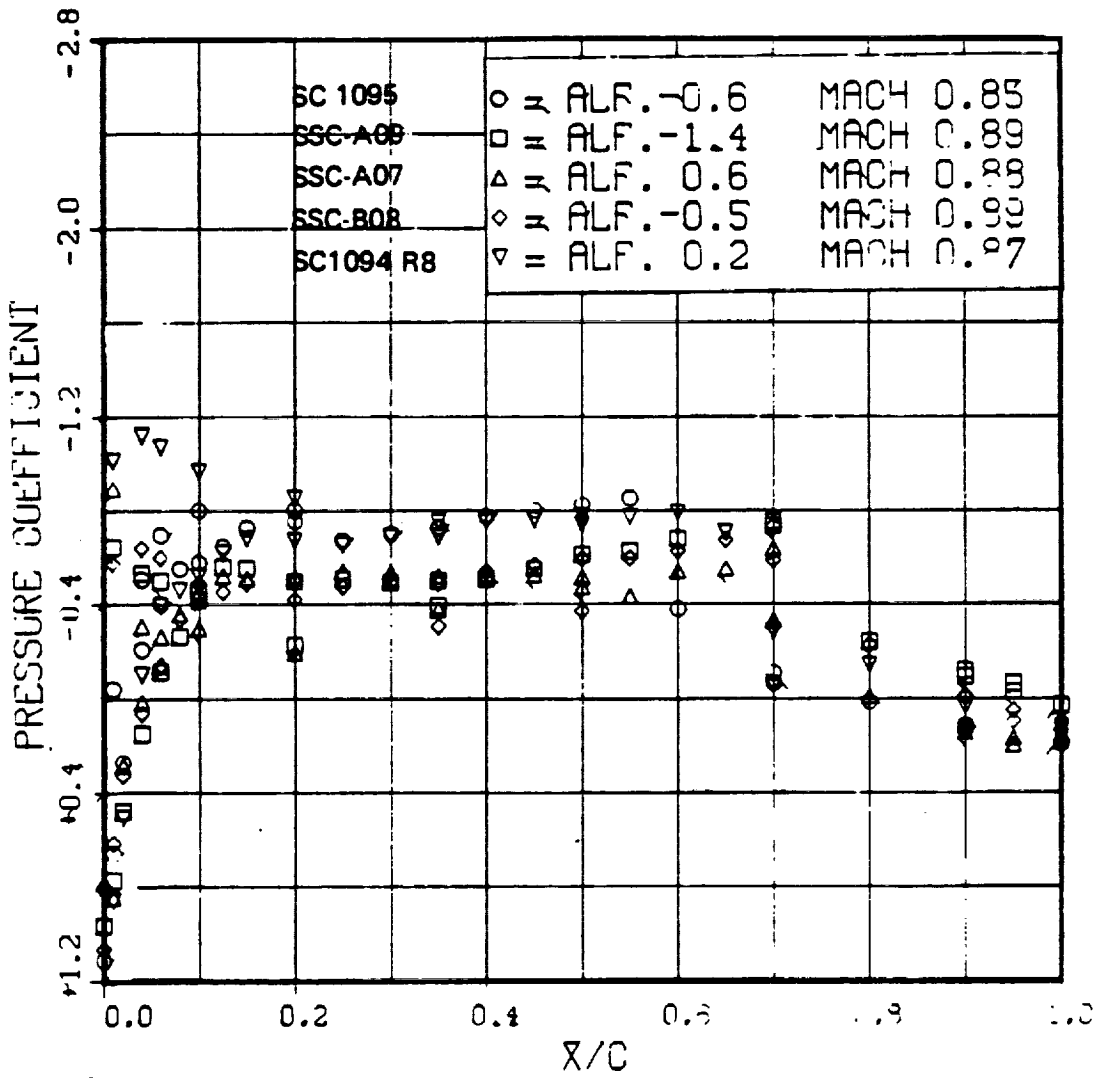
(a) M = .825

Figure 32.— Pressure coefficient distribution for low lift at high Mach numbers



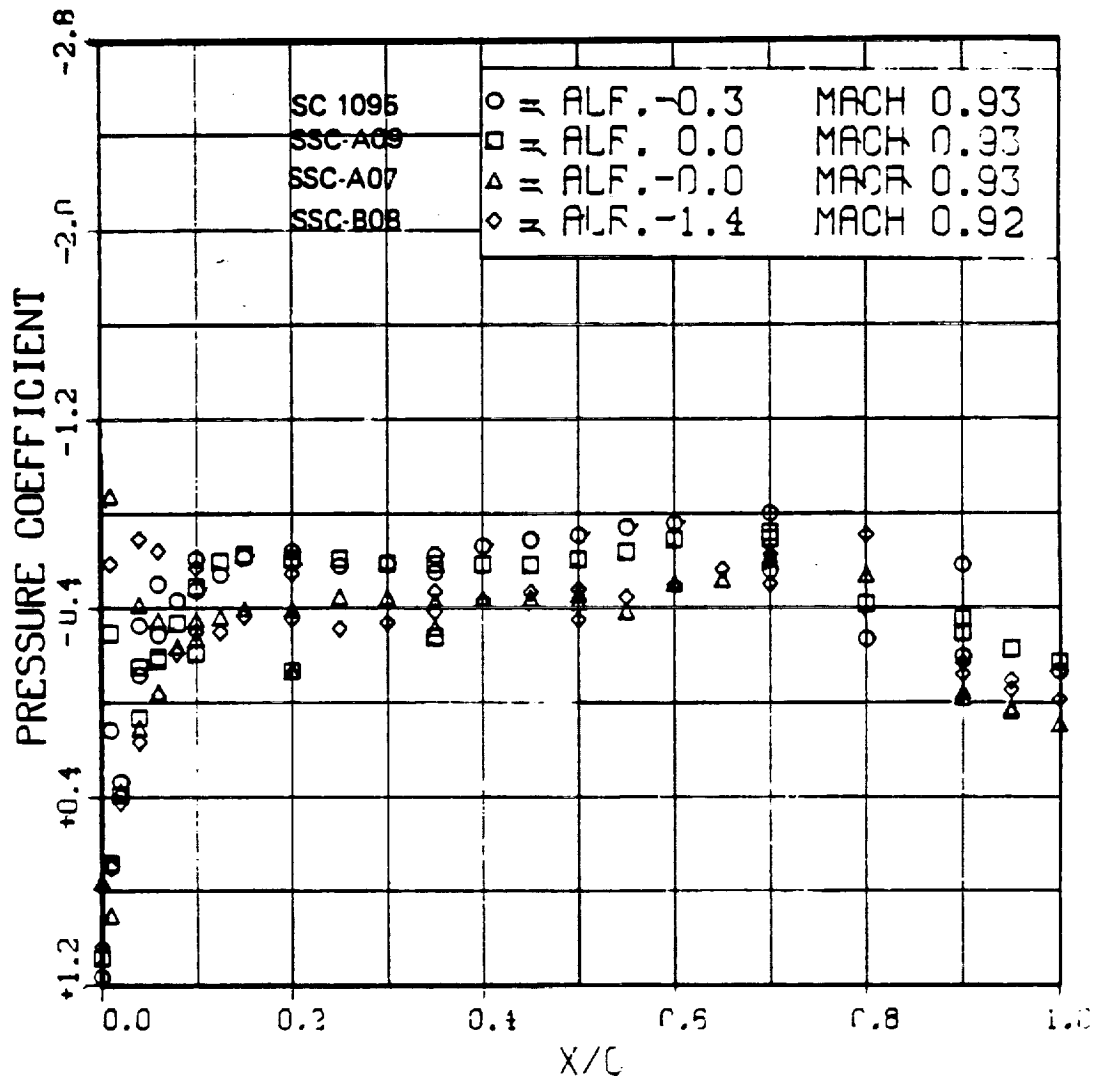
(b) M = .85

Figure 32.-Continued.



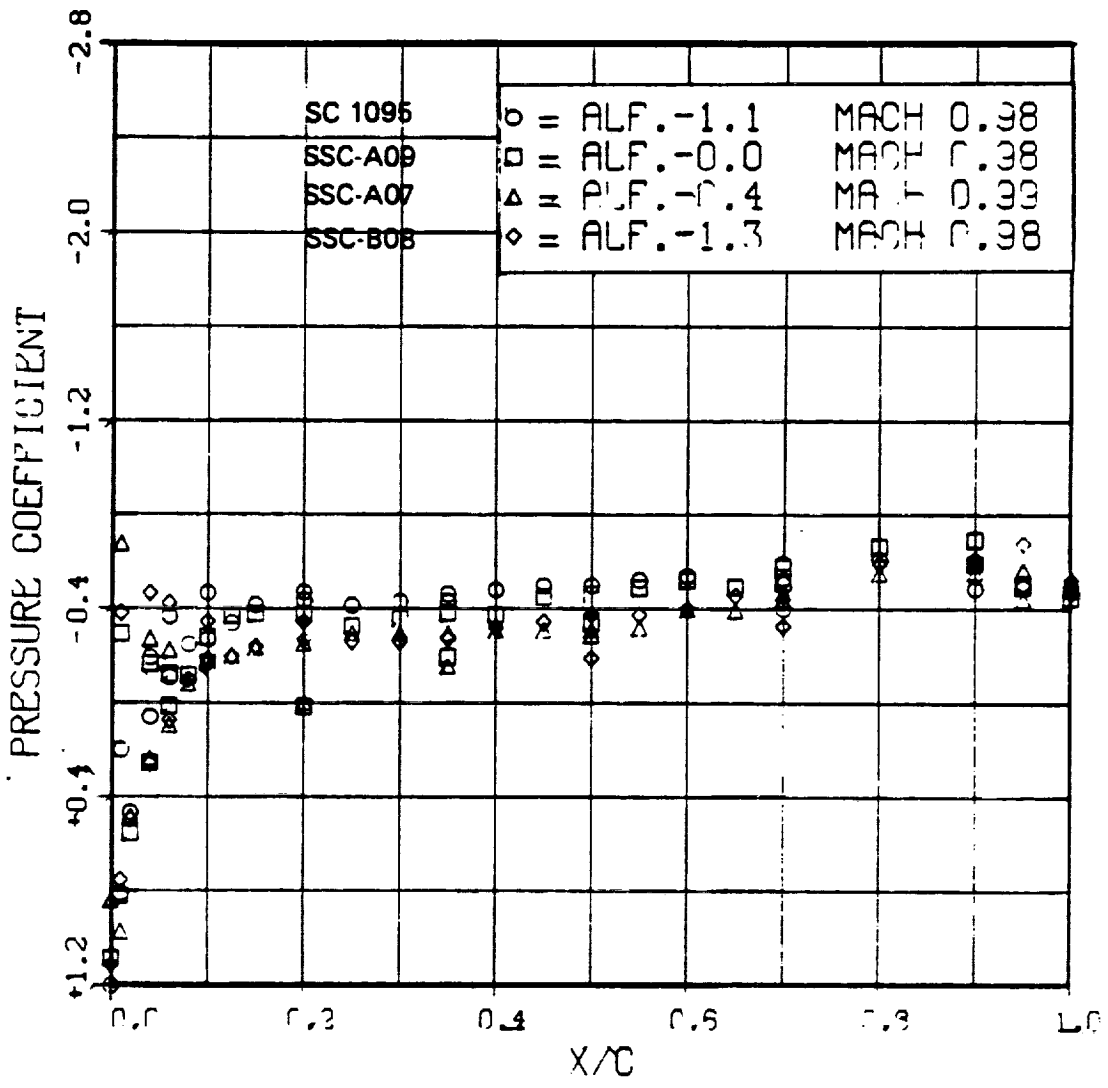
(c) M = .88

Figure 32.- Continued.



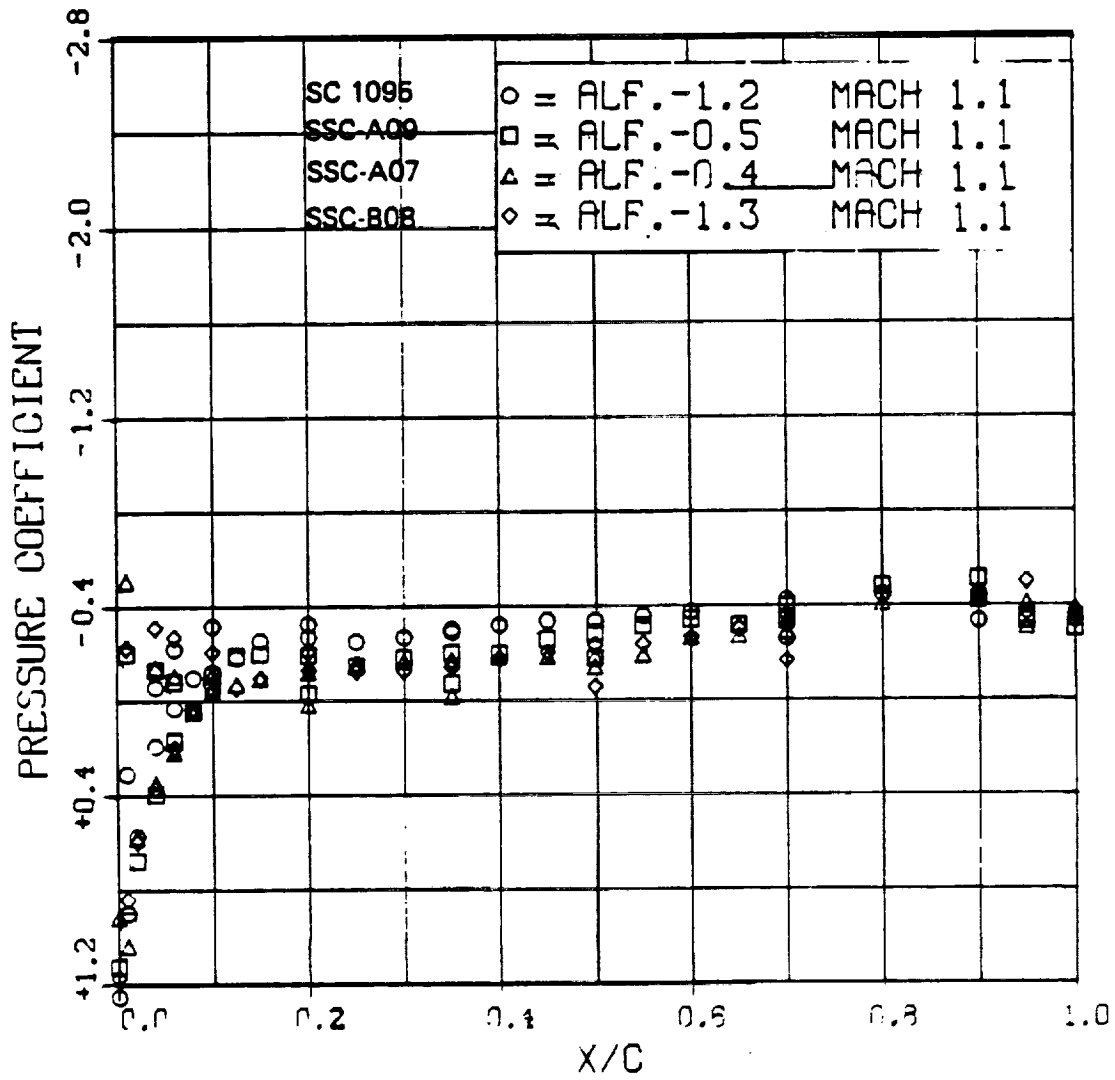
(d) M = .90

Figure 32.- Continued.



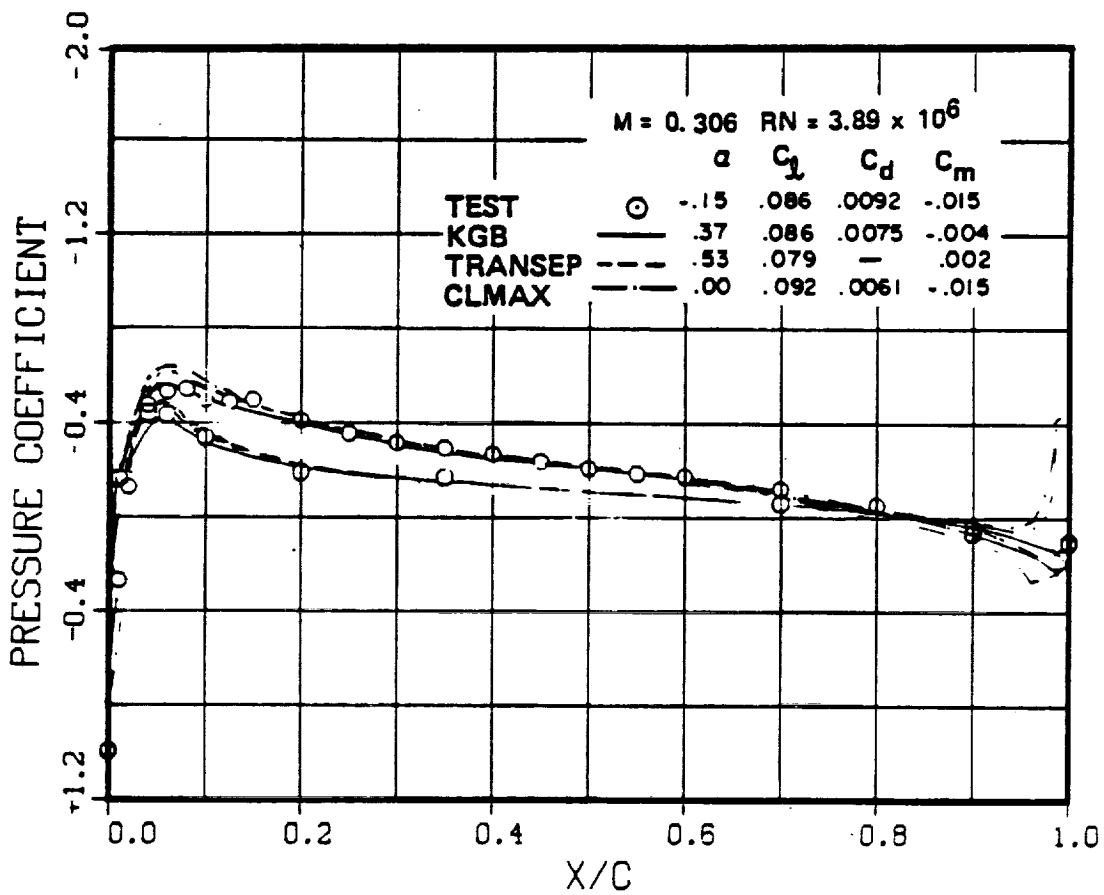
(e) M = .98

Figure 32.-Continued.



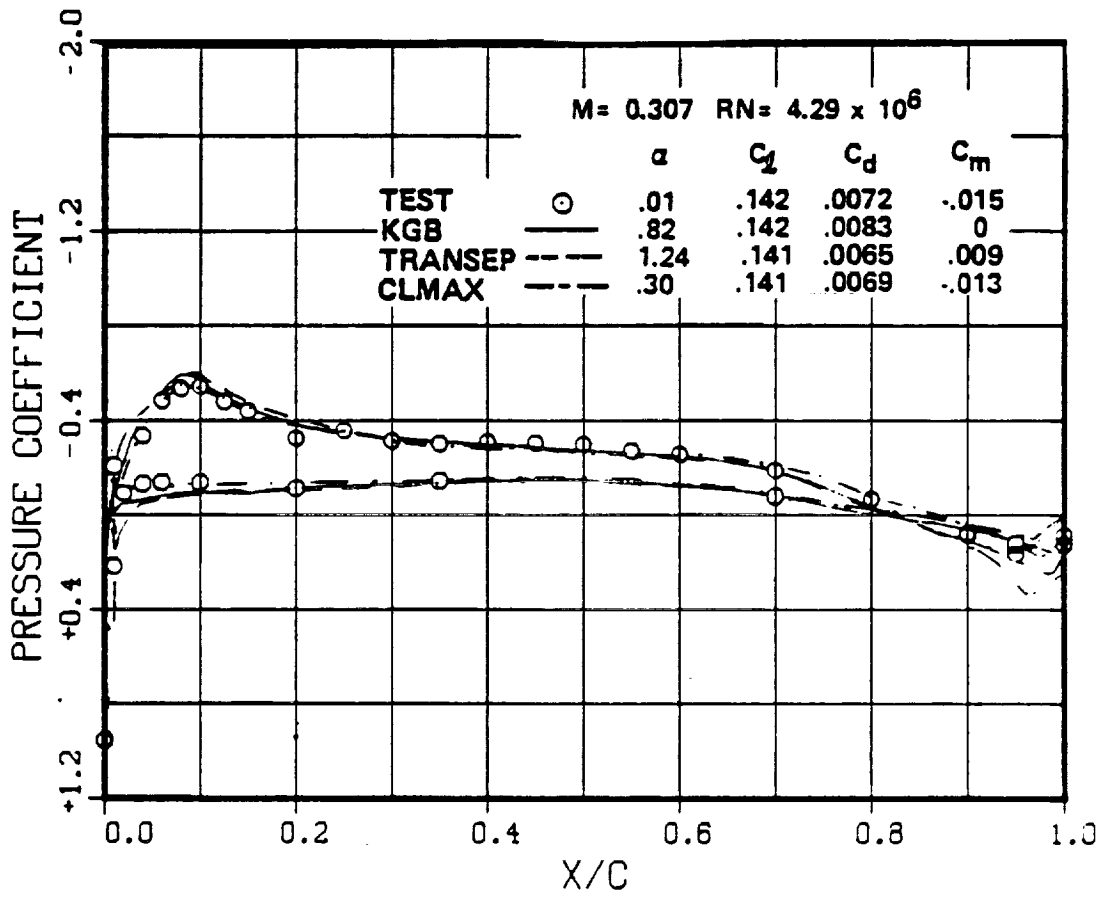
(f) M = 1.07

Figure 32.-Concluded.



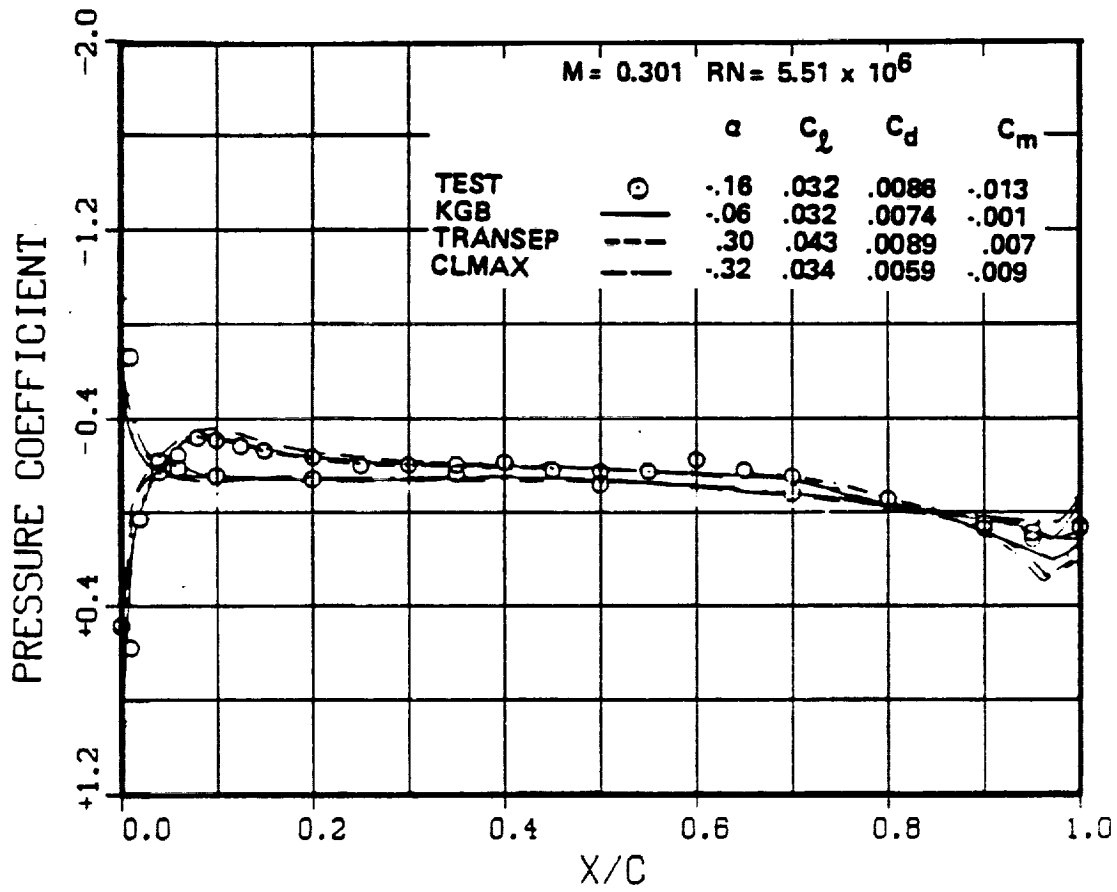
(a) SC1095

Figure 33. - Pressure coefficient correlation, M = 0.30, C_l = 0.



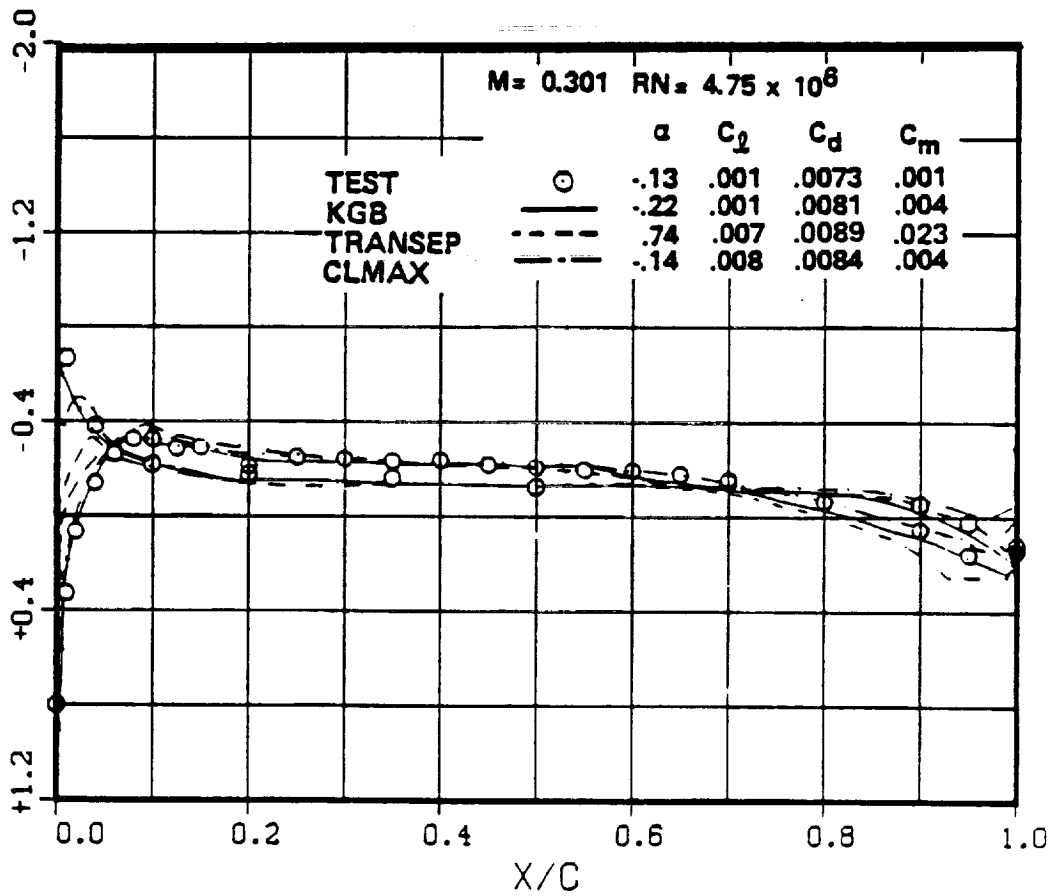
(b) SSC-A09

Figure 33.-Continued.



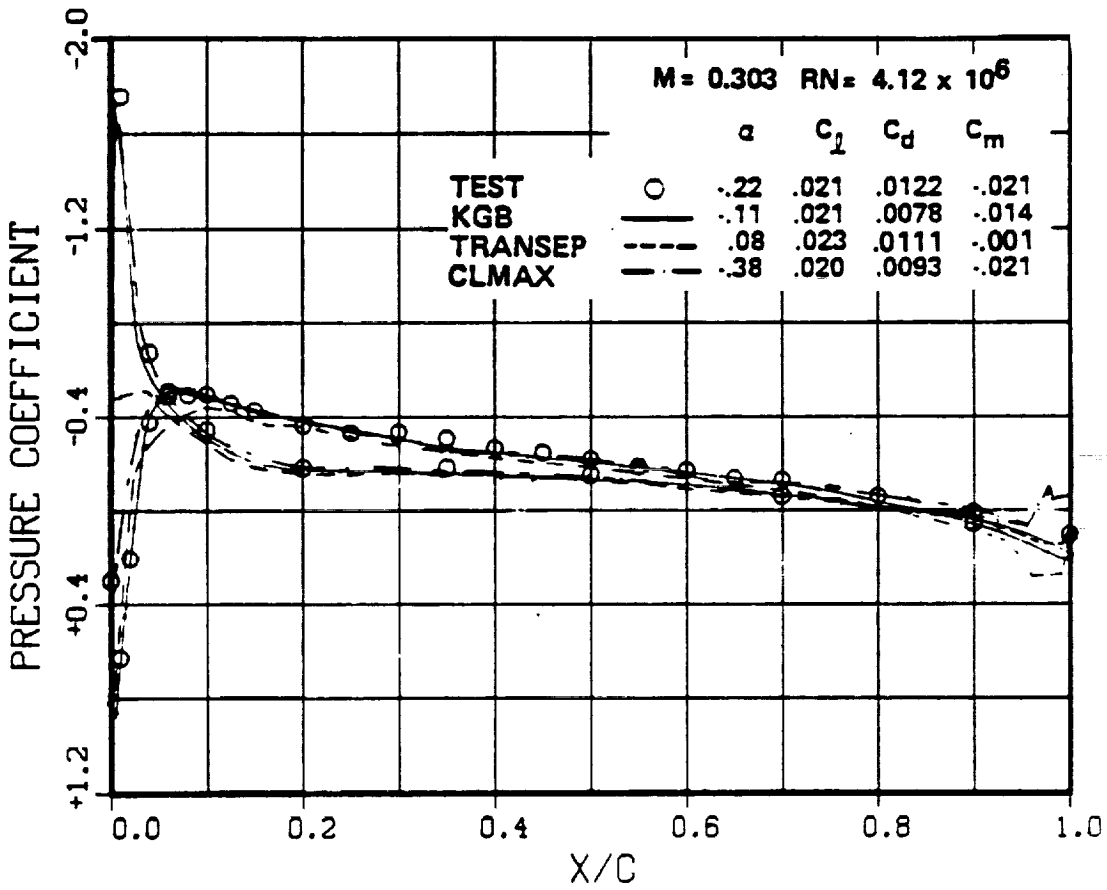
(c) SSC-A07

Figure 33. - Continued.



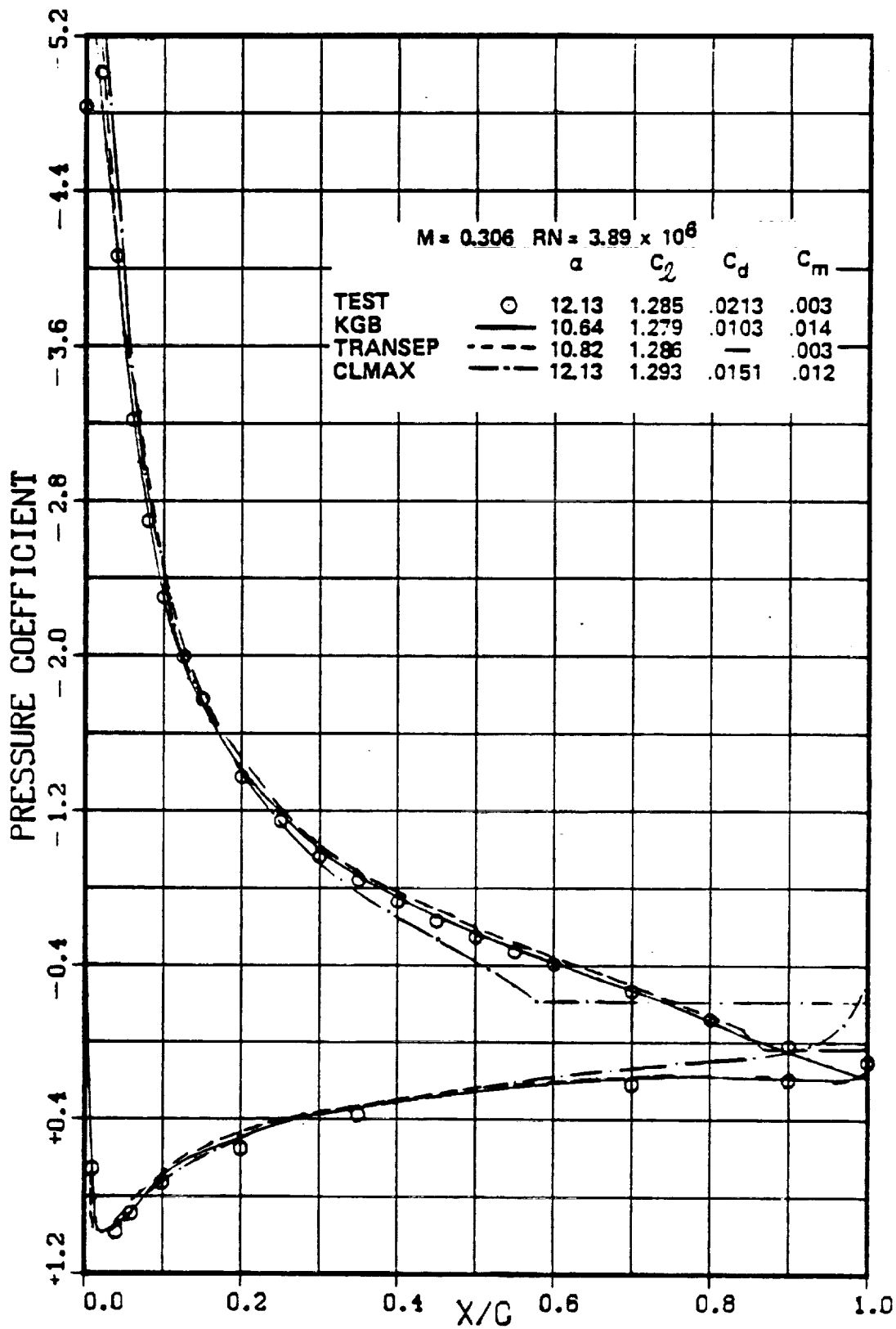
(d) SSC-B08

Figure 33.-Continued.



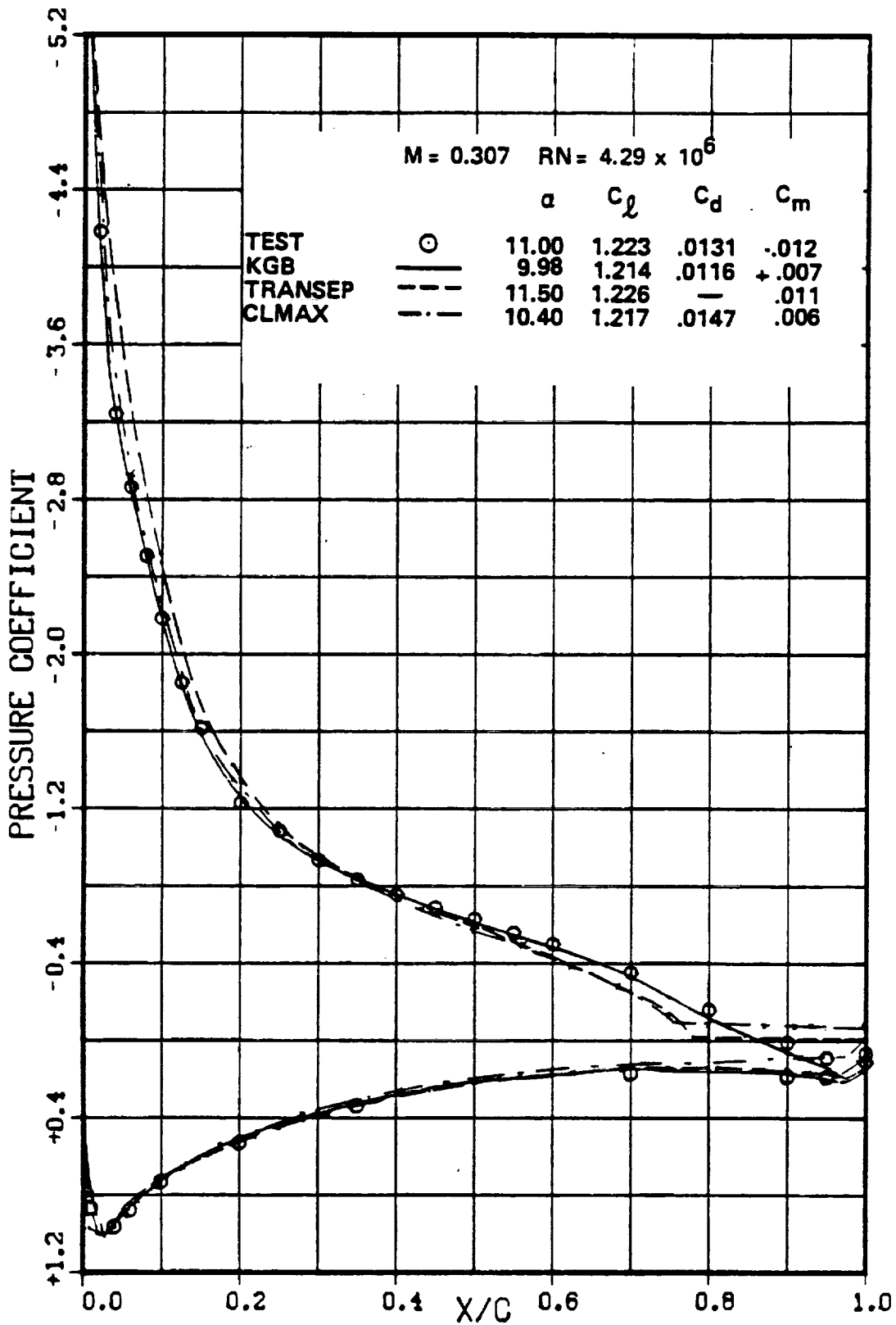
(e) SC1094 R8

Figure 33.- Concluded.

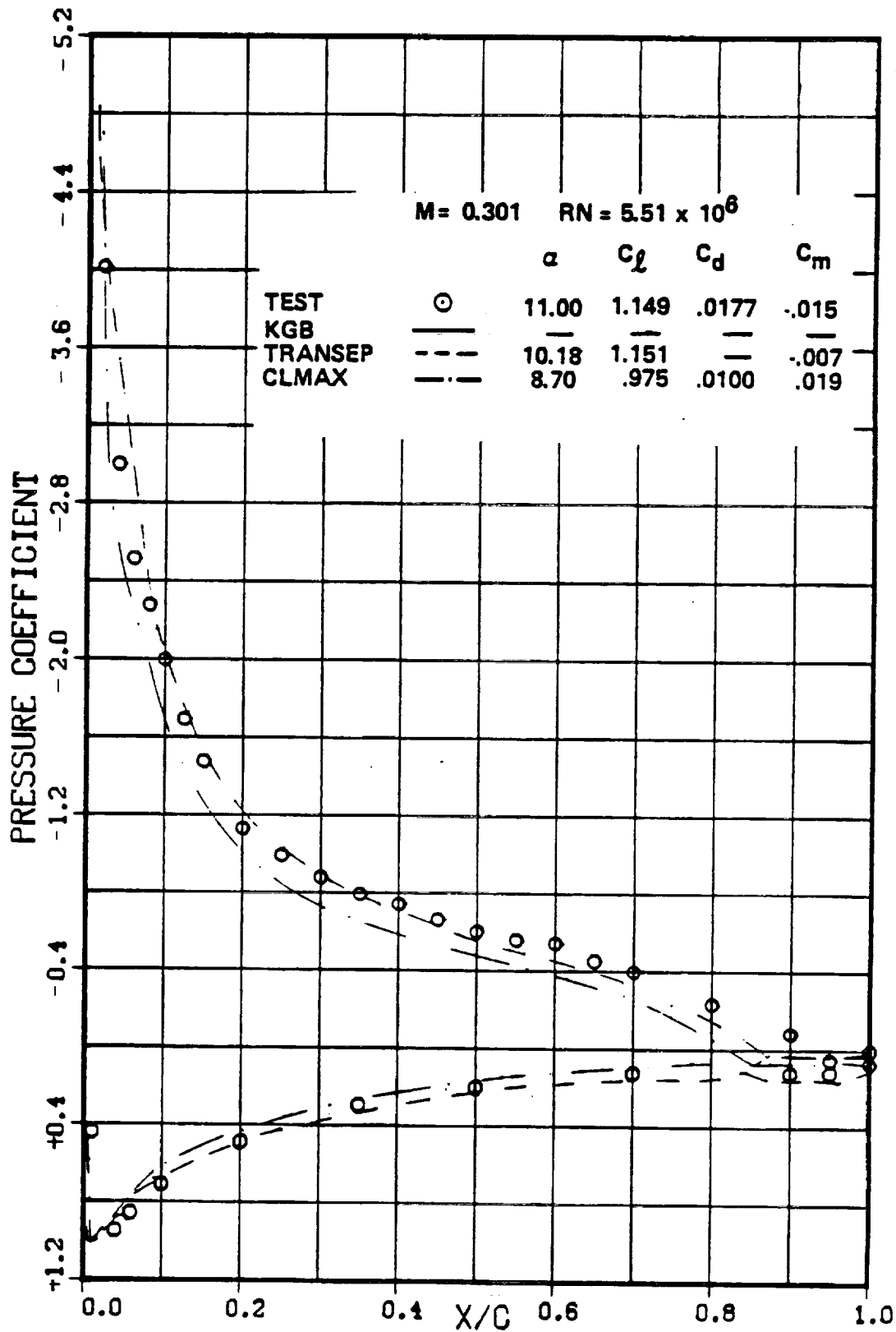


(a) SC1095

Figure 34.—Pressure coefficient correlation, $M = 0.30$, $C_1 = 1.2$.

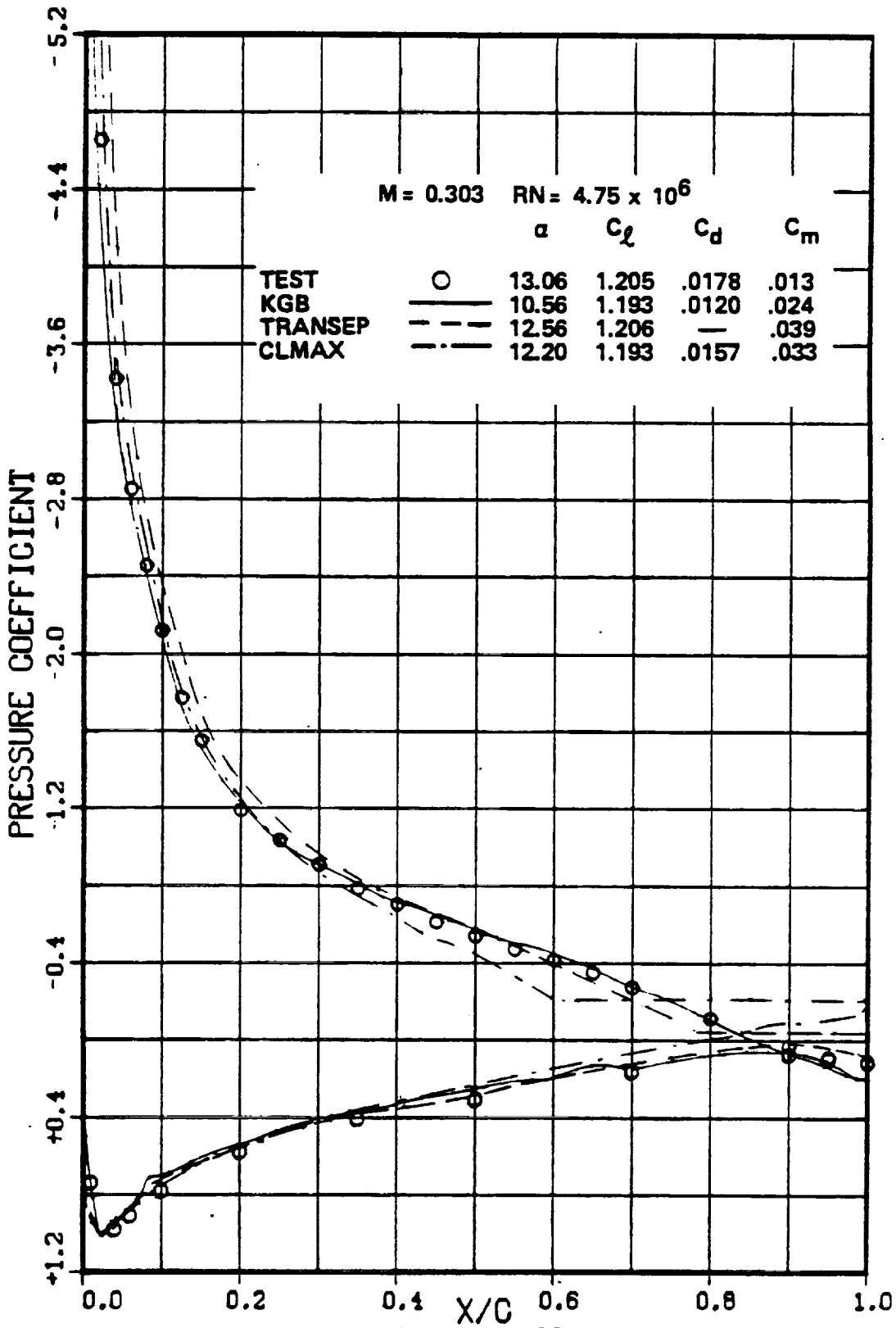


(b) SSC-A09
Figure 34.—Continued.

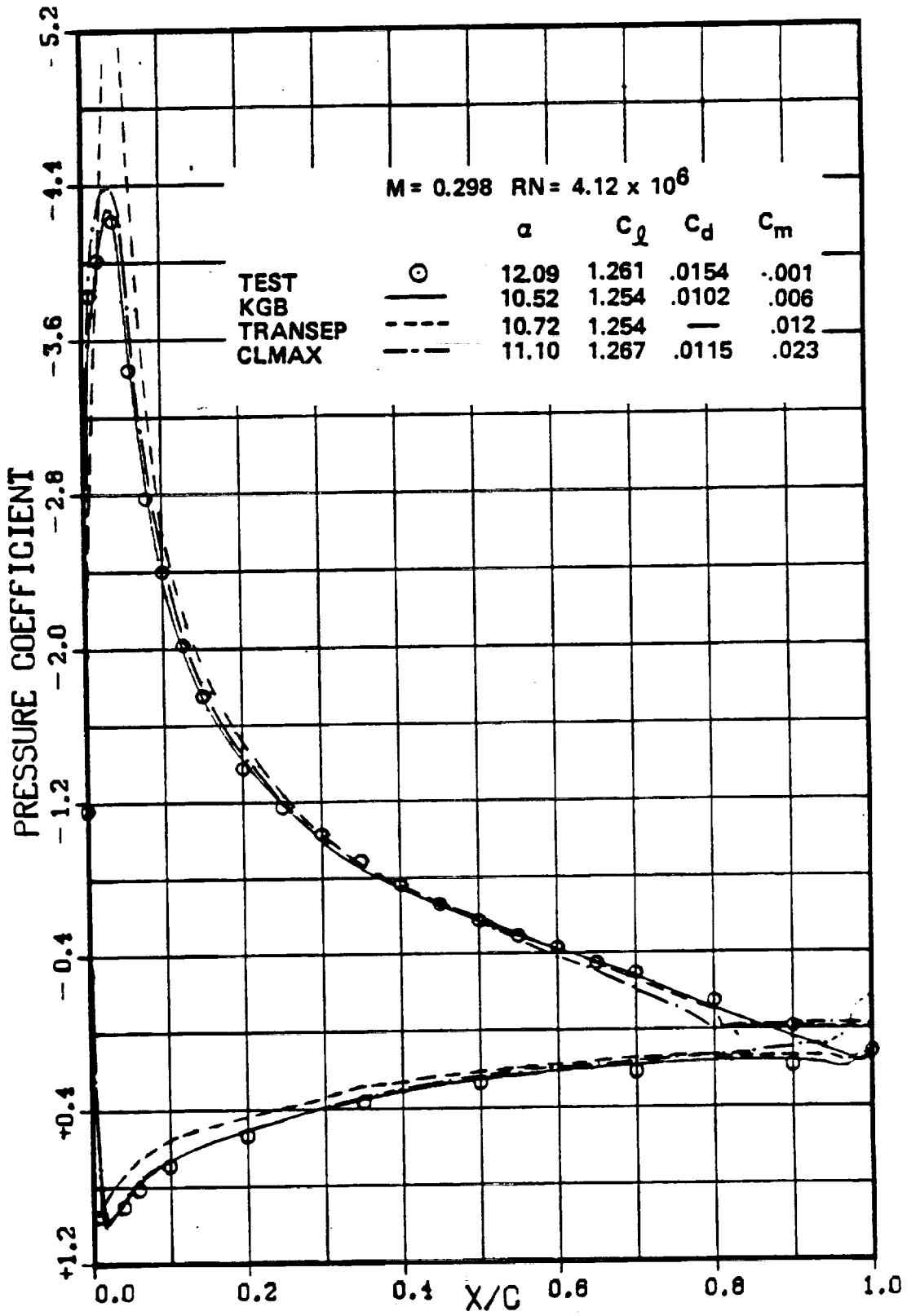


(c) SSC-A07

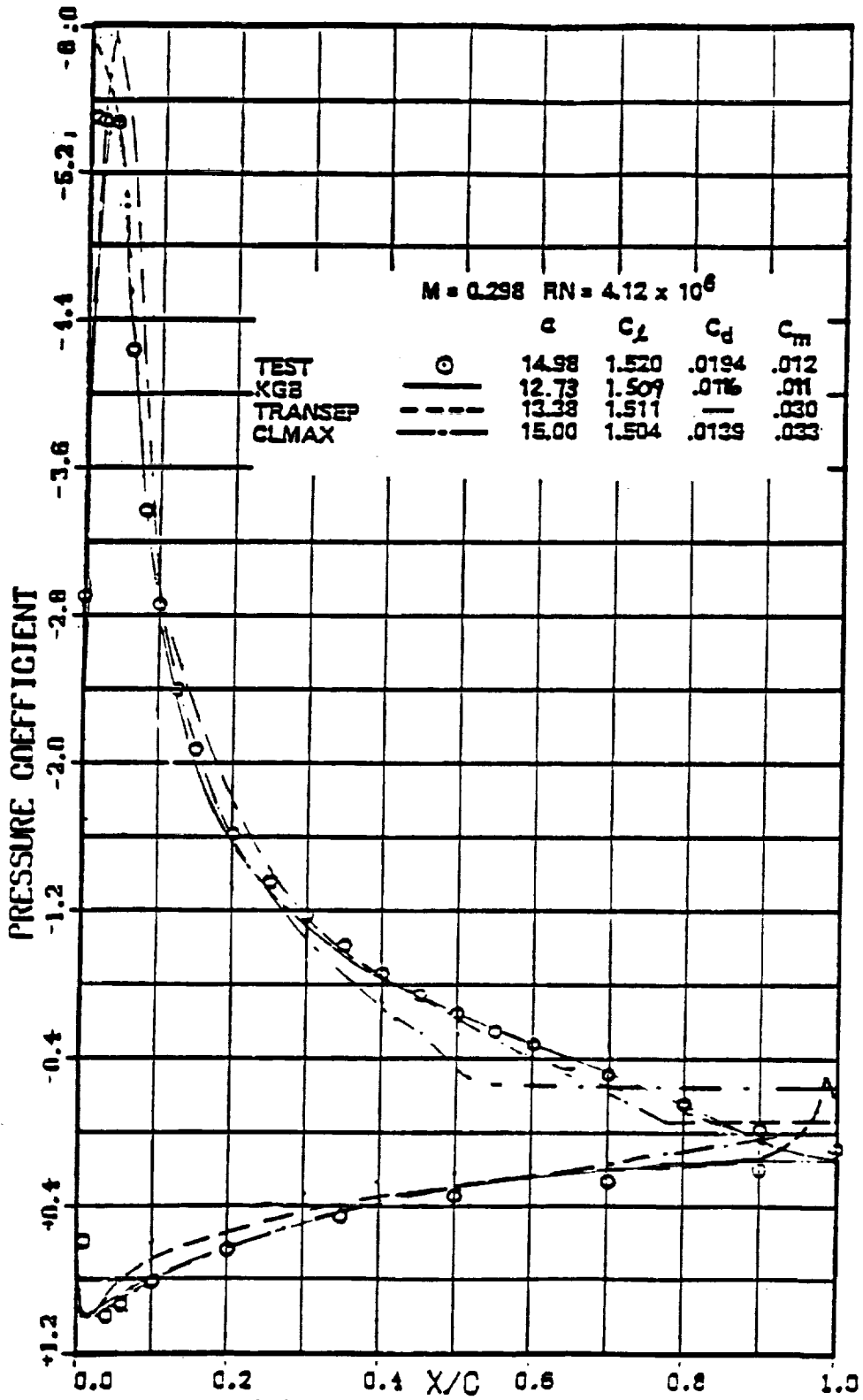
Figure 34.-Continued.



(d) SSC-B08
Figure 34.-Continued.

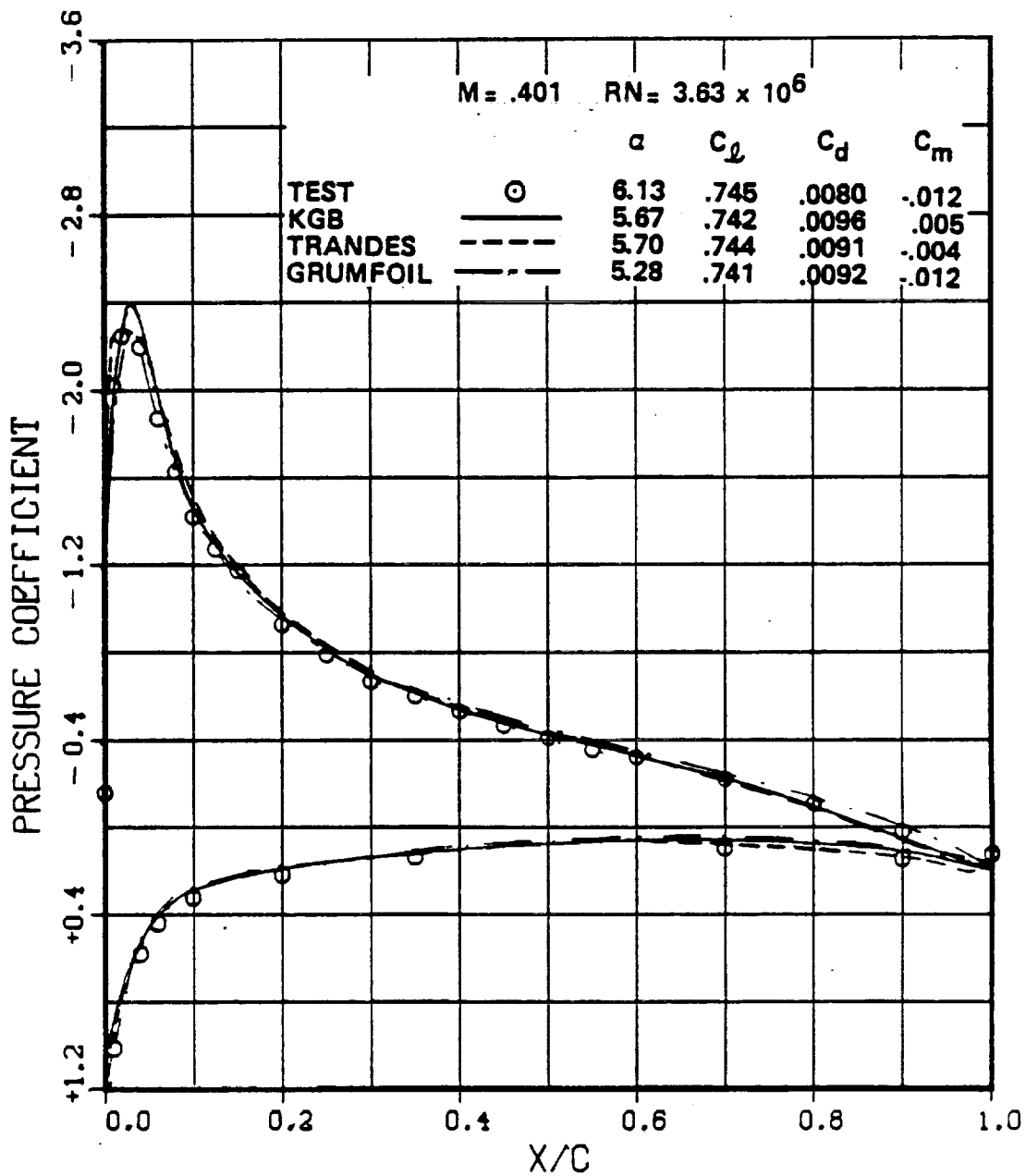


(e) SC1094 R8
Figure 34.—Continued.



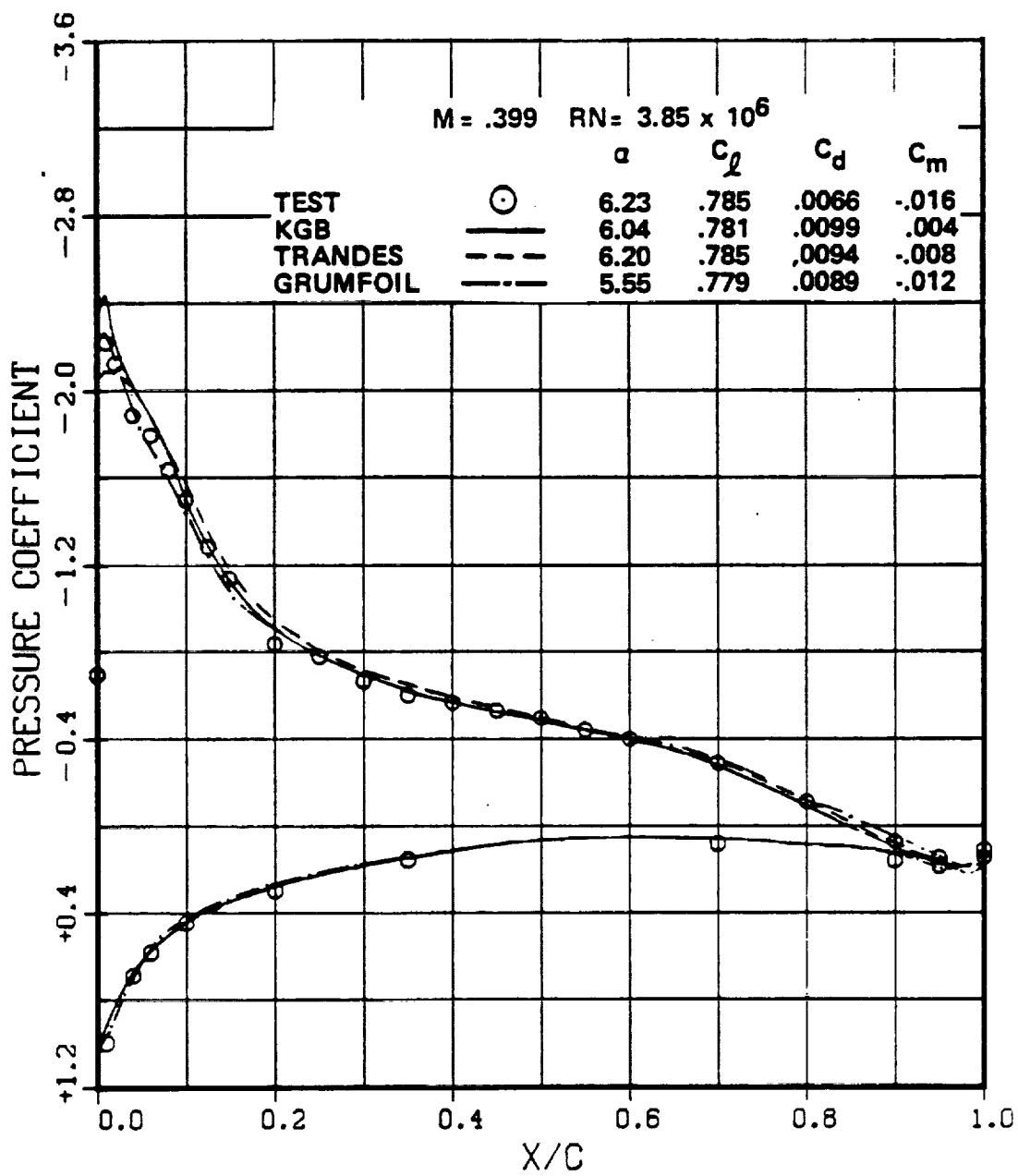
(f) SC1094 R8, $C_1 = 1.5$

Figure 34.- Concluded.



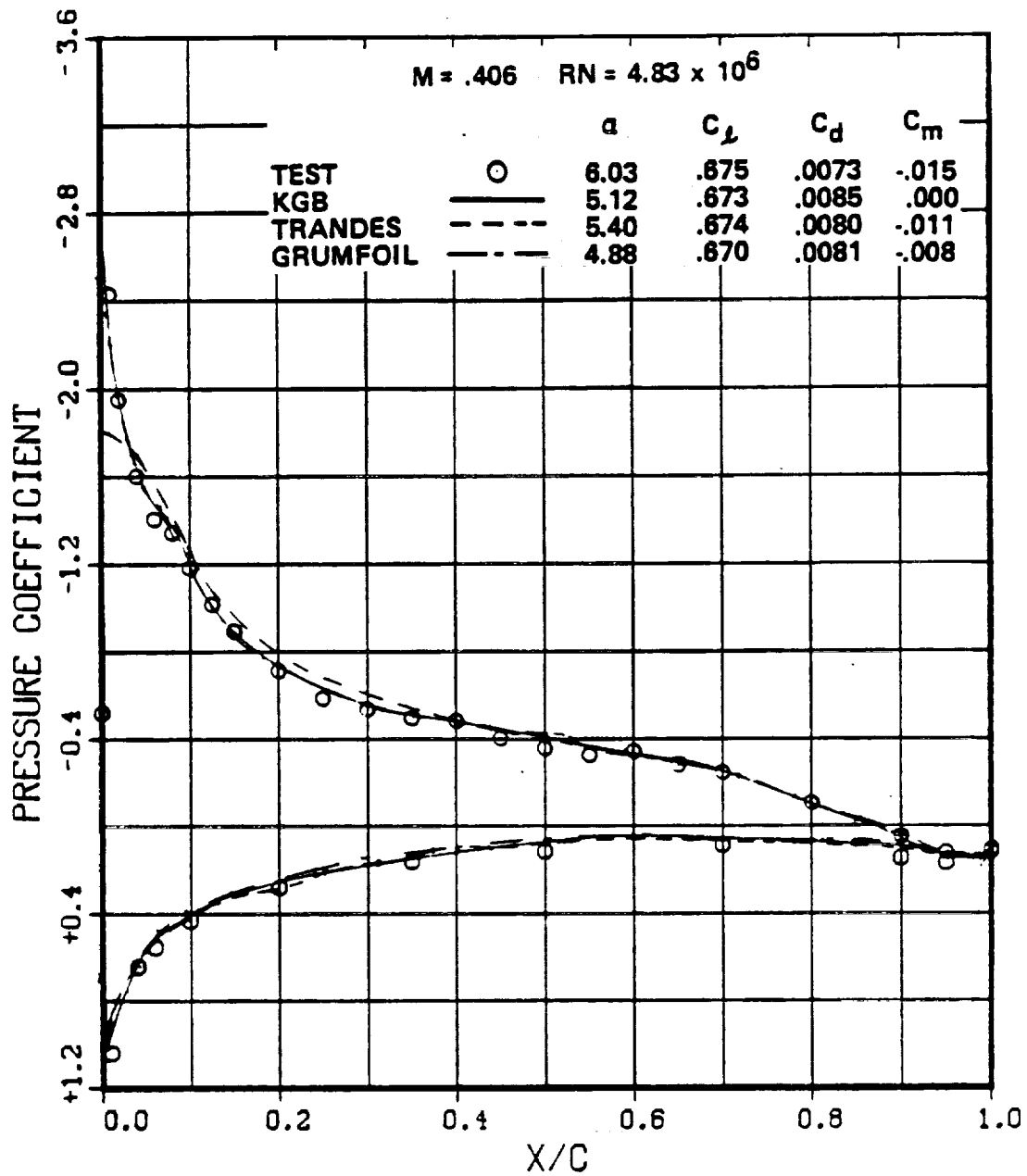
(a) SC1095

Figure 35.- Pressure coefficient correlation, $M = 0.4$, $C_L = .7$.



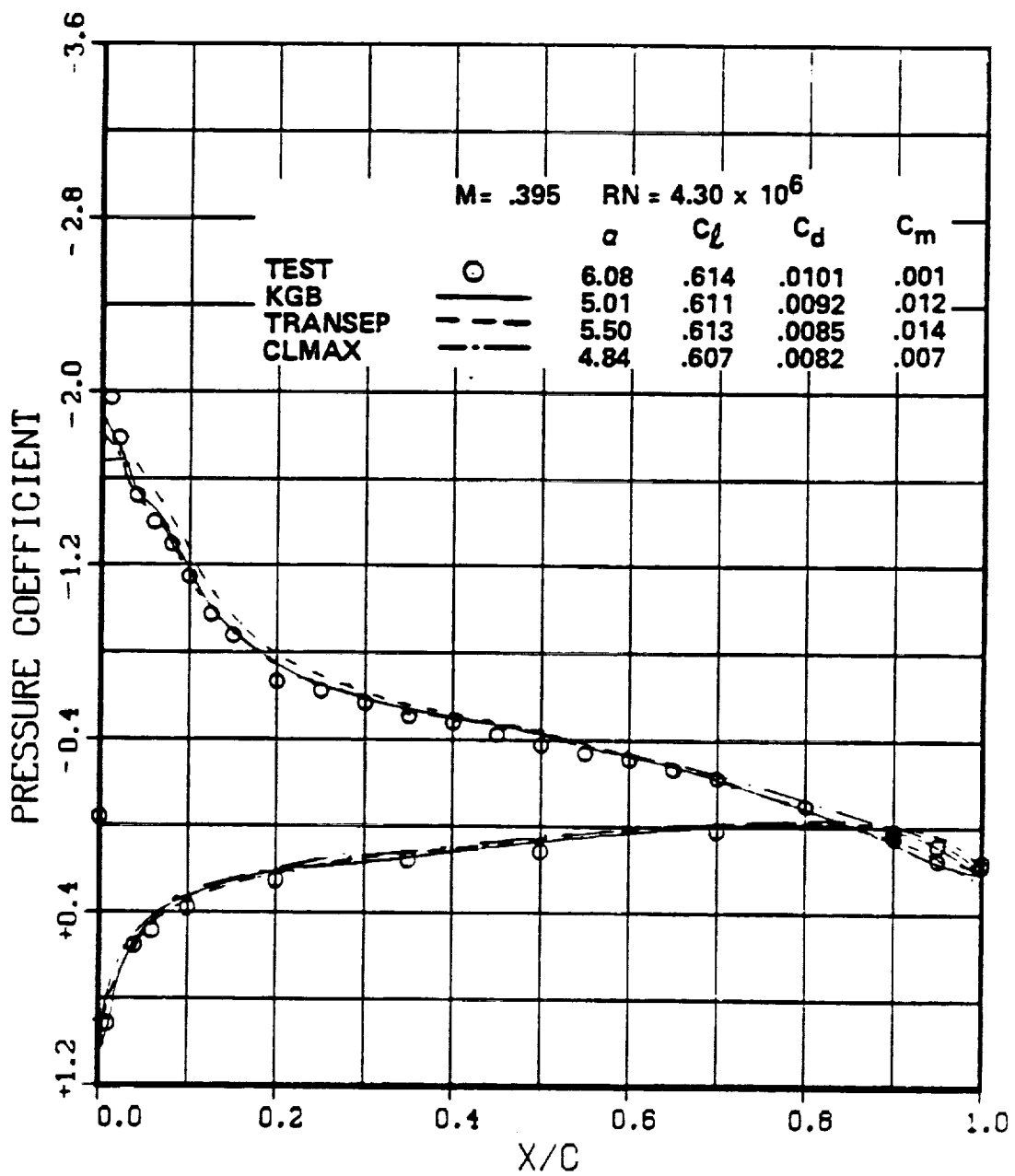
(b) SSC-A09

Figure 35.—Continued.



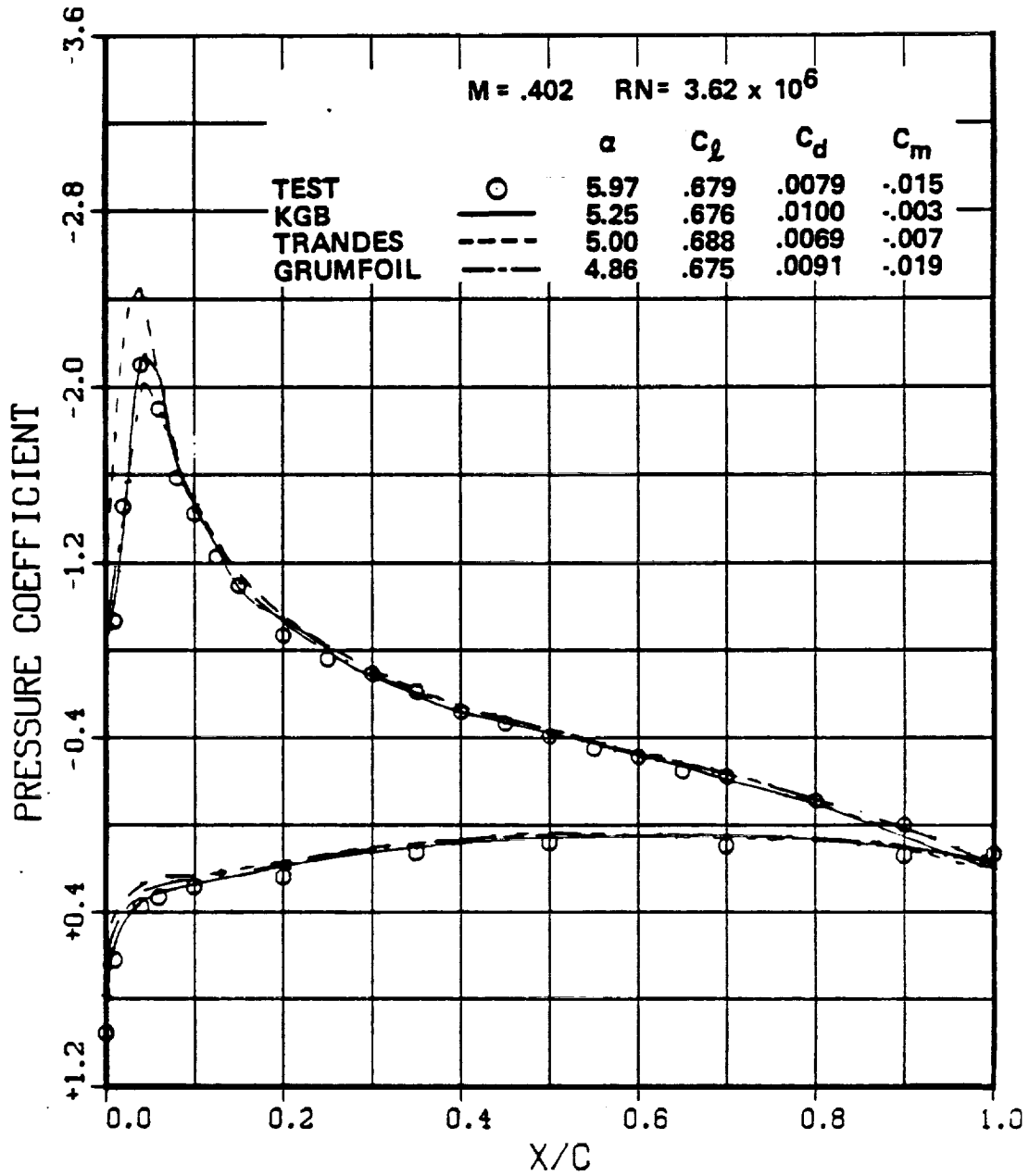
(c) SSC-A07

Figure 35.- Continued.



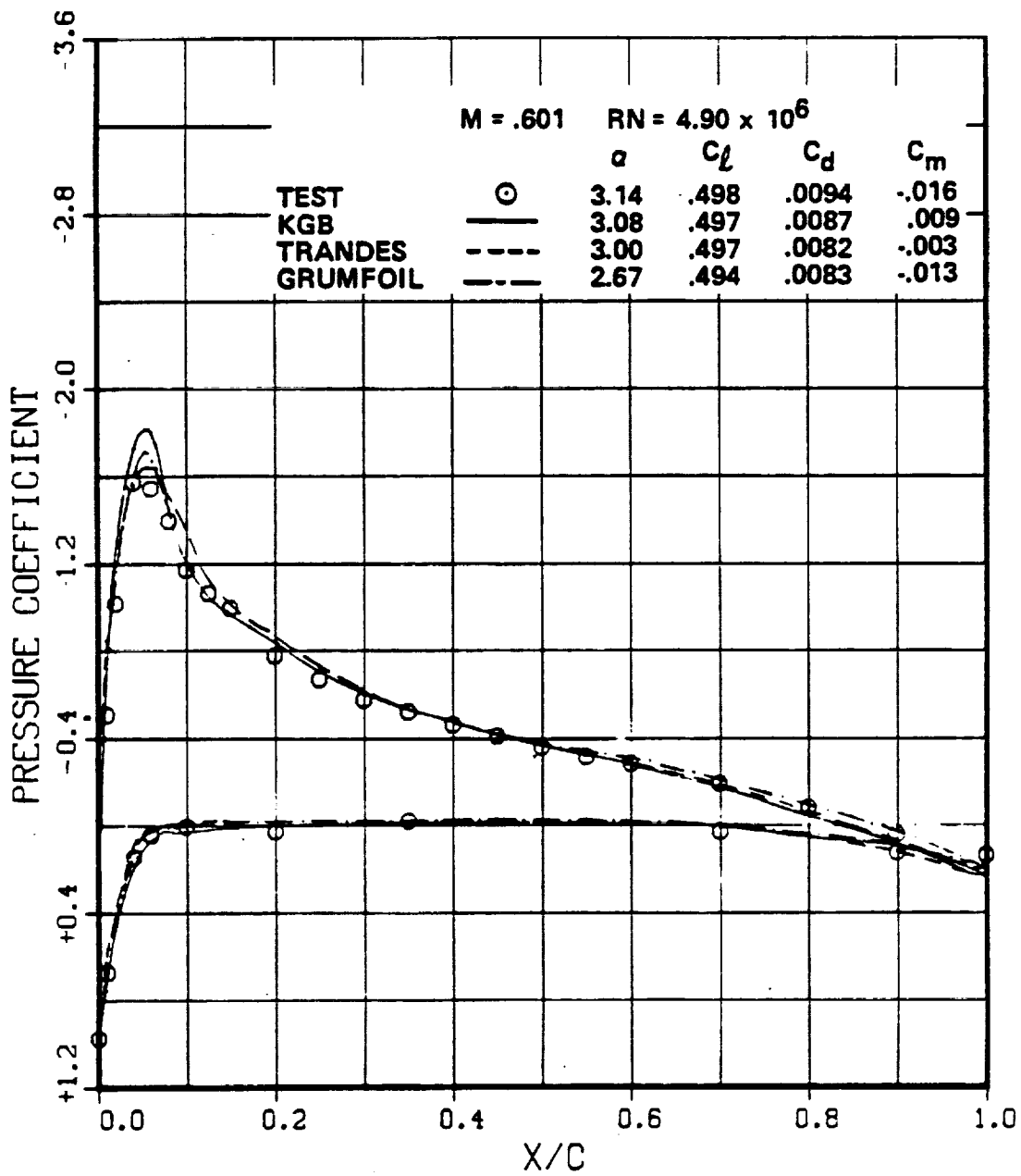
(d) SSC-B08

Figure 35.- Continued.



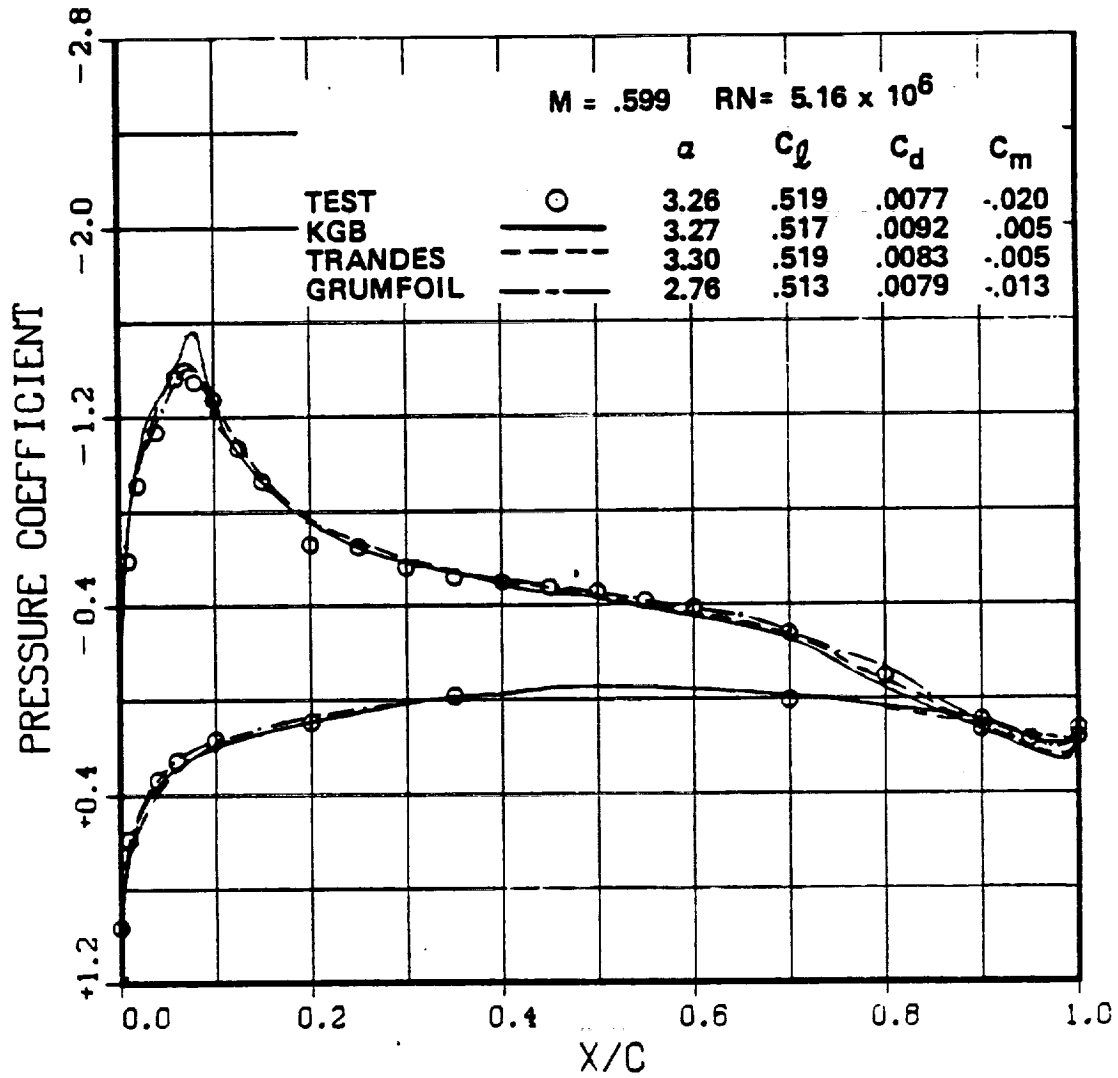
(e) SC1094 R8

Figure 35.- Concluded.



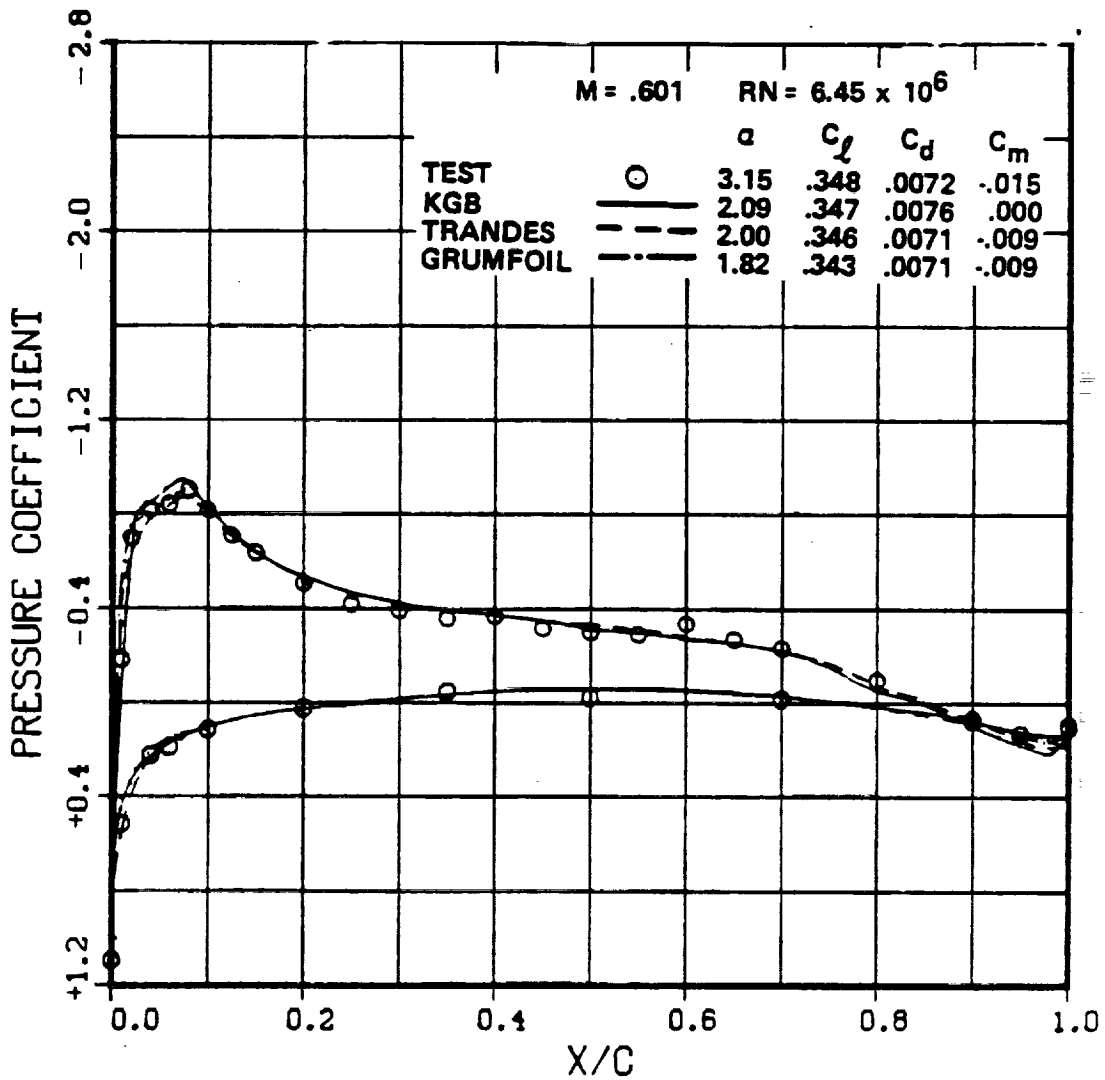
(a) SC1095

Figure 36.- Pressure coefficient correlation, $M = 0.6$, $C_1 = .4$.



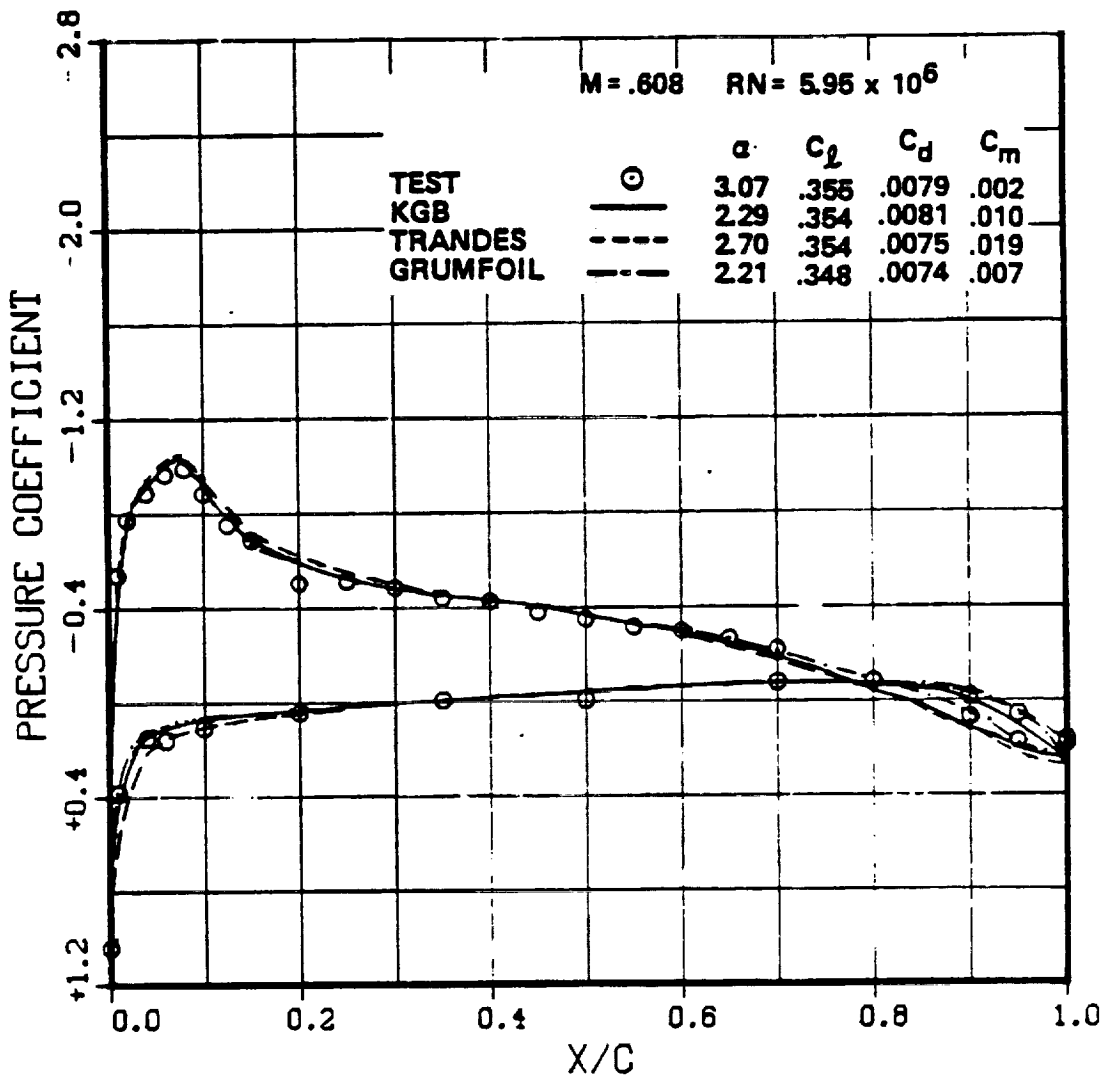
(b) SSC-A09

Figure 36. - Continued.



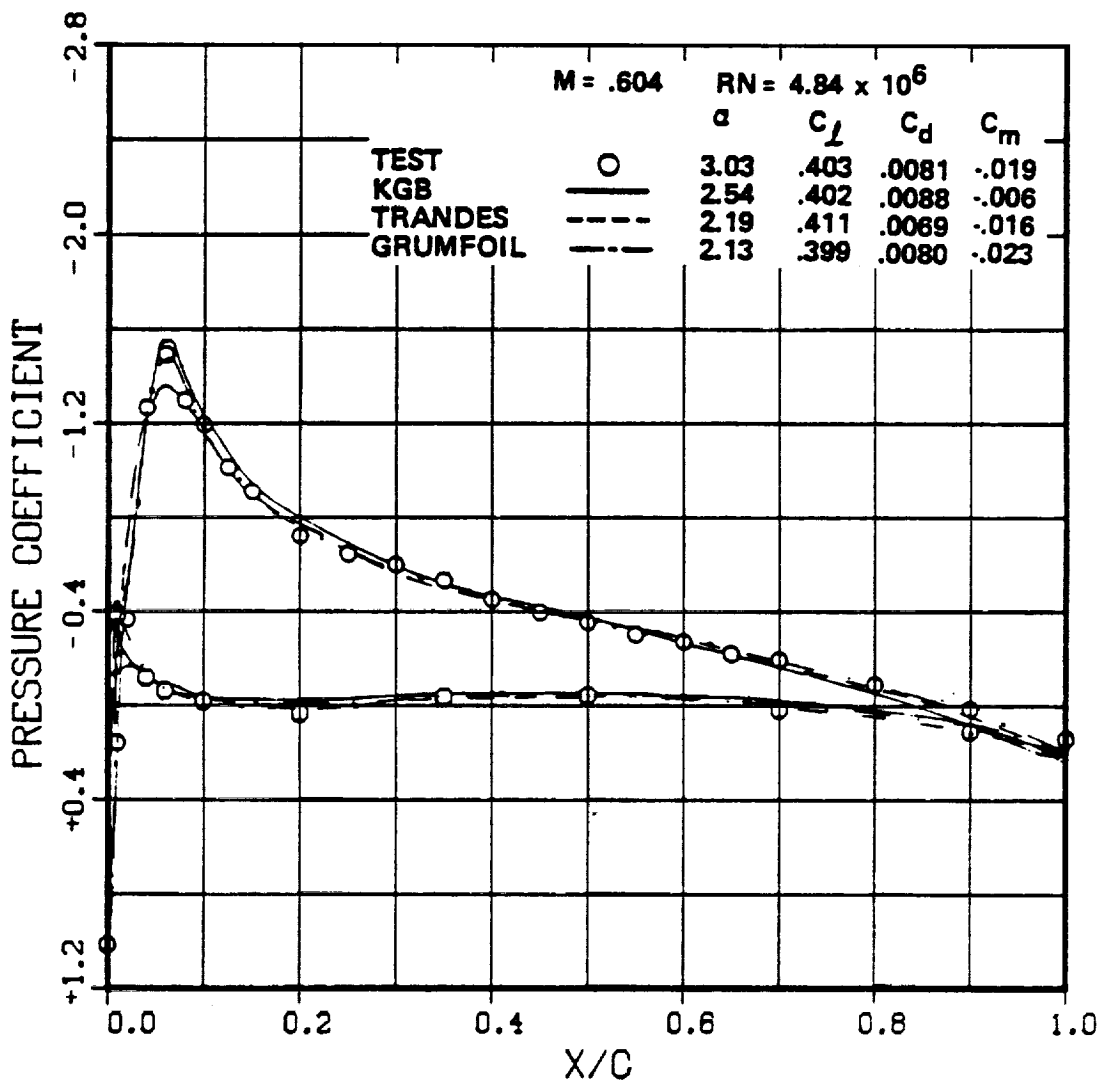
(c) SSC-A07

Figure 36. - Continued.



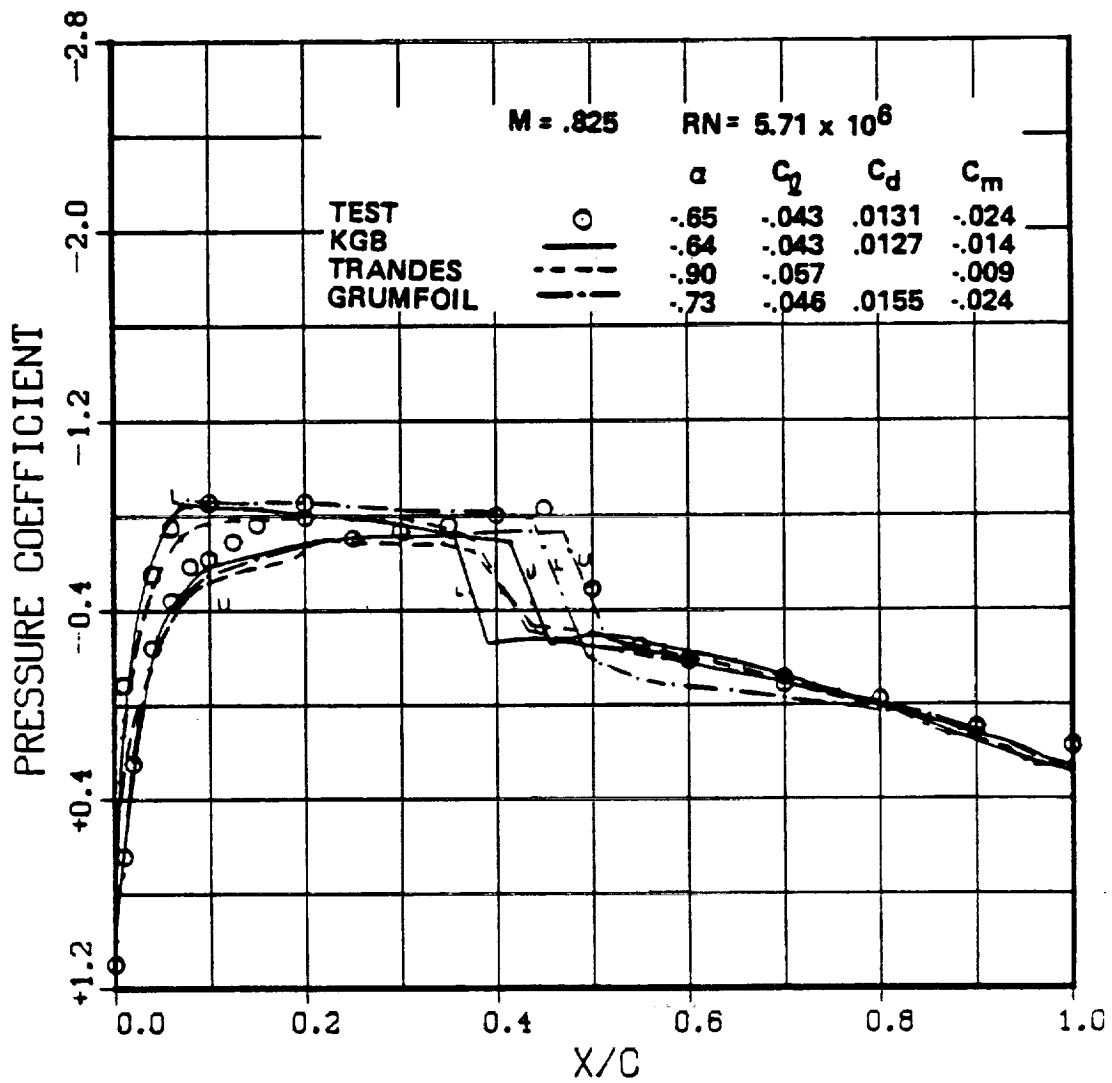
(d) SSC-B08

Figure 36.- Continued.



(e) SC1094 R8

Figure 36. - Concluded.



(a) SC1095

Figure 37.—Pressure coefficient correlation, $M = 0.825$, $C_1 = 0$.

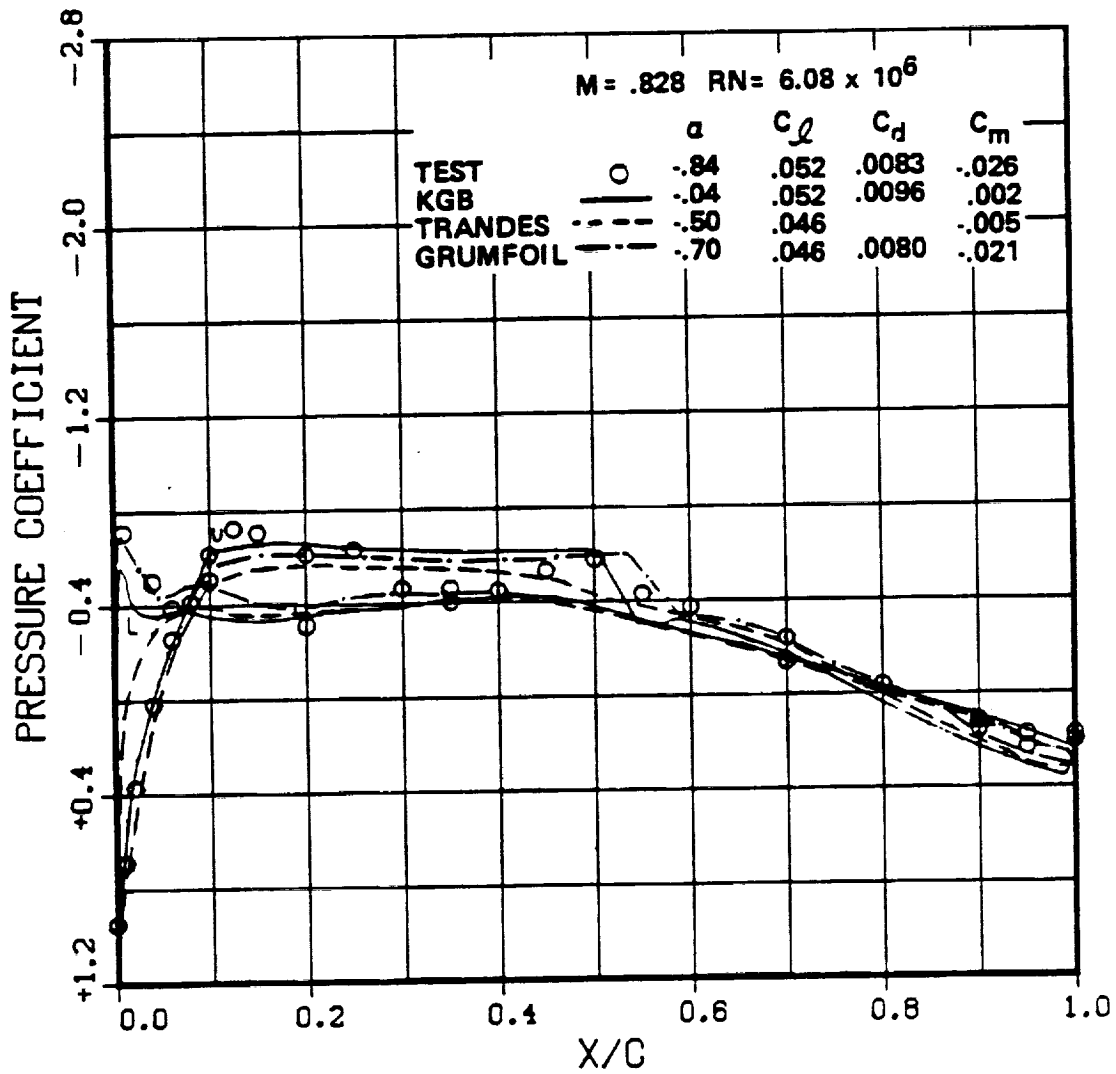
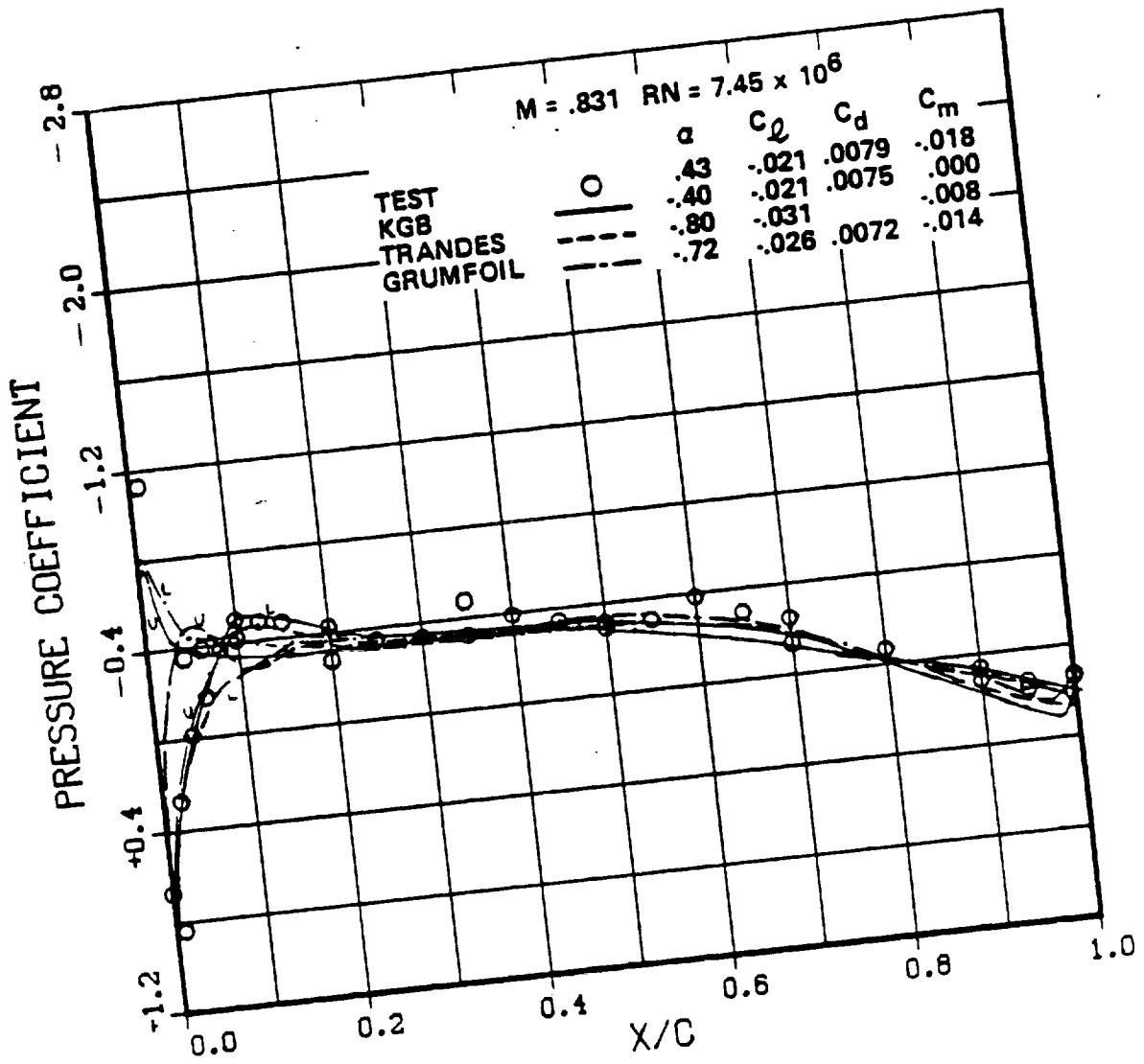
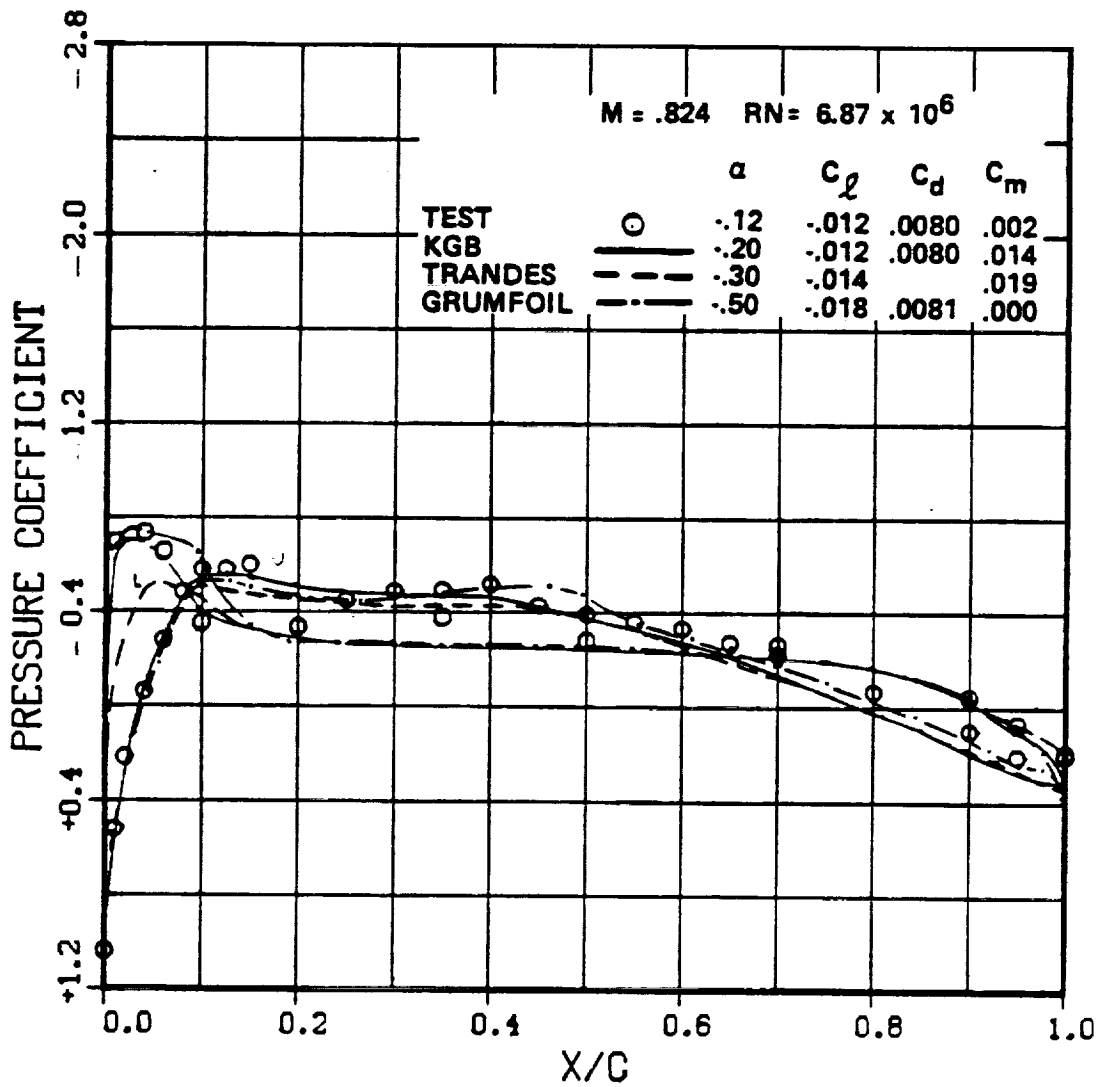


Figure 37.—Continued.



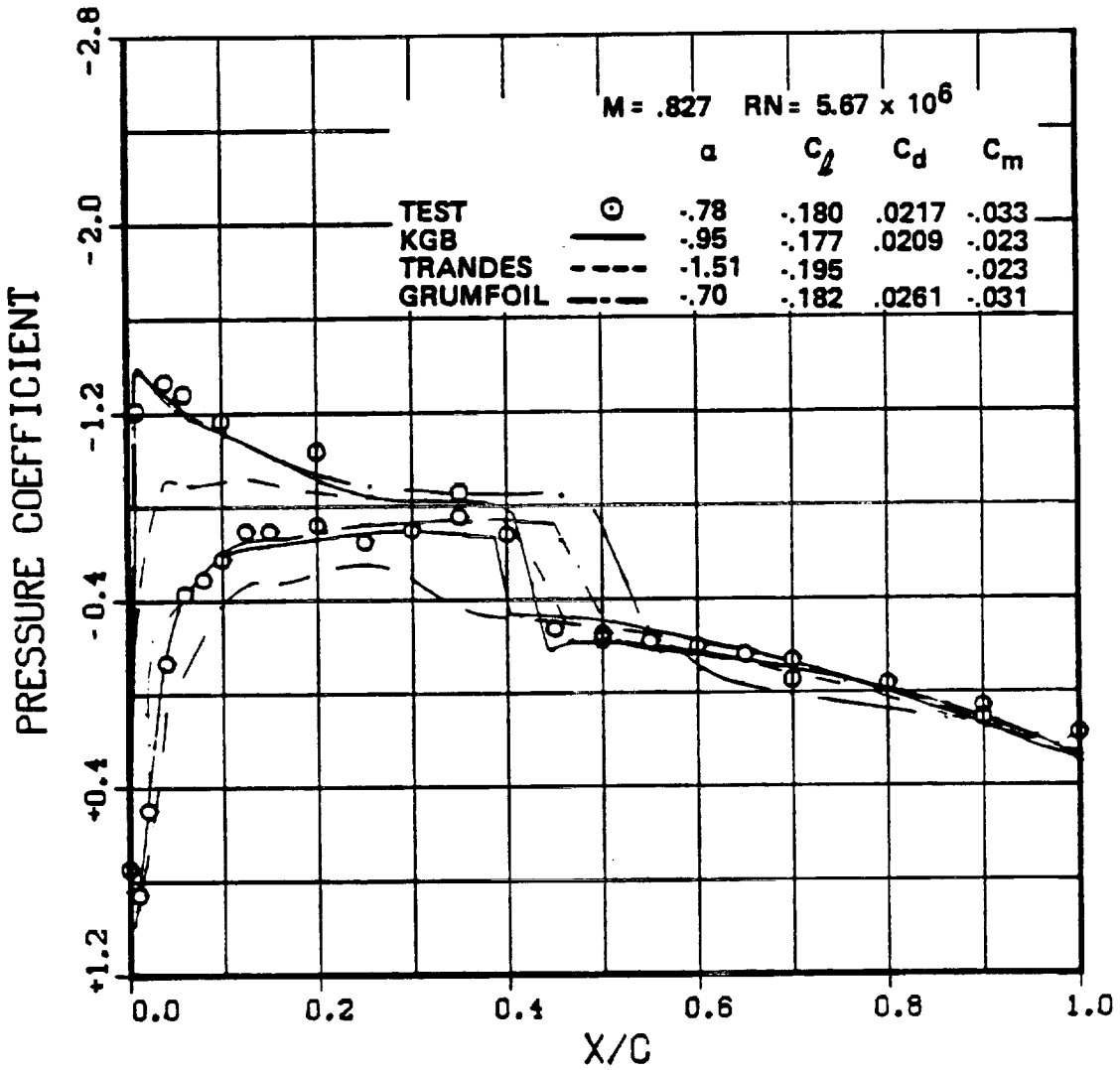
(c) SSC-A07

Figure 37. - Continued.



(d) SSC-B08

Figure 37.-Continued.



(e) SC1094 R8

Figure 37.—Concluded.

APPENDIX A
TABULATED DATA

Heading Description for Tabulated Data

ALPHA Angle of attack, deg
CDBAL Balance - derived drag coefficient
CDP Wake rake - derived drag coefficient
CLBAL Balance - derived lift coefficient
CLP Airfoil surface pressure - derived
CMBAL Balance - derived quarter chord pitching moment
 coefficient
CMP Airfoil surface pressure - derived pitching moment
 coefficient

Configuration 1 = SC1095
Configuration 2 = SSC-A09
Configuration 3 = SSC-A07
Configuration 4 = SSC-B08
Configuration 5 = SC1095 R8
Configuration 6-10 = SSC-A09 Out-of-Contour Test Configuration
 (See page 9 and Table IV)

L/D BAL Balance - derived lift-drag ratio
L/D P Surface and wake rake pressure derived lift-drag ratio
MACH Free stream Mach number
PT Data point number within each run
RN Reynolds number based on airfoil chord
RUN Test run number (see also Table V)

RUN 37 MACH=.810 RN= 5.50*10**6 CONFIGURATION 1
 PT ALPHA CLBAL CDBAL CFBAL CLP CDP CMP L/D BAL L/D P
 1 -6.21 -.469 0.0050 0.014 -.679 0.0090 0.031 -5.7 -7.7

RUN 38 MACH=.830 RN= 5.62*10**6 CONFIGURATION 1
 PT ALPHA CLBAL CDBAL CFBAL CLP CDP CMP L/D BAL L/D P
 1 -6.28 -.469 0.0079 0.022 -.637 0.0066 0.035 -5.3 -7.5

RUN 39 MACH=.399 RN= 3.57*10**6 CONFIGURATION 1
 PT ALPHA CLBAL CDBAL CFBAL CLP CDP CMP L/D BAL L/D P
 1 -0.03 0.137 -.030 0.020 0.0075 -.017 2.7
 2 -0.20 0.209 -.029 0.004 0.0076 -.016 11.1
 3 6.15 0.094 -.012 0.747 0.0001 -.012 92.5

RUN 40 MACH=.403 RN= 3.61*10**6 CONFIGURATION 1
 PT ALPHA CLBAL CDBAL CFBAL CLP CDP CMP L/D BAL L/D P
 1 0.00 0.230 -.027 0.122 0.0069 -.017 17.7
 2 6.13 0.007 -.012 0.753 0.0075 -.012 99.5
 3 5.91 0.073 -.013 0.731 0.0075 -.012 97.7

RUN 41 MACH=.702 RN= 5.30*10**6 CONFIGURATION 1
 PT ALPHA CLBAL CDBAL CFBAL CLP CDP CMP L/D BAL L/D P
 1 -0.79 0.035 0.0104 -.010 0.013 0.0075 -.022 3.3 1.0
 2 -0.49 0.077 0.0094 -.017 0.050 0.0077 -.023 8.2 6.4
 3 -0.50 0.066 0.0093 -.017 0.046 0.0077 -.023 6.9 5.6
 4 -0.52 0.069 0.0099 -.017 0.046 0.0076 -.023 6.9 5.0

RUN 42 MACH=.754 RN= 5.53*10**6 CONFIGURATION 1
 PT ALPHA CLBAL CDBAL CFBAL CLP CDP CMP L/D BAL L/D P
 1 -0.61 0.032 0.0132 -.016 0.014 0.0089 -.027 2.4 1.5

RUN 43 MACH=.770 RN= 5.50*10**6 CONFIGURATION 1
 PT ALPHA CLBAL CDBAL CFBAL CLP CDP CMP L/D BAL L/D P
 1 -0.65 0.034 0.0072 -.019 0.031 0.0097 -.026 4.0 3.2

RUN 31 MACH=.603 RN= 5.63*10**6 CONFIGURATION 1
 PT ALPHA CLBAL CDBAL CFBAL CLP CDP CMP L/D BAL L/D P
 1 -0.06 -.112 0.0106 -.016 -.052 0.0123 -.026 -6.0 -6.2
 2 -0.90 0.066 0.0205 -.009 0.113 0.0123 -.023 3.2 9.1

RUN 32 MACH=.396 RN= 3.45*10**6 CONFIGURATION 1
 PT ALPHA CLBAL CDBAL CFBAL CLP CDP CMP L/D BAL L/D P
 1 0.01 0.079 -.006 0.090 -.017
 2 6.13 0.750 0.012 0.754 -.013

RUN 33 MACH=.590 RN= 4.77*10**6 CONFIGURATION 1
 PT ALPHA CLBAL CDBAL CFBAL CLP CDP CMP L/D BAL L/D P
 1 0.03 0.112 -.008 0.120 0.0077 -.019 15.6
 2 3.16 0.510 0.004 0.405 0.0084 -.016 57.7
 3 6.20 0.000 0.0004 0.023 0.0106 -.001 104.4
 4 9.31 1.003 0.0718 0.017 0.937 0.0509 -.012 14.0 19.7
 5 11.33 1.077 0.1104 0.009 0.979 0.0707 -.031 9.0 13.4
 6 9.31 1.009 0.0700 0.017 0.935 0.0590 -.011 14.3 15.7
 7 6.20 0.091 0.0090 0.023 0.011 0.0192 -.000 90.6 41.9
 8 3.16 0.512 0.004 0.403 0.0085 -.015 56.4
 9 0.03 0.107 -.000 0.116 0.0073 -.019 16.0
 10 -3.11 -3.19 -.020 0.206 0.0084 -.022 -34.4
 11 0.02 0.092 -.008 0.099 0.0072 -.019 13.0

RUN 34 MACH=.697 RN= 5.20*10**6 CONFIGURATION 1
 PT ALPHA CLBAL CDBAL CFBAL CLP CDP CMP L/D BAL L/D P
 1 -6.24 -.597 0.0663 -.029 -.669 0.0504 -.017 -9.0 -13.5

RUN 35 MACH=.753 RN= 5.41*10**6 CONFIGURATION 1
 PT ALPHA CLBAL CDBAL CFBAL CLP CDP CMP L/D BAL L/D P
 1 -6.22 -.500 0.0641 -.013 -.692 0.0635 -.012 -7.9 -11.1

RUN 36 MACH=.793 RN= 5.56*10**6 CONFIGURATION 1
 PT ALPHA CLBAL CDBAL CFBAL CLP CDP CMP L/D BAL L/D P
 1 -6.22 -.494 0.0752 0.001 -.662 0.0840 0.010 -6.6 -0.0

RUN 55 MACH=0.401 RN= 3.60*10**6 CONFIGURATION 1
PT ALPHA CLBAL CDBAL CFBAL CLP COP CMP L/D BAL L/D P
1 -0.26 0.167 -0.020 0.007 -0.015
2 0.16 0.200 -0.020 0.132 -0.015
3 -0.03 0.170 -0.021 0.114 -0.015
4 6.04 0.062 -0.006 0.749 -0.011
5 4.01 0.060 -0.007 0.744 -0.010
6 -0.05 0.101 -0.021 0.112 -0.015

RUN 56 MACH=0.900 RN= 6.04*10**6 CONFIGURATION 1
PT ALPHA CLBAL CDBAL CFBAL CLP COP CMP L/D BAL L/D P
1 -0.07 0.013 0.0977 -0.034 0.100 -0.049 0.1
2 -2.20 -0.095 0.1007 -0.010 -0.077 -0.012 -0.9
3 -1.09 -0.046 0.1009 -0.022 0.039 -0.030 -0.5
4 0.15 0.022 0.1005 -0.033 0.117 -0.052 0.2
5 0.91 0.075 0.1003 -0.040 0.176 -0.066 0.0
6 0.05 0.010 0.1027 -0.033 0.105 -0.051 0.1
7 -0.72 -0.020 0.0970 -0.026 0.055 -0.042 -0.3

RUN 57 MACH=1.071 RN= 5.94*10**6 CONFIGURATION 1
PT ALPHA CLBAL CDBAL CFBAL CLP COP CMP L/D BAL L/D P
1 0.15 0.030 0.0906 -0.032 0.106 -0.049 0.3
2 -1.23 -0.045 0.0883 -0.019 0.010 -0.034 -0.5
3 0.01 0.021 0.0916 -0.030 0.099 -0.047 0.2
4 0.70 0.057 0.0942 -0.036 0.144 -0.056 0.6
5 -0.74 -0.025 0.0900 -0.023 0.049 -0.041 -0.3
6 0.09 0.020 0.0924 -0.030 0.101 -0.040 0.2
7 -0.56 -0.017 0.0893 -0.024 0.059 -0.042 -0.2

RUN 60 MACH=0.399 RN= 3.05*10**6 CONFIGURATION 2
PT ALPHA CLBAL CDBAL CFBAL CLP COP CMP L/D BAL L/D P
1 -0.24 0.039 0.114 0.0066 -0.015 17.1
2 6.33 0.735 -0.022 0.700 0.0071 -0.015 109.0
3 6.23 0.725 -0.016 0.783 0.0066 -0.016 119.3
4 5.94 0.700 -0.022 0.751 0.0069 -0.016 109.2
5 0.21 0.073 0.156 0.0067 -0.015 23.4
6 -0.16 0.036 0.110 0.0070 -0.014 16.7
7 0.01 0.055 0.141 0.0071 -0.015 19.9

RUN 44 MACH=0.001 RN= 5.66*10**6 CONFIGURATION 1
PT ALPHA CLBAL CDBAL CFBAL CLP COP CMP L/D BAL L/D P
1 -0.64 0.013 0.0117 -0.010 0.003 0.0100 -0.020 1.1 0.3
RUN 45 MACH=0.025 RN= 5.71*10**6 CONFIGURATION 1
PT ALPHA CLBAL CDBAL CFBAL CLP COP CMP L/D BAL L/D P
1 -0.65 -0.011 0.0216 -0.017 -0.043 0.0131 -0.024 -0.5 -3.2
RUN 46 MACH=0.045 RN= 5.74*10**6 CONFIGURATION 1
PT ALPHA CLBAL CDBAL CFBAL CLP COP CMP L/D BAL L/D P
1 -0.65 -0.010 0.0316 -0.021 0.020 0.0179 -0.043 -0.6 1.5
2 -0.44 0.014 0.0290 -0.026 0.059 0.0191 -0.051 0.5 3.1

RUN 40 MACH=0.401 RN= 3.59*10**6 CONFIGURATION 1
PT ALPHA CLBAL CDBAL CFBAL CLP COP CMP L/D BAL L/D P
1 -0.11 0.177 -0.023 0.099 -0.017
2 6.16 0.049 -0.007 0.744 -0.012
3 -0.26 0.146 -0.023 0.005 -0.017

RUN 49 MACH=0.920 RN= 6.05*10**6 CONFIGURATION 1
PT ALPHA CLBAL CDBAL CFBAL CLP COP CMP L/D BAL L/D P
1 -0.25 0.022 0.0643 -0.001 -0.019 0.004 0.3
2 -2.39 -0.146 0.0761 -0.021 -0.112 -0.016 -1.9
3 -1.17 -0.047 0.0620 0.002 -0.040 -0.017 -0.7
4 -1.94 -0.106 0.0650 -0.007 -0.079 -0.076 -1.6
RUN 51 MACH=0.404 RN= 3.64*10**6 CONFIGURATION 1
PT ALPHA CLBAL CDBAL CFBAL CLP COP CMP L/D BAL L/D P
1 -0.22 0.105 -0.020 0.102 -0.017
2 6.04 0.099 -0.004 0.744 -0.012

RUN 52 MACH=0.925 RN= 6.01*10**6 CONFIGURATION 1
PT ALPHA CLBAL CDBAL CFBAL CLP COP CMP L/D BAL L/D P
1 0.01 0.051 0.0656 -0.004 0.032 0.005 0.0
2 1.01 0.171 0.0617 -0.007 0.152 -0.005 2.0
3 2.00 0.256 0.0604 -0.004 0.226 0.003 3.7
4 3.10 0.310 0.0766 -0.005 0.300 -0.005 4.2
5 4.09 0.353 0.0842 -0.001 0.357 -0.012 4.2
6 5.10 0.395 0.0945 -0.004 0.301 -0.009 4.1
7 1.03 -0.060 0.0689 -0.002 -0.036 -0.001 -1.0
8 -0.31 -0.020 0.0590 -0.005 0.027 -0.010 -0.3

Table with columns: RUN #, ALPHA, CLBAL, CDBAL, CFBAL, CLP, CDP, CMP, L/D, BAL, L/D, P. Includes sub-sections for RUN 93, RUN 97, RUN 90, and RUN 99.

Table with columns: RUN #, ALPHA, CLBAL, CDBAL, CFBAL, CLP, CDP, CMP, L/D, BAL, L/D, P. Includes sub-sections for RUN 95, RUN 100, and RUN 101.

Table with columns: RUN #, ALPHA, CLBAL, CDBAL, CFBAL, CLP, CDP, CMP, L/D, BAL, L/D, P. Includes sub-sections for RUN 95 and RUN 101.

RUN 102 MACH=.605 RN= 7.30*10**6 CONFIGURATION 3
 PT ALPHA CLBAL CDBAL CFBAL CLP CDP CMP L/D BAL L/D P
 1 0.43 -.034 0.0039 -.014 -.025 0.0077 -.019 -0.6 -3.2
 2 0.45 -.032 0.0042 -.013 -.024 0.0076 -.019 -7.6 -3.1

RUN 103 MACH=.031 RN= 7.45*10**6 CONFIGURATION 3
 PT ALPHA CLBAL CDBAL CFBAL CLP CDP CMP L/D BAL L/D P
 1 0.43 -.037 0.0047 -.012 -.021 0.0079 -.010 -5.5 -2.6
 2 0.43 -.036 0.0078 -.011 -.023 0.0083 -.017 -4.6 -2.7

RUN 104 MACH=.057 RN= 7.52*10**6 CONFIGURATION 3
 PT ALPHA CLBAL CDBAL CFBAL CLP CDP CMP L/D BAL L/D P
 1 0.45 -.007 0.0116 0.002 -.004 0.0101 -.012 -0.6 -0.4
 2 0.45 -.012 0.0103 0.001 0.002 0.0100 -.013 -1.2 0.2
 3 0.19 -.007 0.0103 0.012 -.007 0.0115 0.002 -9.4 -7.4
 4 1.52 0.134 0.0064 -.020 0.115 0.0091 -.014 15.6 12.5
 5 2.64 0.254 0.0024 -.046 0.200 0.0119 -.046 100.2 23.9
 6 2.62 0.266 0.0023 -.047 0.209 0.0113 -.043 114.1 25.2
 7 0.53 -.002 0.0119 -.001 -.001 0.0103 -.011 -0.1 -0.1
 8 0.51 0.004 0.0132 0.001 0.005 0.0107 -.011 0.3 0.5

RUN 105 MACH=.603 RN= 7.61*10**6 CONFIGURATION 3
 PT ALPHA CLBAL CDBAL CFBAL CLP CDP CMP L/D BAL L/D P
 1 0.56 0.032 0.0175 0.005 -.020 0.0143 0.020 1.0 -1.9
 2 0.56 0.030 0.0166 0.005 -.031 0.0146 0.023 1.0 -2.1

RUN 106 MACH=.901 RN= 7.61*10**6 CONFIGURATION 3
 PT ALPHA CLBAL CDBAL CFBAL CLP CDP CMP L/D BAL L/D P
 1 0.57 0.045 0.0239 0.001 0.016 0.0216 0.005 1.9 0.7

RUN 100 MACH=0.605 RN= 4.75*10**6 CONFIGURATION 3
 PT ALPHA CLBAL CDBAL CFBAL CLP CDP CMP L/D BAL L/D P
 1 0.06 -.030 -.006 -.017 -.012
 2 0.02 0.590 -.001 0.593 -.029

RUN 109 MACH=0.920 RN= 7.94*10**6 CONFIGURATION 3
 PT ALPHA CLBAL CDBAL CFBAL CLP CDP CMP L/D BAL L/D P
 1 -0.03 -.014 0.0341 0.000 0.011 0.001 -0.4
 2 -1.37 -.229 0.0247 0.029 -.209 -0.22 -9.3
 3 -1.44 -.127 0.0294 -.012 -.127 0.224 -4.3
 4 -0.25 -.014 0.0330 0.004 0.015 0.026 -0.4
 5 1.12 0.091 0.0401 0.009 0.107 -.044 2.3
 6 2.03 0.141 0.0420 0.008 0.170 0.069 3.4
 7 0.19 0.252 0.0540 -.026 0.263 -.023 4.7
 8 -0.20 -.016 0.0335 0.004 0.012 0.023 -0.5

RUN 110 MACH=0.901 RN= 7.92*10**6 CONFIGURATION 3
 PT ALPHA CLBAL CDBAL CFBAL CLP CDP CMP L/D BAL L/D P
 1 -0.19 0.003 0.0506 -.019 0.016 -.007 0.1
 2 -1.21 -.000 0.0490 -.016 -.005 -.006 -1.4
 3 -0.41 -.011 0.0506 -.010 0.003 -.005 -0.2
 4 1.05 0.093 0.0567 -.029 0.104 -.019 1.6
 5 2.10 0.149 0.0600 -.036 0.170 -.029 2.5
 6 -0.03 0.019 0.0504 -.022 0.027 -.009 0.3

RUN 111 MACH=1.071 RN= 7.92*10**6 CONFIGURATION 3
 PT ALPHA CLBAL CDBAL CFBAL CLP CDP CMP L/D BAL L/D P
 1 -0.03 0.015 0.0514 -.026 0.031 -.013 0.3
 2 -1.32 -.004 0.0497 -.022 -.003 -.011 -1.7
 3 -0.30 -.011 0.0491 -.024 -.000 -.012 -0.2
 4 1.12 0.009 0.0519 -.032 0.102 -.022 1.7
 5 2.04 0.143 0.0554 -.040 0.150 -.030 2.6
 6 -0.01 0.019 0.0550 -.027 0.020 -.013 0.3

RUN 122 MACH=.411 RN= 4.49*10**6 CONFIGURATION 4
 PT ALPHA CLBAL CDBAL CFBAL CLP CDP CMP L/D BAL L/D P
 5 -0.00 -.029 0.017 -.004 0.009
 6 6.00 0.567 0.013 0.600 0.0097 0.002 62.4

```

RUN 124 MACH= .303  RN= 4.75*10**6  CONFIGURATION 4
PT ALPHA  CLBAL  CDBAL  CBAL  CLP  CDP  CMP  L/D  BAL  L/D  P
1 -0.03 -0.010 0.019 0.027 0.0101 0.000 0.000 2.7 0.4
2 -5.37 -526 0.010 -0.71 0.0187 -0.005 -0.005 -25.3 0.000
3 3.37 -340 0.028 -309 0.0098 0.004 0.004 -36.4 0.000
4 -1.33 -130 0.022 -100 0.0097 0.001 -0.001 -10.3 0.001
5 -0.21 -931 0.021 0.003 0.0110 0.002 0.002 0.2 0.002
6 3.37 -346 0.028 -303 0.0091 0.002 -0.002 -33.4 0.002
7 3.03 0.272 0.019 0.317 0.0127 0.000 0.000 26.9 0.000
8 6.00 0.570 0.018 0.614 0.0101 0.001 0.001 40.0 0.001
9 9.07 0.858 0.014 0.895 0.0120 0.004 0.004 47.3 0.004
10 11.10 1.015 0.022 1.033 0.0262 0.016 0.016 54.5 0.016
11 12.07 1.035 0.0499 0.019 1.022 0.0443 0.009 20.0 0.009
12 13.05 0.969 0.0934 0.009 0.949 0.0805 -0.020 10.4 0.020
13 13.98 0.907 0.0874 -0.11 1.015 0.0746 -0.026 10.4 0.026
14 14.95 0.803 0.0934 -0.10 0.970 0.0849 -0.030 9.5 0.030
15 15.92 0.832 0.0991 -0.50 0.974 0.1211 -0.058 8.4 0.058
16 17.07 0.804 0.1171 -0.73 0.972 0.1756 -0.068 6.9 0.068
17 18.42 0.620 0.1011 -0.92 0.971 0.1770 -0.075 6.1 0.075
18 -0.26 -0.077 0.019 -0.004 0.0089 0.001 -0.001 5.4 0.001
19 -1.09 -0.152 0.016 -0.079 0.0085 0.000 -0.000 4.9 0.000

```

```

RUN 128 MACH= .404  RN= 4.40*10**6  CONFIGURATION 4
PT ALPHA  CLBAL  CDBAL  CBAL  CLP  CDP  CMP  L/D  BAL  L/D  P
1 -0.16 -0.004 0.005 0.004 0.0077 0.001 0.001 0.5 0.001
2 12.04 1.094 0.000 1.025 0.0373 0.009 0.009 27.4 0.009
3 5.90 0.599 0.000 0.601 0.0188 0.001 0.001 55.4 0.001

```

```

RUN 129 MACH= .600  RN= 5.95*10**6  CONFIGURATION 4
PT ALPHA  CLBAL  CDBAL  CBAL  CLP  CDP  CMP  L/D  BAL  L/D  P
1 -0.02 0.010 0.003 0.019 0.0079 0.000 0.000 2.3 0.000
2 -5.39 -495 0.022 -524 0.0345 -0.017 -0.017 -15.2 0.017
3 -3.42 -327 0.003 -342 0.0138 0.004 0.004 -26.3 0.004
4 -1.32 -103 0.013 -120 0.0078 0.002 0.002 -15.4 0.002
5 -0.10 0.017 0.007 0.008 0.0049 0.002 0.002 0.0 0.002
6 3.07 0.374 0.003 0.355 0.0079 0.002 0.002 44.7 0.002
7 6.06 0.723 0.005 0.678 0.0104 0.000 0.000 65.1 0.000
8 9.27 0.972 0.016 0.869 0.0458 0.012 0.012 10.9 0.012
9 10.20 0.957 0.1049 0.004 0.876 0.0667 0.000 9.1 0.000
10 11.43 0.891 0.1247 -0.33 0.805 0.1023 -0.000 7.1 0.000
11 12.31 0.829 0.1297 -0.41 0.900 0.1278 -0.030 6.4 0.030
12 13.03 0.818 0.1339 -0.57 0.897 0.1340 -0.032 6.1 0.032
13 13.92 0.839 0.1498 -0.78 0.890 0.1296 -0.027 5.6 0.027
14 16.27 0.822 0.1781 -0.61 0.893 0.1441 -0.064 4.6 0.064
15 -0.00 -0.071 0.009 -0.070 0.0073 0.002 0.002 -10.6 0.002
16 -0.11 0.012 0.003 0.008 0.0074 0.001 0.001 1.1 0.001
17 1.11 0.146 0.000 0.141 0.0072 0.002 0.002 19.5 0.002
18 3.05 0.364 0.003 0.347 0.0078 0.002 0.002 44.5 0.002
19 6.15 0.736 0.004 0.685 0.0101 0.008 0.008 67.4 0.008
20 9.25 0.979 0.011 0.871 0.0457 0.013 0.013 10.9 0.013
21 10.21 0.950 0.1161 -0.01 0.890 0.0634 0.009 0.2 0.009
22 11.28 0.906 0.1338 -0.25 0.884 0.0901 -0.003 6.8 0.003
23 12.16 0.844 0.1294 -0.48 0.894 0.1209 -0.022 6.5 0.022
24 -0.05 0.020 0.007 0.010 0.0070 0.003 0.003 7.3 0.003

```

```

RUN 124 MACH= .490  RN= 5.14*10**6  CONFIGURATION 4
PT ALPHA  CLBAL  CDBAL  CBAL  CLP  CDP  CMP  L/D  BAL  L/D  P
1 -0.07 -0.033 0.015 0.008 0.0087 0.003 0.003 0.9 0.003
2 -5.52 -544 0.004 0.0204 0.0323 -0.012 -0.012 -15.8 0.012
3 -3.54 -377 0.010 -0.237 0.0110 -0.002 -0.002 -32.4 0.002
4 -1.23 -142 0.010 -112 0.0085 0.003 0.003 -8.6 0.003
5 -0.20 -0.046 0.015 -0.005 0.0085 0.002 0.002 0.6 0.002
6 3.14 0.298 0.011 0.347 0.0089 0.002 0.002 39.0 0.002
7 6.07 0.612 0.008 0.651 0.0090 0.003 0.003 71.9 0.003
8 9.11 0.907 0.020 0.907 0.0167 0.019 0.019 40.0 0.019
9 11.14 0.953 0.0889 0.011 0.952 0.0587 0.019 10.7 0.019
10 12.22 0.920 0.0980 0.004 0.924 0.0794 -0.003 9.5 0.003
11 13.04 0.894 0.1040 -0.06 0.914 0.0917 -0.018 8.4 0.018
12 14.18 0.831 0.1144 -0.30 0.898 0.1158 -0.036 7.3 0.036
13 15.18 0.809 0.1204 -0.33 0.893 0.1396 -0.047 6.7 0.047
14 15.00 0.790 0.1350 -0.46 0.877 0.1544 -0.054 5.0 0.054
15 17.07 0.734 0.1478 -0.72 0.881 0.1804 -0.081 5.0 0.081
16 -0.92 -0.135 0.014 -0.000 0.0086 0.001 -0.001 -9.2 0.001
17 -0.36 -0.060 0.012 -0.019 0.0083 0.001 0.001 -2.4 0.001

```


RUN 142 MACH=.402 RN= 4.29*10**6 CONFIGURATION 4
 PT ALPHA CLBAL CDBAL CFBAL CLP CDP CMP L/D BAL L/D P
 1 0.01 0.059 0.017 0.022 0.0070 0.002 3.1
 2 6.00 0.631 0.012 0.615 0.0070 0.000 70.9
 3 10.13 1.015 0.013 0.986 0.0142 0.008 69.2
 4 11.17 1.007 0.019 1.042 0.0220 0.014 47.2
 5 12.09 1.093 0.023 1.026 0.0376 0.012 27.1
 6 13.06 1.024 0.007 0.980 0.0704 -0.011 13.0
 7 -0.05 0.009 0.020 0.016 0.0074 0.001 2.1
 RUN 144 MACH=0.923 RN= 7.33*10**6 CONFIGURATION 4
 PT ALPHA CLBAL CDBAL CFBAL CLP CDP CMP L/D BAL L/D P
 1 -0.17 -0.015 0.0300 -0.024 0.005 -0.030 -0.5
 2 -1.95 -0.215 0.0219 -0.025 -0.134 -0.031 -9.0
 3 -1.35 -0.147 0.0196 -0.033 -0.039 -0.043 -7.5
 4 -0.11 0.000 0.0230 -0.024 0.090 -0.029 0.0
 5 1.02 0.112 0.0370 0.005 0.190 0.013 3.0
 6 2.05 0.170 0.0567 -0.001 0.219 -0.004 3.2
 7 3.15 0.235 0.0661 0.007 0.237 0.039 3.5
 8 4.23 0.290 0.0695 0.002 0.280 0.040 4.2
 9 -0.16 0.002 0.0280 -0.026 0.082 -0.030 0.1
 RUN 145 MACH=0.903 RN= 7.27*10**6 CONFIGURATION 4
 PT ALPHA CLBAL CDBAL CFBAL CLP CDP CMP L/D BAL L/D P
 1 -0.21 -0.026 0.0545 -0.051 0.000 -0.037 -0.5
 2 -1.33 -0.107 0.0442 -0.042 -0.017 -0.028 -1.7
 3 -0.10 -0.020 0.0542 -0.052 0.003 -0.037 -0.4
 4 1.04 0.064 0.0664 -0.050 0.176 -0.043 1.4
 5 2.09 0.116 0.0475 -0.069 0.242 -0.053 2.5
 6 -0.31 -0.043 0.0492 -0.051 0.069 -0.038 -0.6

RUN 149 MACH=.402 RN= 3.62*10**6 CONFIGURATION 5
 PT ALPHA CLBAL CDBAL CFBAL CLP CDP CMP L/D BAL L/D P
 1 -0.09 0.024 -0.020 0.042 0.0090 -0.022 4.7
 2 -0.07 0.023 -0.016 0.037 0.0079 -0.021 4.7
 3 -0.17 0.006 -0.016 0.030 0.0064 -0.022 3.6
 4 -0.19 -0.001 -0.017 0.003 0.0003 -0.022 3.7
 5 5.97 0.665 -0.006 0.679 0.0079 -0.015 65.9
 6 5.97 0.661 -0.005 0.673 0.0062 -0.015 61.9
 RUN 150 MACH=.401 RN= 3.60*10**6 CONFIGURATION 5
 PT ALPHA CLBAL CDBAL CFBAL CLP CDP CMP L/D BAL L/D P
 1 -0.16 -0.007 -0.013 0.031 0.0003 -0.022 3.7
 2 -5.56 -0.549 0.0794 0.000 -0.466 0.0709 -0.027 -6.0
 3 -3.45 -0.300 -0.015 -0.303 0.0121 -0.020 -25.0
 4 -1.27 -0.132 -0.014 -0.077 0.0003 -0.024 -9.3
 5 -0.23 -0.020 -0.012 0.029 0.0000 -0.022 3.6
 6 2.91 0.311 -0.007 0.361 0.0000 -0.019 45.3
 7 6.02 0.962 -0.006 0.606 0.0077 -0.015 89.0
 8 0.92 0.062 -0.009 0.971 0.0094 -0.007 102.6
 9 10.90 1.162 -0.001 1.179 0.0113 0.001 104.2
 10 12.00 1.233 0.004 1.246 0.0135 0.007 92.1
 11 13.01 1.200 0.011 1.295 0.0100 0.014 60.7
 12 13.99 1.325 0.0454 0.012 1.316 0.0203 0.021 29.1
 13 14.96 1.316 0.0666 0.017 1.317 0.0312 0.019 19.7
 14 16.01 1.216 0.0911 -0.016 1.265 0.0547 0.003 13.3
 15 16.01 1.019 0.1023 -0.112 1.297 0.2060 -0.082 5.4
 16 18.20 0.998 0.1663 -0.117 1.193 0.2134 -0.075 5.4
 17 -1.03 -0.139 -0.007 -0.057 0.0079 -0.023 -7.3
 18 -0.41 -0.074 -0.005 0.006 0.0082 -0.022 0.7

RUN 151 MACH=.501 RN= 4.30*10**6 CONFIGURATION 5
 PT ALPHA CLBAL CDBAL CFBAL CLP CDP CMP L/D BAL L/D P
 1 -0.41 -0.059 -0.012 -0.001 0.0082 -0.024 -0.2
 2 -5.37 -0.550 0.0026 -0.462 0.0053 -0.023 -5.5
 3 -3.48 -0.308 0.0615 -0.310 0.0395 -0.032 -9.3
 4 -1.42 -0.176 -0.012 -0.116 0.0000 -0.026 -13.2
 5 -0.36 -0.057 -0.011 -0.008 0.0000 -0.024 -0.0
 6 2.99 0.335 -0.009 0.378 0.0078 -0.019 40.4
 7 6.00 0.691 -0.015 0.713 0.0064 -0.013 64.7
 8 9.00 0.960 0.0219 0.006 0.973 0.0194 0.003 50.0
 9 10.06 1.017 0.0304 0.009 1.030 0.0310 0.007 26.5
 10 11.19 1.036 0.0633 0.001 1.040 0.0514 -0.002 16.4
 11 12.00 1.060 0.0829 -0.014 1.066 0.0623 -0.009 12.0
 12 13.02 1.050 0.1052 -0.014 1.074 0.0772 -0.020 10.0
 13 14.15 1.040 0.1291 -0.032 1.093 0.1006 -0.034 8.1
 14 15.00 1.060 0.1513 -0.049 1.094 0.1200 -0.044 7.1
 15 16.02 1.024 0.1648 -0.065 1.091 0.1533 -0.064 6.2
 16 18.03 1.032 0.2103 -0.103 1.130 0.2026 -0.071 4.9
 17 18.04 1.003 0.2017 -0.102 1.133 0.1919 -0.060 5.0
 18 0.46 0.032 -0.010 0.091 0.0081 -0.023 11.1
 19 0.04 -0.011 -0.012 0.044 0.0005 -0.023 5.1

RUN 146 MACH=1.066 RN= 7.20*10**6 CONFIGURATION 4
 PT ALPHA CLBAL CDBAL CFBAL CLP CDP CMP L/D BAL L/D P
 1 -0.34 -0.042 0.0552 -0.056 0.076 -0.040 -0.0
 2 -1.31 -0.110 0.0659 -0.044 -0.012 -0.031 -1.7
 3 -0.06 -0.020 0.0543 -0.050 0.094 -0.040 -0.4
 4 0.94 0.051 0.0683 -0.063 0.155 -0.044 1.1
 5 -0.12 -0.024 0.0559 -0.050 0.006 -0.041 -0.4
 RUN 147 MACH=0.401 RN= 4.25*10**6 CONFIGURATION 4
 PT ALPHA CLBAL CDBAL CFBAL CLP CDP CMP L/D BAL L/D P
 1 -0.06 0.034 -0.007 0.010 0.010 2.4
 2 6.12 0.630 -0.020 0.602 0.010 13.4
 3 12.21 1.007 -0.005 0.925 0.010 6.7
 4 -0.26 0.004 -0.006 -0.004 0.010 0.2

Table with columns: RUN, ALPHA, CUBAL, CDBAL, CFBAL, CLP, COP, CFP, L/D, BAL, L/D, P. Rows for RUN 206, 207, 208, 209, 211. Each row includes Mach number and various coefficients.

Table with columns: RUN, ALPHA, CUBAL, CDBAL, CFBAL, CLP, COP, CFP, L/D, BAL, L/D, P. Rows for RUN 200, 202, 203, 204. Each row includes Mach number and various coefficients.

RUN 241 MACH=.806 RN= 6.03e10**6 CONFIGURATION 7
 PT ALPHA CUBAL COBAL CFBAL CLP CDP CMP L/D BAL L/D P
 2 0.09 -.006 0.0140 -.013 -.030 0.0163 -.017 -5.0 -2.3

RUN 242 MACH=.746 RN= 5.79e10**6 CONFIGURATION 7
 PT ALPHA CUBAL COBAL CFBAL CLP CDP CMP L/D BAL L/D P
 1 0.0 -.045 0.0109 -.015 -.017 0.0114 -.010 -4.1 -1.5

RUN 243 MACH=.701 RN= 5.90e10**6 CONFIGURATION 7
 PT ALPHA CUBAL COBAL CFBAL CLP CDP CMP L/D BAL L/D P
 1 -0.45 -.113 0.0115 -.010 -.007 0.0130 -.020 -9.0 -6.3
 2 -0.53 -.105 0.0116 -.017 -.009 0.0149 -.020 -9.0 -5.9

RUN 244 MACH=.796 RN= 5.94e10**6 CONFIGURATION 7
 PT ALPHA CUBAL COBAL CFBAL CLP CDP CMP L/D BAL L/D P
 1 -0.35 -.119 0.0129 -.010 -.094 0.0142 -.020 -9.2 -6.5
 2 -0.34 -.120 0.0132 -.010 -.101 0.0153 -.017 -9.1 -6.5

RUN 245 MACH=.822 RN= 6.02e10**6 CONFIGURATION 7
 PT ALPHA CUBAL COBAL CFBAL CLP CDP CMP L/D BAL L/D P
 1 -0.40 -.107 0.0159 -.011 -.115 0.0147 -.011 -6.7 -7.7
 2 -0.39 -.111 0.0152 -.013 -.111 0.0156 -.011 -7.3 -7.1

RUN 247 MACH=.872 RN= 6.15e10**6 CONFIGURATION 7
 PT ALPHA CUBAL COBAL CFBAL CLP CDP CMP L/D BAL L/D P
 1 -0.43 -.030 0.0256 -.005 -.047 0.0260 0.004 -1.5 -1.7
 2 -0.39 -.035 0.0272 -.007 -.066 0.0292 0.014 -1.3 -2.2

RUN 248 MACH=.896 RN= 6.20e10**6 CONFIGURATION 7
 PT ALPHA CUBAL COBAL CFBAL CLP CDP CMP L/D BAL L/D P
 1 -0.40 -.039 0.0400 -.002 -.011 0.0393 -.012 -1.0 -0.3
 2 -0.43 -.040 0.0423 0.000 -.011 0.0418 -.012 -0.9 -0.3

RUN 236 MACH=.404 RN= 3.06e10**6 CONFIGURATION 7
 PT ALPHA CUBAL COBAL CFBAL CLP CDP CMP L/D BAL L/D P
 10 -0.12 -.010 0.0150 -.003 0.003 0.0006 -.017 -1.1 0.3
 19 -2.34 -.249 0.0091 -.006 -.174 0.0093 -.007 -27.5 -10.7
 20 -1.40 -.160 0.0060 -.003 0.044 0.0066 -.011 -2.6 5.1
 21 -0.01 -.010 0.0071 -.000 0.297 0.0055 -.022 20.4 35.0
 22 6.04 0.590 0.0200 0.001 0.617 0.0103 -.024 21.1 60.1
 23 9.10 0.893 0.0527 0.010 0.926 0.0122 -.019 16.9 75.7
 24 9.10 0.897 0.0512 0.011 0.929 0.0119 -.010 17.5 77.6
 25 11.06 1.060 0.0734 0.016 1.100 0.0166 -.000 14.6 65.9
 27 12.13 0.977 0.0977 -.044 0.975 0.0170 -.077 10.0 9.0
 28 13.02 0.937 0.1145 -.052 0.949 0.0173 -.111 0.2 6.4
 29 13.92 0.905 0.1255 -.071 0.897 0.0163 -.117 7.2 5.0
 30 15.02 0.948 0.1423 -.041 0.966 0.0162 -.090 6.7 6.4

RUN 237 MACH=.404 RN= 3.09e10**6 CONFIGURATION 7
 PT ALPHA CUBAL COBAL CFBAL CLP CDP CMP L/D BAL L/D P
 4 -0.19 0.004 -.020 0.023 0.0090 -.011 2.6
 5 -0.21 -.001 -.022 0.022 0.0060 -.011 2.5
 6 5.96 0.651 -.035 0.611 0.0097 -.026 62.9

RUN 238 MACH=.599 RN= 5.21e10**6 CONFIGURATION 7
 PT ALPHA CUBAL COBAL CFBAL CLP CDP CMP L/D BAL L/D P
 1 -0.20 -.021 -.019 0.014 0.0060 -.013 1.4

RUN 239 MACH=.406 RN= 3.90e10**6 CONFIGURATION 7
 PT ALPHA CUBAL COBAL CFBAL CLP CDP CMP L/D BAL L/D P
 1 -0.05 -.011 0.0134 -.007 0.041 0.0149 -.012 -0.0 2.0

RUN 240 MACH=.602 RN= 5.23e10**6 CONFIGURATION 7
 PT ALPHA CUBAL COBAL CFBAL CLP CDP CMP L/D BAL L/D P
 1 -0.19 -.031 0.0079 -.010 0.030 0.0007 -.011 -4.0 3.4
 2 -2.23 -.273 0.0046 -.014 -.150 0.0099 -.001 -59.1 -15.9
 3 -1.43 -.179 0.0052 -.011 -.003 0.0060 -.005 -34.5 -9.4
 4 -0.34 -.055 0.0040 -.010 0.016 0.0060 -.009 -9.1 1.0
 5 2.97 0.334 0.0142 -.101 0.331 0.0096 -.025 23.5 34.2
 6 6.19 0.712 0.0361 -.004 0.678 0.0164 -.020 19.7 41.2
 7 9.29 0.940 0.0974 0.002 0.602 0.0464 -.013 9.7 10.1
 8 10.20 0.935 0.1197 -.013 0.902 0.0609 -.027 7.0 13.0
 9 11.25 0.897 0.1300 -.032 0.924 0.0904 -.037 6.5 9.3
 10 12.16 0.800 0.1505 -.042 0.894 0.1177 -.046 5.0 7.5
 11 13.16 0.823 0.1501 -.080 0.796 0.1629 -.124 5.2 4.9
 12 14.19 0.822 0.1750 -.095 0.761 0.1773 -.124 4.7 4.4
 13 16.26 0.810 0.2061 -.112 0.772 0.2152 -.129 4.0 3.6
 14 -0.99 -.151 0.0099 -.008 -.003 0.0091 -.016 -15.2 -9.1
 15 0.05 -.036 0.0104 -.007 0.024 0.0008 -.017 -3.5 2.7

REFERENCES

- 1) Carlson, L. A.: A FORTRAN Program for Transonic Airfoil Analysis Or Design. NASA CR-2821, June, 1977.
- 2) Bauer, F; Garabedian, P.; Korn, D. and Jamison, A.: Supercritical Wing Section II, Lecture Notes in Economics and Mathematical Systems. Vol. 108. Springer-Verlag, 1975.
- 3) Maskew, B.: CLMAX Program Description. AMI Report 7711, December, 1977.
- 4) Hicks, R. M; and Vanderplaats, G. N: Application of Numerical Optimization to Design of Low-Speed Airfoils. NASA TM X-3213, 1975.
- 5) Melnick, R. E; Chow, R. R; Mead, H. R.; and Jameson, A.: An Improved Viscid/Inviscid Interaction Procedure for Transonic Flow Over Airfoils. Grumman Aerospace Corporation, February, 1980.
- 6) Jepson, W. D.: Two Dimensional Test of Four Airfoil Configurations With An Aspect Ratio of 7.5 and a 16-inch Chord Up to a Mach Number of 1.1. SER-50977, Final Report for Contract N60921-73-C-0057, April 5, 1977.
- 7) Allen, H. J: and Vincenti, W. G: Wall Interference In A Two-Dimensional-Flow Wind Tunnel, With Consideration of the Effect of Compressibility. NACA Report No. 782, 1944.
- 8) Hilton, W. F: High Speed Aerodynamics. Longmans, Green and Co., 1951.
- 9) Bazin, M.: A Critique of Transonic Airfoil Testing Techniques. Part I, System of Industrial Tests in S3MA. L'Aeronautique et L'Astronautique, No. 31, pp. 1-8, Vol. 7, 1971.

1. Report No. NASA CR-166587		2. Government Accession No.		3. Recipient's Catalog No.	
4. Title and Subtitle An Experimental Evaluation of Advanced Rotorcraft Airfoils in the NASA Ames Eleven-Foot Transonic Wind Tunnel				5. Report Date February 1984	
				6. Performing Organization Code	
7. Author(s) Robert J. Flemming				8. Performing Organization Report No. SER-510106	
9. Performing Organization Name and Address Sikorsky Aircraft Division United Technologies Corporation N. Main St., Stratford, CT 06602				10. Work Unit No. T3334Y	
				11. Contract or Grant No. 14800-039	
12. Sponsoring Agency Name and Address National Aeronautics and Space Administration Washington, D.C. 20546				13. Type of Report and Period Covered Contractor Report March 1982-April 1983	
				14. Sponsoring Agency Code	
15. Supplementary Notes Point of Contact: Raymond Hicks, Applied Aerodynamics Branch NASA Ames Research Center, M/S 227-6 Moffett Field, CA 94035 (415) 965-5656					
16. Abstract Five full scale rotorcraft airfoils were tested in March and April 1982 in the NASA Ames Eleven-Foot Transonic Wind Tunnel for full scale Reynolds numbers at Mach numbers from 0.3 to 1.07. The models, which spanned the tunnel from floor to ceiling, included two modern baseline airfoils, the SC1095 and SC1094 R8, which have been previously tested in other facilities. Three advanced transonic airfoils, designated the SSC-A09, SSC-A07, and SSC-B08, were tested to confirm predicted performance and provide confirmation of advanced airfoil design methods. This test has shown that the eleven-foot tunnel is suited to two-dimensional airfoil testing.					
17. Key Words (Suggested by Author(s)) Airfoils Wind Tunnel Test Aerodynamics Correlation Helicopters Transonic Airfoils			18. Distribution Statement Unclassified - Unlimited Subject category 02		
19. Security Classif. (of this report) Unclassified		20. Security Classif. (of this page) Unclassified		21. No. of Pages 152	22. Price*

